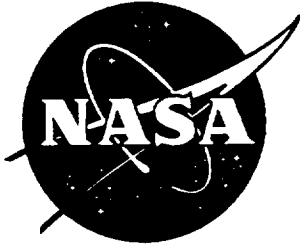


NASA Contractor Report



Progressive Failure and Life Prediction of Ceramic and Textile Composites

David Y Xue, Yucheng Shi, Madhu Katikala, William M. Johnston, Jr.
and Michael F. Card
Analytical and Material Services
Hampton, Virginia

Contract NAS8-40638

March 1998

National Aeronautics and
Space Administration
George C. Marshall Space Flight Center
Huntsville Alabama 35812

PROGRESSIVE FAILURE AND LIFE PREDICTION OF CERAMIC AND TEXTILE COMPOSITES

(CONTRACT: NAS8-40638)

(Final Report, March, 1998)

ABSTRACT

An engineering approach to predict the fatigue life and progressive failure of multilayered composite and textile laminates is presented. Analytical models which account for matrix cracking, statistical fiber failures and nonlinear stress-strain behavior have been developed for both composites and textiles. The analysis method is based on a combined micromechanics, fracture mechanics and failure statistics analysis. Experimentally derived empirical coefficients are used to account for the interface of fiber and matrix, fiber strength, and fiber-matrix stiffness reductions. Similar approaches were applied to textiles using Repeating Unit Cells. In composite fatigue analyses, Walker's equation is applied for matrix fatigue cracking and Heywood's formulation is used for fiber strength fatigue degradation.

The analyses have been compared with experiments with good agreement. Comparisons were made with Graphite-Epoxy, C/SiC and Nicalon/CAS composite materials. For textile materials, comparisons were made with triaxial braided and plain weave materials under biaxial or uniaxial tension. Fatigue predictions were compared with test data obtained from plain weave C/SiC materials tested at AS&M.

Computer codes were developed to perform the analyses. Composite Progressive Failure Analysis for Laminates is contained in the code CPFail. Micromechanics Analysis for Textile Composites is contained in the code MicroTex. Both codes were adapted to run as subroutines for the finite element code ABAQUS as CPFail-ABAQUS and MicroTex-ABAQUS. Graphic User Interface (GUI) was developed to connect CPFail and MicroTex with ABAQUS.

PROGRESSIVE FAILURE AND LIFE PREDICTION OF CERAMIC AND TEXTILE COMPOSITES

CONTENTS:

ABSTRACT

SUMMARY

Part A:	CPFail Analysis
A-1.	Background and Theory
A-2.	CPFail Laminate Analysis
A-3.	CPFail/ABAQUS Structural Progressive Failure Analysis
Part B:	MicroTex Analysis
B-1.	Background and Theory
B-2.	MicroTex Laminate Analysis
B-3.	MicroTex/ABAQUS Structural Progressive Failure Analysis
Part C:	Experiments
Part D:	Publications
Part E:	Commercialization Plan
Part F:	Computer Codes

SUMMARY

This document is the final report for the SBIR project of NASA CONTRACT NAS8-40638, entitled 'Progressive Failure and Life Prediction of Ceramic and Textile Composites'.

An engineering approach to predict the fatigue life and progressive failure of multilayered composite and textile laminates is developed. Analytical models which account for matrix cracking, statistical fiber failures and nonlinear stress-strain behavior have been developed for both composites and textiles. The analysis method is based on a combined micromechanics, fracture mechanics and failure statistics analysis. Experimentally derived empirical coefficients are used to account for the interface of fiber and matrix, fiber strength, and fiber-matrix stiffness reductions. Similar approaches were applied to textiles using Repeating Unit Cells. In composite fatigue analyses, Walker's equation is applied for matrix fatigue cracking and Heywood's formulation is used for fiber strength fatigue degradation.

The analyses have been compared with experiments with good agreement. Comparisons were made with Graphite-Epoxy, C/SiC and Nicalon/CAS composite materials. For textile materials, comparisons were made with triaxial braided and plain weave materials under biaxial or uniaxial tension. Fatigue predictions were compared with test data obtained from plain weave C/SiC materials tested at AS&M.

Progressive analyses for conventional composite materials and textile composites are named as **CPFail** (Composite **P**rogressive **F**ailure Analysis) and **MicroTex** (**M**icro-mechanics analysis for **T**extile composites).

The report contains three major parts: CPFail, MicroTex and Experiments. CPFail and MicroTex include Theoretical parts and user's manuals for the corresponding software codes.

The final products contain four computer software codes with graphics user interfaces: (1) CPFail-ABAQUS, (2) CPFail, (3) MicroTex-ABAQUS and (4) MicroTex.

CPFail-ABAQUS is a code which combines ABAQUS structural analysis and CPFail material degradation analysis for conventional composite materials.

CPFail is an independent code of material degradation analysis for conventional composite materials.

MicroTex-ABAQUS is a code which combines ABAQUS structural analysis and MicroTex textile composite material degradation analysis.

MicroTex is an independent code for textile composite material degradation analysis.

Part A. CPFail (Composite Progressive Failure) Analysis

A-1. Background and Theory

INTRODUCTION

An engineering approach **CPFail** (Composite Progressive Failure Analysis) has been developed to predict composite laminate failure and fatigue life under tensile damage. The stiffness reduction of each layer is computed based on: 1) in the fiber direction, the calculated fiber failure ratio and composite fracture; 2) in the direction normal to the fiber, the estimated matrix cracking. The laminate property is affected by the stiffness reduction of each ply. The analysis consists of micro-mechanics, fracture mechanics and statistics principles to model and predict the mechanical response and failure mechanism of polymer and ceramic matrix composites. The technique uses experimentally derived empirical coefficients to account for the interface of fiber and matrix, fiber strength and fiber-matrix stiffness reductions. In fatigue analysis, the Walker fatigue equation is used for counting matrix fatigue damage and the Heywood fatigue formulation is applied to estimate the fiber strength reduction. Analytical results are generated for Graphite-Epoxy, Nicalon/CAS, and C/SiC and compared with experiments.

The advent of new ceramic materials suitable for high temperature applications makes the capability to predict strength from fundamental principles extremely important. Reinforced materials such as C/SiC and SiC/SiC are finding applications in newly proposed launch vehicles and high performance engines. High temperature induced thermal stress and cyclic loading play an important role in the damage of these new materials.

A number of mathematical models have been proposed for predicting damage in fiber-reinforced composites [1-8]. Composite laminate damage normally starts with matrix cracking in the direction normal to the fibers. The matrix cracking will reach a saturation level with the increase of the applied load or the number of loading cycles. The stiffness of the laminate is controlled by the fiber property of each layer, that is the number of undamaged fibers in the layer.

In this part, the basic principles of the analysis are described. A simplified method of predicting matrix cracking is compared with experimental results for graphite-epoxy laminates. Stress-strain predictions for Nicalon-CAS material are compared with experiments at two temperatures and a study of the strength of angle-ply material is presented. Finally stress-strain curve and fatigue S-N curve for 0-90 C/SiC material are presented and compared with experiment.

CPFail has been successfully combined into ABAQUS structural analysis. Thus complex structural progressive failure analysis can be performed with the CPFail damage criteria. A simple example of a tension plate with a center hole was demonstrated to show the progressive plate damage and stress release process.

ANALYTICAL THEORY

A previous study [1] has developed an analysis to predict the fiber breakage in a single composite layer under tension loads. For continuously reinforced ceramic matrix composites, the failure mechanisms involve fiber/matrix debonding, fiber-bridged matrix cracking, and fiber failure in the wake of matrix cracking. In the analysis, the fiber-bridged matrix crack was

idealized by a continuum model in which the effect of the bridging fibers was modeled by an equivalent closure pressure on the crack surface. A rigorous shear-lag model developed by Budiansky et al. [2] was used to evaluate the closure pressure distribution along the crack surface and to compute the shear stress transfer along the debonded, frictionally sliding fiber/matrix interface. A closed-form micro-mechanics analysis was used to compute the thermal and mechanical (axial and transverse) stress along the fiber/matrix interface region. The micro-mechanics, the shear-lag, and the continuum fracture mechanics models were integrated with a statistical model to predict the fiber failure ratio. Fiber failure and matrix cracking reduce the composite modules and number of intact fibers to the point of failure.

The present study improved the analysis procedure and applied the analysis to compute the behavior of multilayer composites. Experimental results showed inelastic strain can occur when the applied stress exceeds a “yielding stress”. A parameter related to the ply stress ratio is introduced to reduce the fiber and matrix stiffness after the “yielding”. Matrix stiffness reduction due to the cracking in the direction normal to the fibers is estimated according to the tensile stress in this direction. A stepwise loading procedure is required since the stress-strain curve is nonlinear due to the material degradation caused by fiber breakage, matrix cracking and inelastic yielding. The analysis steps are summarized in Figure A1-1.

1) Micromechanics analysis:

A three-phase (fiber-matrix-composite) micromechanics model (Fig. A1-1) was developed for computing the normal stresses σ_{rr} at the fiber-matrix interface. Using classical elasticity solutions, the resulting 15 equations containing 15 unknown coefficients were solved numerically to obtain the solutions. The shear stresses, σ_{rz} and $\sigma_{\theta z}$ were assumed to be zero. The computed interface normal stress will be used in the next step of shear-lag analysis.

Using a classical elasticity approach, the following expressions can be assumed for the stresses in fiber (f), matrix (m) and composites (c).

$$\begin{aligned}\sigma_{rr}^f &= \left[2B_f \right] + \left[-2D_f \right] \cos(2\theta) \\ \sigma_{\theta\theta}^f &= \left[2B_f \right] + \left[2D_f + 12E_{ff}r^2 \right] \cos(2\theta) \\ \sigma_{r\theta}^f &= \left[2D_f + 6E_{ff}r^2 \right] \sin(2\theta)\end{aligned}\tag{A1-1}$$

$$\begin{aligned}\sigma_{rr}^m &= \left[\frac{A_m}{r^2} + 2B_m \right] + \left[-2D_m - 6\frac{F_m}{r^4} - 4\frac{G_m}{r^2} \right] \cos(2\theta) \\ \sigma_{\theta\theta}^m &= \left[-\frac{A_m}{r^2} + 2B_m \right] + \left[2D_m + 12E_{mm}r^2 + 6\frac{F_m}{r^4} \right] \cos(2\theta) \\ \sigma_{r\theta}^m &= \left[2D_m + 6E_{mm}r^2 - 6\frac{F_m}{r^4} - 2\frac{G_m}{r^2} \right] \sin(2\theta)\end{aligned}\tag{A1-2}$$

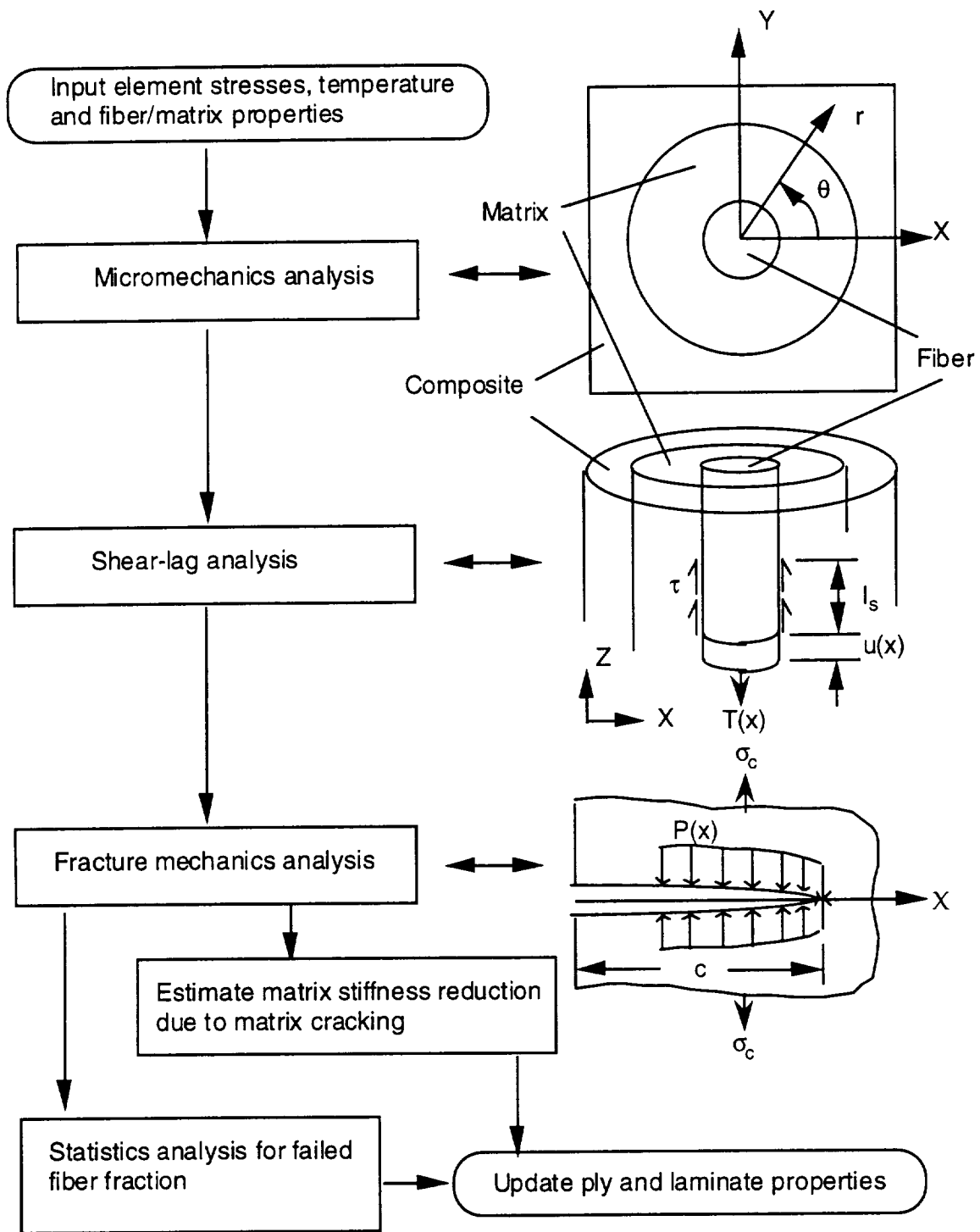


Fig. A1-1. Flow-chart of combined micromechanics, fracture mechanics and statistical approach of composite damage prediction

$$\begin{aligned}
\sigma_{rr}^c &= \left[\frac{A_c}{r^2} + 2B_c \right] + \left[-2D_c - 6\frac{F_c}{r^4} - 4\frac{G_c}{r^2} \right] \cos(2\theta) \\
\sigma_{\theta\theta}^c &= \left[-\frac{A_c}{r^2} + 2B_c \right] + \left[2D_c + 6\frac{F_c}{r^4} \right] \cos(2\theta) \\
\sigma_{r\theta}^c &= \left[2D_c - 6\frac{F_c}{r^4} - 2\frac{G_c}{r^2} \right] \sin(2\theta)
\end{aligned} \tag{A1-3}$$

The constitutive relation in fiber and matrix is assumed to be the same as of isotropic materials,

$$\begin{Bmatrix} \varepsilon_{rr} \\ \varepsilon_{\theta\theta} \\ \varepsilon_{zz} \\ \gamma_{r\theta} \end{Bmatrix} = \begin{bmatrix} \frac{1}{E} & \frac{-\mu}{E} & \frac{-\mu}{E} & 0 \\ \frac{-\mu}{E} & \frac{1}{E} & \frac{-\mu}{E} & 0 \\ \frac{-\mu}{E} & \frac{-\mu}{E} & \frac{1}{E} & 0 \\ 0 & 0 & 0 & \frac{2(1+\mu)}{E} \end{bmatrix} \begin{Bmatrix} \sigma_{rr} \\ \sigma_{\theta\theta} \\ \sigma_{zz} \\ \sigma_{r\theta} \end{Bmatrix} + \begin{Bmatrix} \alpha\Delta T \\ \alpha\Delta T \\ \alpha\Delta T \\ 0 \end{Bmatrix} \tag{A1-4}$$

The constitutive relation of the composite material is,

$$\begin{Bmatrix} \varepsilon_{rr} \\ \varepsilon_{\theta\theta} \\ \varepsilon_{zz} \\ \gamma_{r\theta} \end{Bmatrix} = \begin{bmatrix} \frac{1}{E_{22}} & \frac{-\mu_{23}}{E_{22}} & \frac{-\mu_{21}}{E_{22}} & 0 \\ \frac{-\mu_{23}}{E_{22}} & \frac{1}{E_{22}} & \frac{-\mu_{21}}{E_{22}} & 0 \\ \frac{-\mu_{12}}{E_{11}} & \frac{-\mu_{12}}{E_{11}} & \frac{1}{E_{11}} & 0 \\ 0 & 0 & 0 & \frac{2(1+\mu_{23})}{E_{22}} \end{bmatrix} \begin{Bmatrix} \sigma_{rr} \\ \sigma_{\theta\theta} \\ \sigma_{zz} \\ \sigma_{r\theta} \end{Bmatrix} + \begin{Bmatrix} \alpha_{22}\Delta T \\ \alpha_{22}\Delta T \\ \alpha_{11}\Delta T \\ 0 \end{Bmatrix} \tag{A1-5}$$

with the strain-displacement relation,

$$\varepsilon_{rr} = \frac{\partial u_r}{\partial r}, \quad \varepsilon_{\theta\theta} = \frac{1}{r} \frac{\partial u_\theta}{\partial \theta} + \frac{u_r}{r}, \quad \gamma_{r\theta} = \frac{1}{r} \frac{\partial u_r}{\partial \theta} + \frac{\partial u_\theta}{\partial r} - \frac{u_\theta}{r} \tag{A1-6}$$

The displacement in fiber, matrix and composite can be written as,

$$\begin{aligned}
u_r^f &= \left(\frac{1+\mu_f}{E_f} \right) \left\{ \left[2(1-2\mu_f)B_f r \right] + \left[-2D_f r - 4\mu_f E_{ff} r^3 \right] \cos(2\theta) \right\} + \left[(1+\mu_f)\alpha_f \Delta T - \mu_f \overline{\varepsilon_{zz}} \right] r \\
u_\theta^f &= \left(\frac{1+\mu_f}{E_f} \right) \left[2D_f r + 2(3-2\mu_f)E_{ff} r^3 \right] \sin(2\theta)
\end{aligned}
\tag{A1-7}$$

$$\begin{aligned}
u_r^m &= \left(\frac{1+\mu_m}{E_m} \right) \left\{ \left[-\frac{A_m}{r} + 2(1-2\mu_m)B_m r \right] + \left[-2D_m r - 4\mu_m E_{mm} r^3 + 2\frac{F_m}{r^3} + \frac{4(1-\mu_m)G_m}{r} \right] \cos(2\theta) \right\} \\
&\quad + \left[(1+\mu_m)\alpha_m \Delta T - \mu_m \overline{\varepsilon_{zz}} \right] r \\
u_\theta^m &= \left(\frac{1+\mu_m}{E_m} \right) \left[2D_m r + 2(3-2\mu_m)E_{mm} r^3 + 2\frac{F_m}{r^3} - \frac{2(1-2\mu_m)G_m}{r} \right] \sin(2\theta)
\end{aligned}
\tag{A1-8}$$

$$\begin{aligned}
u_r^c &= \left(\frac{1}{E_{22}} \right) \left\{ \left[-\frac{(1+\mu_{23})A_c}{r} + 2(1-\mu_{23}-2\mu_{12}\mu_{21})B_c r \right] \right. \\
&\quad + \left[-2(1+\mu_{23})D_c r + 2\frac{(1+\mu_{23})F_c}{r^3} + \frac{4(1-\mu_{12}\mu_{21})G_c}{r} \right] \cos(2\theta) \left. \right\} \\
&\quad + \left[(\mu_{12}\alpha_{11} + \alpha_{22})\Delta T - \mu_{12}\overline{\varepsilon_{zz}} \right] r \\
u_\theta^c &= \left(\frac{1}{E_{22}} \right) \left[2(1+\mu_{23})D_c r + 2\frac{(1+\mu_{23})F_c}{r^3} - \frac{2(1-\mu_{23}-2\mu_{12}\mu_{21})G_c}{r} \right] \sin(2\theta)
\end{aligned}
\tag{A1-9}$$

Using the following 15 boundary conditions, Eqs. (A1-10),

$$\begin{aligned}
\sigma_{rr}^f(a, 45^0) &= \sigma_{rr}^m(a, 45^0) \\
\sigma_{rr}^f(a, 0^0) &= \sigma_{rr}^m(a, 0^0) \\
\sigma_{r\theta}^f(a, 45^0) &= \sigma_{r\theta}^m(a, 45^0) \\
\sigma_{rr}^m(b, 45^0) &= \sigma_{rr}^c(b, 45^0) \\
\sigma_{rr}^m(b, 0^0) &= \sigma_{rr}^c(b, 0^0) \\
\sigma_{r\theta}^m(b, 45^0) &= \sigma_{r\theta}^c(b, 45^0) \\
u_r^f(a, 45^0) &= u_r^m(a, 45^0) \\
u_\theta^f(a, 45^0) &= u_\theta^m(a, 45^0) \\
u_r^f(a, 0^0) &= u_r^m(a, 0^0)
\end{aligned}$$

$$\begin{aligned}
u_c^m(b, 45^0) &= u_r^c(b, 45^0) \\
u_r^m(b, 0^0) &= u_r^c(b, 0^0) \\
u_\theta^m(b, 0^0) &= u_\theta^c(b, 0^0) \\
\sigma_{rr}^c(\infty, 0^0) &= \overline{\sigma_0} \\
\sigma_{\theta\theta}^c(\infty, 0^0) &= \overline{\sigma_{90}} \\
\frac{1}{\pi b^2} \left[\iint_{\text{fiber}} \sigma_{zz}^f r dr d\theta + \iint_{\text{matrix}} \sigma_{zz}^{mm} r dr d\theta \right] &= \overline{\sigma_{zz}}
\end{aligned} \tag{A1-10}$$

15 unknown coefficients B_f , D_{ff} , E_{ff} , A_m , B_m , D_m , E_{mm} , F_m , G_m , A_c , B_c , D_c , F_c , G_c and $\overline{\epsilon_{zz}}$ can be solved from Eqs. (A1-11)

$$\begin{aligned}
2B_f - \frac{A_m}{a^2} - 2B_m &= 0 \\
-2D_f + 2D_m + 6\frac{F_m}{a^4} + 4\frac{G_m}{a^2} &= 0 \\
2D_f + 6a^2 E_{ff} - 2D_m - 6a^2 E_{mm} + 6\frac{F_m}{a^4} + 2\frac{G_m}{a^2} &= 0 \\
\frac{1}{b^2} A_m + 2B_m - \frac{1}{b^2} A_c - 2B_c &= 0 \\
-2D_m - \frac{6}{b^4} F_m - 4\frac{G_m}{a^2} + 2D_c + 6\frac{F_c}{a^4} + 4\frac{G_c}{a^2} &= 0 \\
2D_m + 6b^2 E_{mm} - \frac{6}{a^4} F_m - 2\frac{G_m}{a^2} - 2D_c + 6\frac{F_c}{a^4} + 2\frac{G_c}{a^2} &= 0 \\
\frac{2(1+\mu_f)(1-2\mu_f)a}{E_f} B_f + \frac{1+\mu_m}{E_m a} A_m - \frac{2a(1+\mu_m)(1-2\mu_m)}{E_m} B_m + a(\mu_m - \mu_f) \overline{\epsilon_{zz}} \\
&= \left[(1+\mu_f)\alpha_f - (1+\mu_m)\alpha_m \right] \Delta T \\
-\frac{2(1+\mu_f)a}{E_f} D_f - \frac{2(1+\mu_f)(3-2\mu_f)a^3}{E_f} E_{ff} + \frac{2(1+\mu_m)a}{E_m} D_m \\
+ \frac{2(1+\mu_m)(3-2\mu_m)a^3}{E_m} E_{mm} + \frac{2(1+\mu_m)}{E_m a^3} F_m - \frac{2(1+\mu_m)(1-2\mu_m)a^3}{E_m a} G_m \\
&= 0 \\
-\frac{2(1+\mu_f)a}{E_f} D_f - \frac{4\mu_f(1+\mu_f)a^3}{E_f} E_{ff} + \frac{2(1+\mu_m)a}{E_m} D_m \\
+ \frac{4\mu_m(1+\mu_m)a^3}{E_m} E_{mm} - \frac{2(1+\mu_m)}{E_m a^3} F_m - \frac{4(1+\mu_m)(1-\mu_m)a^3}{E_m a} G_m \\
&= 0
\end{aligned}$$

$$\begin{aligned}
& -\frac{(1+\mu_m)}{E_m b} A_m + \frac{2(1-2\mu_m)(1+\mu_m)b}{E_m} B + \frac{(1+\mu_{23})}{E_{22}b} A_c \\
& -\frac{2(1-\mu_{23}-2\mu_{12}\mu_{21})b}{E_{22}} B_c + (\mu_{12}-\mu_m)b\overline{\epsilon_{zz}} \\
& = b[\mu_{12}\alpha_{11} + \alpha_{22} - (1+\mu_m)\alpha_m]\Delta T \\
\\
& -\frac{2(1+\mu_m)b}{E_m} D_m - \frac{4\mu_m(1+\mu_m)b^3}{E_m} E_{mm} + \frac{2(1+\mu_m)}{E_m b^3} F_m + \frac{4(1-\mu_m)(1+\mu_m)}{E_m b} G_m \\
& + \frac{2(1+\mu_{23})b}{E_{22}} D_c - \frac{2(1+\mu_{23})}{E_{22}b^3} F_c - \frac{4(1-\mu_{12}\mu_{21})}{E_{22}b} G_c \\
& = 0 \\
\\
& \frac{2(1+\mu_m)b}{E_m} D_m + \frac{2(1+\mu_m)(3-2\mu_m)b^3}{E_m} E_{mm} + \frac{2(1+\mu_m)}{E_m b^3} F_m - \frac{2(1-2\mu_m)(1+\mu_m)}{E_m b} G_m \\
& - \frac{2(1+\mu_{23})b}{E_{22}} D_c - \frac{2(1+\mu_{23})}{E_{22}b^3} F_c + \frac{2(1-\mu_{23}-\mu_{12}\mu_{21})}{E_{22}b} G_c \\
& = 0 \\
\\
& 2B_c - 2D_c = \overline{\sigma_0} \\
& 2B_c + 2D_c = \sigma_{90} \\
& 4a^2\mu_f B_f + 4(b^2 - a^2)\mu_m B_m + [E_f a^2 + (b^2 - a^2)E_m]\overline{\epsilon_{zz}} \\
& = b^2\overline{\sigma_{zz}} + [\alpha_f E_f a^2 + \alpha_m E_m (b^2 - a^2)]\Delta T
\end{aligned} \tag{A1-11}$$

2) Shear-lag analysis:

A shear-lag model (Fig. A1-1) was used to model each fiber along the matrix crack and the slip region at the fiber-matrix interface. The interface shear stress τ is related to the normal interface stress σ_{rr} through the friction coefficient μ , as:

$$\tau = \mu \sigma_{rr} |_{r=a} \tag{A1-12}$$

where μ is a empirical parameter, needs to be determined from experiments or numerical estimation.

The crack opening displacement, $u(x)$, can be expressed by

$$u(x) = AT(x)^2 + BT(x) + C \tag{A1-13}$$

where $T(x)$ is the fiber bridging traction, A, B and C are functions of interface shear stress τ and applied loads. Both $u(x)$ and $T(x)$ are unknown functions, and require a fracture mechanics analysis to solve the problem.

3) Fracture Mechanics Analysis:

In the fracture mechanics analysis (Fig. A1-1), the crack opening displacement, $u(x)$, can be computed by another form, as:

$$u(x) = \frac{2c\sigma_c}{\pi E_c} \int_0^1 \left[1 - \frac{p(t)}{\sigma_c} \right] \ell n \left| \frac{\sqrt{1-t^2} + \sqrt{1-x^2}}{\sqrt{1-t^2} - \sqrt{1-x^2}} \right| dt \quad (\text{A1-14})$$

where c is the initial crack length, estimated according to the size of the fiber diameter and fiber volume fraction [1], σ_c is the applied stress and E_c is the composite stiffness in the fiber direction.

The bridging pressure, $p(x)$, and the bridging traction $T(x)$ are related as:

$$p(x) = V_f T(x) \quad (\text{A1-15})$$

where V_f is the fiber volume friction. The bridging traction $T(x)$ then can be solved by using an iterative procedure from the following integral equation:

$$AT(x)^2 + BT(x) + C = \frac{2c\sigma_c}{\pi E_c} \left[\pi \sqrt{(1-x^2)} - \frac{V_f}{\sigma_c} \int_0^1 T(t) \ell n \left| \frac{\sqrt{1-t^2} + \sqrt{1-x^2}}{\sqrt{1-t^2} - \sqrt{1-x^2}} \right| dt \right] \quad (\text{A1-16})$$

After solving for the bridging pressure, the composite stress intensity factor, K , at the fiber-bridged crack can be calculated as:

$$K = 2\sqrt{\frac{c}{\pi}} \int_0^1 \frac{(\sigma_c - p(x))dx}{\sqrt{1-x^2}} \quad (\text{A1-17})$$

The matrix stress intensity factor, K_m , is:

$$K_m = K \sqrt{\frac{E_m}{V_m E_c}} \quad (\text{A1-18})$$

where E_m and V_m is the matrix stiffness and volume friction. Matrix crack propagation is predicted when

$$K_m \geq K_{mc} \quad (\text{A1-19})$$

where K_{mc} the critical matrix stress intensity factor should be determined from experiments or the literature.

4) Statistical Fiber Failure:

From the shear-lag model, the fiber failure statistical value can be found as:

$$P_f = 1 - \exp \left[\frac{-4\pi a l_s}{k_0} \left(\frac{T_z}{\sigma_0} \right)^M \right] \quad (A1-20)$$

where P_f is the fiber failure probability, M is Weibull modules, $T_z = \sigma_c / V_{fi}$, V_{fi} is the initial fiber volume fraction. σ_0 is the equivalent fiber strength, an empirical parameter with the units MPa or KSi, k_0 is a unit parameter. $k_0 = 1 \text{ m}^2$, for MPa units; $k_0 = 1550 \text{ in}^2$, for KSi units. The predicted fiber failure probability of the composite is sensitive to the fiber strength properties. Therefore, an accurate knowledge of the σ_0 and M values for the fibers inside the matrix is necessary. Using the fiber original strength properties prior to the composite fabrication overestimates the strength prediction. In general, the mean strength of the fibers is reduced during composite fabrication [11].

The final fiber volume fraction can be estimated as:

$$V_{fn} = V_{fi} (1 - P_f) \quad (A1-21)$$

YIELDING PARAMETER

An important improvement of this analysis in this study is to introduce a yielding parameter to control the stiffness changes of fiber and matrix after a ply passed its yielding point. In the current analysis it is known that a single ply starts yielding when the matrix stress intensity factor in the fiber direction exceeds its critical value, $K_m \geq K_{mc}$. To reduce the dependence of the solution on the load steps, the parameter is designed to be related to the ratio of the current ply stress (in the fiber direction) over the critical ply stress. The critical ply stress is the ply stress at yielding. The reduced stiffness is assumed to be:

$$E = E_0 \left(\frac{\sigma_z}{\sigma_{zc}} \right)^{-\beta} \quad (A1-22)$$

where E_0 is the original, undamaged fiber or matrix stiffness. The yielding parameter β needs to be determined according to the composite material testing data. Basically β will control the slope of stress-strain curve after the yielding point.

MATRIX DAMAGE NORMAL TO THE FIBERS

A simplification of matrix stiffness reduction is based on the fact that 1) the fiber modules dominates the stiffness of the laminate, and 2) matrix cracking reaches its saturation level at the very early (low) loading stages. In the analysis the matrix elastic modules was reduced to 30% of the original value when the matrix fracture stress intensity factor reached the critical value. A linear matrix stiffness reduction was assumed before the critical stress intensity level was reached.

The matrix cracking in the off-fiber direction will be estimated according to the tension stress level in that direction. Assume the size of initial matrix cracking is same as the size c estimated in the fiber direction, the matrix stress intensity factor then can be derived by setting $p(x)=0$ in Eq. (A1-17), as

$$K_{m0} = \sigma_{c0} \sqrt{\pi c} \quad (A1-23)$$

where σ_{c0} is the stress in the off-fiber direction. Assume that if K_{m0} is larger than K_{mc} , matrix cracking reaches a saturation level, the Young's Modules of matrix E_m reduces to 30% of its original value. Before that level E_m has a linear decline:

$$E_m = E_{m0} \delta, \quad \text{if } K_{m0} \geq K_{mc}; \quad (A1-24)$$

$$E_m = E_{m0} \left[1 - \frac{K_{m0}}{K_{mc}} (1 - \delta) \right], \quad \text{if } K_{m0} \leq K_{mc} \quad (A1-25)$$

Since the fiber property dominates in the composite laminate response, the value of δ is not critical to the laminate property. In the present study $\delta = 0.3$. Eqs. (A1-24) and (A1-25) greatly simplify the computation of off-fiber matrix cracking. Comparison with experimental results showed that the simplification was reasonable.

FAILURE CRITERIA

Two criteria were used to test for ply failure:

- 1) $V_f = V_{limit}$ ($V_{limit} = 0.1 \sim 0.3$) in any ply, or
- 2) $K_{m0} \geq K_{mc}$ in all plies

If either condition was met, the laminate was assumed to have failed.

EMPIRICAL PARAMETERS

The analytical theory contains four empirical parameters, μ (Eq. A1-12), β (Eq. A1-22), K_{mc} (Eq. A1-19), and σ_0 (Eq. A1-20). As indicated in Figure A1-2, they can be used to adjust the shape of the stress-strain curve.

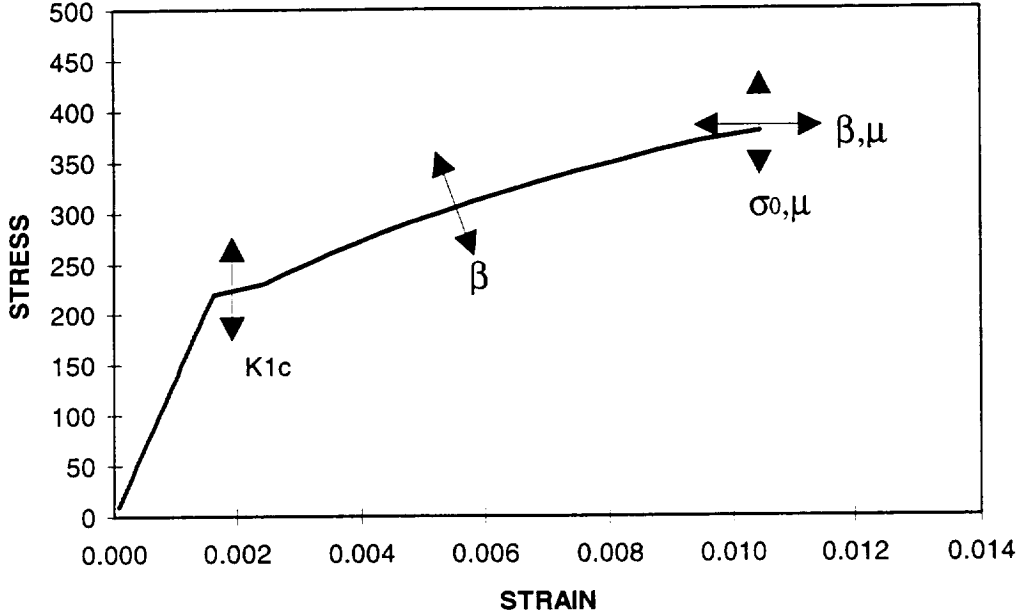


Fig. A1-2 Effects of empirical parameters

CPFail FATIGUE ANALYSIS MODEL

The fatigue analysis includes matrix cracking fatigue and fiber fatigue since the static analysis includes matrix and fiber damages.

The matrix cracking fatigue is counted by using a modified Walker fatigue equation:

$$\frac{da}{dN} = CK_m^n \quad (A1-26)$$

where da is the crack increase, N is the number of loading circles, K_m is the stress intensity factor associated with the maximum stress of the loading circle. C and n are empirical parameters.

In the current analysis, the failure of the fiber is controlled by the equation (A1-20) as:

$$P_f = 1 - \exp \left[\frac{-4\pi a l_s}{k_0} \left(\frac{T_z}{\sigma_0} \right)^M \right] \quad (A1-20)$$

where σ_0 is the equivalent fiber strength. The fatigue of fiber breakage is assumed to be developed with the reduction of σ_0 . To estimate the fatigue reduction of the equivalent strength σ_0 , a fatigue formulation (Heywood) was introduced as:

$$\begin{aligned}\sigma_a &= \pm \sigma_t \left[1 - \sigma_m / \sigma_t \right] \left[A_0 + \gamma(1 - A_0) \right] \\ A_0 &= \left[1 + \frac{p_3 \bar{n}^4}{1 + \sigma_t / p_1} \right] \frac{1}{1 + p_3 \bar{n}^4}, \\ \gamma &= \frac{\sigma_m}{\sigma_t} \frac{1}{1 + (\sigma_t \bar{n} / p_2)^4}, \\ \bar{n} &= \text{Log}(N)\end{aligned}\tag{A1-27}$$

where

σ_a is the Alternating stress,

σ_m is the Mean stress, $\sigma_m = 0.5(\sigma_{\max} + \sigma_{\min}) = 0.5(1 + R_m)\sigma_{\max}$,

σ_t is the Tension strength,

R_m is the stress ratio, $R_m = \frac{\sigma_{\min}}{\sigma_{\max}}$.

The parameters p_1 , p_2 and p_3 are material related, and for aluminum alloy $p_1=153.26$ MPa, $p_2=2206.9$ MPa and $p_3=0.0031$. The following figure (Figure A1-3) shows the effects of parameter changes on the Heywood formulation.

For a given maximum stress, strength, and stress ratio, a relation of alternating stress and the number of the load circles (S-N curve) can be established. The region under the S-N curve is the safe area, so the S-N curve actually represents a fatigue strength curve. In the current analysis, assuming $\sigma_t = \sigma_0 = \sigma_{\max}$, the result curve represents fatigue reduction of σ_0 . Considering the interface of matrix fatigue and fiber fatigue, the final reduced strength is assumed to be:

$$\sigma_0 = (\sigma_a + \sigma_m) R_k^{-\zeta}\tag{A1-28}$$

where $R_k = K_m / K_{mc}$ is the ratio of matrix stress intensity factor, ζ is an empirical parameter.

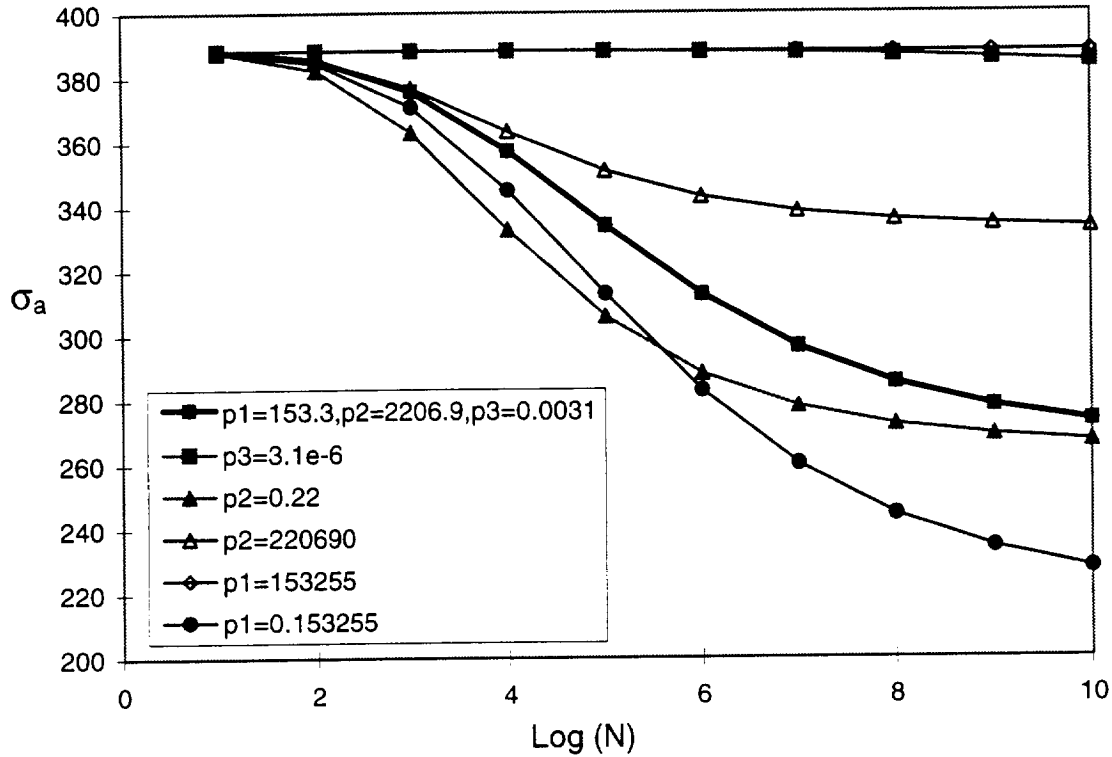


Figure A1-3. Parameter effects on the curve of Log(N) Vs. Maximum Stress (MPa)

ANALYSIS RESULTS

MATERIAL PROPERTIES

To verify the developed analysis tool several kinds of composite materials, Graphite/epoxy, Nicalon/CAS, C/SiC and SiC/SiC have been chosen for the comparison between analyses and test. Following are the material properties used in the present study. (E_f - fiber young's modules, μ_f - fiber Poisson's ratio, α_f - fiber thermal expansion coefficient, V_f - fiber volume fraction, σ_0 - fiber mean strength, d_f - fiber diameter, M - fiber Weibull modules, E_m - matrix Young's modules, μ_m - matrix Poisson's ratio, α_m - matrix thermal expansion coefficient, K_{mc} - critical matrix stress intensity factor, T - temperature).

Nicalon/CAS

Nicalon fiber:

$E_f =$	195.0 (176.0)*	GPa
$\mu_f =$	0.2	
$\alpha_f =$	3.0E-6 (4.0E-6)*	$1/^\circ C$
$V_f =$	0.65	
$M =$	10	
$\sigma_0 =$	388.4	MPa

$$d_f = 7.00E-5 \quad \text{m}$$

CAS matrix:

$$E_m = 95.0 \quad \text{GPa}$$

$$\mu_m = 0.3$$

$$\alpha_m = 5.0E-6 \quad / ^\circ C$$

$$K_{mc} = 2.16(1.73)^* \quad \text{MPa} \cdot m^{(1/2)}$$

$$T = 0 \quad ^\circ C$$

(* Properties at $T=400 \quad ^\circ C$)

Empirical parameters:

$$\mu = 0.01 \quad \text{Friction parameter}$$

$$\beta = 2.4 \quad \text{Nonlinear parameter}$$

$$\delta = 0.3 \quad \text{Matrix damage limit}$$

Graphite/Epoxy

Graphite fiber:

$$E_f = 221.0 \quad \text{GPa}$$

$$\mu_f = 0.48$$

$$\alpha_f = -7.58E-7 \quad / ^\circ C$$

$$V_f = 0.65$$

$$M = 10$$

$$\sigma_0 = 388.4 \quad \text{MPa}$$

$$d_f = 7.00E-6 \quad \text{m}$$

Epoxy matrix:

$$E_m = 3.45 \quad \text{GPa}$$

$$\mu_m = 0.2$$

$$\alpha_m = 8.433E-5 \quad / ^\circ C$$

$$K_{mc} = 0.67 \quad \text{MPa} \cdot m^{(1/2)}$$

$$T = 0 \quad ^\circ C$$

Empirical parameters:

$$\mu = 0.01 \quad \text{Friction parameter}$$

$$\beta = 2.4 \quad \text{Nonlinear parameter}$$

$$\delta = 0.3 \quad \text{Matrix damage limit}$$

Carbon/SiC

Carbon fiber:

$$E_f = 231.0 \quad \text{GPa}$$

$$\mu_f = 0.2$$

$$\alpha_f = -6.0E-5 \quad / ^\circ C$$

$$\begin{aligned}
 V_f &= 0.40 \\
 M &= 10 \\
 \sigma_0 &= 388.4 && \text{MPa} \\
 d_f &= 7.00\text{E-}6 && \text{m}
 \end{aligned}$$

SiC. matrix:

$$\begin{aligned}
 E_m &= 35.10 && \text{GPa} \\
 \mu_m &= 0.22 \\
 \alpha_m &= 1.10\text{E-}5 && / ^\circ\text{C} \\
 K_{mc} &= 0.5 && \text{MPa}\cdot\text{m}^{(1/2)} \\
 T &= 0 && ^\circ\text{C}
 \end{aligned}$$

Empirical parameters:

$$\begin{aligned}
 \mu &= 0.3 && \text{Friction parameter} \\
 \beta &= 0.1 && \text{Nonlinear parameter} \\
 \delta &= 0.1 && \text{Matrix damage limit}
 \end{aligned}$$

Laminate Response

Figure A1-4 (taken from Reference 5) shows a schematic of the expected three stages of laminate response: 1) an initial rapid matrix cracking, 2) a stable period of matrix cracking saturation, and 3) fast fiber breakage. The present analysis models matrix cracking and fiber breakage and accounts for delamination and crack-coupling/interfacial debonding in the empirical parameters.

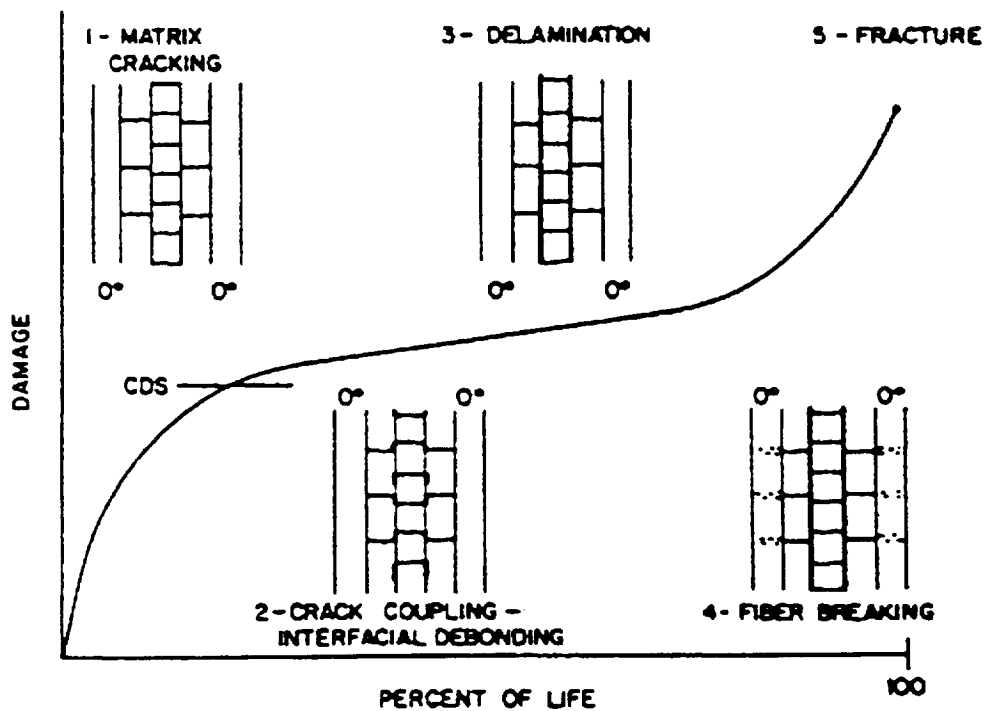


Fig. A1-4 Damage development in composite laminates (Ref. 5)

Stiffness Degradation

To evaluate the accuracy of the stiffness degradation predictions comparisons were made with the test data given in Reference 3 for graphite-epoxy material. The present results and the experimental results are compared in Figure A1-5. The reduction in the axial laminate modules for a strain level of 0.01 is presented for several laminates. Agreement with test is reasonably good.

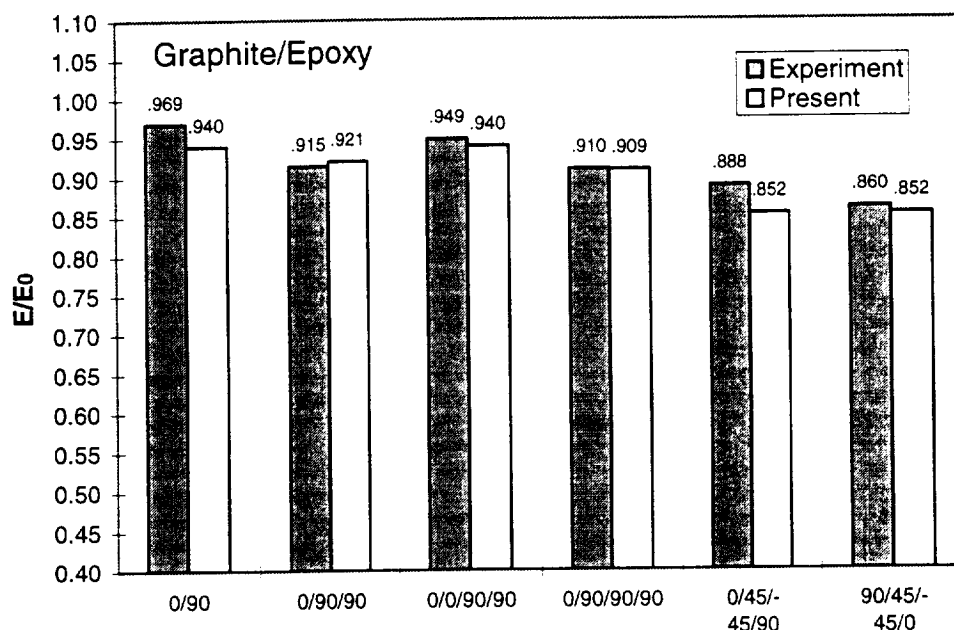


Fig. A1-5 Stiffness reduction prediction comparison with experiments (Ref. 3)

Nicalon/CAS Comparison

Unidirectional ply stress-strain curves were computed for a Nicalon/CAS composite investigated experimentally in Reference 9. Data was obtained at room temperature (0°C) and 400°C . The solid and dashed stress-strain curves from analyses are compared in Fig. A1-6 and show good agreement with the testing data.

Room temperature angle ply laminate results for Nicalon/CAS material are plotted in Figure A1-7. The higher strength results for 15 and 30 degree laminates are unexpected, and are believed to have resulted from the absence of shear effects in the current analysis.

The complexity of the room temperature response of a (0/-45/45/90)_s Nicalon/CAS laminate is illustrated in Figures A1-8 and A1-9. The stress-strain curve in Figure A1-6 can be seen to have a discontinuity corresponding to yielding behavior. Figure A1-9 shows the reduction in stiffness of the laminate and several areas where changes in ply behavior are occurring.

C/SiC Results

Room temperature stress-strain and stiffness reduction for (0/90)_s C/SiC material are presented in Figure A-10 and A-11. The results are compared with experimental results. The calculations appear to have reasonable agreement with the test data.

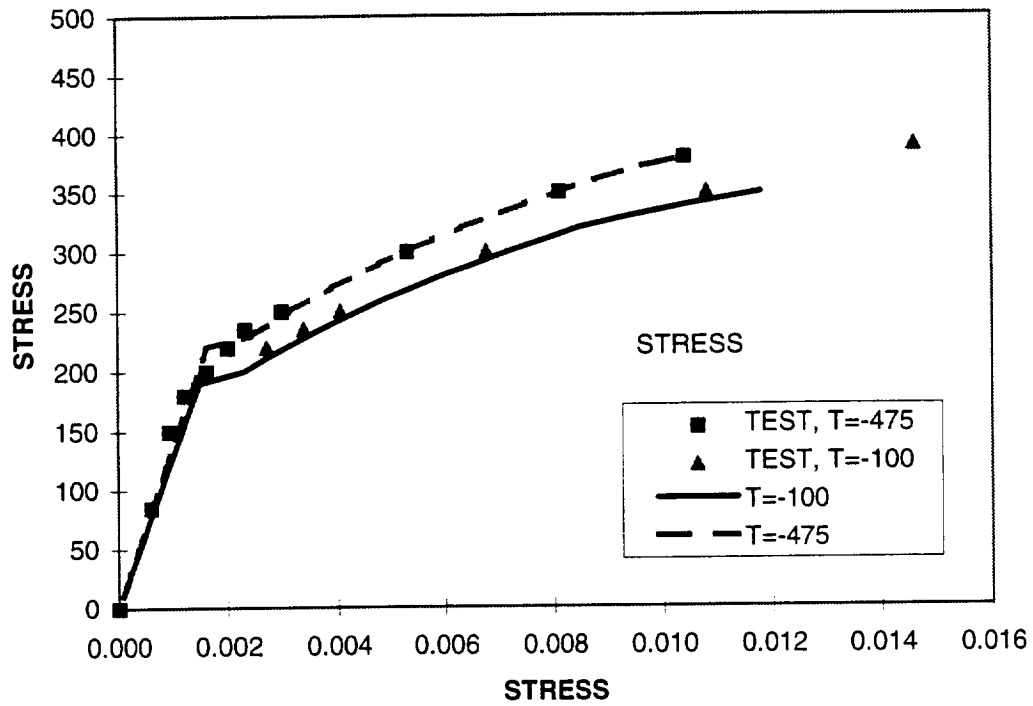


Fig. A1-6 Comparison of stress strain results for the Nicalon/CAS composite

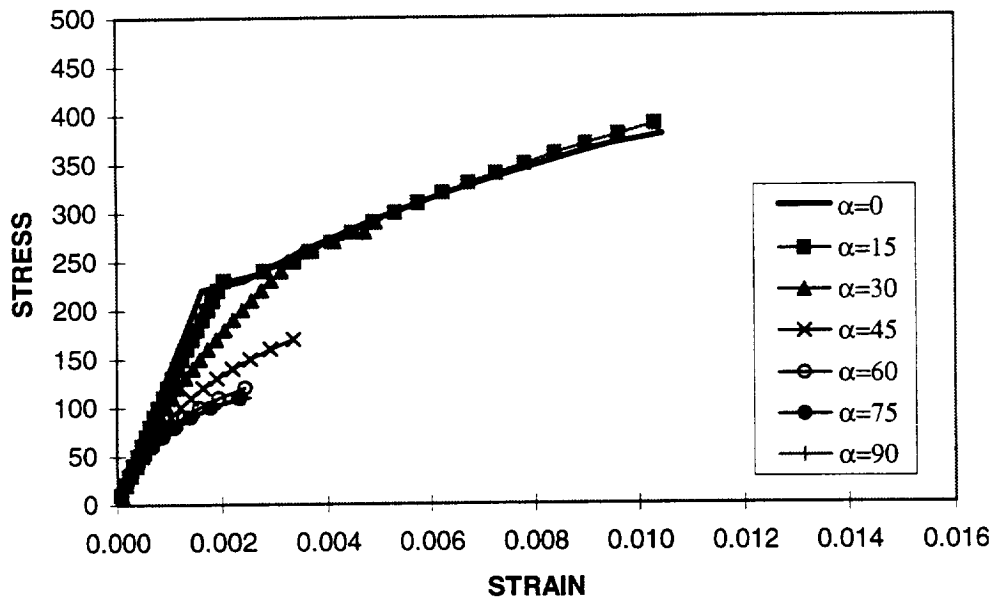


Fig. A1-7 Stress-strain relation of angle ply laminates

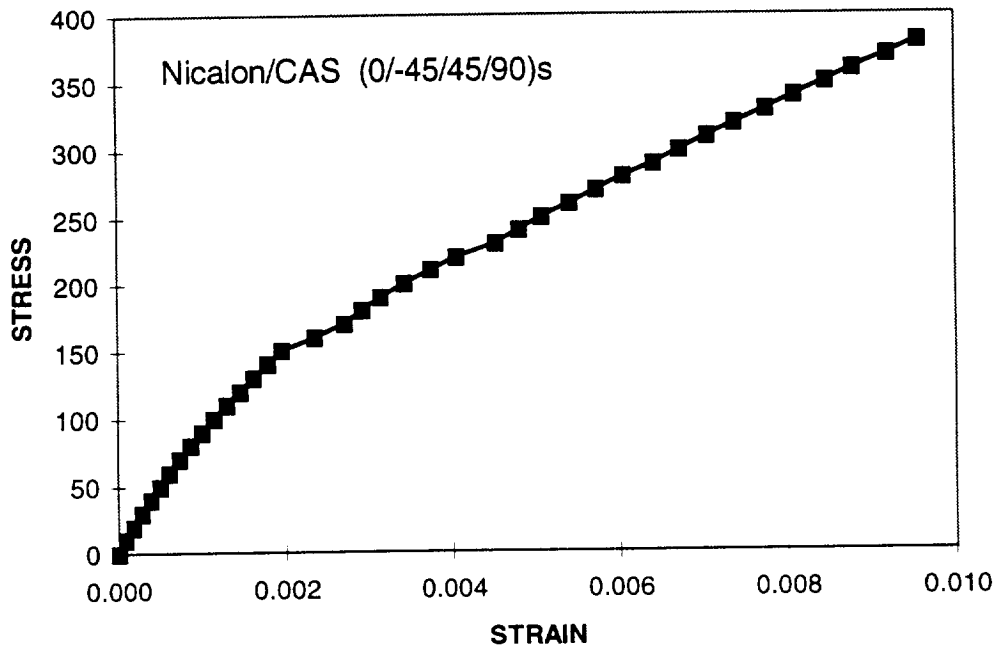


Fig. A1-8 Stress-strain relation of Nicalon/CAS (0/45/-45/90)s laminate under tension

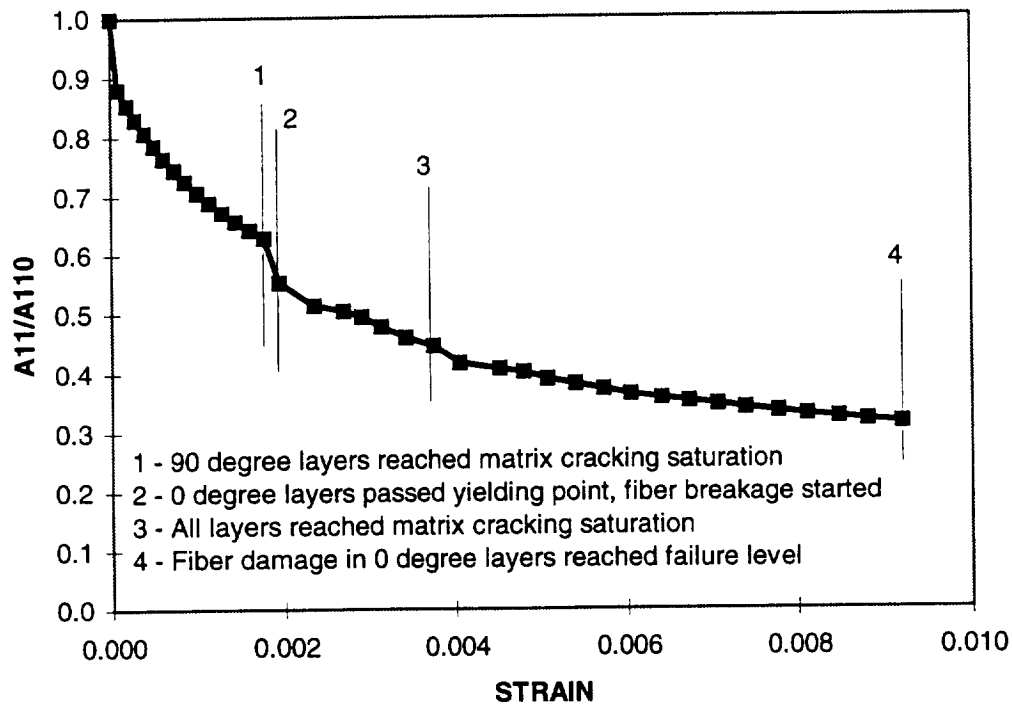


Fig. A1-9 Stiffness reduction of Nicalon/CAS (0/45/-45/90) laminate under tension

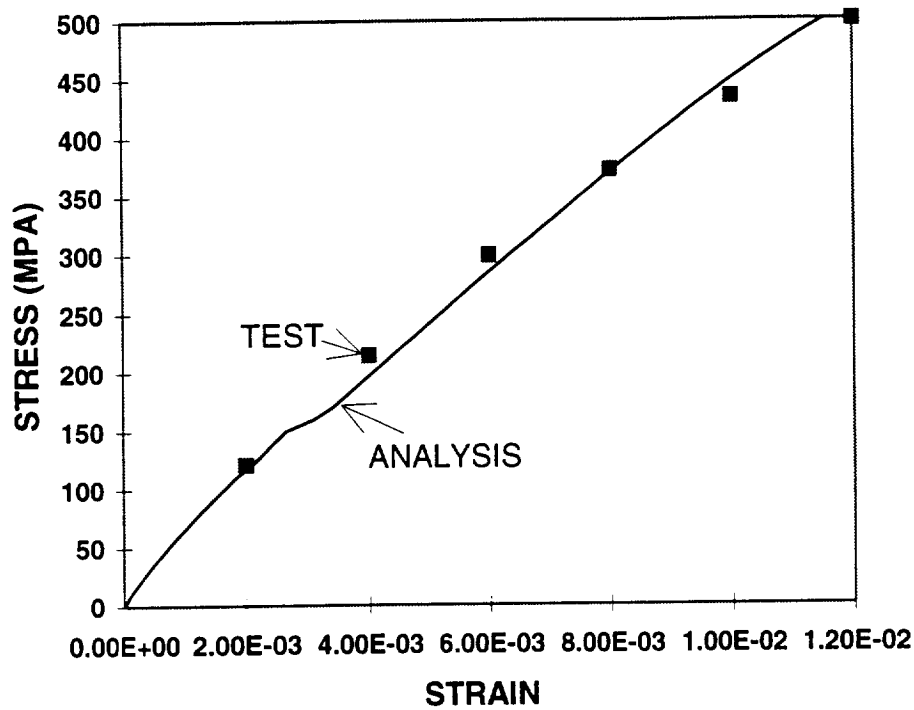


Fig. A1-10 Stress-strain relation of a C/SIC laminate

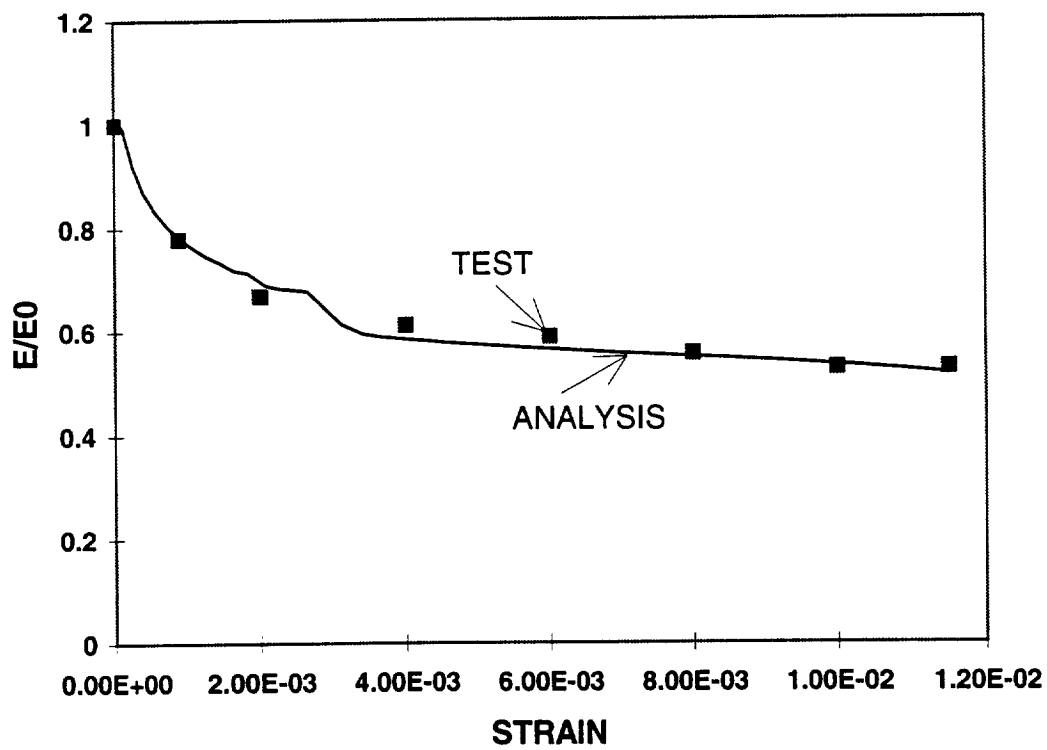


Fig. A1-11 Stiffness reduction of a C/SIC laminate

C/SiC Fatigue Results

A comparison (Figure A-12) is made for analysis and test results for a C/SiC specimen. The testing data is from NASA Marshall Center and the analysis is made by applying the CPFail (Composite Progressive Failure) fatigue analysis. The stress ratio is the ratio of applied maximum stress (σ_{\max}) divided by the static failure stress.

$$\text{Load ratio, } R_m = \frac{\sigma_{\min}}{\sigma_{\max}} = 0.1.$$

The fatigue empirical parameters are:

Walker constants: $A = 3.13\text{E-}15$, $\alpha = 8.4$

Heywood parameters: $p_1 = 0.153 \text{ MPa}$, $p_2 = 2206.9 \text{ MPa}$, $p_3 = 0.0031$

Fatigue coefficient: $\zeta = 0.075$

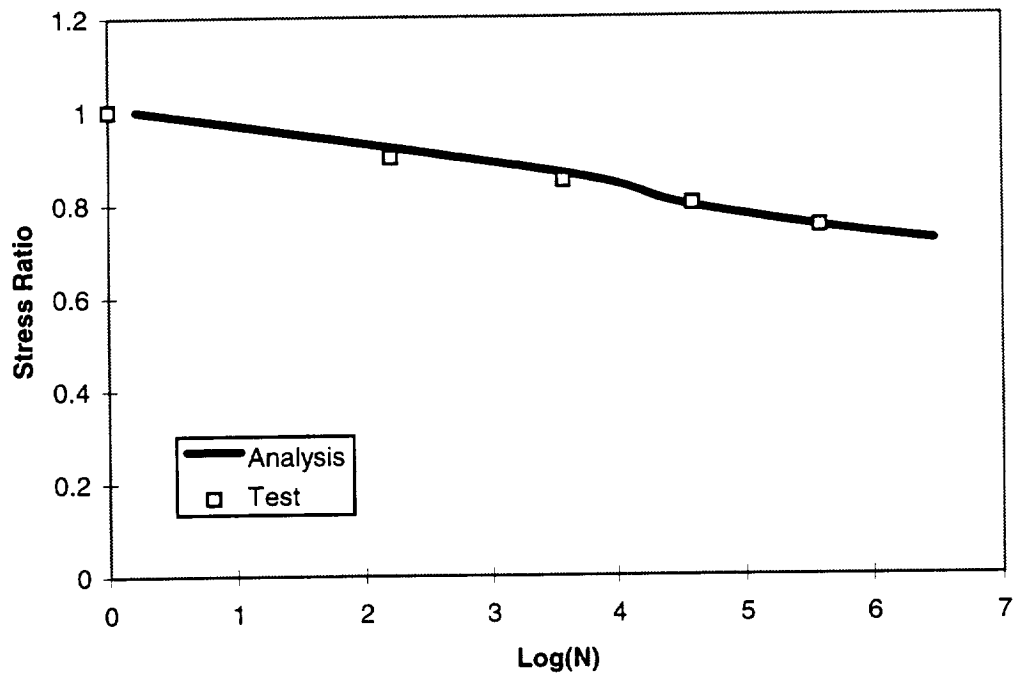


Figure A1-12. C/SiC fatigue result comparison

ABAQUS-CPFail Structural Progressive Failure Analysis

Composite structural progressive failure has been demonstrated by integrating the material damage criteria developed in CPFail, and the ABAQUS's user defined material subroutine and step load increment analysis capability.

A 20-ply tensile test specimen containing a centrally located circular hole is being used to investigate damage progression. The composite laminate is 8-inches long and 1-inch wide with a hole diameter of 0.25 inches. The thickness of each ply is 0.00515 inches, and the laminate stacking sequence is $[0/(+45/-45)_3/90_3]_s$. The specimen is fabricated from T300/1034-C graphite/epoxy. A finite element mesh for the analysis is shown in the following figure. The sides of the laminate are free, and the loaded ends are clamped. Load is introduced by displacing the ends. The lamina properties for this laminate are:

Longitudinal Young's modules	E11 = 21300 ksi
Transverse Young's modules	E22 = 1650 ksi
Poission's ratio	$\nu_{12} = 0.3$
In-plane shear modules	G12 = 897 ksi

The model was created from PATRAN, then translated as an ABAQUS input file. Totally it has 768 elements and 844 nodes, in order to simplify the model, each element has 8 layers with different thicknesses. Using S4R element, each element has 4 integration points. The material property recalculation will be performed in every layer and integration point.

Results are shown in Figures AA-1 ~ AA-10. Figures (a) are for stiffness (E11) damage distribution, and Figures (b) are for stress (S11) distribution. E11 and S11 are in the local fiber directions. Red color shows relatively high value and blue color shows relatively low value. It can be seen that with the loading increase, the stress concentration locations moved out off hole edge, as the material damage developed. This stress release due to local material damage is an important phenomenon in structural failure studies. Figures AA-1 ~ AA-10 are for 0 degree layer behavior. The 45 degree layer behavior are shown in Figures AA-11 and AA-12.

Figure AA-1 (a). Stiffness E11 distribution for 0 degree layer at step 1

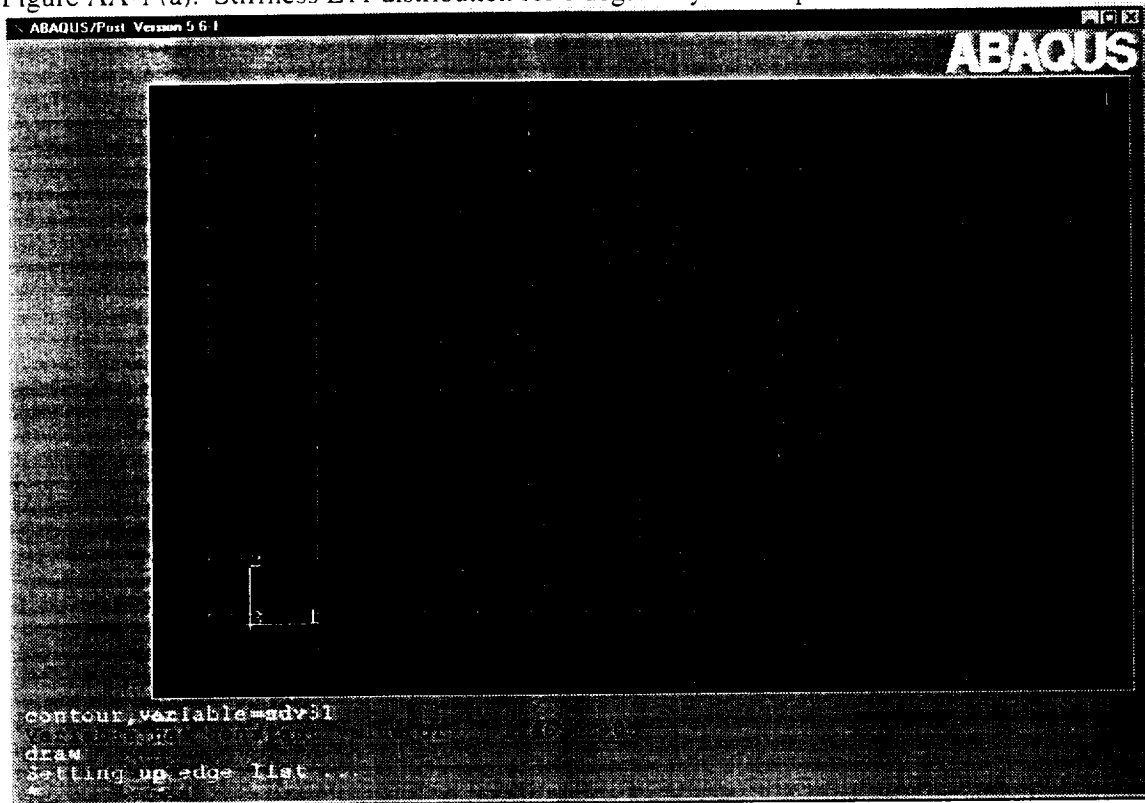


Figure AA-1 (b). Stress S11 distribution for 0 degree layer at step 1

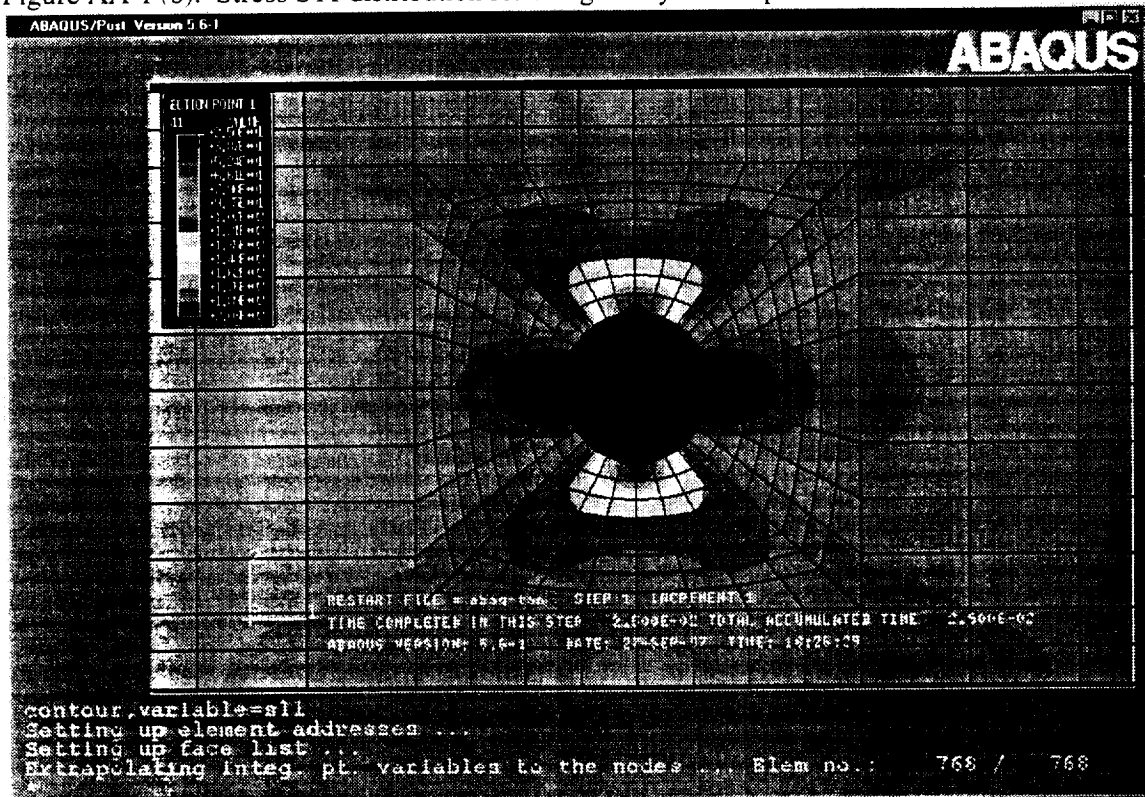


Figure AA-2 (a). Stiffness E11 distribution for 0 degree layer at step 2

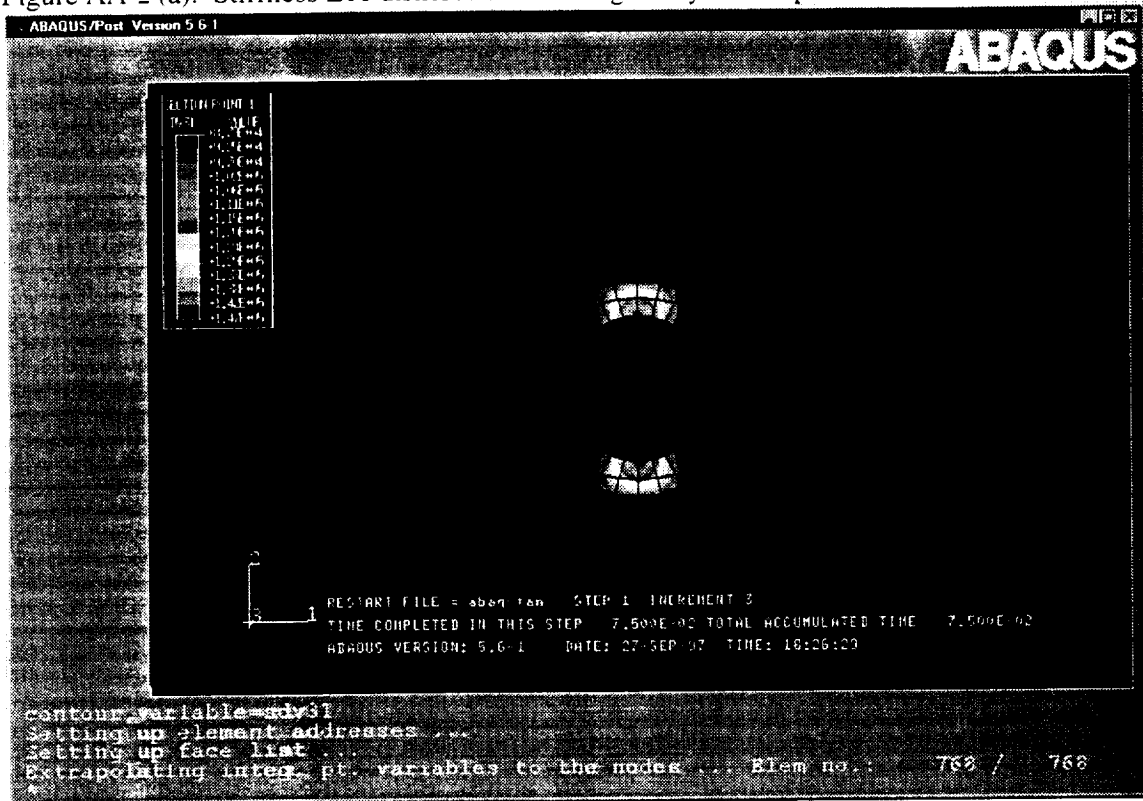


Figure AA-2 (b). Stress S11 distribution for 0 degree layer at step 2

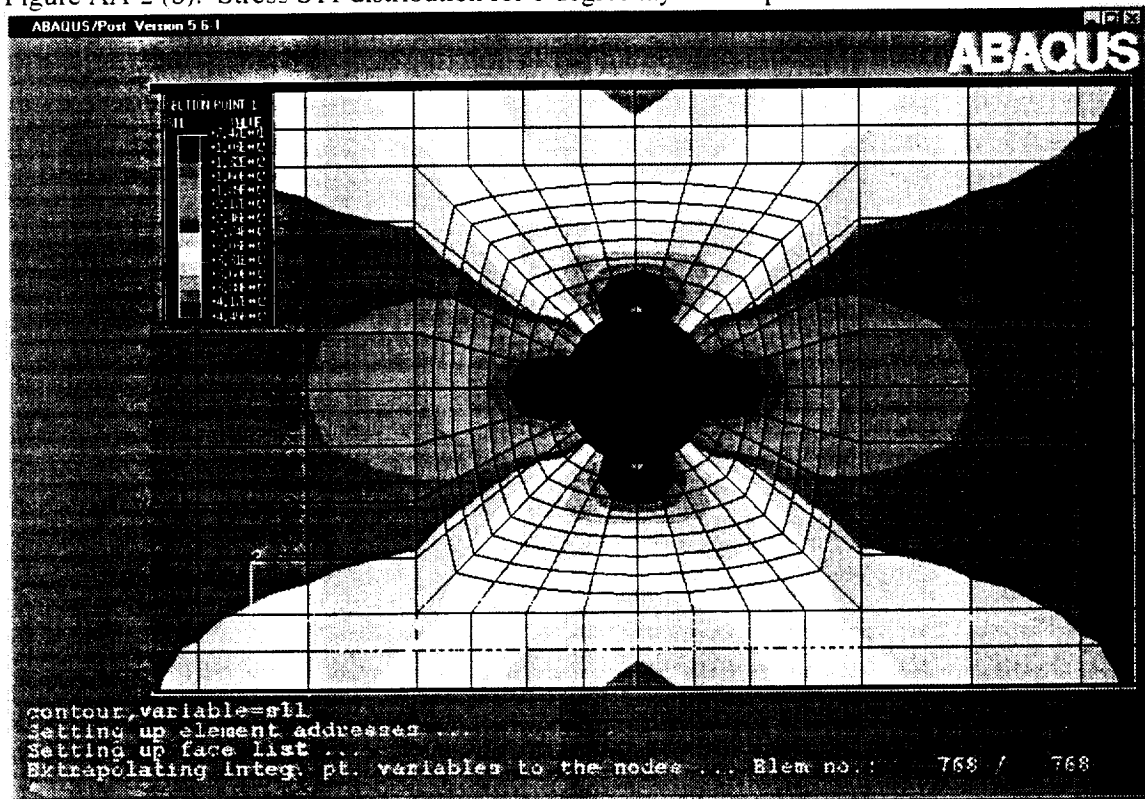


Figure AA-3 (a). Stiffness E11 distribution for 0 degree layer at step 3

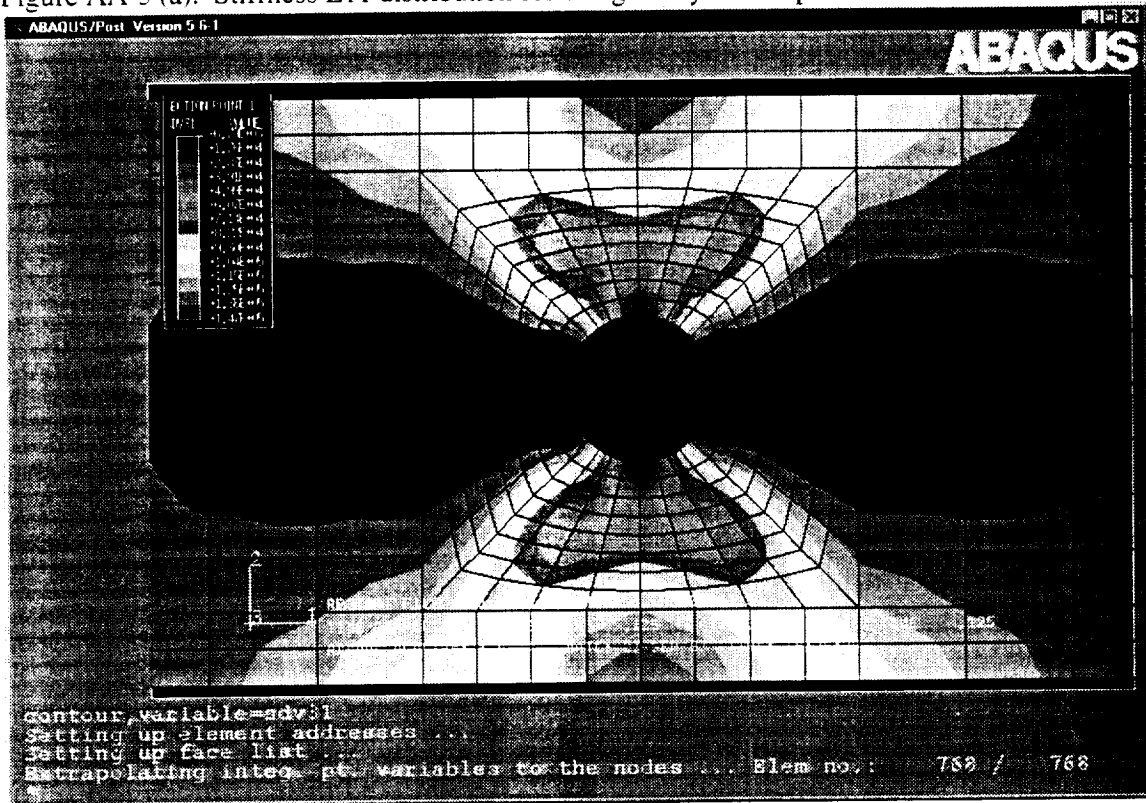


Figure AA-3 (b). Stress S11 distribution for 0 degree layer at step 3.

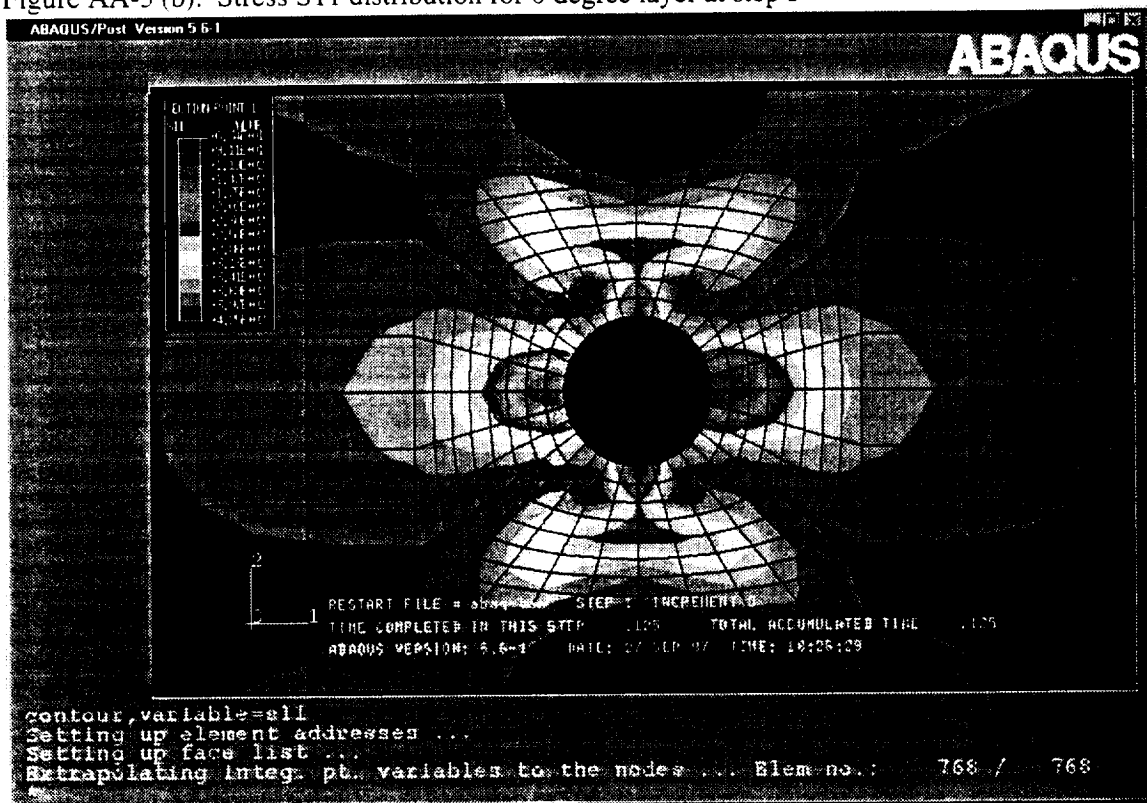


Figure AA-4 (a). Stiffness E11 distribution for 0 degree layer at step 4

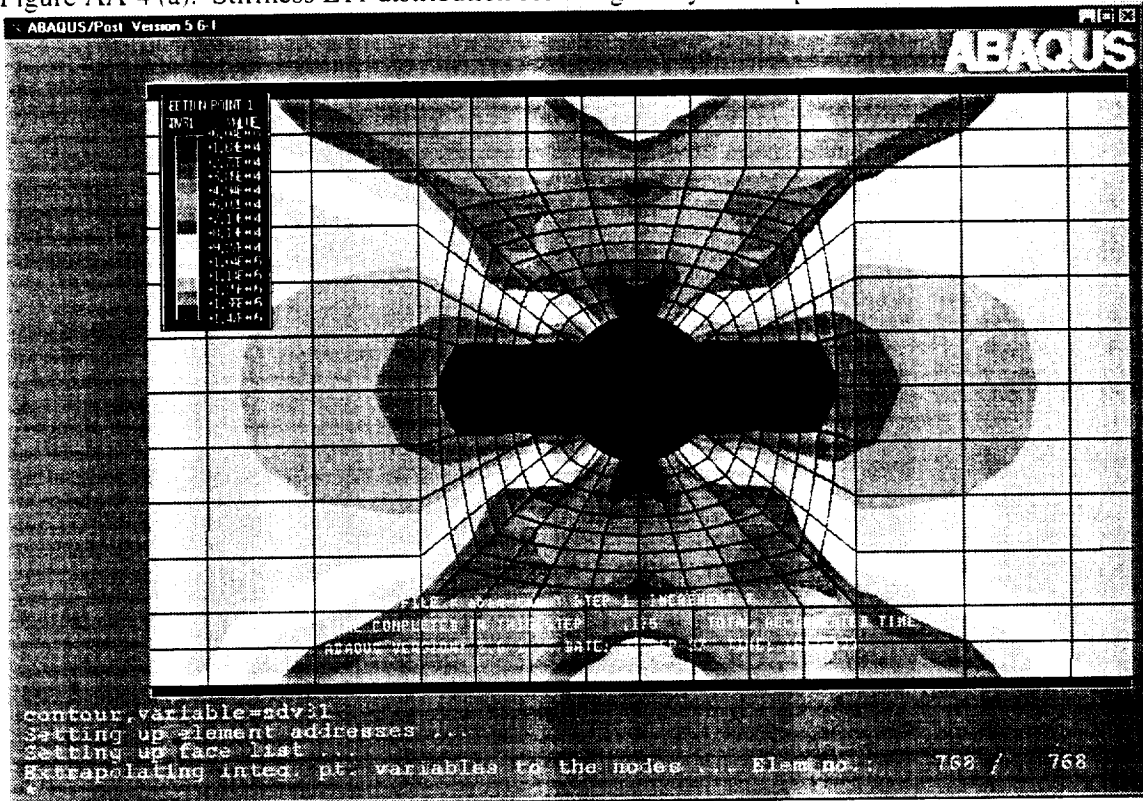


Figure AA-4 (b). Stress S11 distribution for 0 degree layer at step 4

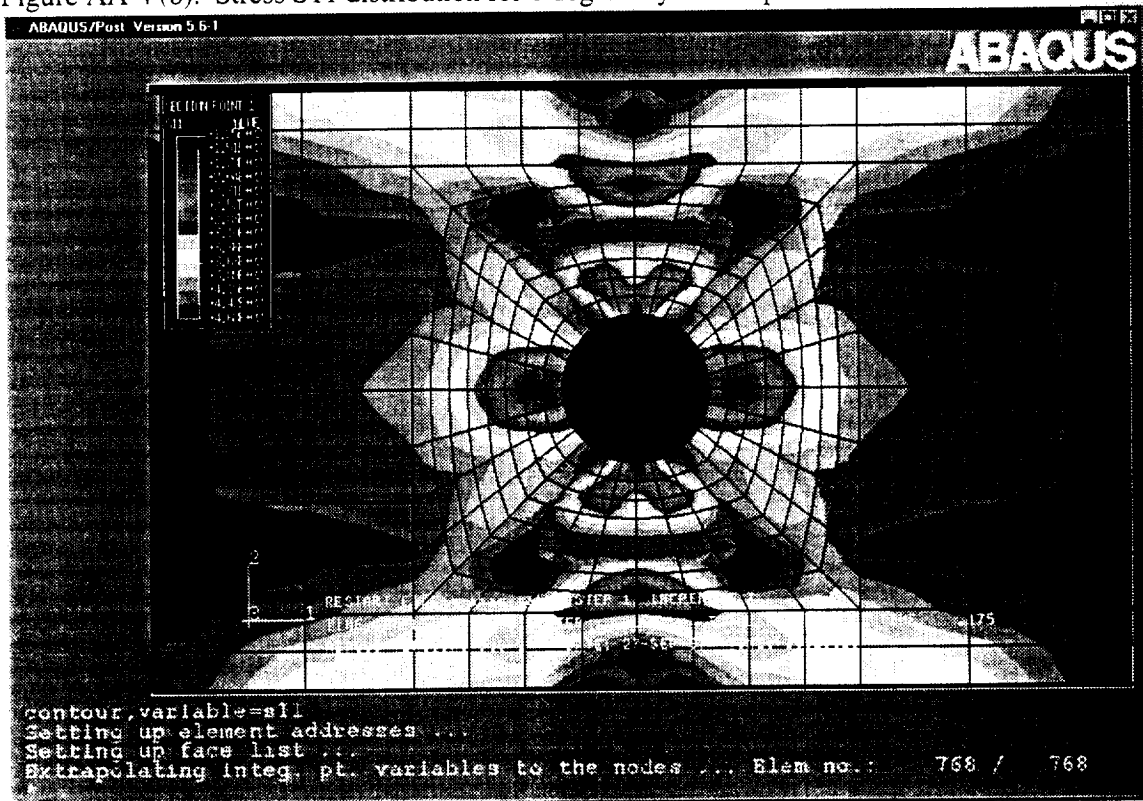


Figure AA-5 (a). Stiffness E11 distribution for 0 degree layer at step 5

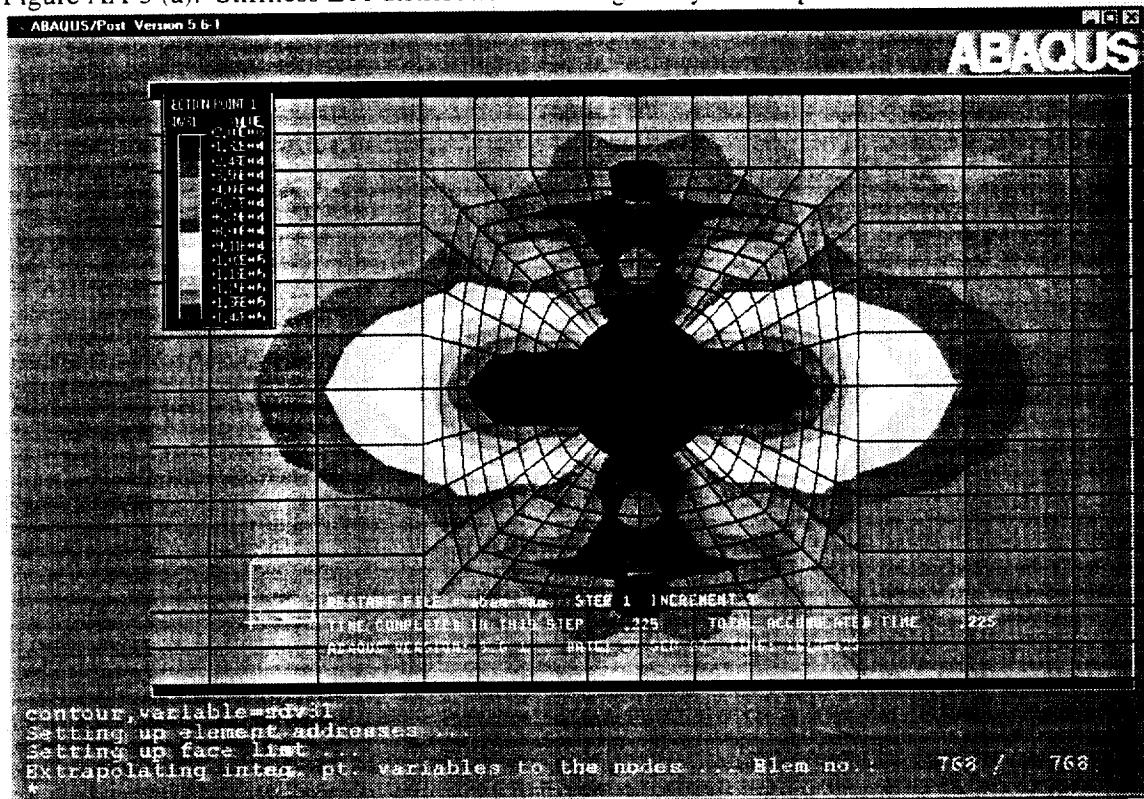


Figure AA-5 (b). Stress S11 distribution for 0 degree layer at step 5

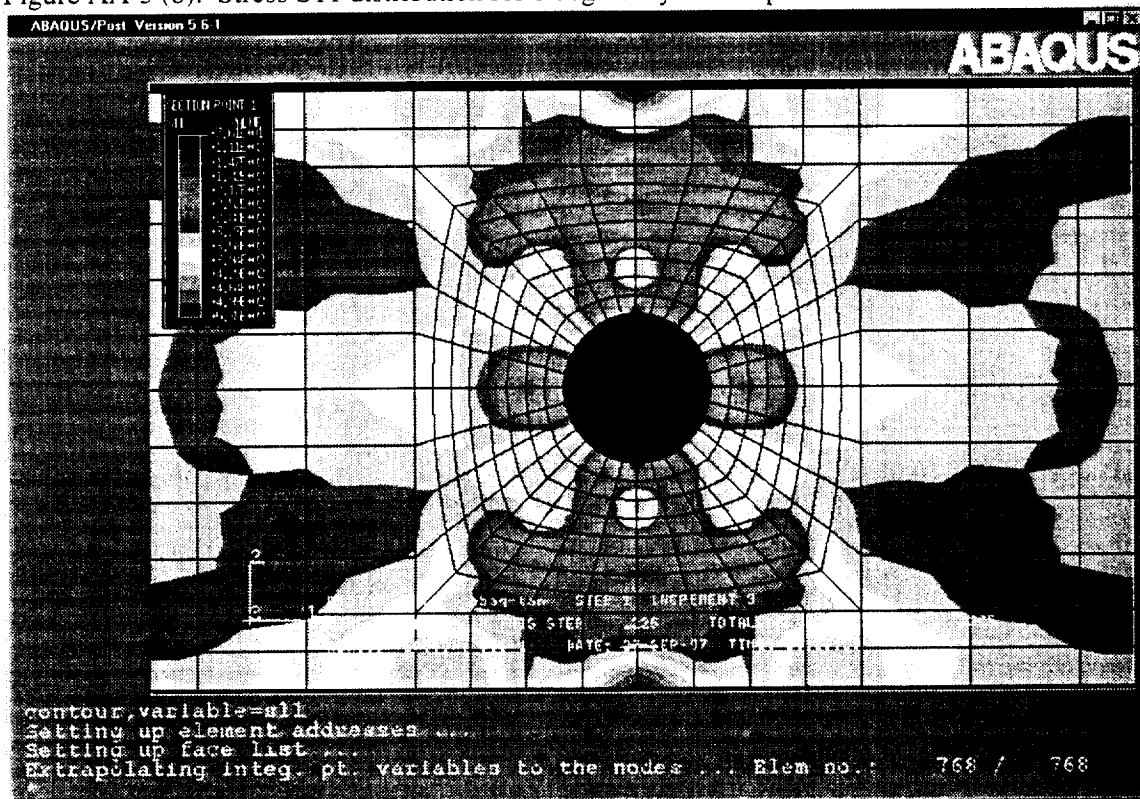


Figure AA-6 (a). Stiffness E11 distribution for 0 degree layer at step 6

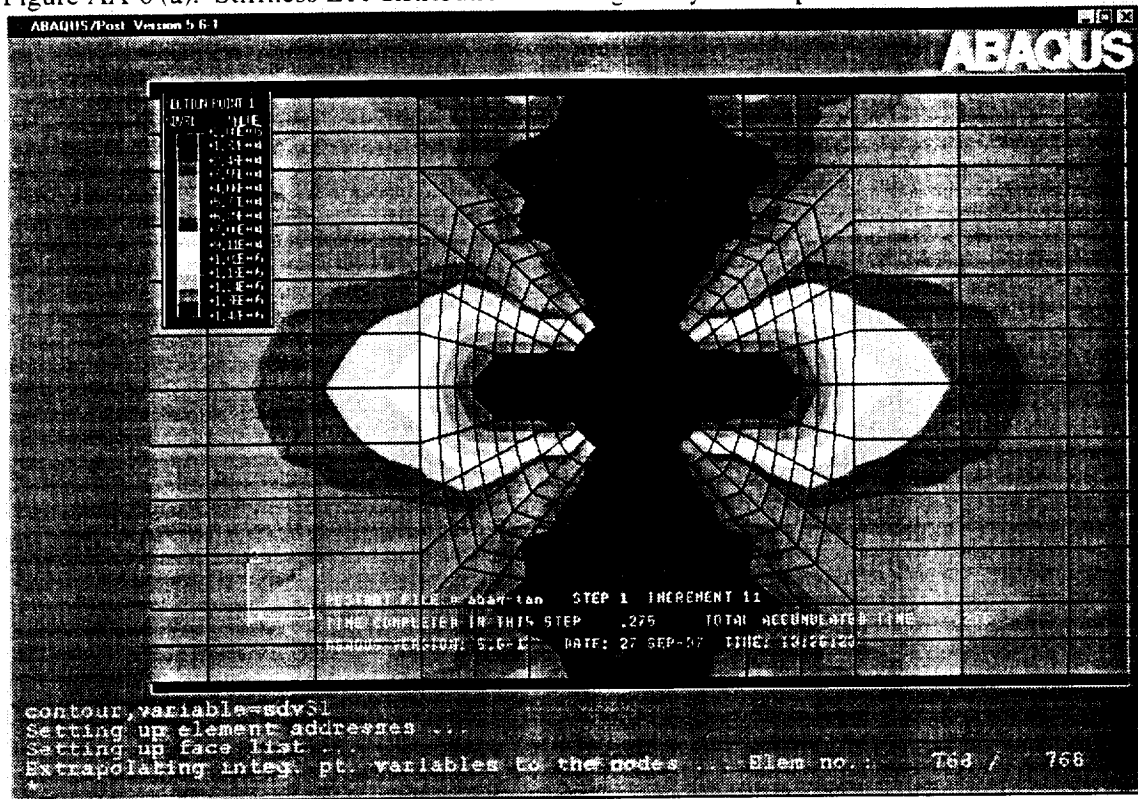


Figure AA-6 (b). Stress S11 distribution for 0 degree layer at step 6

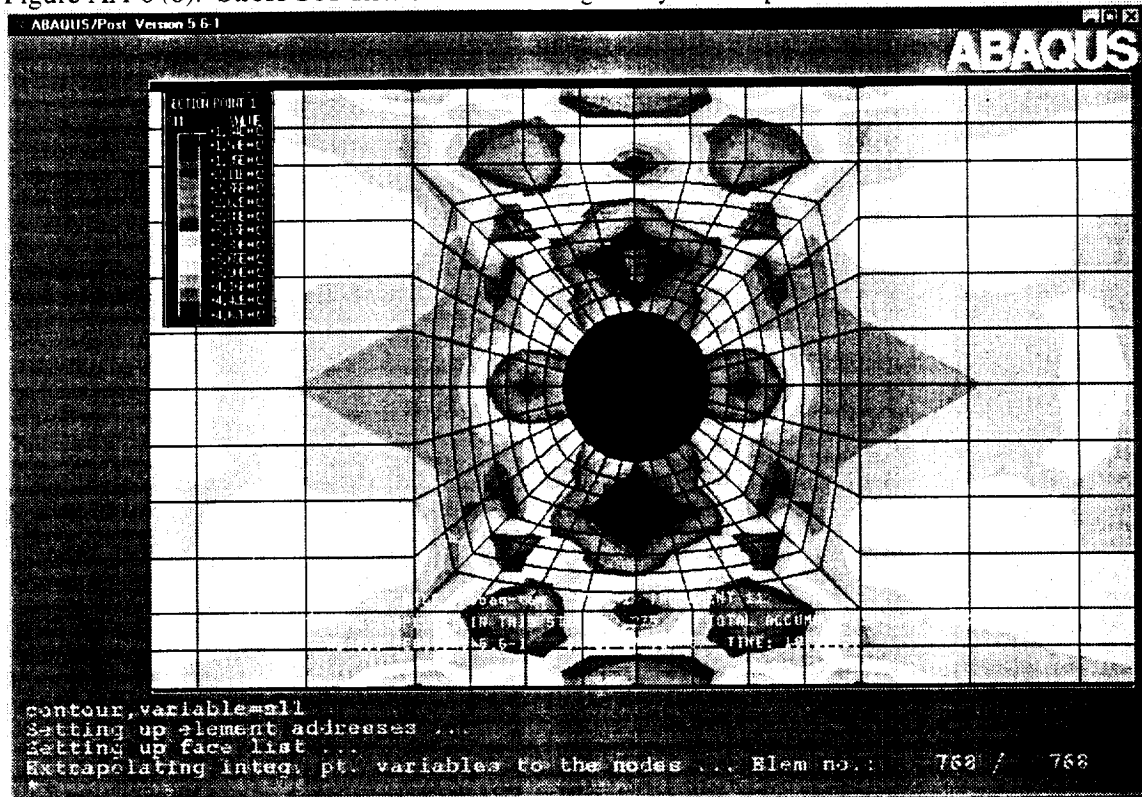


Figure AA-7 (a). Stiffness E11 distribution for 0 degree layer at step 7

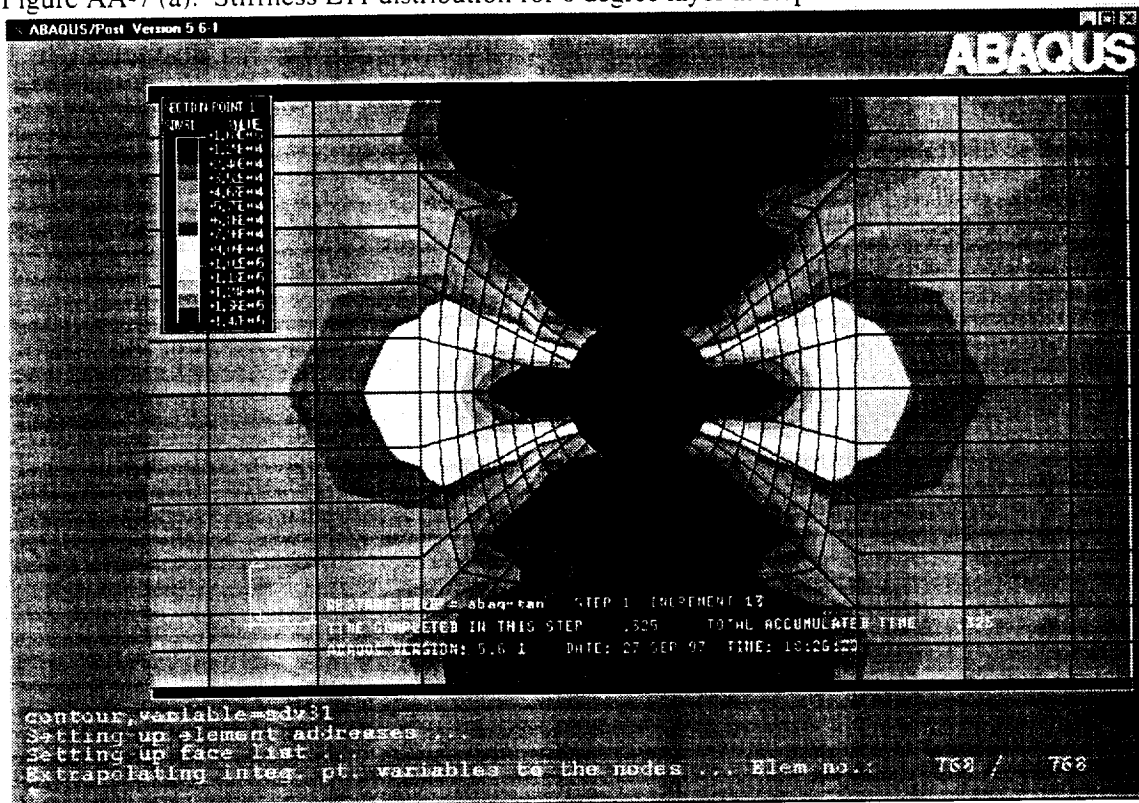


Figure AA-7(b). Stress S11 distribution for 0 degree layer at step 7

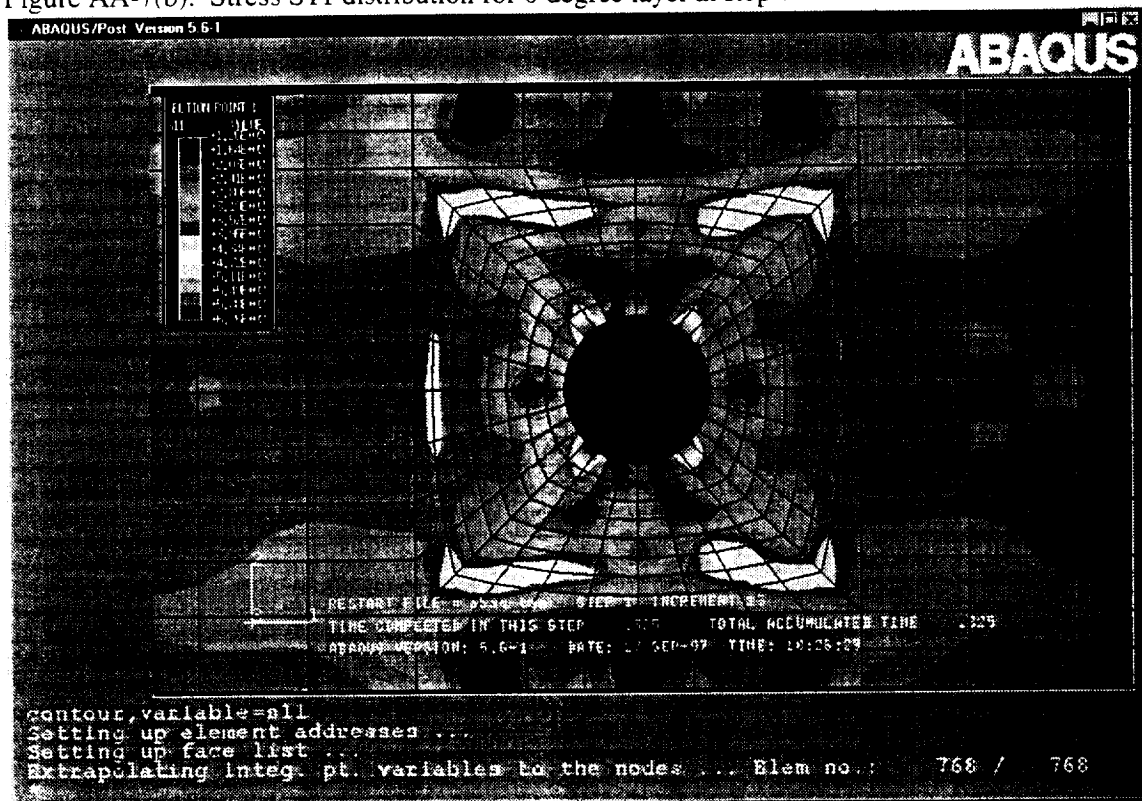


Figure AA-8 (a). Stiffness E11 distribution for 0 degree layer at step 8

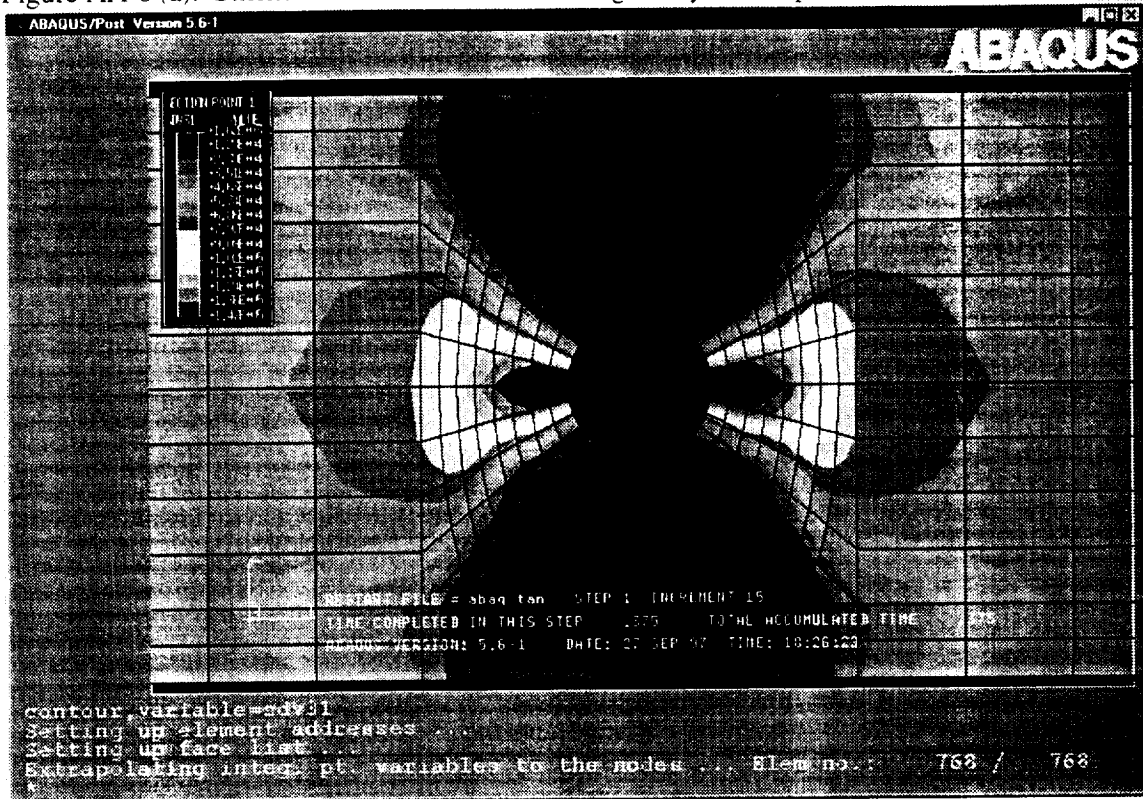


Figure AA-8 (b). Stress S11 distribution for 0 degree layer at step 8

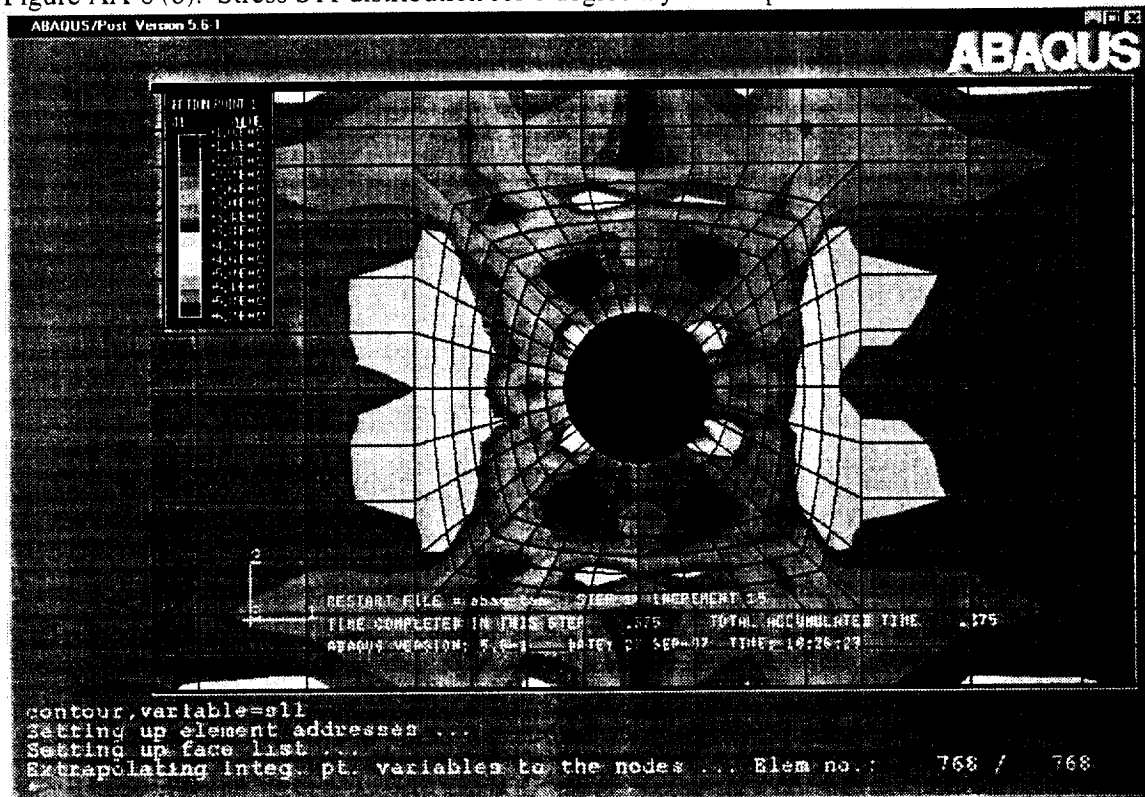


Figure AA-9 (a). Stiffness E11 distribution for 0 degree layer at step 9

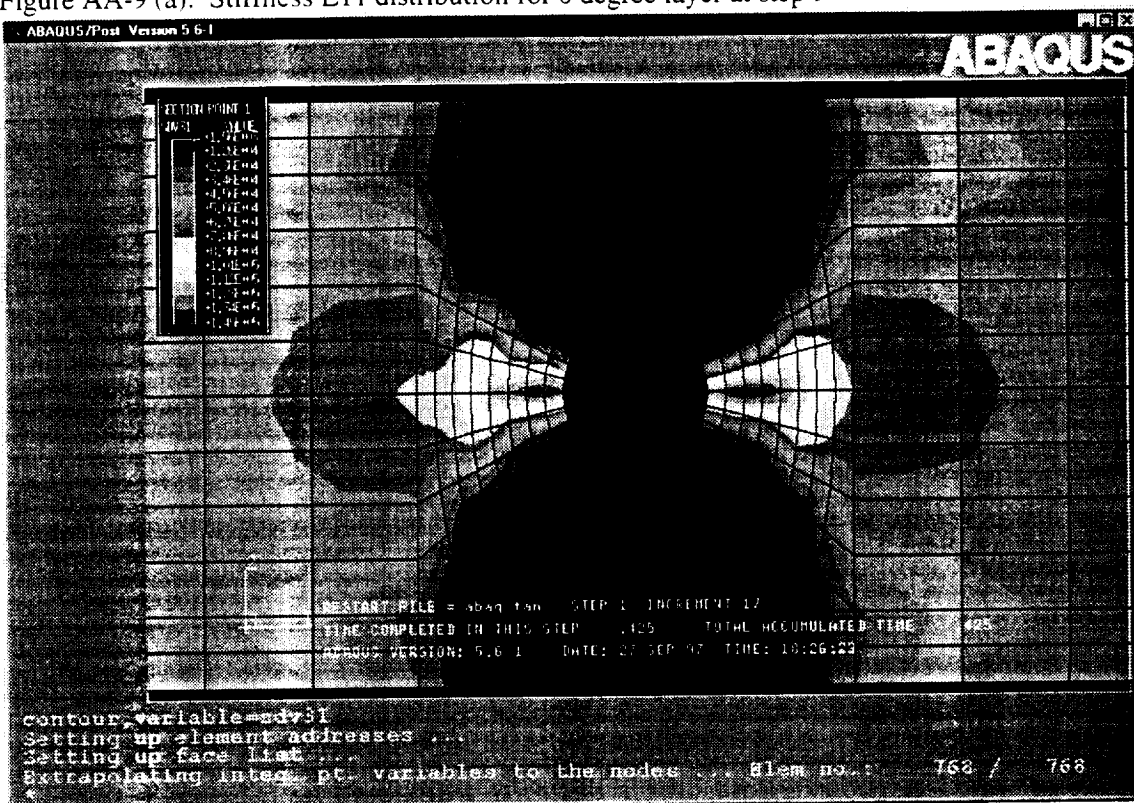


Figure AA-9 (b). Stress S11 distribution for 0 degree layer at step 9

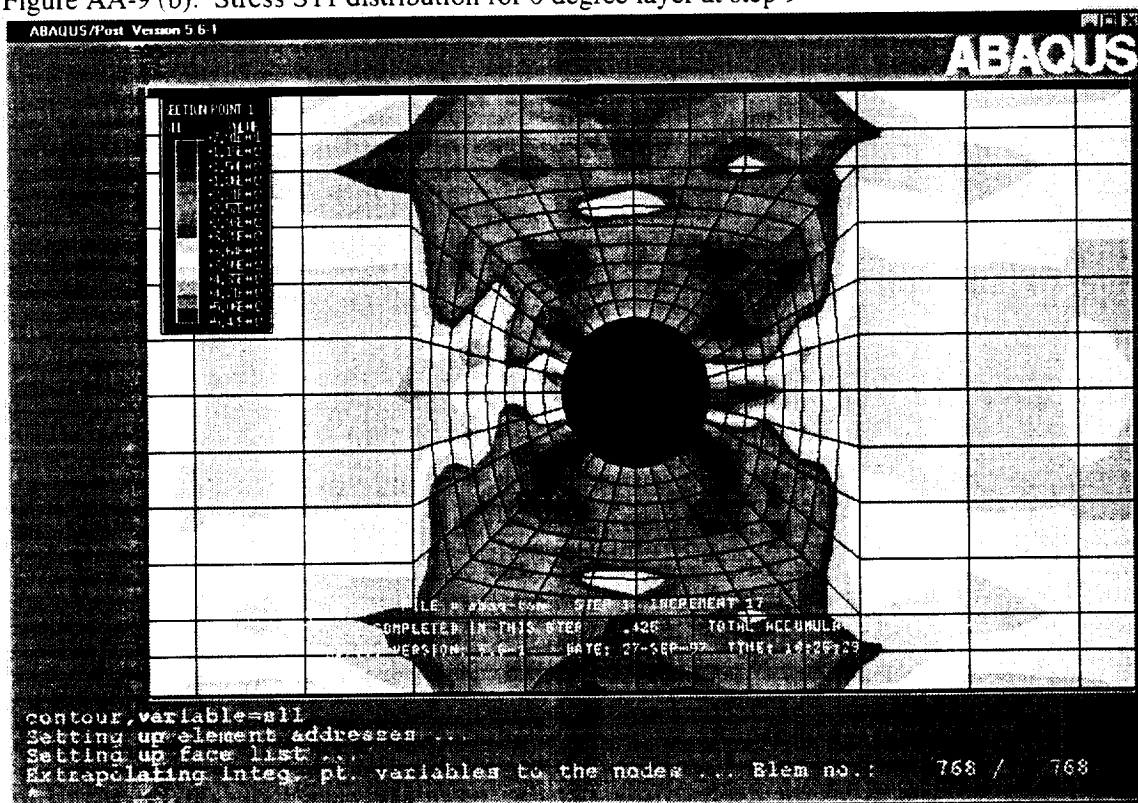


Figure AA-10(a). Stress EFT distribution for a 3-dimensional part.

Figure AA-10 (b) shows a screenshot of the ABAQUS/Post Version 5.6.1 interface. The main window displays a stress S11 distribution for a 0-degree layer at step 10. The visualization is a complex, star-shaped mesh structure with a central circular hole and four smaller holes. The stress distribution is visualized using a color scale from -1.0E+00 to 1.0E+00. The ABAQUS logo is visible in the top right corner. The bottom status bar shows the following information:

```

contour,variable=all
Setting up element addresses ...
Setting up face list
Extrapolating integ. pt. variables to the nodes ... Elem no.: 768 / 768

```

Figure AA-11 (a). Stiffness E11 distribution for 45 degree layer at step 2-3

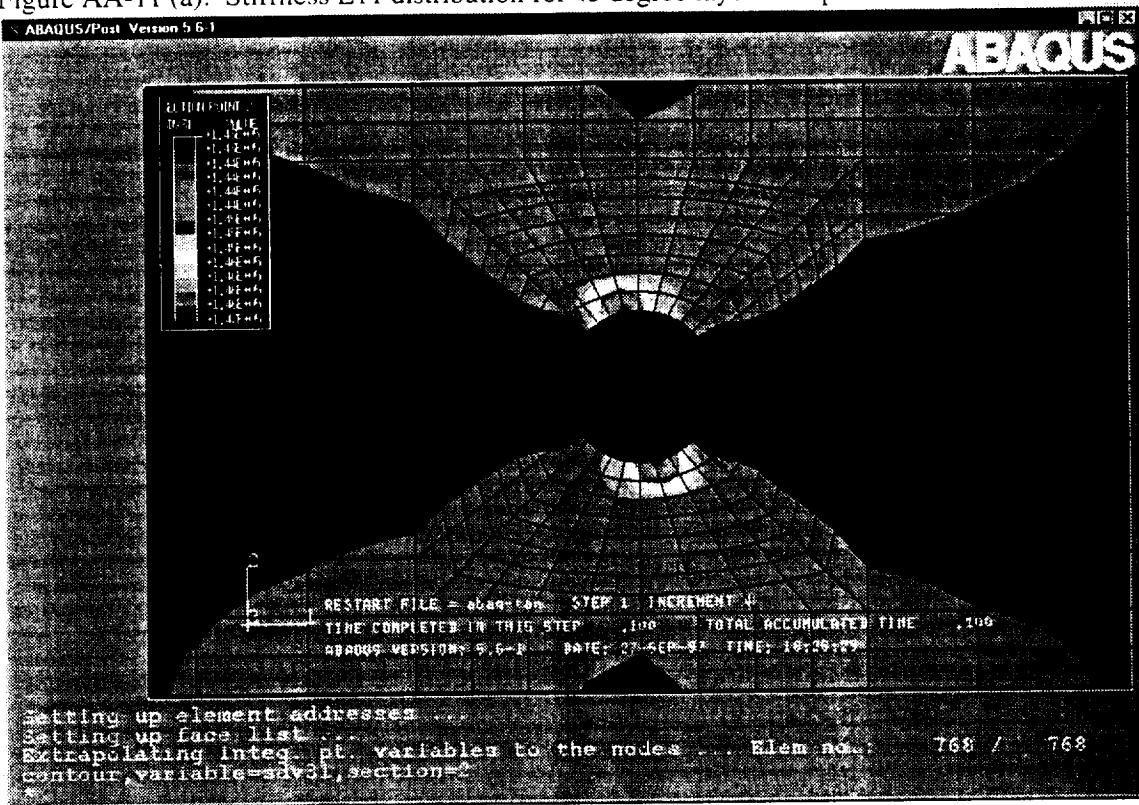


Figure AA-11 (b). Stress S11 distribution for 45 degree layer at step 2-3

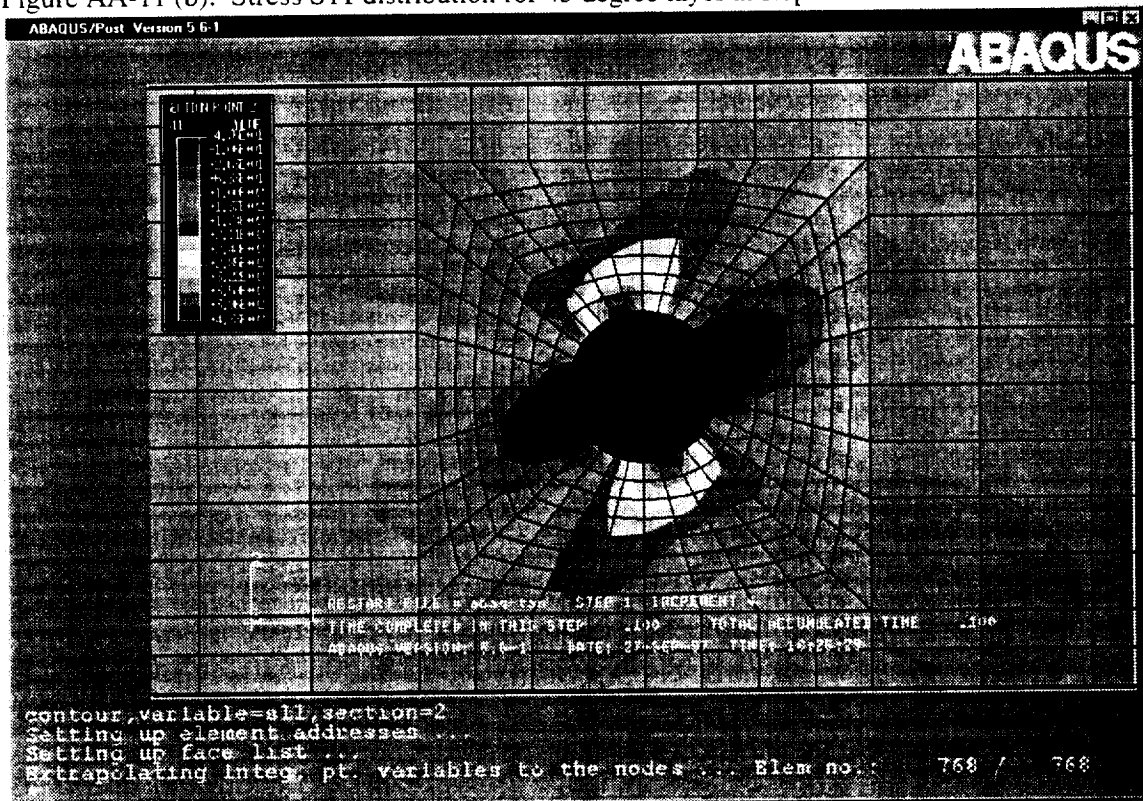
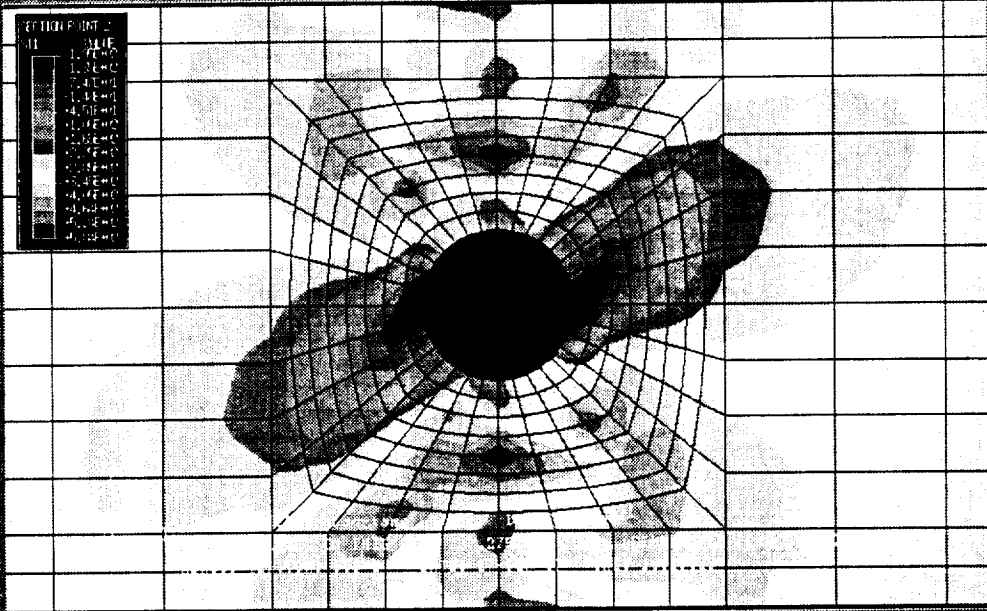


Figure 11-11 shows a screenshot of the ABAQUS/Post Version 5.6-1 interface. The main window displays a 3D finite element model of a mechanical part, likely a bracket or a similar structure, with a color-coded stress distribution. A legend on the left side of the window indicates the color scale for the stress variable, ranging from 0.00e+00 to 1.00e+06. The bottom status bar shows the current view is 'RESTART FILL # 51' and 'STEP 1 INCREMENT 1'. The bottom right corner displays the element count: '768 / 768'.

Figure 7-14-12 (b) Contour plot of the effective stress in the middle section of the part.

ABAQUS/Post Version 5.6-1

ABAQUS

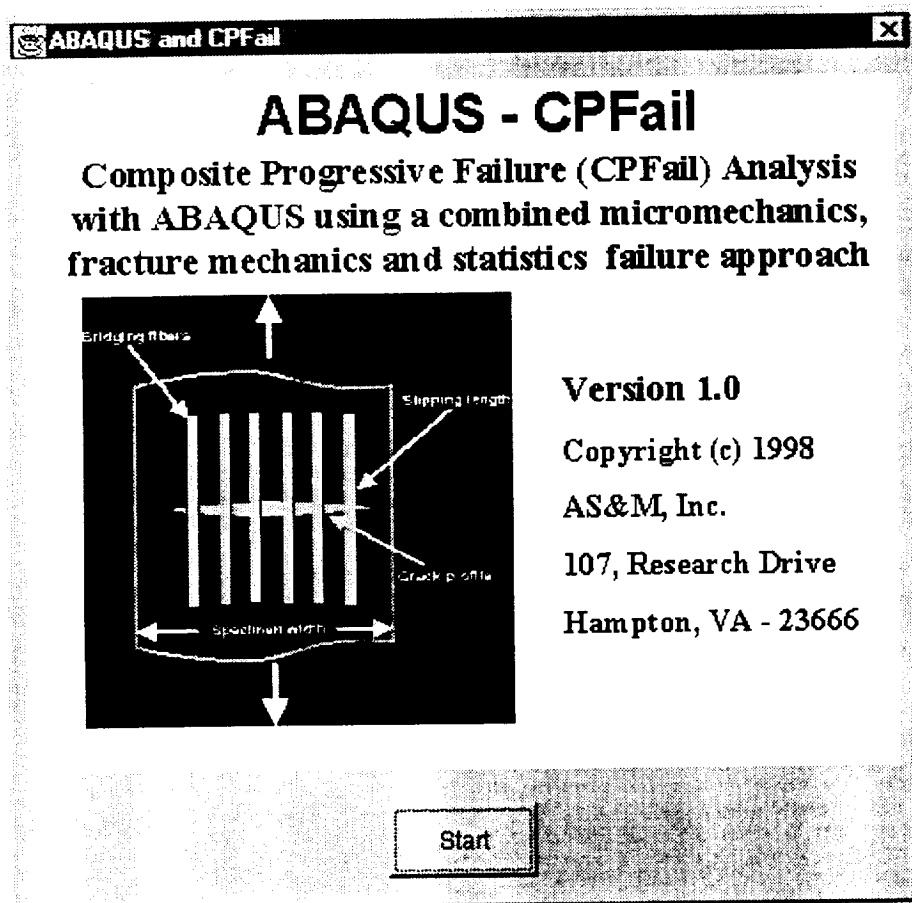


contour, section=2
P1
contour, variable=s11, section=2
Extrapolating integ. pt. variables to the nodes... Elem. no.: 768 / 768

REFERENCES

- 1) Rajiv A. Naik, "A combined Micro-mechanics, Fracture Mechanics, and Statistical Approach for Life Prediction of Ceramic Matrix and Metal Matrix Composites," Final Report, NASA MSFC Phase I SBIR Contract Number NAS8-40505, 1995.
- 2) Budiansky, B., Hutchinson, J. W., and Evans, A.G.; "Matrix Fracture in Fiber-Reinforced Ceramics," Journal of Mechanics and Physics of Solids, Vol.34, No. 2, 1986. pp. 167-189.
- 3) C. E. Harris and D. H. Allen, "A continuum damage model of fatigue-induced damage in laminated composites," SAMPE Journal, July/August 1988, pp. 43-51.
- 4) D. H. Allen, C. E. Harris and S. E. Groves, "A Thermomechanical Constitutive Theory for Elastic Composites with Distributed Damage- Part I and II," International Journal of Solids and Structures, 23(9), 1987, pp. 1301-1338.
- 5) R. Talreja, "Modeling of Damage Development in Composites Using Internal Variables Concepts. Danish Center for Applied Mathematics and Mechanics, The Technical University of Denmark, No. 321, March, 1986.
- 6) A. L. Highsmith and K. L. Reifsnider, "Stiffness Reduction Mechanisms in Composite Laminates," Damage in Composite Materials, ASTM STP 775, K. L. Reifsnider, Ed., ASTM, 1982, pp. 103-177.
- 7) J. Aboudi, "Stiffness Reduction of Cracking Solids," Engineering Fracture Mechanics, Vol. 26, No. 5, 1987, pp. 637-650.
- 8) Reifsnider, K. L., Henneke, E. G., Stinchcomb, W. W., and Duke, J. C.: "Damage Mechanics and NDE of Composite Laminates", Mechanics of Composite Materials. Recent Advances, Pergamon, 1983, pp. 399-420.
- 9) Delale, F., Liaw, B. M., Zhang, S.J., and Zhang, H. Q., "Tensile Behavior of Ceramic Matrix Composites at Room and Elevated Temperatures," Proceedings of the Ninth International Conference on Composite Materials (ICCM/9), Madrid, July 12-16, 1993. pp. 55-62.
- 10) Shuler, S.F., Holmes, J. W., Wu, X. and Roach, D.: "Influence of Loading Frequency on the Room-Temperature Fatigue of a Carbon-Fiber/SiC-Matrix Composite," J. Am.Ceram. Soc. **76** [4] 2327-2336. (1994).
- 11) Sutcu, M., "Weibull Statistics Applied to Fiber Failure in Ceramic Composites and Work of Fracture," Acta Metall., Vol. 37, No. 2, pp. 651-661.

A-2. CPFail-ABAQUS User's Manual



CONTENTS

I. Preface

- I-1) Introduction
- I-2) System requirement
- I-3) User knowledge requirement
- I-4) Installation and execution
- I-5) Composite material degradation capabilities
- I-6) Limitations

II. Getting Started

- II-1) Preparing an initial ABAQUS input file
- II-2) Using GUI to input material parameters and rewrite cpf-1.inp file for CPFail-ABAQUS analysis

III. GUI Help

- III-1) Initial ABAQUS file
- III-2) [File]
- III-3) [Model]
- III-4) [Database]
- III-5) [Options]
- III-6) [Abaqus]
- III-7) How to adjust parameters

IV. Example

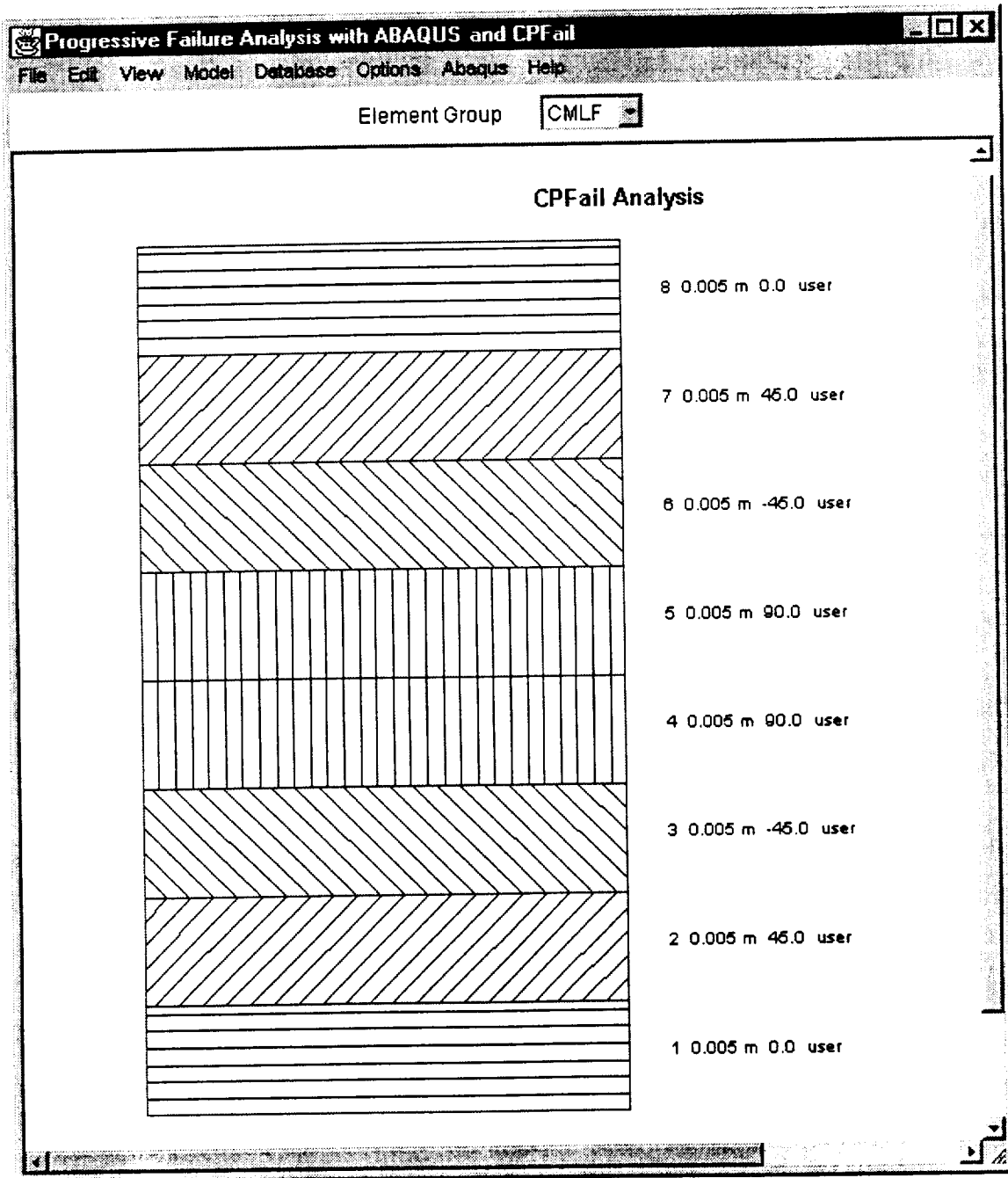
- IV-1) Initial and final ABAQUS runstream files:
- IV-2) Material properties and parameters
- IV-3) Progressive Damage

I. Preface

I-1) Introduction

CPFail is an analysis code for computing the composite material degradation due to tensile damage. CPFail-ABAQUS combines the material degradation with ABAQUS structural analysis through the ABAQUS user defined material entry UMAT. With a step loading procedure, it can show the structural progressive failure process or predict the structure fatigue life.

A user friendly GUI (Graphic User Interface) is designed for helping user to input material information and use ABAQUS's UMAT with CPFail material degradation analysis.



I-2) System requirement

CPFail-ABAQUS can be run on PC or UNIX system. The system requirement for running CPFail-ABAQUS is the same as the requirement for running ABAQUS software.

Since the GUI is written by JAVA, it also requires JDK(Java Development Kit 1.1.3 or higher version) on the PC or UNIX system.

I-3) User knowledge requirement

User should be able to run ABAQUS standard linear static analysis and ABAQUS-POST.

User may not know how to use UMAT in ABAQUS.

User is required to input necessary material information and practice adjusting empirical parameters.

I-4) Installation, path and execution

Installation:

The software is distributed in tar format file `asm.tar`. The file contains all the required data files, source files and java class files required to execute the programs. To install the software components copy change directory to the destination directory and extract the files using the command: `tar -xvf asm.tar`. This command creates the ASM main directory and sub directories to copy the CPFail, MicroTex and ABAQUS interface programs.

The ABAQUS-CPFail is developed using Sun's JDK 1.1.4. To execute these components Java runtime environment of version 1.1.3 or higher is required. Refer the JDK or JRE documentation for installation of Java.

Path:

After extracting the files, the following two path settings have to be completed.

1) The ABAQUS executable file with its path, `xxx/xxx/xxx/abaqus`, has to be set for GUI before running any sample problems. The path, `xxx/xxx/xxx/`, is the path where the ABAQUS software installed and **abaqus** is the ABAQUS executable file for UNIX version. This setting can be made by either manually editing the configuration file (`abaqus.cfg`) or by executing the program and modifying through the GUI using the menu command Configuration under Options menu.

2) In ABAQUS subroutines, SDVIDI and UMAT, user need to set the full path `xxx/xxx/ASM/CPF/ABAQUS-CPF/pathname.dat` by modifying the corresponding line in each subroutine. These two subroutines are included in the file `user-t.rut` under the directory of `xxx/xxx/ASM/CPF/ABAQUS-CPF/`.

Execution:

The executable commands for ABAQUS-CPFail are listed below:

go to directory	<code>/ASM/CPF/ABAQUS-CPF</code>	and
execute	<code>java asm.abaqus.ABApp CMLIFE</code>	command

Original code Files:

The following files are the original code files, user should carry over when change software installation directory, user can also carry over `xxx.cml`, `xxx.ini` and `xxx.inp` files for previous cases:

user-t.rut
/asm/abaqus/*. * (all files)
abcmLife.gif
abaqus.env
abaqus.cfg
CMPly.db
CMMatrix.db
CMFiber.db

I-5) Composite material degradation capabilities

The degradation can be specified to be happened in the whole structure or in the part of the structure with user defined areas (element groups) and layers.

The material degradation analysis will be performed at each element, each layer and each integration point in the selected area. For large scale problem, it may necessary to specify part of the structure to have CPFail degradation analysis.

More than one kind of material can be selected to have material degradation.

I-6) Limitations

Composite material degradation is caused by tensile damage with the effect of shear stress.

Only applicable to ABAQUS shell elements.

Loading formats for static and fatigue progressive failure analyses are pre-designed in GUI, and can not be changed, since the material degradation is loading path dependent. Step linear analysis procedure is used, small load increments are necessary to catch material and structure nonlinear behavior due to damage.

Geometry nonlinearity is not available for this progressive damage analysis.

II. Getting Started

II-1) Preparing an initial ABAQUS input file

- a) The initial ABAQUS input file is an ABAQUS standard static analysis runstream file (for example, cpf-1.ini) for a structure analysis problem with structure FE model, loading and boundary conditions. This file should be pre-tested with no errors in ABAQUS execution. Use ABAQUS shell elements only. The initial file should be written in upcase except the names of linked files. No blank space after comma in the material and section definition lines.
- b) If not whole structure, but only part of the structure or some of the material needs material degradation analysis, specify different element group and material names in these areas.
- c) The materials which will not be degraded in the analysis should be completed in the initial ABAQUS runstream file, cpf-1.ini. GUI will not modify those materials.
- d) The materials which will be degraded in the analysis can have dummy values in the initial file, and should be defined in a normal format, not defined in the format of user defined material. Their true properties and some additional material parameters will be inputted from GUI, and the corresponding ABAQUS user defined material format will be created by GUI.
- e) GUI can modify laminate section and orientation settings in the initial file.

II-2) Using GUI to input material parameters and produce ABAQUS runstream file xxx.inp file for CPFail-ABAQUS analysis

- a) Open CPFail-ABAQUS GUI window
- b) Create material database:
Go to [Database], select [Fiber] and [CPFail matrix] if user wants to input material properties from fiber and matrix properties; select [Ply] if user wants to input ply properties. (The material degradation analysis will be based on fiber and matrix properties, the program will convert ply property to fiber and matrix properties.)
- c) Ply, Fiber or Matrix Database:
 - * Define a new ID or select one from database. (The ID will be used in [Model]/[User Materials]).
 - * Input or modify material properties. Refer to III-3(d) or III-7 for detailed material information.
 - * input a name for user's own remarks
- d) Close [Database] windows. Go to [File]/[New], in the Import Model window select the prepared initial runstream file cpf-1.ini, click [Open]. All material names defined in the initial file will be appeared in GUI.
- e) Go to [Model]/[User Material], select the material name which need the degradation analysis and click [User Defined ?]. Select [Material Type] for material input format, 'Ply' or 'Matrix and Fiber'. Select material ID which is defined in [Database]. Click [Edit] for [Material Special Parameters], refer to III-3(d) and III-7 for the explanations of the special parameters.

f) Lamination modification

The GUI main window shows graphic laminate information for an element group selected in the [Element Group] dialog box. All element groups defined in the initial file, cpf-1.ini, will appear in the dialog box. User can modify the laminate by going to [Model]/[Geometry] and [Model]/[Orientations].

g) Select analysis

- * Go to [Model]/[Control Parameters], fill [Title] with user's remarks, select 'Static Analysis' or 'Fatigue Analysis'.
- * Select damage output location: Element and Layer. This location should have user defined material.
- * Static Analysis: input the number of total analysis steps
- * Fatigue Analysis: input [Load Ratio] and [Maximum Cycles (Log N)]
- * Note: Load values are inputted in the initial file

h) Save file

Go to [File], click [Save] or [Save As] to save the change in a GUI format file, xxx.cml. This file can be reopen later by using [File]/[Open].

I) Execute analysis

Go to [Model]/[Analysis], chose or input a runstream file name, for example cpf-2.inp, in [File name], then click [Save]. The GUI will produce a ABAQUS runstream file, cpf-2.inp (and several internal files), execute cpf-2.inp for the structural analysis defined in cpf-1.ini with CPFail defined material degradation effects.

Check cpf-2.sta, cpf-2.msg or cpf-2.log to find out if the ABAQUS analysis finished or not.

J) Results

- * Go to [View]
 - Open 'strain-stress' for strain-stress at each steps (no last step) for static analysis ; or at each Log(N) cycles for fatigue analysis, at selected output location
 - Open 'Damage' for material degradation information at selected output location
- * Use ABAQUS-POST to display stress, strain, displacement and other results.
- * Use ABAQUS-POST to display reduced material properties:
 - SDV31=E11
 - SDV32=E22
 - SDV34=G12
 - where E11, E22 and G12 are the ply Young's modules in the ply local coordinates.
- * For fatigue analysis, the number of Log N is corresponding to (step -3). So, to display results at cycle, Log N = 2, the corresponding ABAQUS step = 2+3 = 5.

k) Structural fatigue S-N curve

It should be pointed out that in the fatigue analysis the step number is for loading cycle, Log(N). In each fatigue analysis case, load will be a constant and the Log(N) of final fatigue cycle will be computed. Thus for one load level, it can only produce one point on the curve (S-N) of Maximum stress verses Fatigue cycle Log(N). In order to have a complete S-N curve, several load levels should be executed. The fatigue failure (final) cycle, Log(N) is printed in the stress-strain result file (s-s.dat) and can be read from [View] window.

III. GUI Help

III-1) Initial ABAQUS file

CPFail-ABAQUS GUI (Graphic User Interface) is designed to help user to input material parameters and use the proper UMAT entry and analysis steps in ABAQUS for progressive failure analysis. This GUI does not have the functions for structural modeling. So the structure model including element mesh, material, shell section, boundary, constraints and loading conditions should be pre-prepared in a file called initial file. The GUI will copy all structure model and material information from the initial file and can make changes only on (1) the material part to form user defined material entries, (2) shell sections and (3) loading format. The laminate which contains the user defined materials should be defined by using '*SHELL SECTION' not '*SHELL GENERAL SECTION'. GUI will not change the material properties for which are not selected as user defined materials.

GUI will not debug the errors in the initial file.

In the initial file all the units should be in SI units. GUI will allow user to input material properties in US unit, but will convert them to SI units in ABAQUS runstream files. So, all ABAQUS results will also be read in SI units.

III-2) [File]

- (a) [New]: Open a case from an initial xxx.inp ABAQUS file, for example, cpf.ini.
- (b) [Open]: Open a case from a previously saved xxx.cml GUI file
- (c) [Save]: Save the current modified case to the original xxx.cml file
- (d) [Save As]: Save the current case to a new GUI file, for example, xxx-1.cml
- (e) [Print]: Print out the lamination figure in the window
- (f) [Exit]: Close GUI

III-3) [View]

- (a) [Strain-Stress]: View file 's-s.dat'. This file presents strain vs. stress at each load step (no last step) for static analysis; or Log(N) vs. maximum stress for fatigue analysis.
- (b) [Damage]: View file 'out.volume'. This file presents material damage information by showing the remaining fiber volume fraction and matrix stiffness ratio.
- (c) [Text File]: View text files

III-4) [Model]

- (a) [Geometry]:

Modify section (lamination) properties. Suggest to choose '1' integration point to reduce computation time.

(b) [Control Parameters]:

- * Select damage output location: Element and Layer. Only one location for a structural analysis. Stress-strain, remaining fiber volume fraction and matrix stiffness ratio will be written out at this location. Whole structure damage status can be viewed by showing total stiffness distribution using ABAQUS-POST.
- * Select static analysis steps. Increment load value = load/steps.
- * Select fatigue analysis load factor and maximum loading cycles, Log(N)
Load factor = Minimum load / Maximum load in a loading cycle.
- * For both static and fatigue analyses load values are inputted from the initial file.

(c) [User Materials]

Select material name which will have degradation analysis

- * Material Name: (should be in upcase) All material names defined in the initial file will be in the list. Also user can create new material name.
Select the materials which will have degradation analysis, click [User Defined], (one by one).
- * Material Type: Select material property input format
'Matrix and Fiber' --- input material properties from matrix and fiber properties
'Ply' --- input composite ply properties
- * --- Material ID: Select material ID from the list which is created in [Database]
- * Material Special Parameters: Empirical parameters, see (d) for details.
- * Create NEW or DELETE existing materials in xxx.inp file.

(d) [Material Special Parameters]:

Material special parameters are designed for user to adjust material or laminate behavior due to damage, fatigue, delamination, material nonlinearity or plasticity.

- * Matrix Damage Limit: matrix modules remaining ratio after matrix cracking, E_m / E_{m0} .
- * Nonlinear Coefficient: Adjust for material nonlinear behavior due to yielding, plasticity, damage or delamination. The nonlinear effect is bigger for larger value, for example, 0.01 (linear) ~ 2.4 (nonlinear).
- * Process Temperature: Composite laminate manufacture curing temperature.
- * Walker Constant C and n: from Walker's fatigue statistic equation for matrix fatigue cracking. Suggested value: C= 3.13E-15 and n=8.4

$$\frac{da}{dN} = CK_m^n$$

- * Fatigue Coefficient: Empirical fatigue parameter. A smaller value corresponds for smaller damage and longer life. A positive value of (0.01 ~ 3.0).
- * Fatigue Final Strain: The fatigue failure criteria to define fatigue life cycles. User assumes that the structure failed as the strain (ϵ_{ll}) at the monitor point reaches this value.

- * Heywood Parameters p1 ~ p3: from Heywood's fatigue statistic equation for fiber strength fatigue reduction. The effects of p1 ~ p3 are shown in the following figure. Suggest value: $p_1 = 0.153$ MPa, $p_2 = 2206.9$ MPa, $p_3 = 0.0031$

$$\sigma_a = \pm \sigma_t \left[1 - \sigma_m / \sigma_t \right] \left[A_0 + \gamma(1 - A_0) \right]$$

$$A_0 = \left[1 + \frac{p_3 \bar{n}^4}{1 + \sigma_t / p_1} \right] \frac{1}{1 + p_3 \bar{n}^4},$$

$$\gamma = \frac{\sigma_m}{\sigma_t} \frac{1}{1 + (\sigma_t \bar{n} / p_2)^4},$$

$$\bar{n} = \text{Log}(N)$$

(e) [Orientations]

Define new or modify old orientations according to ABAQUS format

(f) [Analyze]

- * If the case is started from a previous xxx.cml file (when user opened the case), GUI will ask if user wants save the change (to xxx.cml).
- * User should then give a runstream xxx.inp file name, for example, cpf-2.inp. User can create a new name or select one from the window list and overwrite it.
- * Click [Save], GUI will create the runstream file and execute it.

III-4) [Database]

(a) User can build new or modify old matrix, fiber and ply property databases.

(b) Matrix Critical Stress Intensity Factor, Kmc, (0.1 ~ 5.0)

(c) Weibull Modules (M) and Mean Fiber Strength (σ_0)

Empirical parameters from modified Weibull fiber damage statistic equation, M=10 and $\sigma_0 = 388.0$ MPa are default values.

$$P_f = 1 - \exp \left[\frac{-4\pi a l_s}{k_0} \left(\frac{T_z}{\sigma_0} \right)^M \right]$$

(d) Friction Coefficient

Empirical parameter of matrix-fiber integration (0.01 ~ 1.0)

III-5) [Options]

(a) [Units]:

- * Let user choose SI or US units.
- * All values will be changed according to unit change in GUI and will be written in to ABAQUS runstream file.
- * for running a analysis, user should choose the unit which was used in structural modeling, since GUI will not change any value in model.

- * For building or modifying database, user can choose any units.

(b) [Configuration]:

User should set the path to indicate where the file abaqus.exe exists, for example,
C:\ABAQUS\5_6_1\abaqus.exe

III-6) [Abaqus]

Execute an ABAQUS runstream without GUI modification.

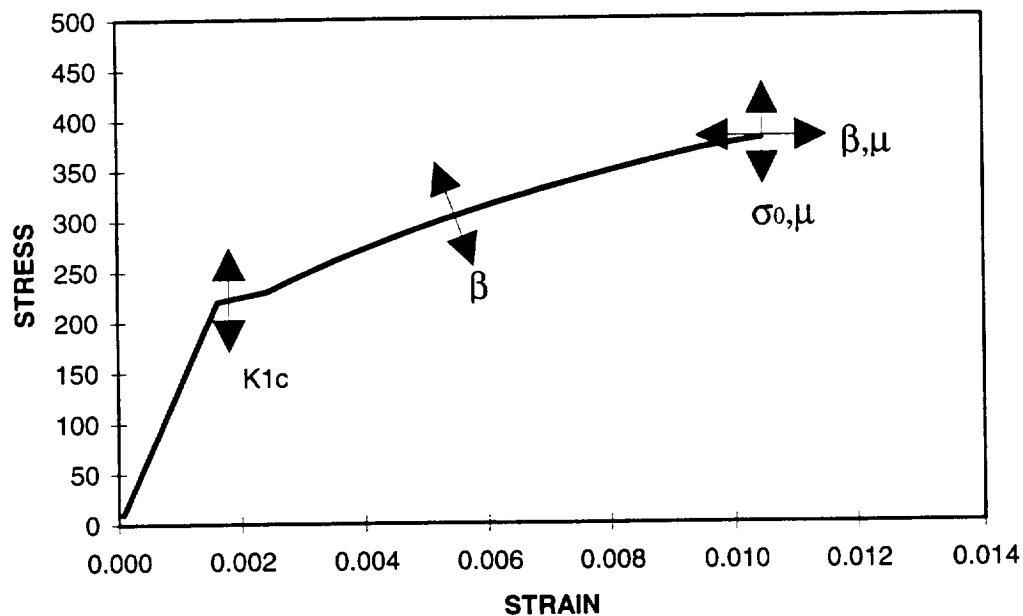
This is an option to let user to rerun a final xxx.inp file or a manually modified xxx.inp file.

III-7) How to adjust parameters

In order to make this material degradation analysis tool more general to composite materials, several empirical parameters need to be adjusted according to different materials or different damage conditions. Default values provide a base for the parameter adjustments, so they should be kept for reference. The following figures shown the effects of parameters on material or structural behaviors.

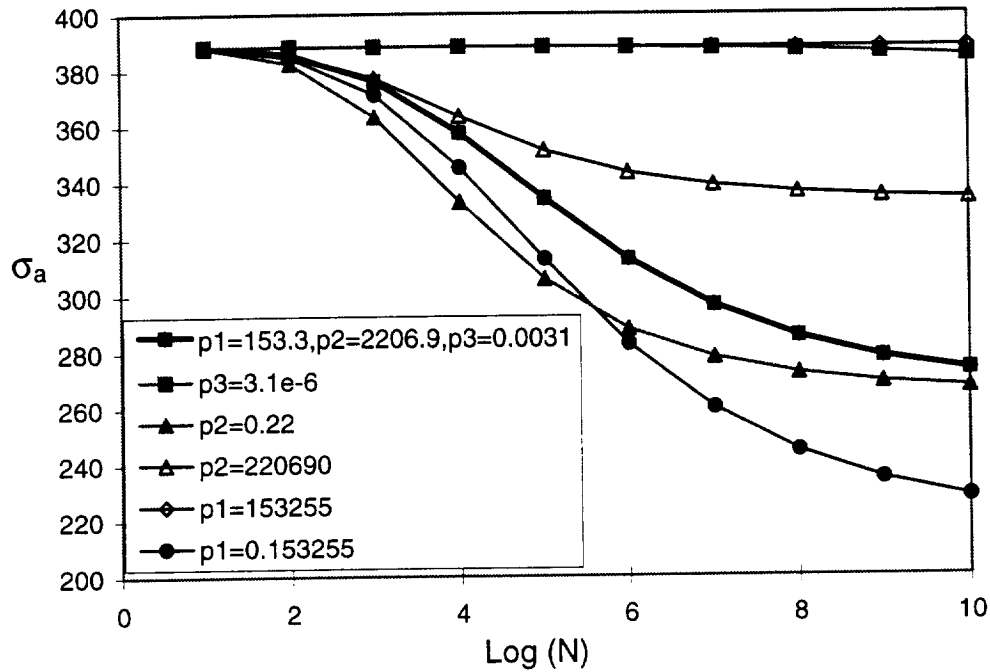
(a) Static analysis:

- * K_{mc} --- Matrix critical stress intensity factor. A larger value will move up 'yielding point'
- * β --- Nonlinear coefficient (0.01 ~ 10). A larger value will have stronger nonlinear behavior.
- * σ_0 --- Mean fiber strength. A larger value will move up the final failure stress
- * μ --- Friction coefficient (0.01 ~ 1.0).



(b) Fatigue analysis:

In addition to the parameters in static analysis, in fatigue analysis Walker fatigue parameters for matrix fatigue and Heywood fatigue parameters ($p1 \sim p3$) for fiber fatigue may need to be adjusted. The Heywood parameters have the effects on S-N curve as shown in the following figure.



IV. Example

IV-1) Initial and final ABAQUS runstream files:

(a) Initial ABAQUS file, cpf.ini, prepared by users

In the following initial file, the elements in group CMLF will have material degradation analysis, the material (USER) then can have dummy values, the real properties will be input through GUI. The element group UNDA will not have degradation analysis, so its material, ORIN, should be correctly defined here and GUI will not change it.

Write a simple static analysis step in the initial file. The real analysis steps will be input from GUI.

```
*HEADING
CPFail-ABAQUS, cpf.ini
*INCLUDE,INPUT=cpf.model
** END OF MESH GENERATION
*SHELL SECTION,ELSET=CMLF,COMPOSITE
.005,1,user,ORI0
.005,1,user,ORI0
*TRANSVERSE SHEAR STIFFNESS
5.0E4,5.0E4
*SHELL SECTION,ELSET=UNDA,COMPOSITE
.005,1,orin,ORI0
.005,1,orin,ORI90
*TRANSVERSE SHEAR STIFFNESS
5.0E4,5.0E4
*MATERIAL,NAME=orin
*ELASTIC,TYPE=LAMINA
146896.55,11379.31,0.3,6186.21,6186.21,6186.21
*MATERIAL,NAME=user
*ELASTIC,TYPE=LAMINA
10.0,2.0,3.0,4.0,5.0,6.0
*ORIENTATION,NAME=ORI0,SYSTEM=RECTANGULAR
1.,0.,0.,0.,1.,0.
3,0.
*ORIENTATION,NAME=ORI90,SYSTEM=RECTANGULAR
1.,0.,0.,0.,1.,0.
3,90.
*STEP
*STATIC
** Boundary condition
*INCLUDE,INPUT=c:\users\cpf.bc
*RESTART,WRITE
*EL PRINT,ELSET=CMLF,SUMMARY=NO,POSITION=NODE
S
E
*MONITOR,NODE=401,DOF=1
*END STEP
```

(b) Final ABAQUS runstream files (xxx.inp) produced from GUI

Through GUI, in group CMLF one layer (0 degree) with material 'user' was added and the layer thickness were changed to 0.05; in group UNDA layer 2 was changed to be 0 degree and thickness were changed to 0.075. The material 'user' was selected as user defined material (to have degradation analysis). The output point is Element=2 and layer=1, which is in the group CMLF. The following files are the GUI result runstream files, under lines show the difference to the initial file. GUI also produced three internal files, control.dat, user_constant.dat and user_material.dat, which are for CPFail analysis and contain material information inputted from GUI.

(b-1) Static Analysis Runstream CPF-S.inp:

In [Model]/[Control Parameters]/[Analysis], select static analysis and 10 steps, the following runstream file will be produced from GUI.

```
*HEADING
CPFail-ABAQUS, cpf.ini
*INCLUDE,INPUT=cpf.model
** END OF MESH GENERATION
*SHELL SECTION,ELSET=CMLF,COMPOSITE
0.05,1,user,ORI0
0.05,1,user,ORI90
0.05,1,user,ORI0
*TRANSVERSE SHEAR STIFFNESS
5.0E4,5.0E4
*MATERIAL, NAME=user
*DEPVAR
40
*USER MATERIAL, CONST=2
2,1
*SHELL SECTION,ELSET=UNDA,COMPOSITE
0.075,1,orin,ORI0
0.075,1,orin,ORI0
*TRANSVERSE SHEAR STIFFNESS
5.0E4,5.0E4
*MATERIAL,NAME=orin
*ELASTIC,TYPE=LAMINA
146896.55,11379.31,0.3,6186.21,6186.21,6186.21
*ORIENTATION,NAME=ORI90,DEFINITION=COORDINATES,SYSTEM=RECTANGULA
R
1,0,0,0,1,0
3,90
*ORIENTATION,NAME=ORI0,DEFINITION=COORDINATES,SYSTEM=RECTANGULAR
1,0,0,0,1,0
3,0
*INITIAL CONDITIONS,TYPE=SOLUTION,USER
*USER SUBROUTINE, INPUT=user-t.rut
*STEP,INC=10
*STATIC,DIRECT
0.1, 1.0
```



```

*INCLUDE,INPUT=cpf.bc
*RESTART,WRITE
*EL PRINT,ELSET=CMLF,SUMMARY=NO,POSITION=NODE
S
E
*MONITOR,NODE=401,DOF=1
*END STEP

```

(b-2) Fatigue Analysis Runstream CPF-F.inp:

In [Model]/[Control Parameters]/[Analysis], select Fatigue Analysis and Maximum Log(N) = 6, Load Ratio = 0.1, the following runstream file will be produced from GUI.

```

*HEADING
CPFail-ABAQUS, cpf.ini
*INCLUDE,INPUT=cpf.model
** END OF MESH GENERATION
*SHELL SECTION,ELSET=CMLF,COMPOSITE
0.05,1,user,ORI0
0.05,1,user,ORI90
0.05,1,user,ORI0
*TRANSVERSE SHEAR STIFFNESS
5.0E4,5.0E4
*MATERIAL, NAME=user
*DEPVAR
40
*USER MATERIAL, CONST=2
2, 1
*SHELL SECTION,ELSET=UNDA,COMPOSITE
0.075,1,orin,ORI0
0.075,1,orin,ORI0
*TRANSVERSE SHEAR STIFFNESS
5.0E4,5.0E4
*MATERIAL,NAME=orin
*ELASTIC,TYPE=LAMINA
146896.55,11379.31,0.3,6186.21,6186.21,6186.21
*ORIENTATION,NAME=ORI0,DEFINITION=COORDINATES,SYSTEM=RECTANGULAR
1,0,0,0,1,0
3,0
*ORIENTATION,NAME=ORI90,DEFINITION=COORDINATES,SYSTEM=RECTANGULAR
R
1,0,0,0,1,0
3,90
*INITIAL CONDITIONS,TYPE=SOLUTION,USER
*USER SUBROUTINE, INPUT=user-t.rut
*STEP
STEP 1
*STATIC
1.0, 1.0

```

```

*INCLUDE,INPUT=cpf.bc
*RESTART, WRITE
*EL PRINT,ELSET=CMLF,SUMMARY=NO,POSITION=NODE
S
E
*MONITOR, NODE=401, DOF=1
*END STEP
*STEP
STEP 2
*STATIC
1.0, 1.0
*END STEP
*STEP
STEP 3
*STATIC
1.0, 1.0
*END STEP
*STEP
STEP 4
*STATIC
1.0, 1.0
*END STEP
*STEP
STEP 5
*STATIC
1.0, 1.0
*END STEP
*STEP
STEP 6
*STATIC
1.0, 1.0
*END STEP
*STEP
STEP 7
*STATIC
1.0, 1.0
*END STEP
*STEP
STEP 8
*STATIC
1.0, 1.0
*END STEP
*STEP
STEP 9
*STATIC
1.0, 1.0
*END STEP

```

IV-2) Material properties and parameters

Several cases of static and fatigue analyses for different materials are listed here for references.

(E_f - fiber young's modules, μ_f - fiber Poisson's ratio, α_f - fiber thermal expansion coefficient, V_f - fiber volume fraction, σ_0 - fiber mean strength, d_f - fiber diameter, M - fiber Weibull modules, E_m - matrix Young's modules, μ_m - matrix Poisson's ratio, α_m - matrix thermal expansion coefficient, K_{mc} - critical matrix stress intensity factor, T - temperature).

(a) Nicalon/CAS

Nicalon fiber:

$E_f =$	195.0 (176.0)*	GPa
$\mu_f =$	0.2	
$\alpha_f =$	3.0E-6 (4.0E-6)*	$/^{\circ}C$
$V_f =$	0.65	
$M =$	10	
$\sigma_0 =$	388.4	MPa
$d_f =$	7.00E-5	m

CAS matrix:

$E_m =$	95.0	GPa
$\mu_m =$	0.3	
$\alpha_m =$	5.0E-6	$/^{\circ}C$
$K_{mc} =$	2.16(1.73)*	MPa- $m^{(1/2)}$
$T =$	0	$^{\circ}C$

(* Properties at $T=400^{\circ}C$)

Empirical parameters:

Friction coefficient =	0.01
Nonlinear coefficient =	2.4
Matrix damage limit =	0.3

(b) Graphite/Epoxy

Graphite fiber:

$E_f =$	221.0	GPa
$\mu_f =$	0.48	
$\alpha_f =$	-7.58E-7	$/^{\circ}C$
$V_f =$	0.65	
$M =$	10	
$\sigma_0 =$	388.4	MPa
$d_f =$	7.00E-6	m

Epoxy matrix:

$E_m =$	3.45	GPa
$\mu_m =$	0.2	

$\alpha_m =$	8.433E-5	$/^{\circ}C$
$K_{mc} =$	0.67	MPa- $m^{(1/2)}$
$T =$	0	$^{\circ}C$
Empirical parameters:		
Friction coefficient =	0.01	
Nonlinear coefficient =	2.4	
Matrix damage limit =	0.3	

(c) Carbon/SiC

Carbon fiber:

$E_f =$	231.0	GPa
$\mu_f =$	0.2	
$\alpha_f =$	-5.40E-7	$/^{\circ}C$
$V_f =$	0.40	
$M =$	10	
$\sigma_0 =$	388.4	MPa
$d_f =$	7.00E-6	m

SiC. matrix:

$E_m =$	35.10	GPa
$\mu_m =$	0.22	
$\alpha_m =$	1.10E-5	$/^{\circ}C$
$K_{mc} =$	0.5	MPa- $m^{(1/2)}$
$T =$	0	$^{\circ}C$

Empirical parameters:

Friction coefficient =	0.3
Nonlinear coefficient =	0.1
Matrix damage limit =	0.1
Fatigue final strain =	0.0115
Fatigue coefficient =	0.075
Walker constant C =	3.13E-15
Walker constant n =	8.4
Heywood parameter p1 =	0.153 MPa
Heywood parameter p2 =	2206.9 MPa
Heywood parameter p3 =	0.0031

IV-3) Progressive Damage

An example of tensile laminate plate with a central hole shows the progressive material damage and stress re-distributions, Figure PD-1 ~ PD-4. In order to reduce computation time, PD-5 shows that material degradation analysis performed only in the elements near the hole.

Figures are plotted by using ABAQUS-POST, valuable = s11 for stress, valuable = sdv31 for stiffness E11.

Figure PD-1 (1). Stiffness E11 distribution for 0 degree layer at step 1

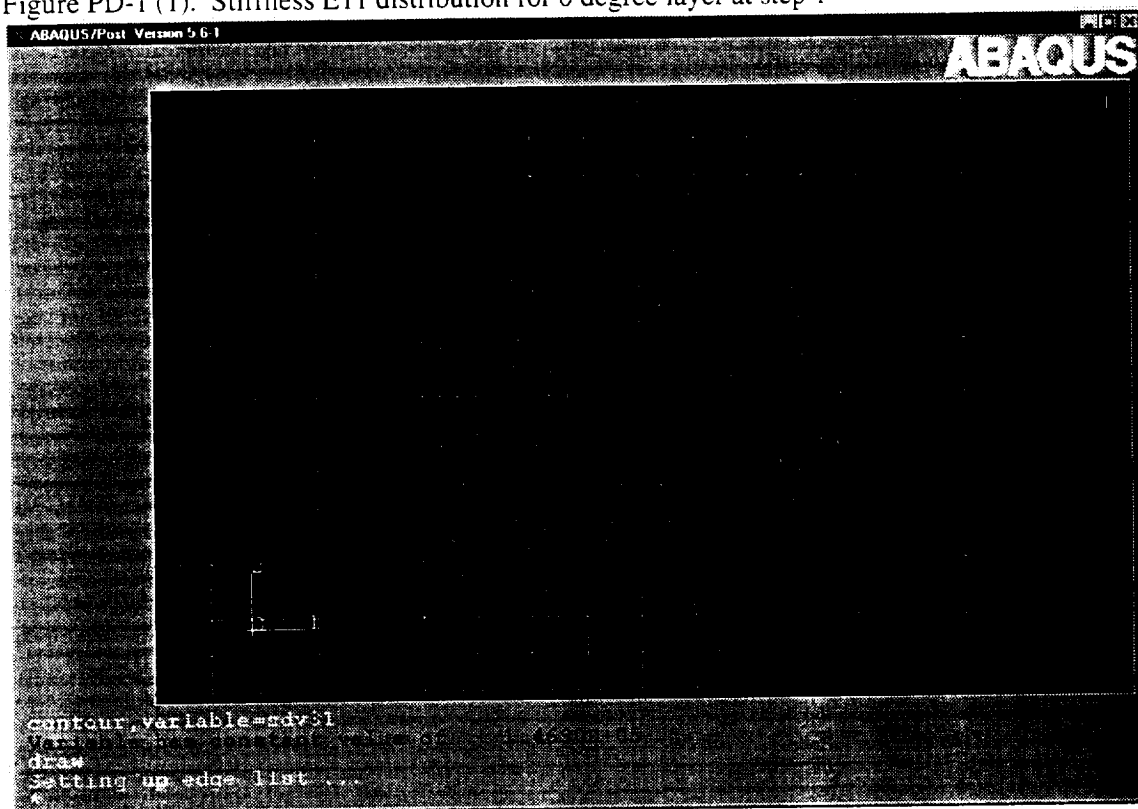


Figure PD-1 (2). Stress S11 distribution for 0 degree layer at step 1

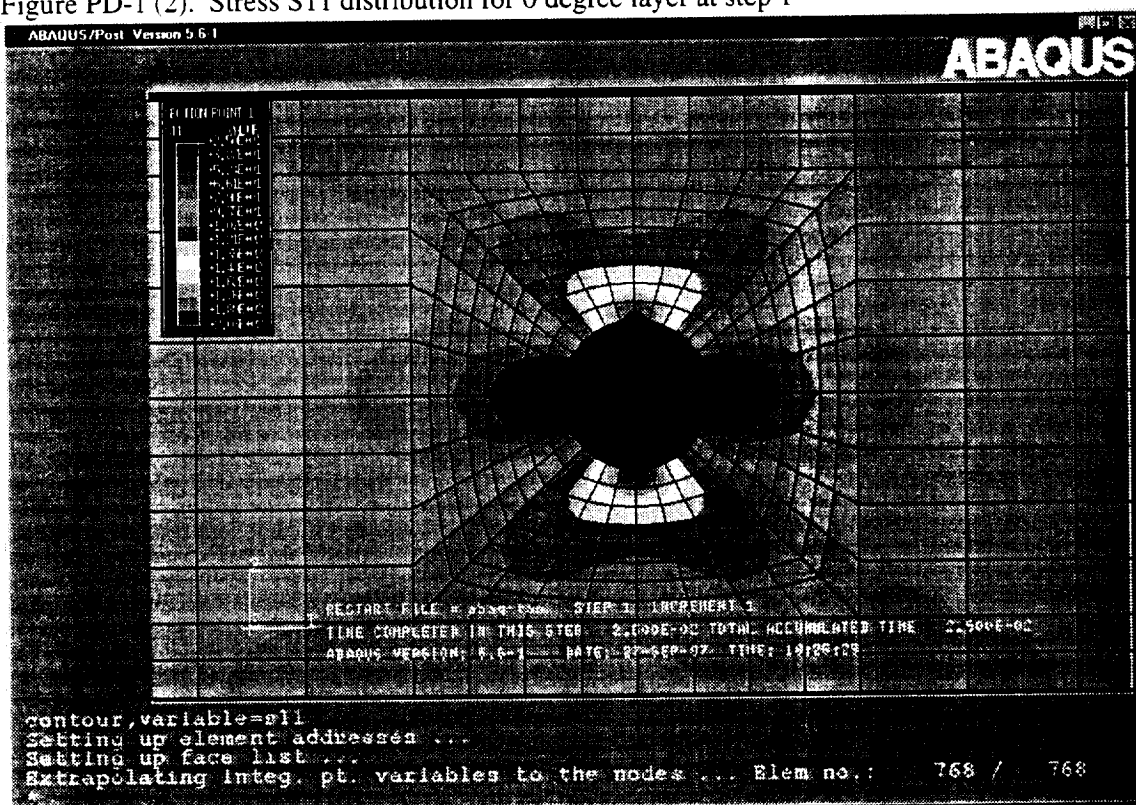


Figure PD-2 (1). Stiffness E11 distribution for 0 degree layer at step 4

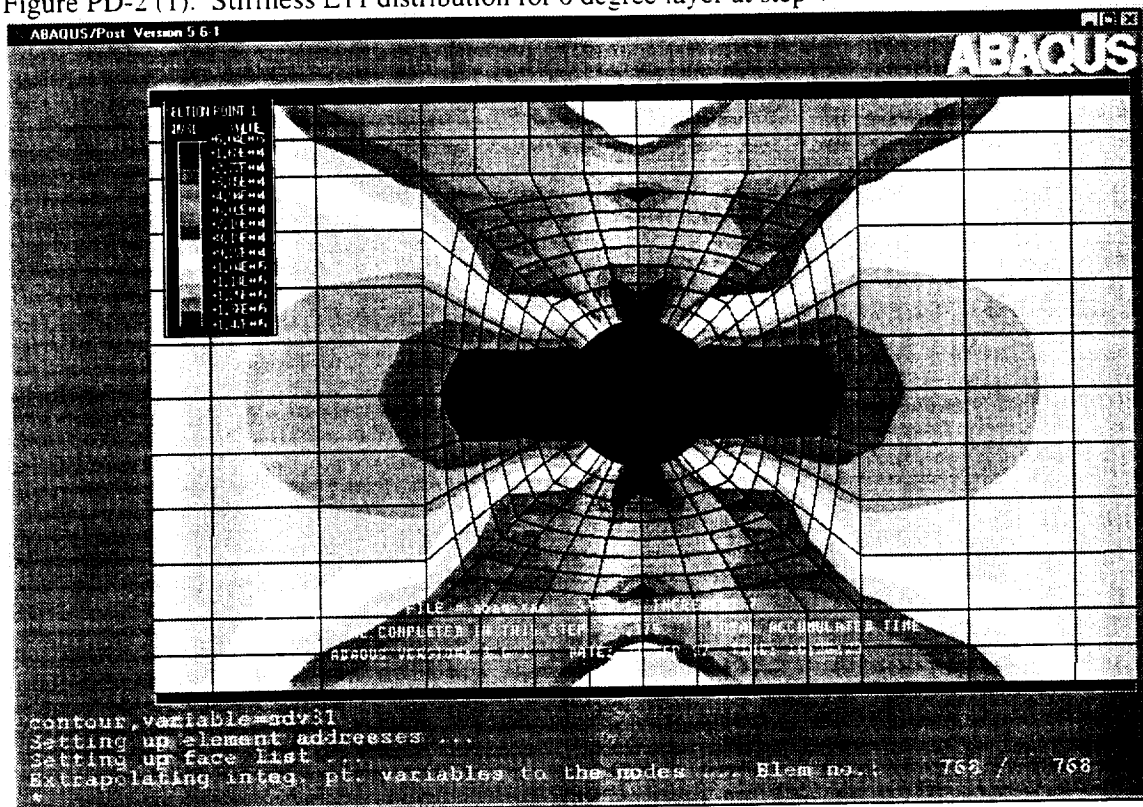


Figure PD-2 (2). Stress S11 distribution for 0 degree layer at step 4

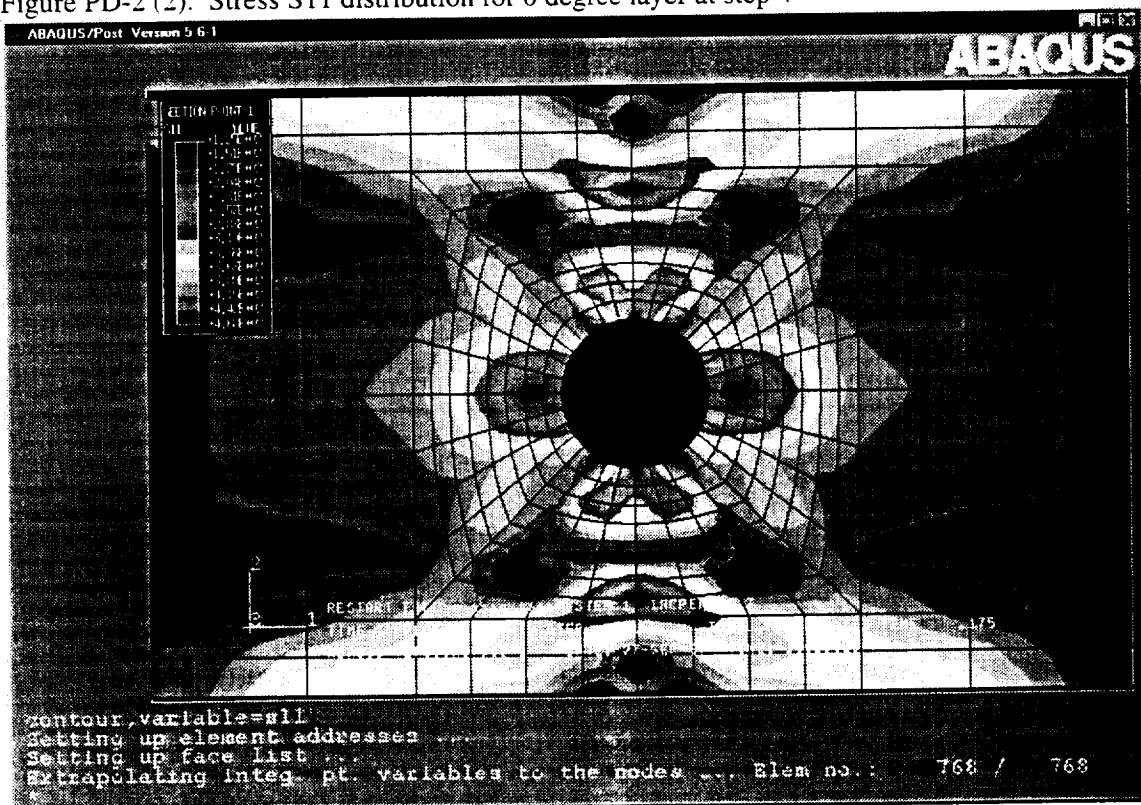


Figure PD-3 (1). Stiffness E11 distribution for 0 degree layer at step 6

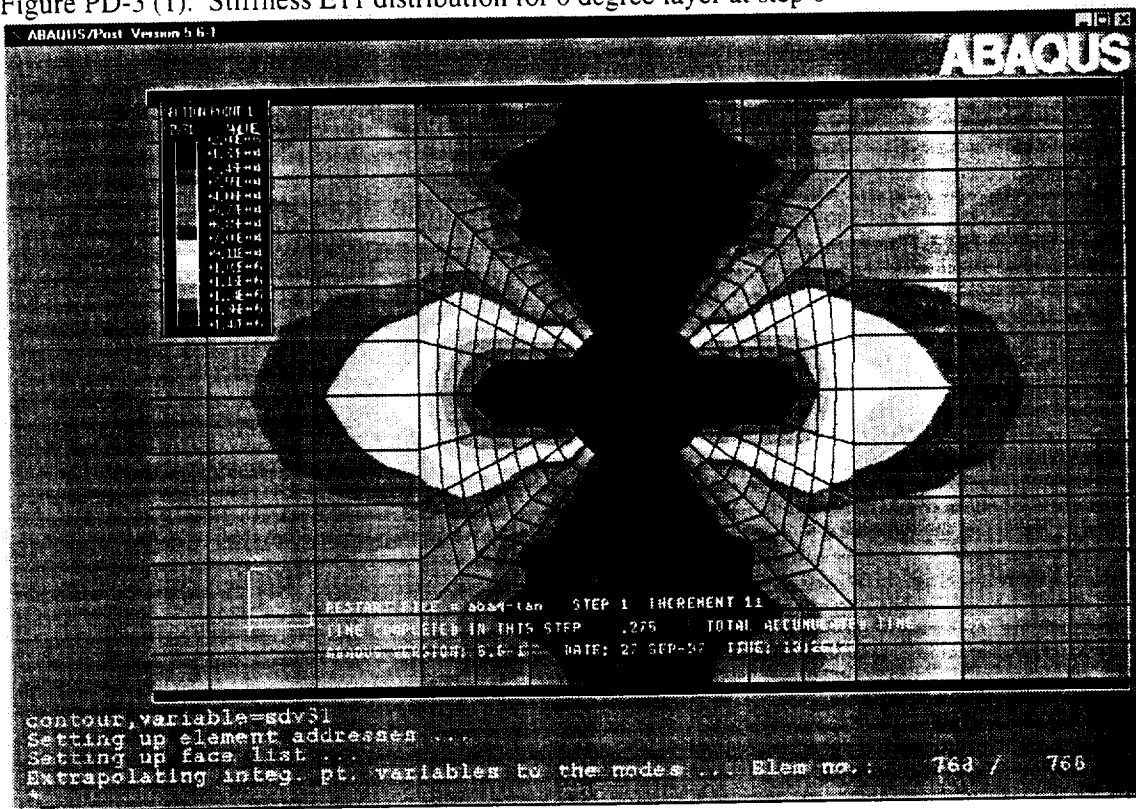


Figure PD-3 (2). Stress S11 distribution for 0 degree layer at step 6

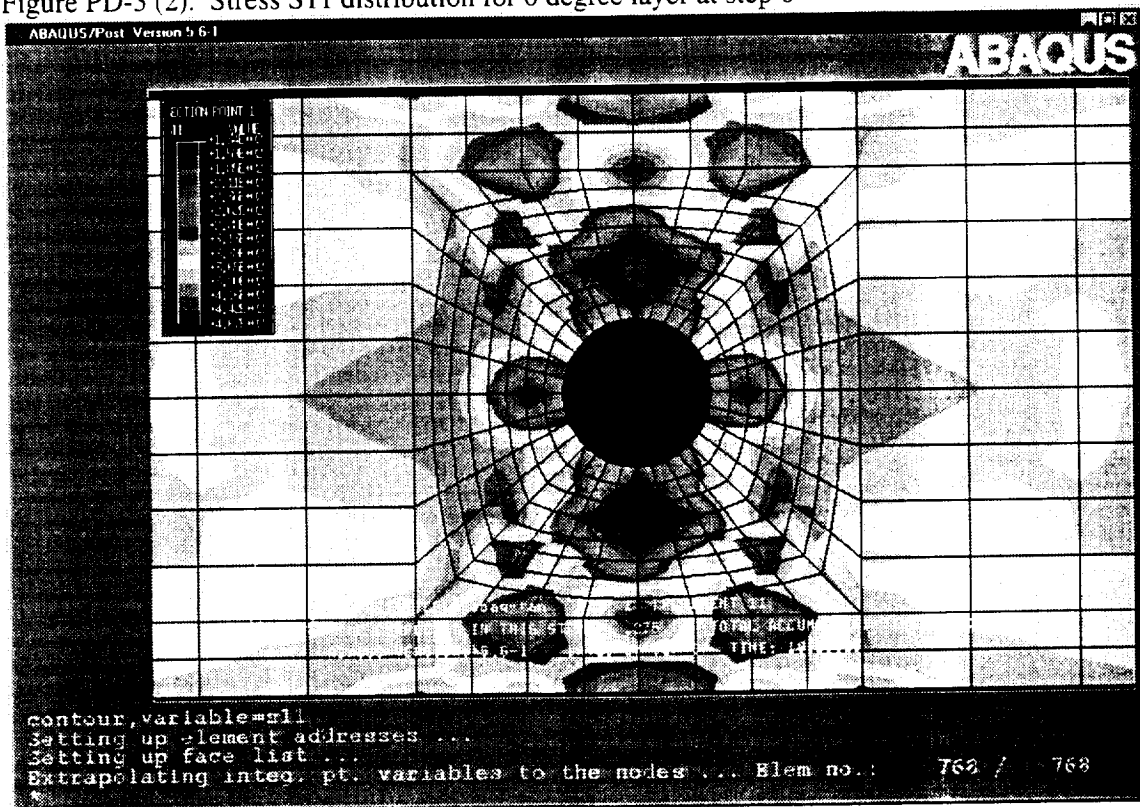


Figure PD-4 (a). Stiffness E11 distribution for 0 degree layer at step 7

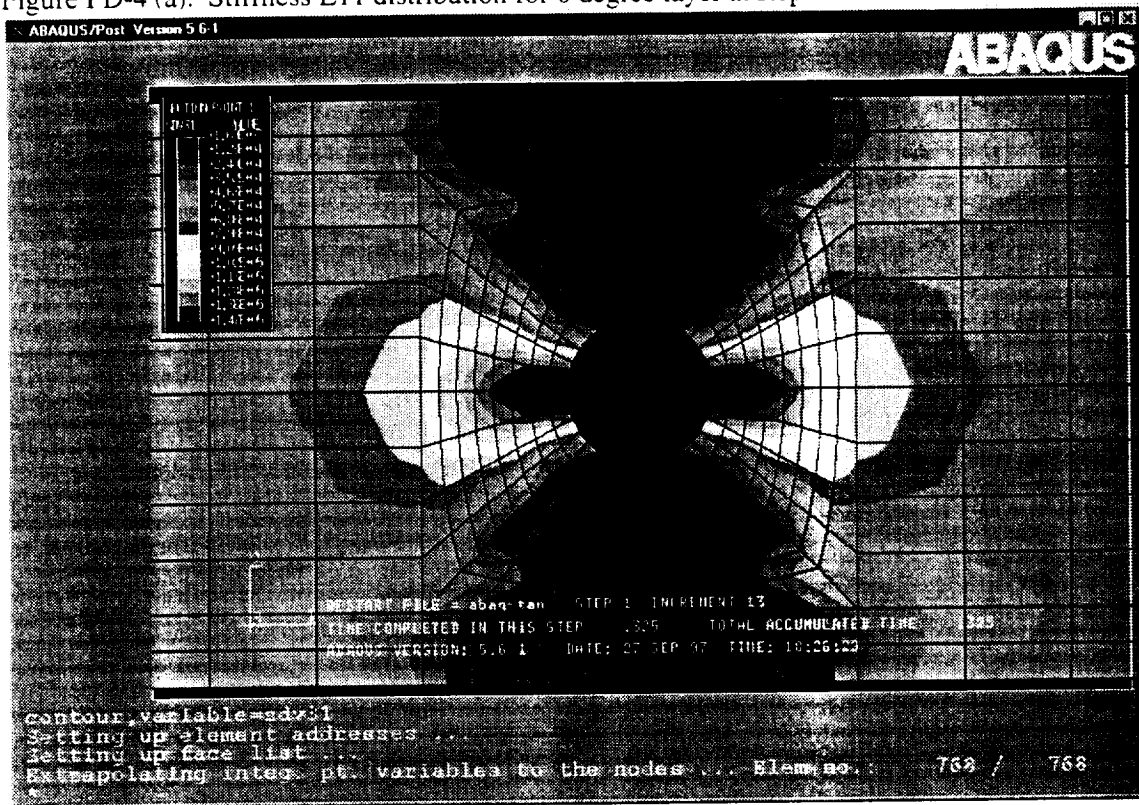


Figure PD-4 (b). Stress S11 distribution for 0 degree layer at step 7

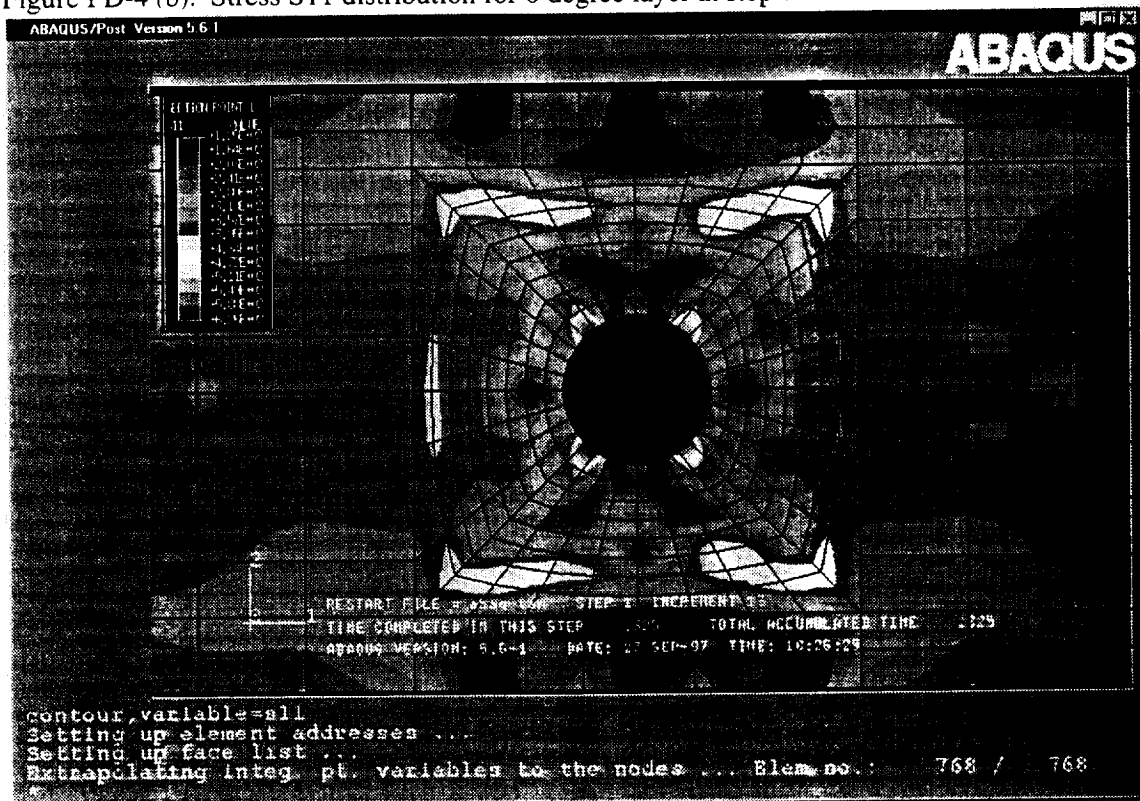


Figure PD-5(1). Stiffness E11 for 0 degree layer at step 4 (partly damage analysis)

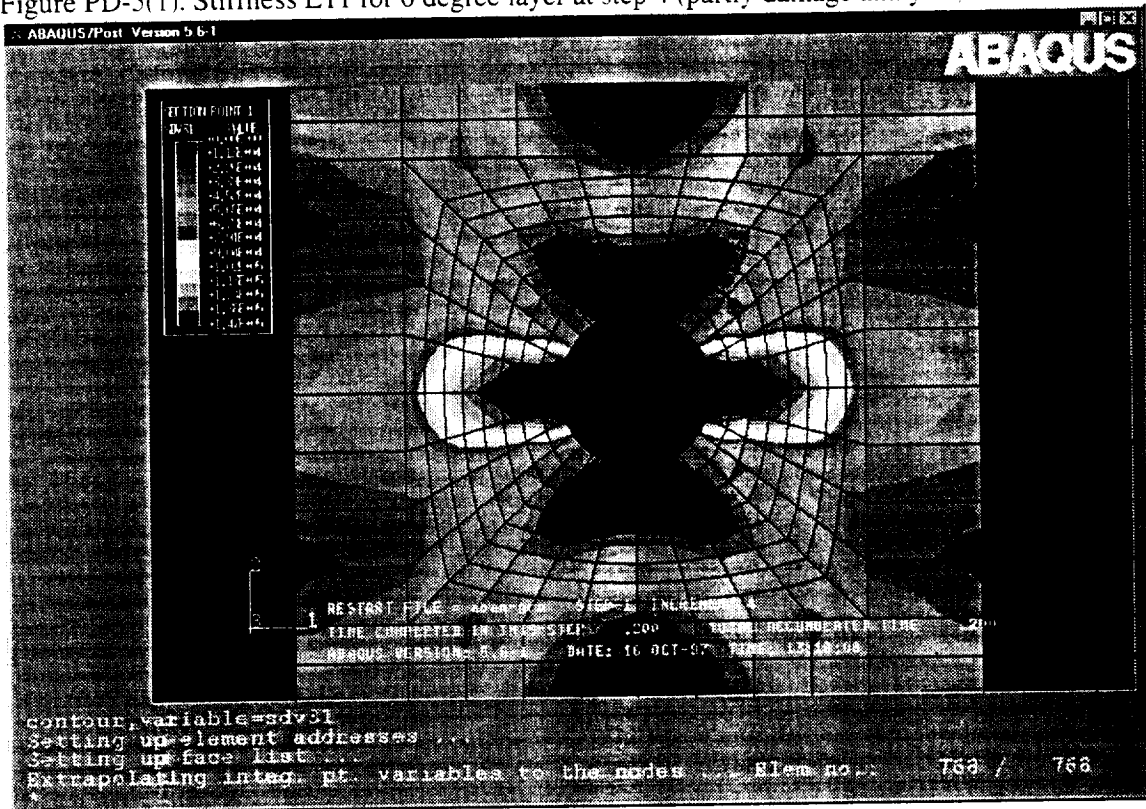
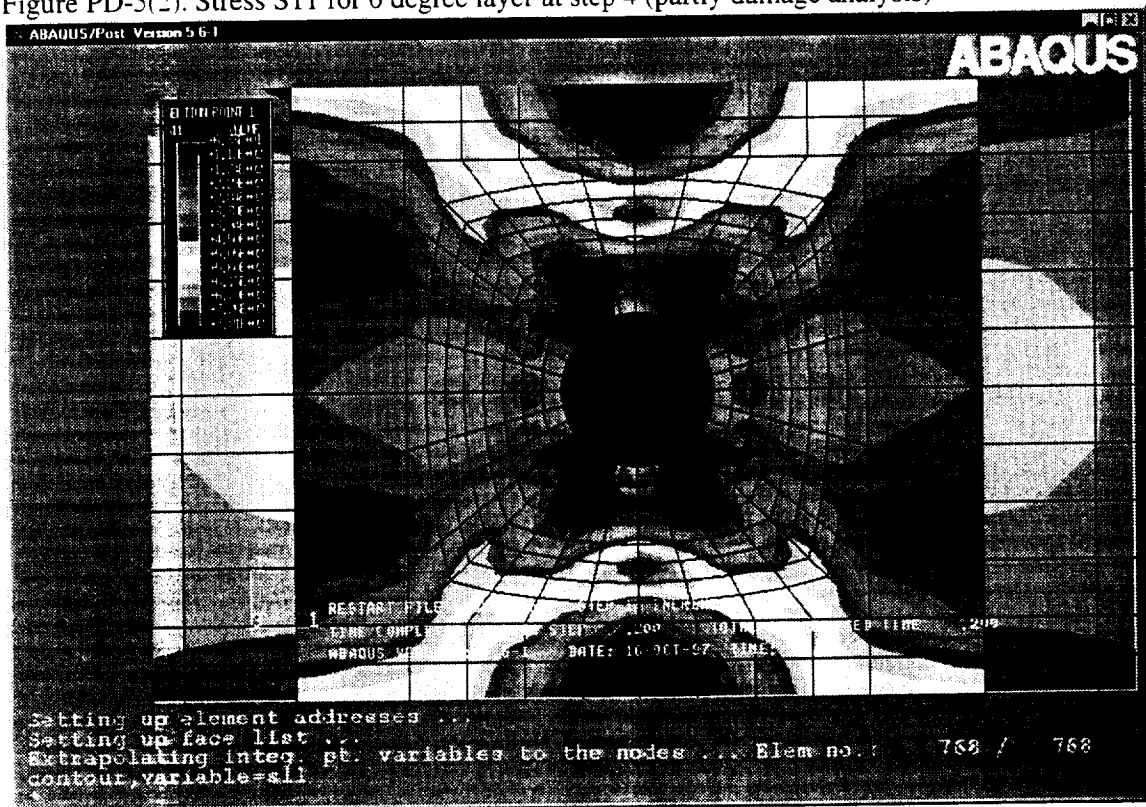
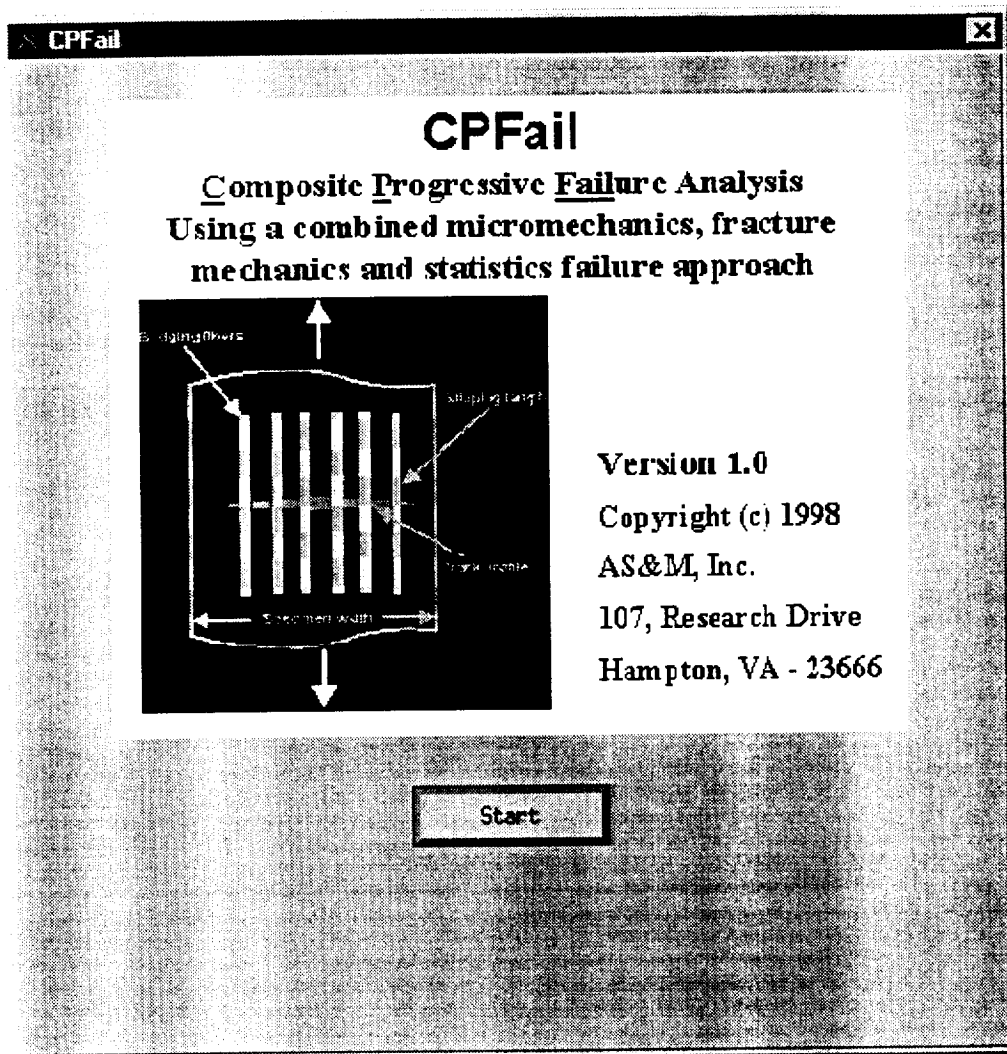


Figure PD-5(2). Stress S11 for 0 degree layer at step 4 (partly damage analysis)



A-3. CPFail User's Manual



CONTENTS

I. Preface

- I-1) Introduction
- I-2) System requirement
- I-3) Installation and execution
- I-6) Limitations

II. Getting Started

- II-1) Using GUI to input material parameters

III. GUI Help

- III-1) [File]
- III-2) [View]
- III-3) [Command]/[Execute] or [Execute]
- III-4) [Model]/[Laminate] or [Laminate]
- III-5) [Model]/[Load] or [Load]
- III-6) [Model]/[Analysis] or [Analysis]
- III-7) [Database]/ or [Fiber], [Matrix] and [Ply]
- III-8) [Options]

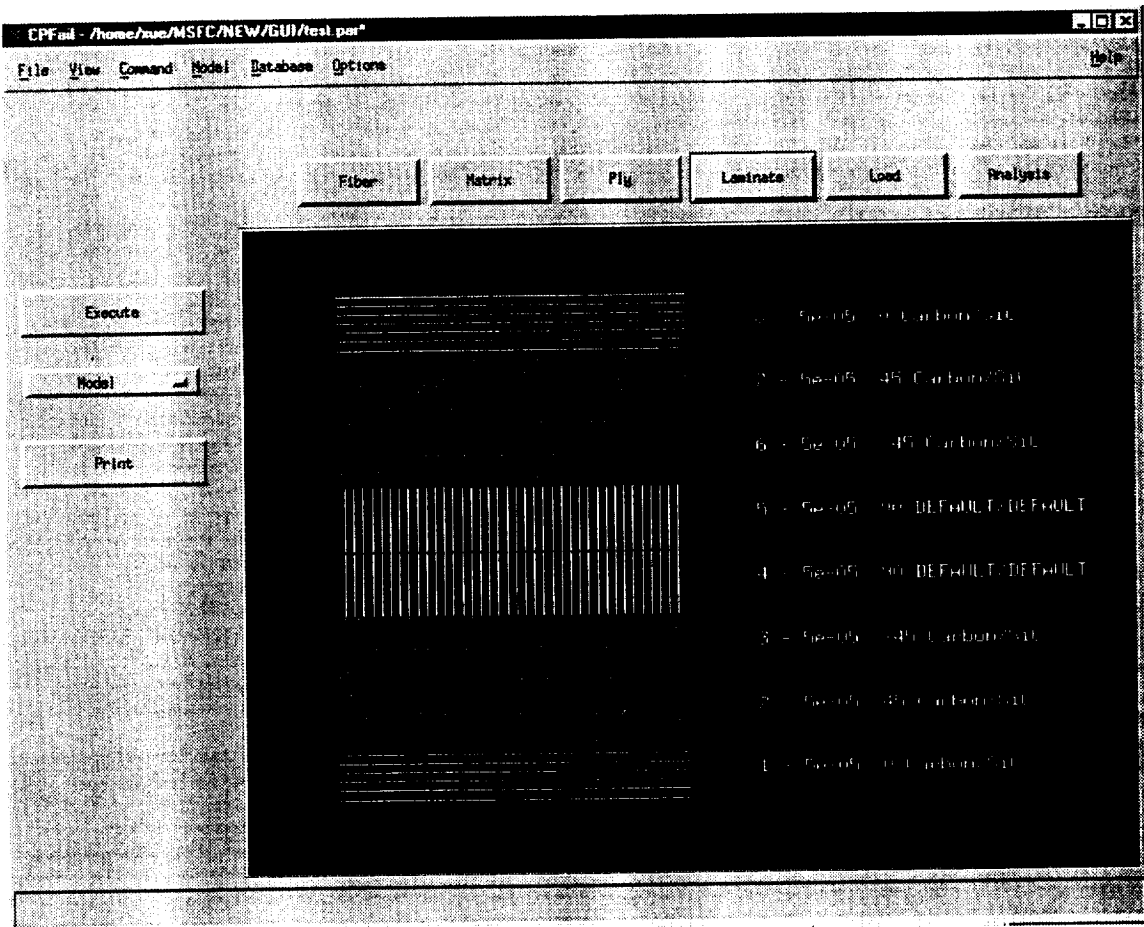
IV. Material Parameters Information

- IV-1) Parameter definition
- IV-2) How to adjust parameters

V. Example of Material Properties and Parameters

- V-1) Nicalon/CAS
- V-2) Graphite/Epoxy
- V-3) Carbon/SiC

I. Preface



I-1) Introduction

CPFail (Composite Progressive Failure Analysis) is an analysis code for computing the composite material degradation due to tensile damage. The material degradation is estimated by using a combined micromechanics, fracture mechanics and statistics failure approach. With a step loading procedure, it can show the structural progressive failure or predict the structure fatigue life. A user friendly GUI (Graphic User Interface) is designed for helping user to input material information and loading condition.

I-2) System requirement

The CPFail is developed in C/C++ using X-Windows and Motif toolkits. It can be run only on UNIX system.

I-3) Installation and execution

Installation:

The software is distributed in tar format file `asm.tar`. The file contains all the required data files, source files and java class files required to execute the programs. To install the software components copy change directory to the destination directory and extract the files using the command: `tar -xvf asm.tar`. This command creates the ASM main directory and sub directories to copy the CPFail, MicroTex and ABAQUS interface programs.

Execution:

The executable command for CPFail is:

go to directory	/ASM/CPF/CPFAIL	and
execute	./cpfail	command

Original code Files:

The following files are the original code files, user should carry over when change software installation directory, user can also carry over xxx.par files for previous cases:

cpfail
cma
fiber.dbf
matrix.dbf
ply.dbf
cpfail.tif

I-4) Limitations

Composite material degradation is caused by tensile damage with the effect of shear stress.

II. Getting Started

a) Open CPFail GUI window

b) Create material database:

In main screen or go to [Database], select [Fiber] and [Matrix] if user wants to input material properties from fiber and matrix properties; select [Ply] if user wants to input ply properties. (The material degradation analysis will be based on fiber and matrix properties; the program will convert ply properties to fiber and matrix properties.)

c) Ply, Fiber or Matrix Database:

- * Define a new name or select one from database. (The material name will be used in [Laminate]).
Ply (Fiber, Matrix) Name: To select an existing material
New Ply (Fiber, Matrix) Name: To create a new material or modify the existing material name
- * Input or modify material properties. Refer to III and IV for detailed material information.
- * input a description for user's own remark

d) Go to [Laminate], input layer thickness, orientation, fiber volume fraction and friction coefficient, select material name, than click [Add] to build a laminate layer by layer.

e) Go to [Load]

- * Select load type: Stress or Displacement
- * Input load values: start initial values and increment values
- * Input analysis environment temperature and composite manufacture processing temperature

f) Go to [Analysis], select Static Analysis or Fatigue Analysis,

f-1. Static Analysis:

- * Input maximum steps
- * Input static analysis parameters: see IV for detailed information
- * Input final strain (in 0 degree direction) to stop analysis

f-2. Fatigue Analysis:

- * Input log maximum cycles, Log(N)
- * Input maximum load value (peak load)
- * Input loading ratio, load ratio = Minimum load / Maximum load
- * Input fatigue analysis parameters: see IV for detailed information
- * Input fatigue final strain (in 0 degree direction)

g) Go to [File]/[Save As], to save the case as a xxx.par GUI file

h) Go to [Execute], to start analysis

- i) Go to [View], to read result figures and text files
See III. GUI Help for detailed information.

j) Structural fatigue S-N curve

It should be pointed out that in the fatigue analysis, the loading cycle increases as, $\text{Log}(N) = 1, 2, 3 \dots$, to the maximum $\text{Log}(N)$. In each fatigue analysis, load will be a constant and the final fatigue cycle, $\text{Log}(N)$, will be computed. Thus for one load level, it can only produce one point on the curve (S-N) of Maximum stress verses Fatigue cycle $\text{Log}(N)$. In order to have a complete S-N curve, several load levels should be executed. The fatigue failure (final) cycle, $\text{Log}(N)$ is printed in the result file, s-s.dat, and can be read from [View]/[Text File] window.

III. GUI Help

III-1) [File]

- (a) [New]: Open a new case, after input, save the case in a new GUI file, xxx.par
- (b) [Open]: Open a case from a previously saved xxx.par GUI file
- (c) [Save]: Save the current modified case to the original xxx.par file
- (d) [Save As]: Save the current case to a new GUI file, for example, xxx-1.par
- (e) [Print]: Print out results or the lamination figure in the window
- (f) [Exit]: Close GUI

III-2) [View]

- (a) [Model]: Lamination figure
- (b) [Ply Damage]: Steps vs. remaining ply fiber volume fraction
- (c) [Lam Prop Change]: Steps vs. laminate stiffness ratio, E_{11} / E_{11}^0 and E_{22} / E_{22}^0 ,
 E^0 s are the undamaged original value
- (d) [Lam Stresses]: Steps vs. laminate stresses
- (e) [Lam Displacements]: Steps vs. laminate displacements
- (f) [Lam Stress-Strain]: Laminate strain vs. stress
- (g) [Text File]: View text files

III-3) [Command]/[Execute] or [Execute] executing analysis

III-4) [Model]/[Laminate] or [Laminate]

- * Input or modify ply numbering, ply thickness, orientation, fiber volume fraction
- * Adjust friction coefficient according to testing results
- * Select material input format: ply property or fib/matrix properties. Select material name from [Database], [Fiber], [Matrix] or [Ply]

III-5) [Model]/[Load] or [Load]

- (a) Load Type: Stress or displacement load. For fatigue analysis, apply stress load only.
- (b) Initial Value: Starting load. For fatigue analysis, it is the maximum (peak) load.
- (c) Increment Value: Constant increment load. For fatigue analysis, it is zero.
- (d) Temp. Difference: Environment temperature
- (e) Process Temperature: Composite manufacture processing temperature

III-6) [Model]/[Analysis] or [Analysis]

(a) Static Analysis:

- * Steps --- Total load increments
- * Matrix Damage Limit --- (0.1 ~ 0.3) see IV for details
- * Nonlinear Coefficient --- (0.01 ~ 10) see IV for details
- * Static Final Strain --- Strain value to stop the static analysis

(b) Fatigue Analysis:

- * Maximum Cycles Log(N) --- User defined stopping point

- * Maximum Load --- Load peak value
- * Load Ratio --- (= Minimum load / Maximum load) in a load cycle
- * Fatigue Final Strain --- Strain value to stop the fatigue analysis
- * Fatigue Parameter --- (0.01 ~ 3.0), see IV for information
- * Walker Constants (C and n) --- (3.13E-15, 8.4), see IV for information
- * Heywood Parameters (p1 ~ p3) --- (0.153 MPa, 2206.9 MPa and 0.0031), see IV for information

III-7) [Database]/ or [Fiber], [Matrix] and [Ply]

(a) User can build new or modify old matrix, fiber and ply property databases.

- * Ply (Fiber, Matrix) Name: To select an existing material
- * New Ply (Fiber, Matrix) Name: To create a new material or modify the existing material name

(b) Matrix Critical Stress Intensity Factor, K_{mc} , (0.1 ~ 5.0)

(c) Weibull Modules (M) and Mean Fiber Strength (σ_0)

Empirical parameters from modified Weibull fiber damage statistic equation,
 $M=10$ and $\sigma_0=388.0$ MPa are default values. See IV for details

(d) Friction Coefficient

Empirical parameter of matrix-fiber integration (0.01 ~ 1.0)

III-8) [Options]:

(a) Units:

- * Let user to choose SI or US units.
- * All values will be changed according to unit change in GUI and will be written in to ABAQUS runstream file.

(b) Graphic Settings:

- * Adjust output figure settings

IV. Material Parameters Information

Material special parameters are designed for user to adjust material or laminate behavior due to damage, fatigue, delamination, material nonlinearity or plasticity.

IV-1) Parameter definition:

- * Weibull Modules (M) and Mean Fiber Strength (σ_0)

Empirical parameters from modified Weibull fiber damage statistic equation, M=10 and $\sigma_0=388.0$ MPa are default values.

$$P_f = 1 - \exp \left[\frac{-4\pi a l_s}{k_0} \left(\frac{T_c}{\sigma_0} \right)^M \right]$$

- * Friction Coefficient: Empirical parameter of matrix-fiber integration (0.01 ~ 1.0)
- * Matrix Damage Limit: matrix modules remaining ratio after matrix cracking
- * Nonlinear Coefficient: Adjust for material nonlinear behavior due to yielding, plasticity, damage or delamination. The nonlinear effect is bigger for lager value, for example, 0.01 (linear) ~ 2.4 (nonlinear).
- * Process Temperature: Composite laminate manufacture curling temperature.
- * Walker Constant C and n: from Walker's fatigue statistic equation for matrix fatigue cracking. Suggested value: C= 3.13E-15 and n=8.4

$$\frac{da}{dN} = CK_m^n$$

- * Fatigue Coefficient: Empirical fatigue parameter. A smaller value corresponds to smaller damage and longer life. A positive value of (0.01 ~ 3.0).
- * Fatigue Final Strain: The fatigue failure criteria to define fatigue life cycles. User assume that the structure failed as the strain (ϵ_{11}) at the monitor point reaches to this value.
- * Heywood Parameters p1 ~ p3: from Heywood's fatigue statistic equation for fiber strength fatigue reduction. The effects of p1 ~ p3 are shown in the following figure. Suggest value: $p_1 = 0.153$ MPa, $p_2 = 2206.9$ MPa, $p_3 = 0.0031$

Heywood equation:

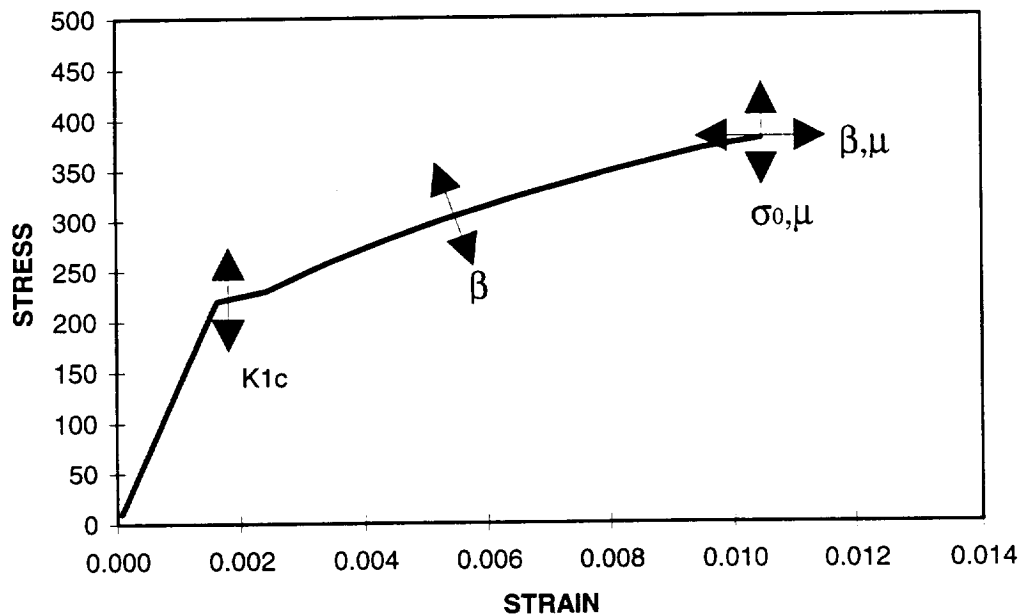
$$\begin{aligned} \sigma_a &= \pm \sigma_t \left[1 - \sigma_m / \sigma_t \right] \left[A_0 + \gamma(1 - A_0) \right] \\ A_0 &= \left[1 + \frac{p_3 \bar{n}^4}{1 + \sigma_t / p_1} \right] \frac{1}{1 + p_3 \bar{n}^4}, \\ \gamma &= \frac{\sigma_m}{\sigma_t} \frac{1}{1 + (\sigma_t \bar{n} / p_2)^4}, \\ \bar{n} &= \text{Log}(N) \end{aligned}$$

IV-2) How to adjust parameters

In order to make this material degradation analysis tool more general to composite materials, the empirical parameters need to be adjusted according to different materials, structure or different damage conditions. Default values provide a base for the parameter adjustments, so they should be kept for references. The following two figures show the effects of parameters on material or structural behaviors.

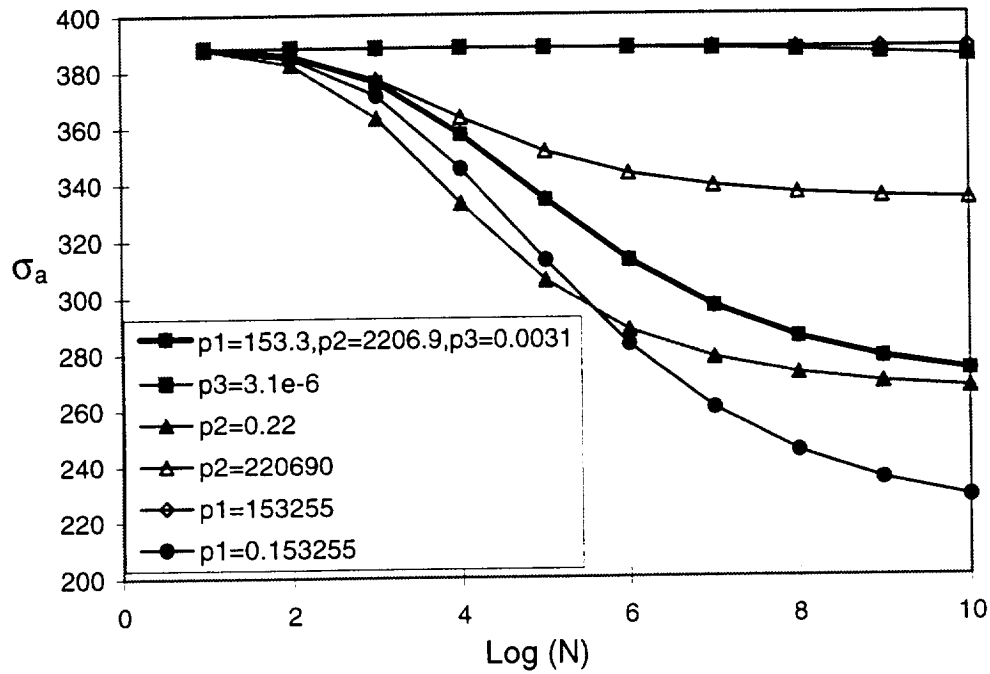
(a) Static analysis:

- * K_{mc} --- Matrix critical stress intensity factor. A larger value will move up 'yielding point'
- * β --- Nonlinear coefficient (0.01 ~ 10). A larger value will have stronger nonlinear behavior.
- * σ_0 --- Mean fiber strength. A larger value will move up the final failure stress
- * μ --- Friction coefficient (0.01 ~ 1.0).



(b) Fatigue analysis:

In addition to the parameters in static analysis, in fatigue analysis Walker fatigue parameters for matrix fatigue and Heywood fatigue parameters ($p1 \sim p3$) for fiber fatigue may need to be adjusted. The Heywood parameters have the effects on S-N curve as shown in the following figure.



V. Examples of Material Properties and Parameters

Several cases of static and fatigue analyses for different materials are listed here for references.

(E_f - fiber young's modules, μ_f - fiber Poisson's ratio, α_f - fiber thermal expansion coefficient, V_f - fiber volume fraction, σ_0 - fiber mean strength, d_f - fiber diameter, M - fiber Weibull modules, E_m - matrix Young's modules, μ_m - matrix Poisson's ratio, α_m - matrix thermal expansion coefficient, K_{mc} - critical matrix stress intensity factor, T - temperature).

V-1) Nicalon/CAS

Nicalon fiber:

$E_f =$	195.0 (176.0)*	GPa
$\mu_f =$	0.2	
$\alpha_f =$	3.0E-6 (4.0E-6)*	/ $^{\circ}C$
$V_f =$	0.65	
$M =$	10	
$\sigma_0 =$	388.4	MPa
$d_f =$	7.00E-5	m

CAS matrix:

$E_m =$	95.0	GPa
$\mu_m =$	0.3	
$\alpha_m =$	5.0E-6	/ $^{\circ}C$
$K_{mc} =$	2.16(1.73)*	MPa- $m^{(1/2)}$
$T =$	0	$^{\circ}C$

(* Properties at $T=400$ $^{\circ}C$)

Empirical parameters:

Friction coefficient =	0.01
Nonlinear coefficient =	2.4
Matrix damage limit =	0.3

V-2) Graphite/Epoxy

Graphite fiber:

$E_f =$	221.0	GPa
$\mu_f =$	0.48	
$\alpha_f =$	-7.58E-7	/ $^{\circ}C$
$V_f =$	0.65	
$M =$	10	
$\sigma_0 =$	388.4	MPa

$d_f = 7.00\text{E-}6$ m
 Epoxy matrix:
 $E_m = 3.45$ GPa
 $\mu_m = 0.2$
 $\alpha_m = 8.433\text{E-}5$ / $^{\circ}\text{C}$
 $K_{mc} = 0.67$ MPa- $m^{(1/2)}$
 $T = 0$ $^{\circ}\text{C}$

Empirical parameters:
 Friction coefficient = 0.01
 Nonlinear coefficient = 2.4
 Matrix damage limit = 0.3

V-3) Carbon/SiC

Carbon fiber:
 $E_f = 231.0$ GPa
 $\mu_f = 0.2$
 $\alpha_f = -5.40\text{E-}7$ / $^{\circ}\text{C}$
 $V_f = 0.40$
 $M = 10$
 $\sigma_0 = 388.4$ MPa
 $d_f = 7.00\text{E-}6$ m

SiC. matrix:
 $E_m = 35.10$ GPa
 $\mu_m = 0.22$
 $\alpha_m = 1.10\text{E-}5$ / $^{\circ}\text{C}$
 $K_{mc} = 0.5$ MPa- $m^{(1/2)}$
 $T = 0$ $^{\circ}\text{C}$

Empirical parameters:
 Friction coefficient = 0.3
 Nonlinear coefficient = 0.1
 Matrix damage limit = 0.1

Fatigue final strain = 0.0115
 Fatigue coefficient = 0.075
 Walker constant C = $3.13\text{E-}15$
 Walker constant n = 8.4
 Heywood parameter p1 = 0.153 MPa
 Heywood parameter p2 = 2206.9 MPa
 Heywood parameter p3 = 0.0031

Part B. Textile Composites

B1. Textile Composite Theory

B1-1. Introduction

Textile composites are being considered for potential structural application in the aerospace and automotive industries because of the better impact and delamination resistance over tape laminates. However, their architectures are also more complex due to the weaving, braiding, and knitting of fiber yarns. Thus, along with fabrication processes and test methodologies, the development of analytical models to predict the mechanical properties and strength of the textile composites is of increasing importance.

A general purpose micro-mechanics analytical technique was developed by Naik [1,2] in the *Textile Composite Analysis for Design* (TEXCAD) code to predict the overall mechanical and thermal properties of textile composites. The calculation of material properties in this code is based on a simple geometry analysis which transforms the repeating unit cell (RUC) of textile composites into a typical micro-structure with uniform strains; failure criterion of textile composites is based on maximum stress or maximum strain criterion of the matrix and yarn materials.

The failure mechanism of the yarn slice in a textile composite is quite similar to that of a laminated composite, which involves fiber/matrix debonding, fiber-bridged matrix cracking, and statistical fiber failure. An analytical model based on micro-mechanics, fracture mechanics, and statistical concept was developed in the Phase I study [3] to predict the failure of laminate composite under high temperature and tension loads. In the analysis, the fiber-bridged matrix crack was idealized by a continuum model in which the effect of the bridging fibers was modeled by an equivalent closure pressure on the crack surface. A rigorous shear-lag model was used to evaluate the closure pressure distribution along the crack surface and to compute the shear stress transfer along the debonded, frictional sliding fiber/matrix interface. A closed-form micro-mechanics analysis was used to compute the thermal and mechanical (axial and transverse) stress along the fiber/matrix interface region.

In this report, an engineering approach (MicroTex) is developed for textile composites to predict the initial thermal and mechanical properties based on simple geometry, to predict damage progress, and to predict the failure of textile composites. The basic procedure is shown in Figure B1-1. The statistical failure criterion based on fracture mechanics, shear-lag theory, and fiber pull-out concept is modified and combined with other maximum stress or maximum strain criteria to provide a complete set of standards for yarn and matrix slices failure prediction. Nonlinear material properties for both matrix and fiber are included in addition to the failure progress of material slices to calculate the three dimensional stiffness reduction of the RUC. The failure of textile composites or its RUC as a structure with yarn and matrix slices as its components is predicted based on the overall stiffness calculation of RUC. Comparisons with various experimental results for various different textile composites are also presented.

Fatigue analysis for the textile composite is presented in this report also. The assumption is that the stiffness reduction due to fatigue loading when the composite is under uniaxial loading contains information necessary for fatigue analysis for this composite under complex stress states. A fatigue model is developed based on this assumption, empirical parameters are determined using testing data for (0/90) C/SiC composite and then applied to for a (0/-60/60) C/SiC composite.

B1-2. Geometry Model of Textile Composites

Real textile composites have very complicated geometry structures. Figure B1-2 shown a two dimensional C/SiC plain weave composite laminate which is one of the simplest textile composites. It consists of stacked, pre-impregnated layers of woven fabric which are cured and consolidated by a process similar to tape laminates. Each yarn is a bundle of filaments (or fibers) and the yarn size is measured by the number of filaments in the yarn. To model this geometry is impossible without certain simplifications.

A general geometry model was developed [1-2] for textile composites based on several assumptions to describe the fabric architectures and then calculate the mechanical and thermal properties of the textile composites. By observing the periodicity of the repeating pattern in a woven (or braided) fabric, it is assumed that a small repeating unit cell (RUC) can be isolated which is sufficient to describe the fabric architecture. Each individual yarn architecture is discretely modeled using sinusoidal undulations at yarn crossovers and a straight portion. And finally, the iso-strain assumption was used to calculate the overall thermal and mechanical properties and average strains over RUC.

This section will give a brief derivation of geometry model for several textile composites, and then the calculation for overall thermal and mechanical properties of RUCs.

Laminated composite

The RUC for this classical lamination is a two dimensional orientated yarn as shown in Figure B1-3. The ply longitudinal and transverse directions are indicated by 1 and 2, respectively. In the model of laminated composite there is only one yarn slice, and there is no matrix slice.

2D weaves and 2D braids

The geometry model of 2D weaves and 2D braids was developed for plain weave, 5-harness satin weave, 8-harness satin weave, plain 2D braid, 5-harness satin 2D braid, and 8-harness satin 2D braid.

The RUC of a 5-harness satin weave and plain 2D braids are shown in Figures B1-4 and B1-5, respectively. The sectional view A-A shows the undulation of a yarns. The known quantities are assumed to be braid angle, θ_b (for weave, 45 degree), yarn spacing, d_o , yarn filament counts n , yarn packing density, p_d , filament diameter, d_f , and the thickness of each layer, H . Those known quantities were used to calculate the unknown quantities such as yarn thickness, yarn cross-sectional areas, yarn crimp angle, overall fiber volume fraction, and yarn undulating paths which are required to discretely model each yarn within the RUC. Here we assume that the fill and warp yarns are identical.

The yarn cross-sectional area, A , was assumed to remain constant along the entire yarn path. With the yarn filament counts, the yarn packing density, and filament diameter, the cross-sectional area could be calculated as

$$A = \frac{\pi d_f^2 n}{4 p_d} \quad (\text{B1-1})$$

Assuming a sinusoidal path, the yarn centerline path can be expressed as

$$Z_c = \pm \frac{H}{4} \sin \left[\frac{L_c \pi \sin(\theta_b)}{L_u} \right] \quad (B1-2)$$

where L_c is measured from the corresponding cross-over point, L_u is the projection of the undulating part of the yarn path. Since the cross-sectional areas of yarns can be written as

$$A = \frac{d_o H}{2} - L_u H \left(1 - \frac{2}{\pi} \right) \sin \theta_b \cos \theta_b \quad (B1-3)$$

we have the projection of the undulating part of the yarn paths from equation (B1-1) and (B1-3) as

$$L_u = \frac{d_o H - 2A}{(1 - 2/\pi) H \sin(2\theta_b)} \quad (B1-4)$$

Then the length of the each yarn can be obtained as

$$L = \frac{K d_o}{\sin(2\theta_b)} + 2 \left(\int_0^{L_u} Z(x) dx - L_u \right) \quad (B1-5)$$

where K is 2 for plain weave or plain 2D braid, 5 for 5-harness satin weave and 5-harness satin 2D braid, and 8 for 8-harness satin weave and 8-harness satin 2D braid. The overall fiber volume fraction becomes

$$V_f = \frac{2 p_d L A}{H d_o^2 K} \quad (B1-6)$$

and the crimp angle as

$$\tan(\theta_c) = \frac{H \pi}{2 L_u} \sin(2\theta_b) \quad (B1-7)$$

1x1, 2D triaxial braids

The RUC of a 2D 1x1 triaxial braids is shown in Figure B1-6. The sectional view A-A shows the undulation of a braider yarn which undulates over and under the axial yarns in the RUC. The known quantities are assumed to be braid angle, θ_b , axial yarn spacing, d_o , yarn filament counts for the axial and braider yarns, n_a and n_b , respectively, yarn packing density, p_d , filament diameter, d_f , and the thickness of each layer, H . Those known quantities were used to calculate the unknown quantities such as yarn thickness, yarn cross-sectional areas, yarn crimp angle, overall fiber volume fraction, and yarn undulating paths which are required to discretely model each yarn within the RUC.

The cross-sectional areas, A_a and A_b , for the axial and braider yarns, respectively, are assumed to remain constant along the entire yarn path. With the yarn filament counts, the yarn packing density, and filament diameter, the cross-sectional areas can be calculated as

$$A_a = \frac{\pi d_f^2 n_a}{4 p_{da}}, A_b = \frac{\pi d_f^2 n_b}{4 p_{db}} \quad (B1-8)$$

The projected lengths, L_a and L_b , of the axial and braider yarn paths are functions of the axial yarn spacing and braid angle, and can be given by

$$L_a = \frac{2d_o \cos(\theta_b)}{\sin(\theta_b)}, L_b = \frac{d_o}{\sin(\theta_b)} \quad (\text{B1-9})$$

respectively. Then the total volume occupied by the axial and braider yarns was given by $(A_a L_a + 4A_b L_b)$. Since the dimensions of the parallelepiped RUC are $L_b \times L_b \times H$, where H is the layer thickness, the overall fiber volume fraction can be calculated as

$$V_f = \frac{p_{da} A_a \cos(\theta_b) + p_{db} A_b \sin(\theta_b)}{H d_o \cos(\theta_b)} \quad (\text{B1-10})$$

if the ratio of the braider yarn thickness, t_b , to axial yarn thickness, t_a , is assumed to be m , we have

$$t_b = \frac{H}{2 + m} \quad (\text{B1-11})$$

This unknown thickness ratio is determined using cross-sectional areas. The braider yarn width, w_b (perpendicular to the yarn direction), is related to the axial yarn spacing by assuming the connection between axial yarns as $w_b = d_o \cos(\theta_b)$. The braider yarn centerline path, on the other hand, is described using sine function as

$$Z_c = \pm \frac{t_a + t_b}{2} \sin \left[\frac{L_c \pi \sin(\theta_b)}{L_u} \right] \quad (\text{B1-12})$$

where L_c was measured from the corresponding cross-over point. The parameter L_u , that is the projection of the undulating part of the yarn path, is related to the cross-sectional areas of axial and braider yarns as

$$A_a = w_a t_a - L_u (t_a + t_b) \left[1 - \frac{2}{\pi} (s + \cos(s)) \right] \quad (\text{B1-13})$$

$$A_b = w_b t_b - \left(\frac{2}{\pi} - 1 \right) \frac{L_u t_b \cos(\theta_b)}{1 + m} \quad (\text{B1-14})$$

$$s = \sin^{-1} \left(\frac{1}{1 + m} \right), w_a = \frac{d_o}{2} - 2s \frac{L_u}{\pi}$$

obviously, equations (B1-13) and (B1-14) has only two unknowns: m and L_u , an iteration scheme is employed to solve these equations, and then the total length of the straight portion of each braider yarn becomes

$$L_{st} = \frac{d_o}{\sin(\theta_b)} - L_u \left[1 + \frac{2 \cos(\theta_b)}{1 + m} \right] \quad (\text{B1-15})$$

and yarn crimp angle θ_c :

$$\tan(\theta_c) = \frac{(t_a + t_b) \pi}{2 L_u} \sin(\theta_b) \quad (\text{B1-16})$$

2x2, 2D triaxial braids

For 2D, 2x2 triaxial braids (see Figure B1-7), the known quantities are assumed to be braid angle, θ_b , axial yarn spacing, d_o , yarn filament counts for the axial and braid yarns, n_a and n_b , respectively, yarn packing density for axial and braid yarns, p_{da} and p_{db} , respectively, filament diameter, d_f , the thickness of each layer, H , and the axial yarn content, y_{av} . Those known quantities are used to calculate the unknown quantities such as yarn thickness, yarn cross-sectional areas, yarn crimp angle, overall fiber volume fraction, and yarn undulating paths which are required to discretely model each yarn within the RUC.

The length of total axial yarn and each braid yarn can be expressed as

$$L_a = 8d_o \cot(\theta_b) \text{ and } L_b = \frac{A_a L_a (1 - y_{av})}{8A_b y_{av}} \quad (\text{B1-17})$$

where A_a and A_b are the cross-sectional areas of axial and braid yarns

$$A_a = \frac{\pi d_f^2 n_a}{4 p_{da}}, A_b = \frac{\pi d_f^2 n_b}{4 p_{db}} \quad (\text{B1-18})$$

With a layer thickness H , the overall fiber volume fraction becomes:

$$V_f = \frac{L_a [p_{da} y_{pa} + (y_{pa} - 1) p_{db}]}{H d_o y_{pa}} \quad (\text{B1-19})$$

Following a similar procedure as 2D, 1x1 triaxial braids, we can form the equation for the yarn thickness ratio $m = t_a / t_b$ as

$$\frac{A_a - d_a H m / (2 + m)}{[(1 + m)(\cos s - \pi/2) + s]} = \frac{A_b - d_a H \cos \theta_b / (2 + m)}{[(1 + m)(1 - \cos s) - s]} \quad (\text{B1-20})$$

where $s = \sin^{-1}\left(\frac{1}{1 + m}\right)$.

We then can calculate the crimp angle as

$$\tan(\theta_c) = \frac{t_b^2 (1 + m) [(1 + m)(\cos s - \pi/2) + s]}{A_a - m d_o t_b} \quad (\text{B1-21})$$

and the projection of the undulating part of the braider yarn path as

$$L_u = \frac{(t_a + t_b) \pi}{2 \tan(\theta_c)} \quad (\text{B1-22})$$

3D spatially oriented composite

The geometry model for 3D spatially oriented composite was developed to describe composites which is made up of straight yarns oriented along different directions. The RUC of a example composite is shown in Figure B1-8. In the RUC of this composite each yarn becomes a yarn slice, and as always, all the interstitial matrix form a matrix slice.

Thermal and mechanical properties of RUC

All the analysis in this report is assumed to apply to the RUC, so that the analyzed specimen of textile composite is so large that all the thermal and mechanical properties computed with its RUC can be considered as the same of the whole specimen.

The overall composite properties are determined by discretizing all the yarns within the RUC. The straight portions of each yarn path are modeled as a single yarn slice. Along an undulating portion, the yarn is divided into piecewise straight slices made perpendicular to its in-plane direction. Thus, the sinusoidal yarn undulating portion is approximated by interconnected straight yarn slices.

The RUC of a textile composite was treated as a system consists of a set of spatially oriented yarn slices and an interstitial matrix material slice. The matrix is assumed to be isotropic, while the yarn slices transversely isotropic. For the m th material slice (yarn or matrix), the three dimensional stiffness matrix $[C']_m$ can always be calculated from given material constants (Young's modulus and Poisson's ratios). Assuming the strains are uniform inside RUC, the stress-strain relation becomes

$$\{\sigma\} = [C]\{\epsilon\} \quad (B1-23)$$

where the 6x6 matrix $[C]$ is the overall stiffness matrix of RUC, which can be expressed as a summation over all the N yarn and matrix slices in terms of the materials slices stiffness matrix:

$$[C] = \sum_{m=1}^N \left(V_m [T]_m^T [C']_m [T]_m \right) \quad (B1-24)$$

where V_m is the volume fraction of the m th material slice, matrix $[T]_m$ is the transformation between the global coordinates and the local coordinates of the m th material slice, and superscript T indicates transpose. With a given loading, the average strains in a RUC, that is also the strains of each material slice, can be calculated from equation (B1-23). The stress components in global coordinates of each material slice can be obtained and transformed to the local material coordinates as

$$\{\sigma\}_m = ([T]_m [C']_m [T]_m^T) \{\epsilon\} \quad (B1-25)$$

Thermal properties are also calculated based on the iso-strain assumption. For the m th material slice, thermal residual stresses are given by

$$\{\sigma_T\}_m = \Delta T [C']_m \left\{ [T]_m^T \{\bar{\alpha}\} - \{\alpha'\}_m \right\} \quad (B1-26)$$

where ΔT is the change in temperature from the stress free state, $\{\alpha'\}_m$ is the coefficients of thermal expansion (CTE) of the m th material slice and $\{\bar{\alpha}\}$ is assumed to be the overall CTE for the RUC, given as

$$\{\bar{\alpha}\} = [C]^{-1} \sum_{m=1}^N \left(V_m [T]_m^T [C']_m \{\alpha'\}_m \right) \quad (B1-27)$$

This formulation enables the calculation of stresses and strains of each material slice when the thermal or mechanical loads are given. This forms the foundation for the damage analysis and failure analysis of textile composites.

B1-3. Statistical Failure Criterion of Yarns

The geometry model of textile composites assumes that the RUC of a textile composite is a system consists of matrix and yarn slices. The geometry model has already considered the orientation and geometry shape of each material slice. For the matrix slice, since the matrix material is assumed to be isotropic, only the volume of one matrix slice is necessary for the geometry modeling, while for a yarn slice, other information like orientation and fiber volume fraction is also important. As we introduced above, the overall stiffness and coefficients of thermal expansion of the RUC, also of the textile composite, are calculated as a summation of all the material slices, the damage properties of the RUC, that are the stiffness reduction and strength of the RUC, are also calculated based on each individual material slice. In what follows we introduce a failure criterion of yarn slices under tension, based on micro-mechanics analysis and a statistical model.

A yarn slice is the same as a laminated composite. It consists of fibers and matrix. The failure criterion proposed here is based on the fiber pull-out concept of laminated composites. As shown in Figure B1-9, assuming the matrix has a crack and the fiber behaves as a bridge that has a traction T , the crack causes the sliding between the matrix and fiber over a length of l , and allows the fiber to open out of the matrix a distance u , that is also half of the crack opening. We assume that the slipping on the fiber-matrix interface is local, that is beyond the distance l , the matrix and fiber are continuous. Within the slipping distance, the stress is redistributed between the matrix and fiber through a shear stress τ on the fiber-matrix interface is called shear stress parameter.

Shear-lag Model

A shear-lag model developed by Marshall and Cox [5] was used in the present analysis to establish the relationship between the fiber traction and the crack opening displacements. This relation is then provided to the fracture mechanics analysis to determine the fiber traction.

As shown in Figure B1-9, assuming purely frictional fiber-matrix bond, the slipping distances can be determined by the length over which the interface shear stresses exceed the maximum shear stress the fiber-matrix interface can resist. The stress σ_m for matrix and σ_f for fiber under far-field stress σ_c can be related to each other by neglecting the effect of shear stress beyond the slipping distance, as

$$\sigma_m(l)/E_m = \sigma_f(l)/E_f \quad (\text{B1-28})$$

where E_m and E_f are longitudinal Young's modulus of matrix and fiber, respectively.

Assume the extension due to stress σ_c is δ for matrix, then the extension for fiber will be $u + \delta$, considering the equilibrium of the matrix and fiber separately, we have a set of equations as:

$$\sigma_m(z)A_m = 2\pi R_z \tau \quad (\text{B1-29})$$

$$TA_f = 2\pi R_z \tau + \sigma_f(z)A_f \quad (\text{B1-30})$$

$$\delta = \int_0^l \frac{\sigma_m(z)}{A_m E_m} dz, \quad (\delta + u) = \int_0^l \frac{\sigma_f(z)}{A_f E_f} dz \quad (\text{B1-31})$$

where R is the radius of the fiber, A_f is the fiber cross-section area, A_m is the area of matrix per fiber, or $A_f / (A_f + A_m) = V_f$ is the fiber volume fraction. Notice that in the slipping area, the shear stress on the fiber-matrix interface reaches its maximum value, the constant shear stress parameter, then equation (B1-31) becomes

$$\delta = \frac{\pi R l^2 \tau}{A_m E_m}, \quad (\delta + u) = \frac{T l}{E_f} - \frac{l^2 \tau}{R E_f} \quad (\text{B1-32})$$

This set of equations then gave the relation between the crack opening displacement and fiber traction as

$$u = \frac{R E_m (1 - V_f)}{4 E_f E_c \tau} T^2 \quad (\text{B1-33})$$

also we have the slipping length when the matrix crack is fully developed can be expressed as

$$\frac{2 l \tau}{a} = \frac{\sigma_c E_m (1 - V_f)}{E_c V_f} \quad (\text{B1-34})$$

and the fiber stress within the slipping region as

$$\sigma_f(z) = \frac{\sigma_c}{V_f} - \frac{2 \tau z}{a} \quad (\text{B1-35})$$

Fracture Mechanics Analysis

The fracture mechanics analysis is required to provide the relationship between the unknown crack opening displacement $u(x)$ and fiber bridge traction $T(x)$. As shown in Figure B1-9, considering a crack under far-field applied stress, σ_c , and a closure pressure, $p(x)$, the crack opening displacement $u(x)$ can be written [5] as:

$$u(x) = \frac{2 c \sigma_c}{\pi E_c} \int_0^1 \left[1 - \frac{p(t)}{\sigma_c} \right] \ln \left| \frac{\sqrt{1-t^2} + \sqrt{1-x^2}}{\sqrt{1+t^2} - \sqrt{1+x^2}} \right| dt \quad (\text{B1-36})$$

where the E_c is the longitudinal Young's Modulus of the composite (or yarn), c is the half crack length. The bridging pressure, $p(x)$, and the bridging traction $T(x)$ is related by the fiber volume fraction, V_f , as:

$$p(x) = V_f T(x) \quad (\text{B1-37})$$

Hence, the bridging traction $T(x)$ can be solved by using an iterative procedure from the following integral equation [3]:

$$\frac{R E_m (1 - V_f)}{4 E_f E_c \tau} T^2(x) = \frac{2 c \sigma_c}{\pi E_c} \left[\pi \sqrt{1-x^2} - \frac{V_f}{\sigma_c} \int_0^1 T(t) \ln \left| \frac{\sqrt{1-t^2} + \sqrt{1-x^2}}{\sqrt{1+t^2} - \sqrt{1+x^2}} \right| dt \right] \quad (\text{B1-38})$$

After the solving of bridging pressure, the stress intensity factor for yarn material, K , at the fiber-bridged crack can be calculated as:

$$K = 2\sqrt{\frac{c}{\pi}} \int_0^1 \frac{(\sigma_c - p(x))}{\sqrt{1-x^2}} dx \quad (B1-39)$$

The matrix stress intensity factor, K_m , can be related to K as:

$$K_m = K \sqrt{\frac{E_m}{(1-V_f)E_c}} \quad (B1-40)$$

where E_m is the matrix Young's modulus. With a given critical stress intensity factor of matrix, K_{1c} , crack propagation is predicted when

$$K_m \geq K_{1c} \quad (B1-41)$$

Statistical Failure Criterion

The Weibull distribution was used to describe the probability of fiber failure. The probability was defined as [6]

$$P_f = 1 - \exp \left[-2\pi a \int_{-\sigma_o}^{\sigma_f} \left(\frac{\sigma_f}{\sigma_o} \right)^m dz \right] \quad (B1-42)$$

where M is the Weibull modulus and σ_o is the mean fiber strength, both are material constants. Substituting equations (B1-34) and (B1-35) in (B1-42), we have

$$P_f = 1 - \exp \left\{ \frac{\pi a^2 \sigma_c^{m+1}}{(m+1)\tau \sigma_o^m V_f^{m+1}} \left[\left(1 - \frac{E_m(1-V_f)}{E_c} \right)^{m+1} - \left(1 + \frac{E_m(1-V_f)}{E_c} \right)^{m+1} \right] \right\} \quad (B1-43)$$

With a given critical value P_{fc} , the fiber failure criterion, or the yarn failure criterion, was set to be

$$P_f \geq P_{fc} \quad (B1-44)$$

B1-4. Failure Criteria and Stiffness Reduction

The statistical failure criterion and other maximum stress or maximum strain strength criteria are combined together to predict the failure of individual material slice and overall textile composite. The maximum stress or maximum strain criteria are adopted from TEXCAD code developed by Naik [3]. The failure criterion in equation (B1-44) is added to predict the tensile failure of yarn slices only. A matrix crack development model is also added for the transverse tensile failure for yarn slices and tensile failure of matrix slices. Textile composite failure is reached when the stiffness corresponding to each load is less than a critical value.

Failure criteria for yarn slice

Yarn material slices failures are divided into matrix dominated failure and fiber dominated failure. Shear failures in all direction and transverse failures belong to matrix dominated failure, and only tensile or compressive failure in the fiber direction are considered as fiber dominated failure.

For matrix dominated yarn slices failure, maximum stress criteria are used, the critical values are user inputted material parameters. For fiber dominated yarn slices failure, when the fracture mechanics model is used, the statistical failure criterion is employed, while for no-fracture mechanics model, the maximum strain criterion is used. The critical values, that is the

maximum and minimum strains are user supplied parameters, and the failure probability is given in the code.

Failure criteria for matrix slice

For matrix material slices, when the in-plane shear load is not applied, the maximum octahedral stress criterion are used. The critical value is calculated from the inputted matrix material strengths.

When there is no in-plane shear load, two failure criteria are employed. In addition to the octahedral stress criterion, a maximum principal stress criterion is used to judge the matrix failure. For fracture model, when the maximum principle stress is tension, the critical value for the maximum principle stress criterion is the stress at which the initial cracks in matrix material as a uniform material start to develop. When no-fracture model is chosen or the maximum principal stress is negative (compressive), the material strength of the matrix is used as the critical value.

Nonlinear Material

The nonlinear response of textile composites in MicroTex came from two sources. The first source is the assumed nonlinear material (matrix and yarns). The user of MicroTex code could chose linear or nonlinear materials. When nonlinear material was chosen, the Young's modulus and shear modulus of the matrix and yarn material was assumed to obey following form:

$$E = E_0 \left[1 + \left(\frac{s}{\beta s_c} \right)^\alpha \right]^{-\left(1 + \frac{1}{\alpha} \right)} \quad (B1-45)$$

where E_0 represents the initial Young's modulus or shear modulus, S is the corresponding stress level, s_c is the critical values of failure criteria used, α and β are empirical constants, for matrix slices, β is taken as unity. For transverse Young's modulus and shear modulus (which are dominated by the matrix behavior) of yarn slices, the empirical constants α and β are taken the same as the matrix slice.

When the fracture mechanics model is chosen, the yarn material properties in fiber direction changes due to the matrix crack development. This affect is included by assuming the Young's modulus in fiber direction of the matrix in yarn slices obeys equation (B1-45), where, of course, β is unity and s_c is the stress at which the fiber bridged crack develops.

Stiffness Reduction due to slice failure

The other source of stiffness reduction comes from material slice failure. When a material slice is failed based on judgments mentioned above in this section, the Young's moduli and shear moduli are reduced coordinately. For matrix material slices, all the moduli are reduced 99% when slice failure is reached. For yarn slices with matrix dominated failure, the corresponding Young's modulus and shear modulus are reduced to 1%, and for yarn slices, with fiber dominated failure, only the Young's modulus in fiber direction is reduced 99%.

Failure criteria for textile composites

The failure of textile composites is judged using the same concept as a structure failure. The textile composites are considered as systems of matrix slices and yarn slices, or a structure its components are material slices. A structure is failed when it cannot carry some kind of

loading, and here a textile composite is failed when the RUC of a textile composite cannot carry some kind of loading . In MiroTex, the composite failure is reached when the stiffness in the loading direction is reduced to a critical value, like 10% of the original value. This critical value is a user input parameter.

B1-5. Numerical Examples for Textile Composites

Numerical examples for various textile composites under various loading are given in this section. The textile architectures studied include laminated composites, 2D triaxial braided composites, and plain weave composites. The materials involved include C/SiC, Graphite/Epoxy, and Nicalon/CAS. The loading includes tension, compression, shear, and temperature change. The results include geometry parameters, overall stiffness, overall coefficients of thermal expansion, strengths, strain-stress relations, and stiffness reduction. The results are compared with available test data. Also in this chapter, the effect of some parameters are investigated.

Some of the material parameters are fixed in all the following examples. They are the Weibull modulus $M=10.0$, the mean fiber strength $\sigma_o = 388.4 \text{ MPa} - m^{(2/m)}$, and the fiber failure probability $P_{fc} = 0.6$.

Tension Failure of Laminated Composites

The laminated composite is treated as a special case of textile composite in MicroTex, that is, layered yarns. Figures B1-10 shows the stress-strain results for Nicalon/CAS laminate composites under tension. The comparison with experimental results[3] was performed for room temperature (25°C) and 400°C, respectively. The mechanical and thermal properties for Nicalon fiber and CAS matrix are given in Table B1-1 (where values in () represent properties at 400°C)[3]. Significant agreement for damage progress and ultimate failure was obtained, the predicted strength and ultimate strain for room temperature case are 380.0MPa and 1.007%, and 390.0MPa and 1.354% for 400°C case. The shear stress parameter is taken as 0.4 in room temperature case and 0.7 in 400°C case, and the composite failure stiffness is assumed as 1% of the initial stiffness. The two nonlinear parameters for yarn (α and β) are taken to be 4.3 and 0.63 for both cases. The increase of shear stress parameter with the increase of temperature is reasonable because the Nicalon/CAS material has a compressive radial thermal stresses at the fiber-matrix interface with increasing temperature.

Table B1-1 Nicalon fiber and CAS matrix thermal and mechanical properties.

Fiber Properties	Matrix Properties
$E_f = 195 \text{ GPa}$ (175 GPa)	$E_m = 95 \text{ GPa}$ (94 GPa)
$\nu_f = 0.2$	$\nu_m = 0.3$
$\alpha_f = 3.0e-06 / ^\circ \text{C}$ (4.0e-06 / °C)	$\alpha_m = 5.0e-06 / ^\circ \text{C}$
	$K_{lc} = 2.16 \text{ MPa}\sqrt{m}$ (1.73 MPa√m)

2D triaxial braided composites

Experimental results for 2D triaxial braided Graphite/Epoxy composites with different architectures under uniaxial or biaxial tension and compression [7-9] are compared to MicroTex predictions. Two sets of notation are used to describe each individual architecture[7]. The first is

a shorthand notation consisting of three letters, the second one is a longhand notation which describes in detail the construction of the braid as shown in Figure B1-11. The first number in the longhand notation indicates the angle for the axial yarns with respect to the longitudinal axis, its subscript designates the size of the axial yarns in thousands of fibers. The second number indicates the angles of the braid yarns with respect to the longitudinal axis; its subscript designates the size of the braid yarns in thousands of fibers. The subscript outside the brackets is the percent of the total volume fraction of the yarns occupied by axial yarns.

Uniaxial tension failure of 2D triaxial braided Graphite/Epoxy composites

Burr and Morris [7] gave experimental data for 2D triaxial braided composites subject to uniaxial tension. The materials are Graphite fiber and Epoxy matrix. Four different braided architectures, so-called LLL, SLL, LLS, and SSL, were investigated. The corresponding shorthand and longhand notation and geometry parameters used in this calculation are listed in Table B1-2, and the calculated geometry parameters of the RUC are given Table B1-3. Since there are no details of material properties, the data from reference [8] are adopted and listed in Table B1-4, and the yarn fiber volume fractions are taken as 0.75. The predicted Young's moduli of the four architectures gives good agreement with the test data (Figure B1-12), that indicate this adoption is reasonable. The comparison of the present strain-stress results with the testing data are shown in Figure B1-13. The shear stress parameters used in the analysis, and the comparison of strengths and ultimate strains are given in Table B1-5. Since only one tension test for each architecture is available, the shear stress parameters in both axial and braided yarns are assumed to be the same.

Table B1-2. Architecture parameters for 2D triaxial braided composites

Architecture	Axial yarn size(K)	Braid yarn size(K)	Braid angle (degree)	Axial Yarn spacing	Axial yarn percentage	Layer thickness
LSS	6	15	45.0	6.95mm	12%	0.500mm
LLS	36	15	45.0	5.35 mm	46%	0.927mm
SLL	30	6	70.0	6.1mm	46%	0.605mm
LLL	75	15	70.0	11.2 mm	46%	0.935mm

Table B1-3. Calculated geometry parameters for 2D triaxial braided composites

Architecture	Axial yarn thickness	Braid yarn thickness	Crimp angle (degree)	Axial Yarn length	Braid yarn length	Volume fraction
LSS	0.36 mm	0.07 mm	3.22	47.60 mm	17.45 mm	0.65
LLS	0.66 mm	0.13 mm	11.68	42.80 mm	15.07 mm	0.61
SLL	0.43 mm	0.09 mm	7.74	17.76 mm	13.03 mm	0.68
LLL	0.67 mm	0.13 mm	5.61	32.61 mm	23.93 mm	0.60

Table B1-4. Yarn and matrix properties used for 2D triaxial braided composites

Material	E_{11} (GPa)	E_{22} (GPa)	G_{12} (GPa)	ν_{12}	ν_{23}	$\alpha_{11}(10^{-6}/^{\circ}C)$	$\alpha_{22}(10^{-6}/^{\circ}C)$
Yarn	144.80	11.73	5.52	0.23	0.30	-0.324	14.0
Matrix	3.45	3.45	1.28	0.35	0.35	40.0	40.0

Table B1-5. Failure Strength and ultimate strain for 2-D braided composite under tension.

Architecture	Shear Stress Parameter(MPa)	Failure Strength (MPa)		Failure Strain (%)	
		exp.[7]	present	exp.[7]	present
LSS	1.5	370.0	370.0	1.24	1.50
LLS	0.6	644.5	640.0	0.91	1.11
SLL	3.0	843.5	840.0	1.33	1.33
LLL	0.006	487.1	490.0	0.93	0.89

Both experiment and prediction indicate for LLS, SLL, and LLL architectures, the load-response is very linear, while for LSS case, the response is nonlinear (Figure B1-13). The analysis indicates the non-linearity of LSS architecture is due to the large shear stresses in braid yarns. Figure B1-14 shows the decrease of tangent axial modulus and failure information for LSS architecture. It indicates that the in-plane shear failure in braided yarns contributes to the non-linearity.

Biaxial tension failure of 2D triaxial braided AS4/1895 composites

Swanson and Smith [9] reported the experimental results of four different braided architectures consisting of AS4/1895 carbon fibers and epoxy matrix subject to biaxial tension loads. The yarn and matrix properties are given in Table B1-6 as AS4/3501-6 lamina with a fiber volume fraction of 0.60. The measured crimp angles given in reference [9] are used in calculating the necessary input data for the MicroTex analysis. Tables B1-7 and B1-8 give the input geometry parameters and calculated dimensions from MicroTex. The predicted axial and hoop stiffness and the in-plane Poisson's ratios are compared with testing data for four different architectures in Figures B1-15 to B1-17. Reasonable agreement can be observed.

MicroTex was then used to predict the composite strength under biaxial tension. The shear stress parameters of axial yarn and braid yarns are assumed to be different, and determined using experimental results for uniaxial tension in the axial and hoop direction, respectively. The obtained shear stress parameters are listed in Table B1-9. The shear stress parameters are then used to predict the strengths of the four different architectures, and the results were compared with testing data in Figures B1-18 to B1-21. The agreement between experimental results and predictions is reasonable for all four architectures under various axial stress and hoop stress ratios.

Table B1-6. Yarn and resin properties used for 2D triaxial braided composites

Material	E_{11} (GPa)	E_{22} (GPa)	G_{12} (GPa)	ν_{12}	ν_{23}
Yarn	127.0	11.0	6.55	0.28	0.30
Matrix	3.45	3.45	1.28	0.35	0.35

Table B1-7. Architecture parameters for 2D triaxial braided composites

Architecture	Axial yarn size(K)	Braid yarn size(K)	Braid angle (degree)	Axial Yarn spacing	Axial yarn percentage	Layer thickness
LSS	9	12	47.0	4.65 mm	20%	0.79 mm
LLS	27	12	45.0	4.54 mm	44%	1.06 mm
SLL	33	6	73.0	9.73 mm	35%	0.64 mm
LLL	54	12	70.0	9.21 mm	43%	1.06 mm

Table B1-8. Calculated geometry parameters for 2D triaxial braided composites

Architecture	Axial yarn thickness	Braid yarn thickness	Crimp angle (degree)	Axial Yarn length	Braid yarn length	Volume fraction
LSS	0.57 mm	0.12 mm	7.11	34.69 mm	13.01 mm	0.47
LLS	0.76 mm	0.15 mm	15.04	36.32 mm	13.00 mm	0.49
SLL	0.46 mm	0.91 mm	4.10	23.80 mm	14.82 mm	0.58
LLL	0.76 mm	0.15 mm	7.44	26.82 mm	20.00 mm	0.50

Table B1-9. Shear stress parameters for 2D triaxial braided composites

Architecture	Shear stress parameter for axial yarns (MPa)	Shear stress parameter for braid yarns (MPa)
LSS	0.60	3.0e-06
LLS	0.12	1.0e-08
SLL	0.50	2.0e-08
LLL	0.012	5.0e-07

Plain weave composite under in-plane shear stress

2-D plain weave composites under tension, compression, and shear loading[8] are analyzed here using MicroTex. The fiber is Hercules AS4 graphite and the matrix is Hercules 3501-6 epoxy, and yarn fiber volume fraction is 0.70, the material properties are given in Table B1-4. The results are compared with testing data[8] in Table B1-10 for strengths and stress-strain relation in Figures B1-22 and B1-23. The shear stress parameters in those calculation were taken as 0.3MPa.

Table B1-10. Comparison of results for plain weave composites

Axial yarn size(K)	Fiber volume fraction	Axial Yarn spacing	Loading	Strength (MPa)	
				Testing	Prediction
3	60.0%	2.22 mm	Tension	753	680
			Compression		620
			Shear	103	104
12	52.2%	3.33 mm	Tension		650
			Compression		590
			Shear	100	81
3	62.0%	2.22 mm	Tension	690	710
			Compression	656	640
			Shear		102

Plain weave C/SiC composites under tension

Testing and analysis on C/SiC plain weave composites under uniaxial tension were performed at AS&M. The material properties for T300 fiber and SiC matrix are listed in Table B1-11, and also the input and calculated geometry parameters in Tables B1-12 and B1-13. The testing data for the two-layer (0/90) plain weave composite are employed to determine the shear stress parameter (we assume that the warp and fill yarns are identical, thus the shear stress parameters for those two yarns are the same) and other parameters like nonlinear parameters for yarns and matrix; the agreement is excellent as shown in Figure B1-24. Those parameters are

then applied to predict the strain-stress relation and strength for the three-layered (0/-60/60) C/SiC plain weave composite, the results are compared in Figures B1-25 with the experimental results. The prediction indicated that the failure of the (0/+60/-60) composite is due to in-plane shear stresses. Considering the assumption of identical warp and fill yarns, the results is reasonable.

The MicroTex code is then employed to analyze the failure processes of this composite under tension at different directions. The results are shown in Figure B1-26. The strength is largely reduced when the applied load is off axial. For axial load (0°), the failure is due to tension failure in loading direction, the strength is 502MPa and the ultimate strain is 0.1235%. For all the others, in-plane shear failure of the yarns causes the composite failure. Also the stress-strain results of two-layer angle-ply plain weave composite are shown in Figure B-27.

Table B1-11. Fiber and matrix properties used for C/SiC Plain weave composites

Material	Young's Modulus (GPa)	Possion's ratio
Fiber	231.0	0.20
Matrix	3.51	0.22

Table B1-12. Architecture parameters for C/SiC plain weave composites

Yarn size(K)	Braid angle	Yarn spacing	Yarn fiber volume fraction	Layer thickness
1	47.0	3.22 mm	0.6	0.60 mm

Table B1-13. Calculated geometry parameters for C/SiC plain weave composites

Yarn thickness	Crimp angle	Yarn length	Volume fraction
0.30 mm	2.26	6.40 mm	0.40

The tension strength of plain weave composites with different crimp angles are given in Figure B1-28 and compared with the laminate composite case. It can be seen that the increase of crimp angle will decrease the composite strength. Detailed analysis also indicated that, when the crimp angle is less than 10° , the composite failure is caused by loading direction tension. When the crimp angle is larger than 10° , failure is caused by local transverse shear failure of axial yarns.

B1-6. Fatigue Simulations for Plain Weave Composites

It is well-known that fatigue analysis is experimental orientated, that experimental works play an critical role. Fatigue testing was performed in this project for both (0/90) and (0/-60/60) C/SiC plain weave composites. The stress ratio and frequency for both cases are 0.1 and 5Hz, respectively. In this section, a fatigue damage model was developed based on the observation of experimental data. This model assumed that the stiffness reduction during the fatigue process contains all the information about the effect of fatigue damage to material strength, and assumed, for simplicity, that the fatigue damage to all the materials (matrix and yarn materials) are proportional.

The fatigue model

The mean strength in the Weibull distribution and all the critical values in material failure criteria are related to the stiffness reduction of the composite to reflect the affect of fatigue loading on the composite strength. They can be expressed as

$$\sigma_N = \sigma_o \left(\frac{E}{E_0} \right)^{M(b_1 + b_2 \sigma_{\max}) \sigma_s} \quad (B1-46)$$

$$\sigma_{cN} = \sigma_c \left(\frac{E}{E_0} \right)^{M(b_1 + b_2 \sigma_{\max}) \sigma_s} \quad (B1-47)$$

where b_1 and b_2 are parameters, M is the Weibull modulus, σ_{\max} is the maximum loading, E/E_0 is the overall stiffness reduction, σ_o is the mean strength of the yarn material, and σ_N is the mean strength after N cycles, σ_c is the original critical value in any failure criteria, and σ_{cN} the critical value after N cycles, and σ_s is the static strength of composite.

Stiffness reduction due to fatigue damage

Fatigue testing for the C/SiC (0/90) plain weave composite analyzed in previous section was performed. Based on the observation of testing data, the stiffness reduction for (0/90) C/SiC plain weave composite under fatigue loading is assumed as:

$$\frac{E}{E_o} = \frac{1}{1 + (c_1 + c_2 \sigma_{\max}) \text{Log}(N)} \quad (B1-48)$$

where N is the number of cycle, σ_{\max} is the maximum stress, c_1 and c_2 are material constants to be determined by experimental data.

Fatigue results

The parameters in equations (B1-46) and (B1-47) are determined from experimental stiffness reduction data and the S-N curve for (0/90) composite. Then those parameters are substituted into these two equations to predict the fatigue damage for (0/-60/60) composite.

Using the stiffness reduction data for (0/90) composite, the two parameters in equation (B1-48) were determined as:

$$c_1 = -1.54e - 02, \quad c_2 = 7.32e - 05 \text{ /MPa}$$

The comparisons of stiffness reductions for maximum stress at 458.85MPa and 410.6MPa were given in Figures B1-29 and B1-30 as examples.

The S-N data of (0/90) composite are then used to determine two constants in equations (B1-46) and (B1-47) with the help of equation (B1-48) which provides the stiffness reduction relation. The two coefficient were obtained as

$$b_1 = 0.0415 \text{ /MPa}, \quad b_2 = -8.22e - 05$$

The comparison with testing data was shown in Figure B1-31.

The four parameters and the static strength of (0/-60/60) C/SiC composite, which were obtained in the previous section as 272.0MPa (experimental strength 289.8MPa), are used to predict the fatigue curve for (0/-60/60) C/SiC plain weave composite. The predicted S-N curve is compared with experimental result in Figure B1-32, and predicted stiffness reductions for maximum stress at 248.0MPa and 258.0MPa are shown in Figure B1-33.

Discussion

Since all the fatigue testing were performed under same stress ratio and frequency, we were unable to include two very important parameters in this model. As a consequence, the static strength is used as one point in the S-N curve.

B1-7. Conclusions

Geometry models for various textile composites are presented in this section. The RUC is used to represent the textile composite by taking advantage of the periodically repeating pattern of textile composite materials. The RUC is represented by a set of yarn and matrix slices based on the sinusoidal assumption of the undulation portion of the yarn paths. Thermal and mechanical properties calculation of the RUC are then carried out based on an iso-strain assumption.

An analytical approach based on fracture mechanics, shear-lag theory, and fiber pull-out concept is developed for a statistical failure criterion of the yarn slice under tension. Statistical analysis based on the fiber pull-out concept is used as a yarn failure criterion, while shear-lag analysis and fracture mechanics are employed to determine relations needed for statistical computation.

Stiffness reduction of RUC comes from the material non-linearity and the failure of material slices. The complete set of failure criteria, including the statistical criterion, is proposed for yarn and matrix slices within the RUC. When a material slice failure is reached, the corresponding moduli are reduced.

A textile composite analysis code, named MicroTex, has been developed by following the above mentioned engineering approach. The following capabilities were included: geometry analysis for various textile composite architectures; calculation of mechanical and thermal properties, such as overall Young's moduli, Poisson's ratios, and coefficients of thermal expansion for RUCs; calculation of strains and local stresses using plate theory or 3D iso-strain model; local material slice failure judgment; stiffness reduction due to material slice failure and non-linear material properties; and overall composite failure judgment.

The textile composite or its RUC is considered as a structure with yarn and matrix slices as its components. When this structure can not resist some kind of loading, the composite or RUC reaches its failure point.

Fatigue analysis is performed based on the assumption that simple fatigue test for the same textile composite is performed.

The prediction based on above analysis are compared with experimental results for laminate composites, plain weave composites under uniaxial loading, and various 2D triaxial braided composites under both uniaxial and biaxial tensions. The agreement is reasonable.

B1-8. Reference

1. R. A. Naik: "Failure analysis of woven and braided fabric reinforced composite", Journal of Composite Materials, Vol. 29, No. 17, pp. 2334-2363, 1995.
2. R. A. Naik: "Analysis of weave and braided fabric reinforced composite," NASA Contractor Report 194930, June, 1994, National Aeronautics and Space Administration, Hampton, VA.
3. R. A. Naik: "A combined micromechanics, fracture mechanics, and statistical approach for life prediction of ceramic matrix and metal matrix composites", Final Report, NASA NSFC Phase I SBIR Contract Number NAS8-40505, 1995
4. B. R. Marshall and B. N. Cox: "The mechanics of matrix cracking in brittle-matrix fiber composites," Acta Metall., Vol. 33, No. 11, pp. 2013-2021, 1985.
5. L. N. McCartney: "Mechanics of matrix cracking in brittle-matrix fiber-reinforced composites," Proceedings of the Royal Society of London, A409, pp. 329-350, 1987.
6. M. Sutcu, "Weibull statistics applied to fiber failure in ceramic composite and work of fracture," Acta Metal., Vol. 37, No. 2, pp. 651-661, 1989.
7. S. T. Burr and D. H. Morris: "Characterization of two-dimensionally braided composites subject to static and fatigue loading", Mechanics of Textile Composite Conference, NASA CP 3311, Part1, Hampton, VA, Dec. 6-8, 1994.
8. R. A. Naik, P. G. Ifju, and J. E. Masters: "Effect of fiber architecture parameters on deformation field and elastic moduli of 2D braided composites," Journal of Composite Materials, Vol. 28, No. 7, pp. 656-681, 1994.
9. S. R. Swanson and L. V. Smith: "Multiaxial stiffness and strength characterization of 2D braid carbon/epoxy fiber composite", Mechanics of Textile Composite Conference, NASA CP 3311, Part1, Hampton, VA, Dec. 6-8, 1994

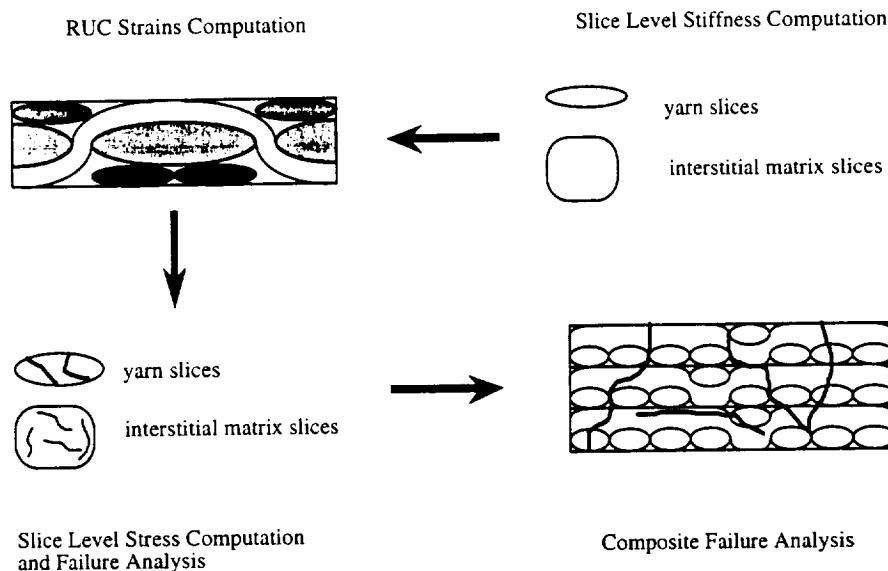


Figure B1-1. MicroTex for textile composites analysis

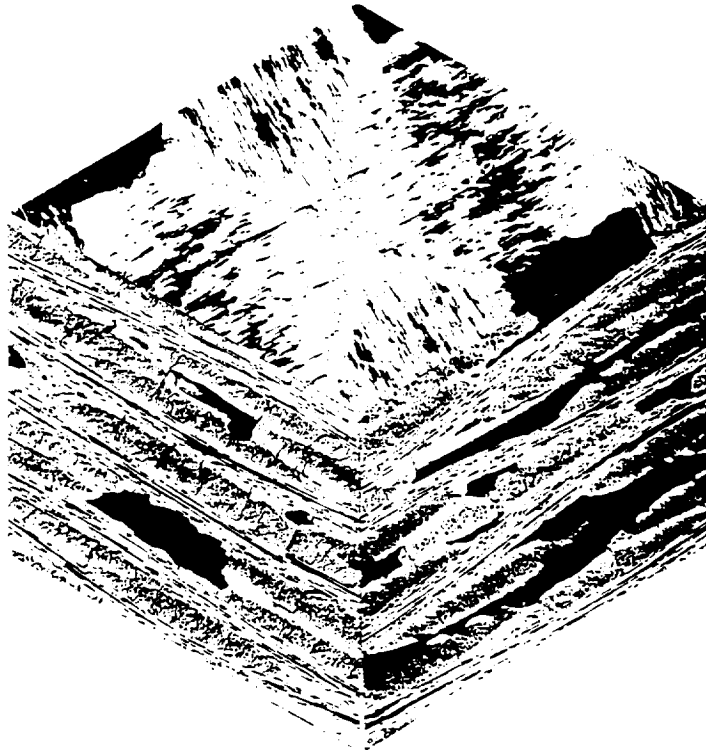
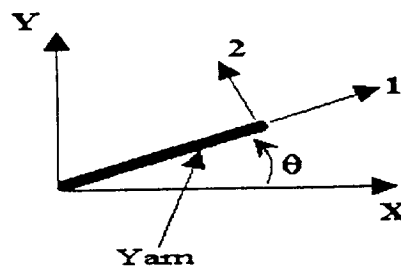


Figure B1-2. A 3D micro-graph of C/SiC plain weave composites

COORDINATE SYSTEMS FOR 2-D LAMINATE



- 1-2-3 Coordinates refer to yarn material coordinates. The 2-axis is assumed to be always perpendicular to the Z-axis.

Figure B1-3. 2D laminated composite and coordinate systems

UNIT CEL FOR 5-HARNESS SATIN WEAVE

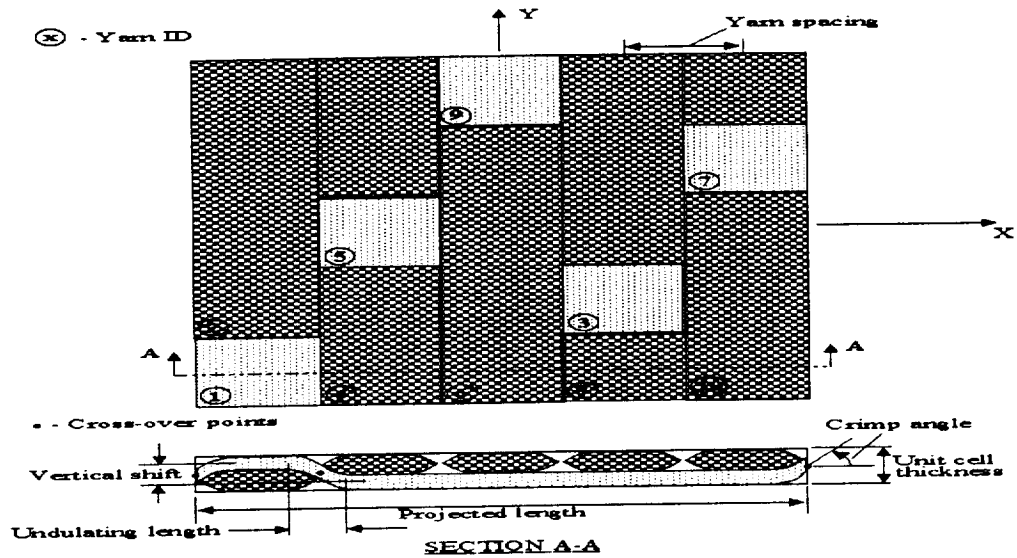
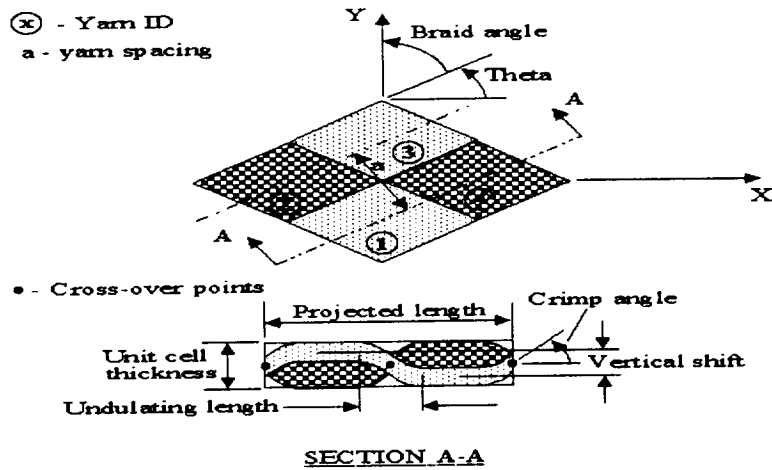


Figure B1-4. RUC of 5-harness satin weave composite

UNIT CELL FOR 2-D BRAIDED COMPOSITE



UNIT CELL MODEL FOR 1x1 2-D TRIAXIAL BRAID

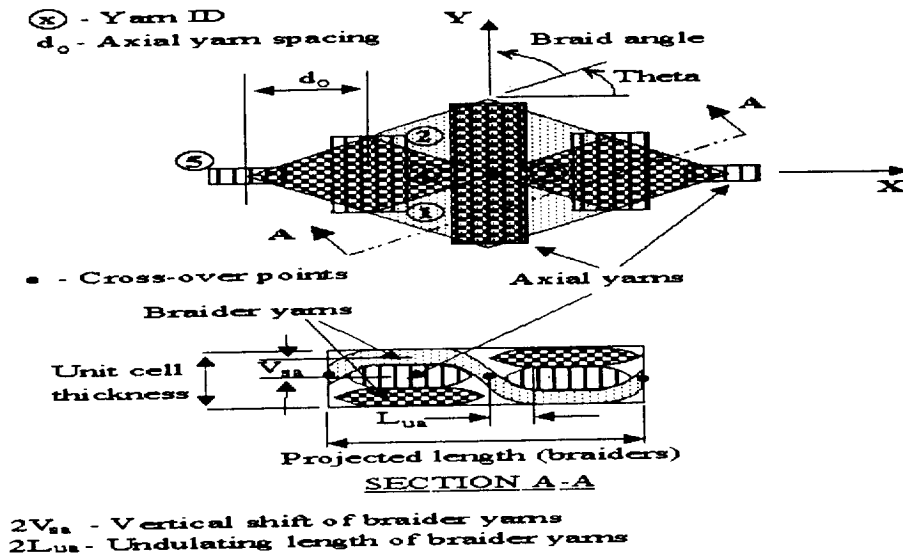


Figure B1-6. RUC of 2D, 1x1 triaxial braid composite

UNIT CELL FOR 2x2, 2-D TRIAXIAL BRAID

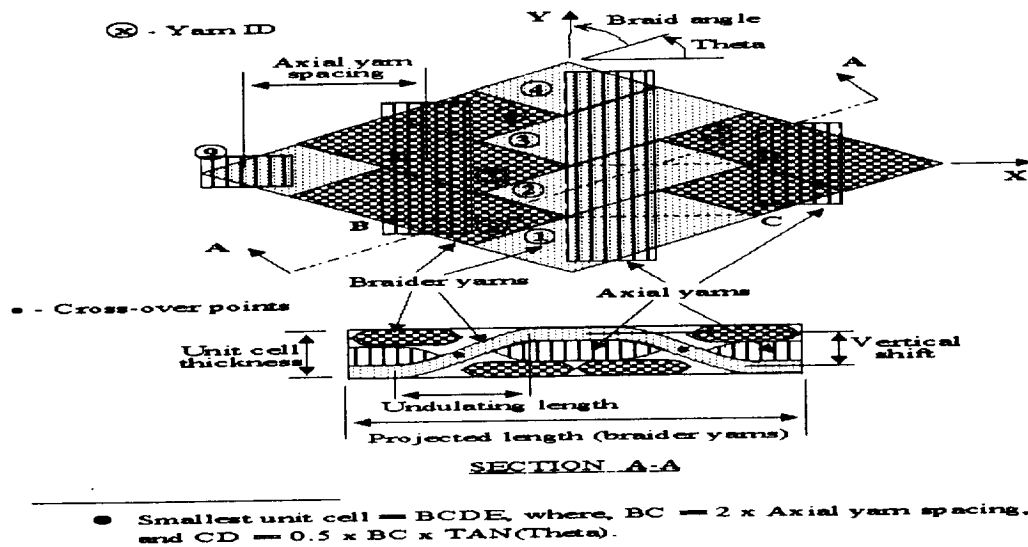
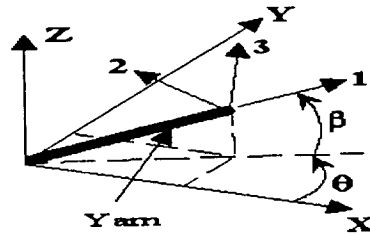


Figure B1-7. RUC of 2D, 2x2 triaxial braid composite

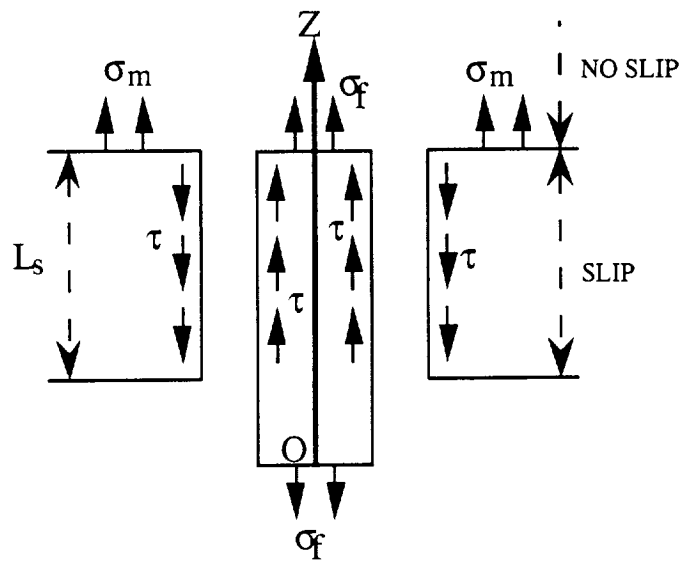
ORIENTATION ANGLES FOR 3-D COMPOSITE



- 1-2-3 Coordinates refer to yarn material coordinates. The 2-axis is assumed to be always perpendicular to the Z-axis.

Figure B1-8. 3D oriented composite

Shear-lag analysis



Fracture mechanics analysis

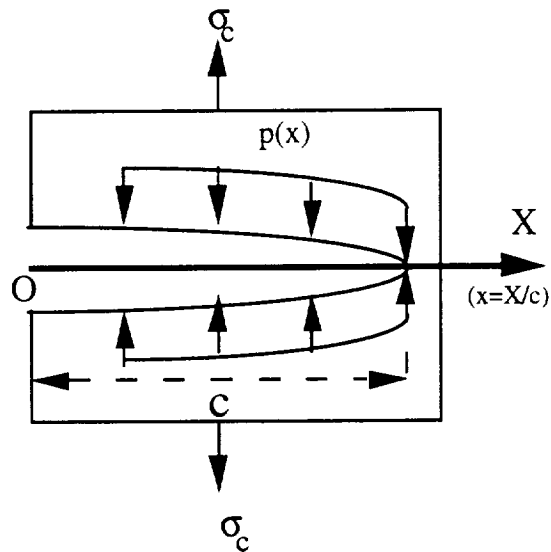


Figure B1-9. Shear-lag analysis and fracture mechanics model

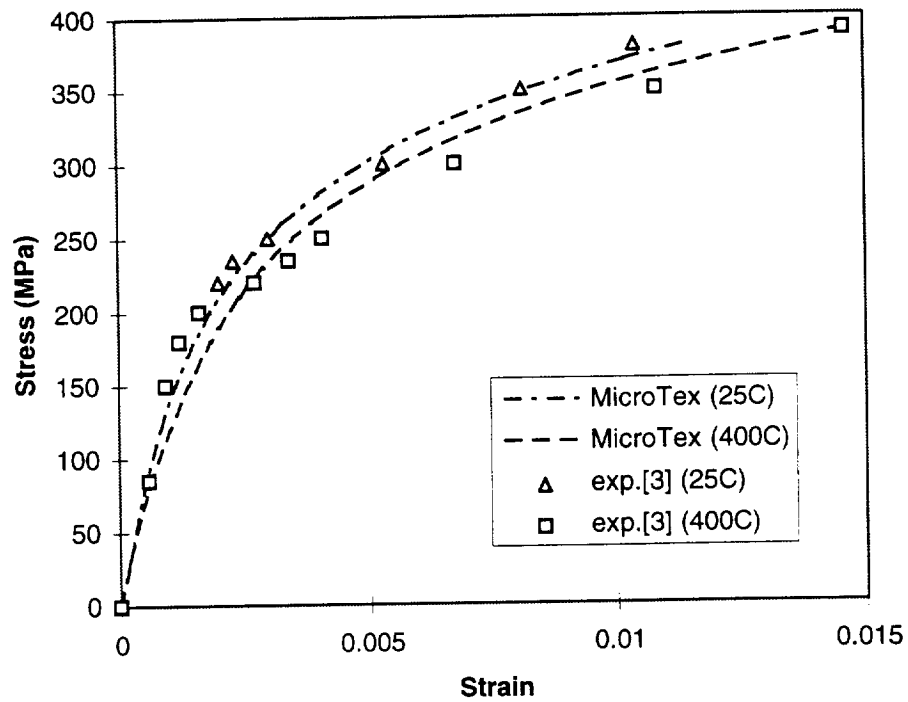


Figure B1-10. Stress-strain Result for Nicalon/CAS laminate composite under tension

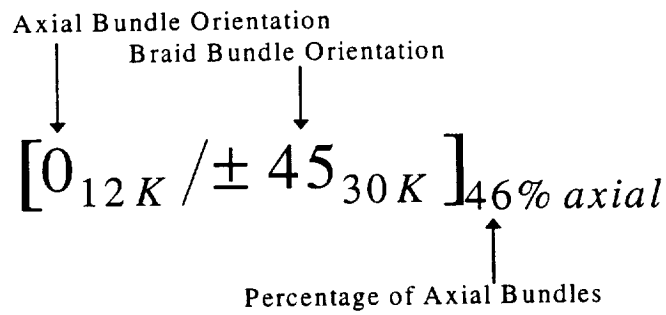


Figure B1-11. Longhand nomenclature for 2D triaxial braided composites

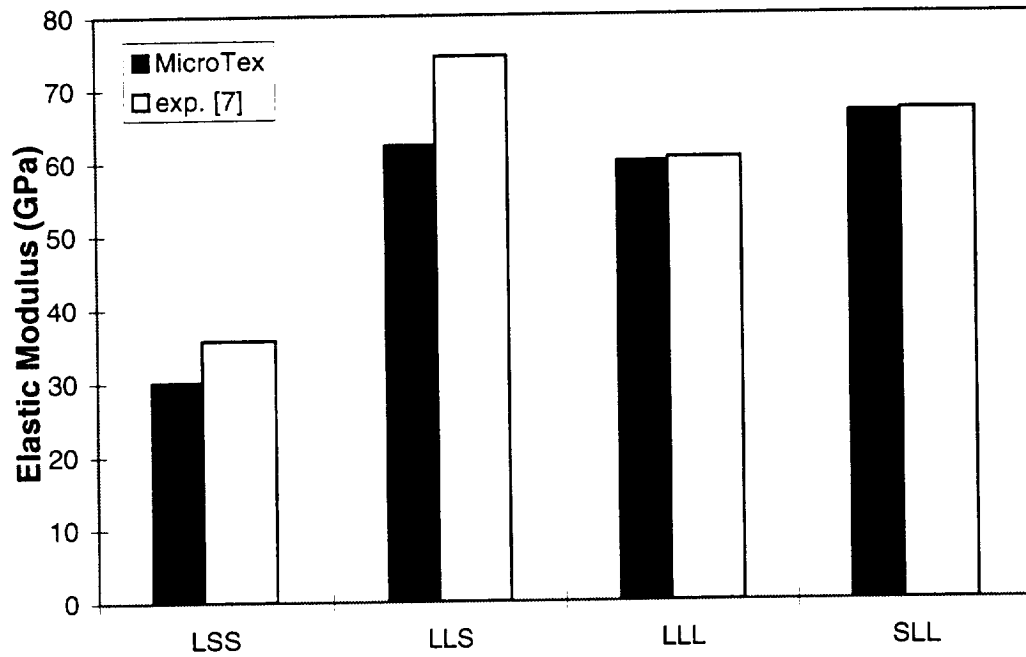


Figure B1-12. Elastic moduli for 2D triaxial braided Graphite/Epoxy composites

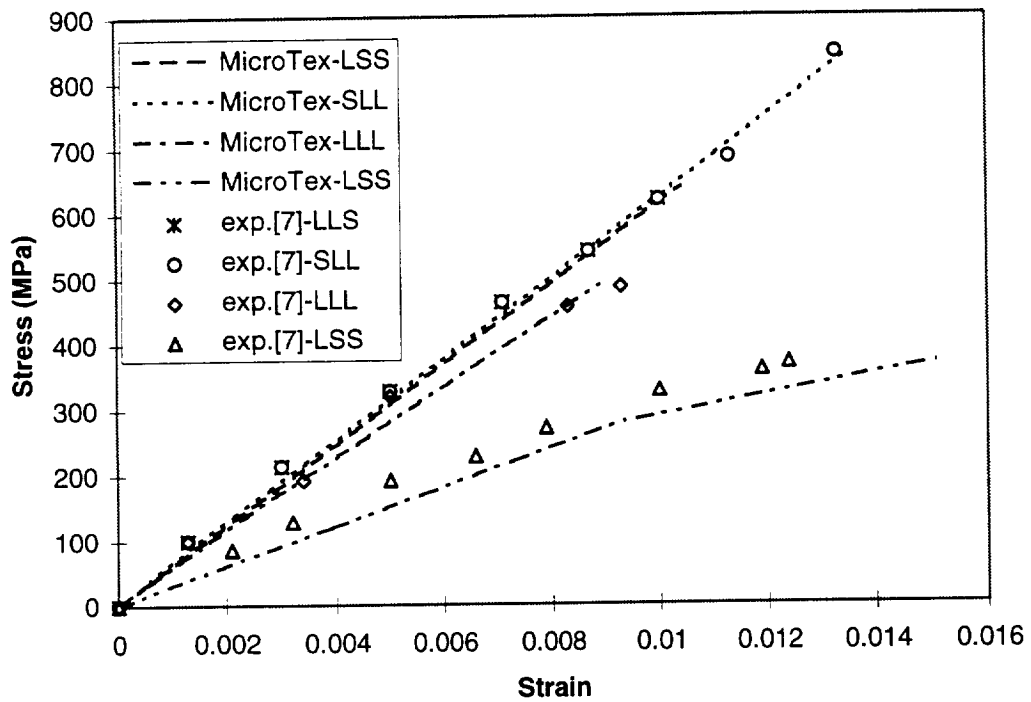


Figure B1-13. Stress-strain results for 2D triaxial braided Graphite/Epoxy composites

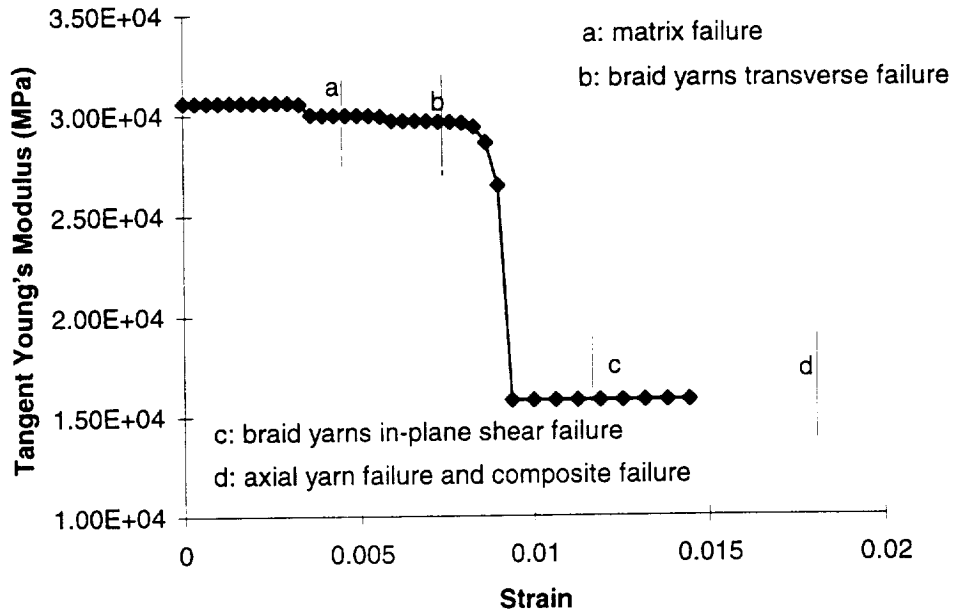


Figure B1-14. Failure process for 2D triaxial braided composite: architecture SLL

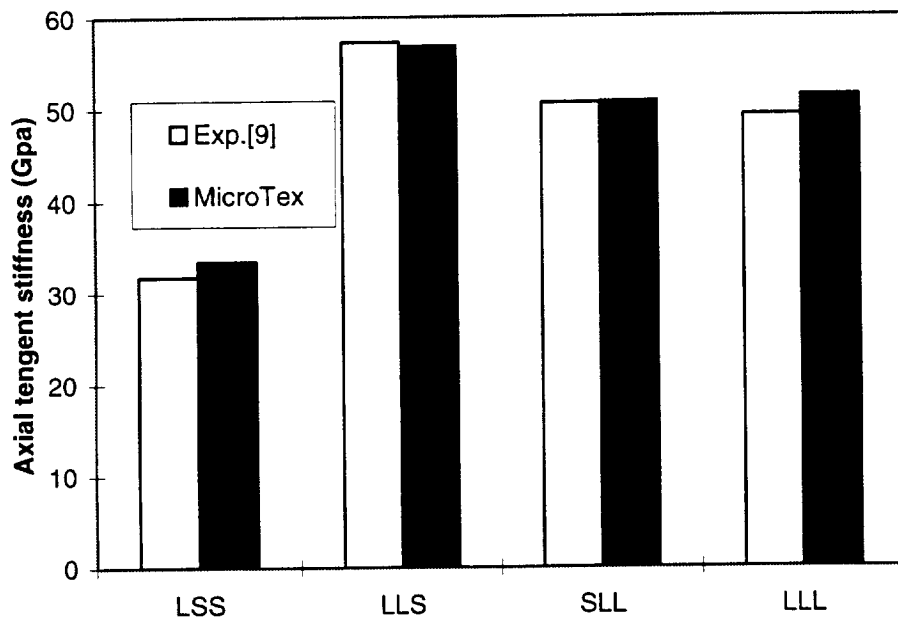


Figure B1-15. Comparison of axial Young's moduli for 2D triaxial braid composites

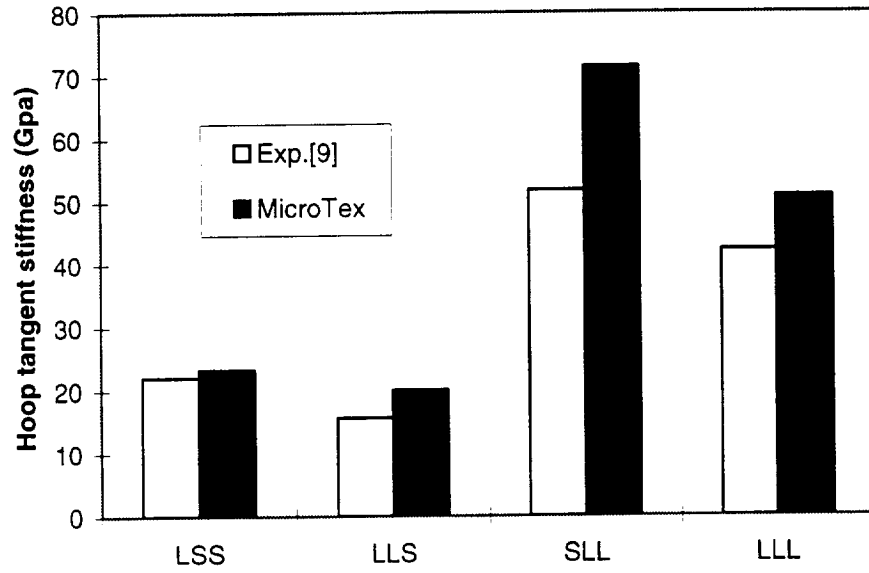


Figure B1-16. Comparison of Young's moduli in hoop direction for 2D triaxial braid composites

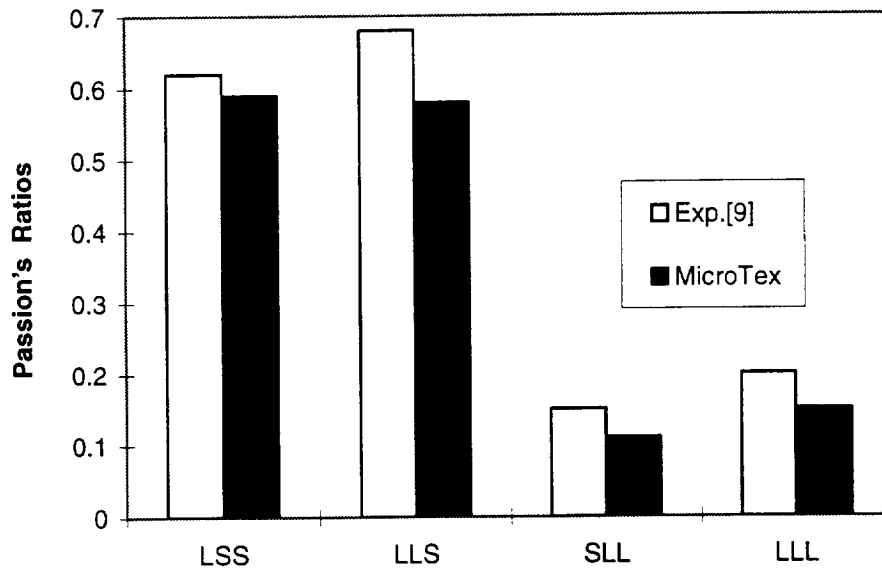


Figure B1-17. Comparison of in-plane Poisson's ratios for 2D triaxial braid composites

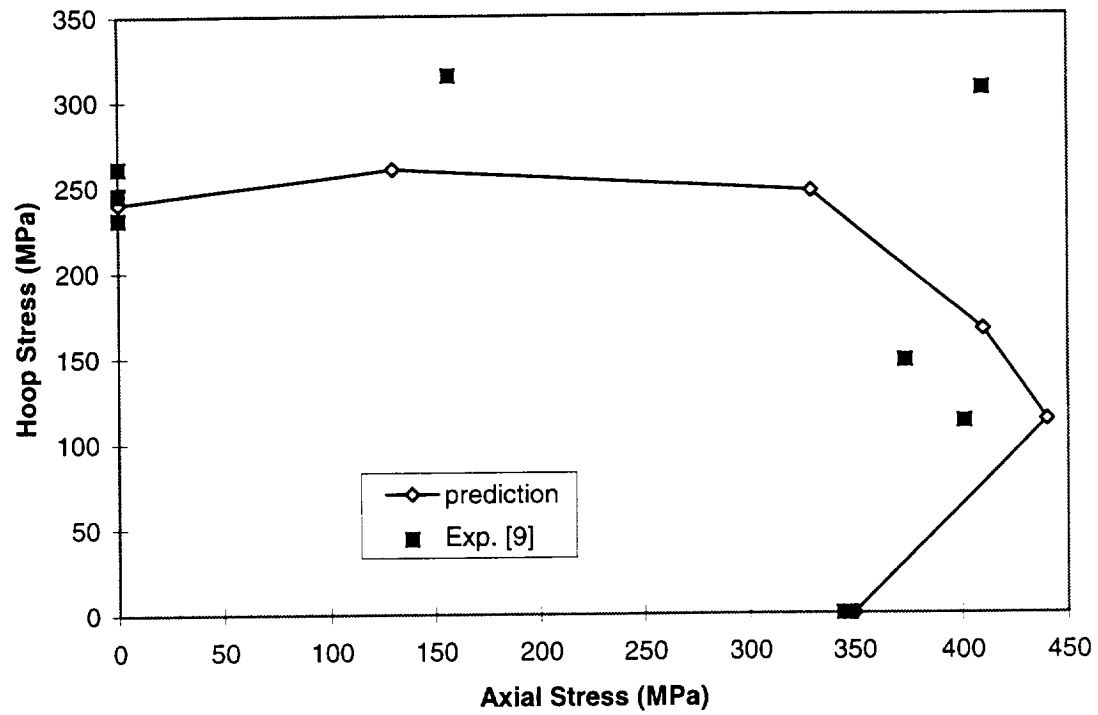


Figure B1-18. Comparison of Strength for Architecture LSS

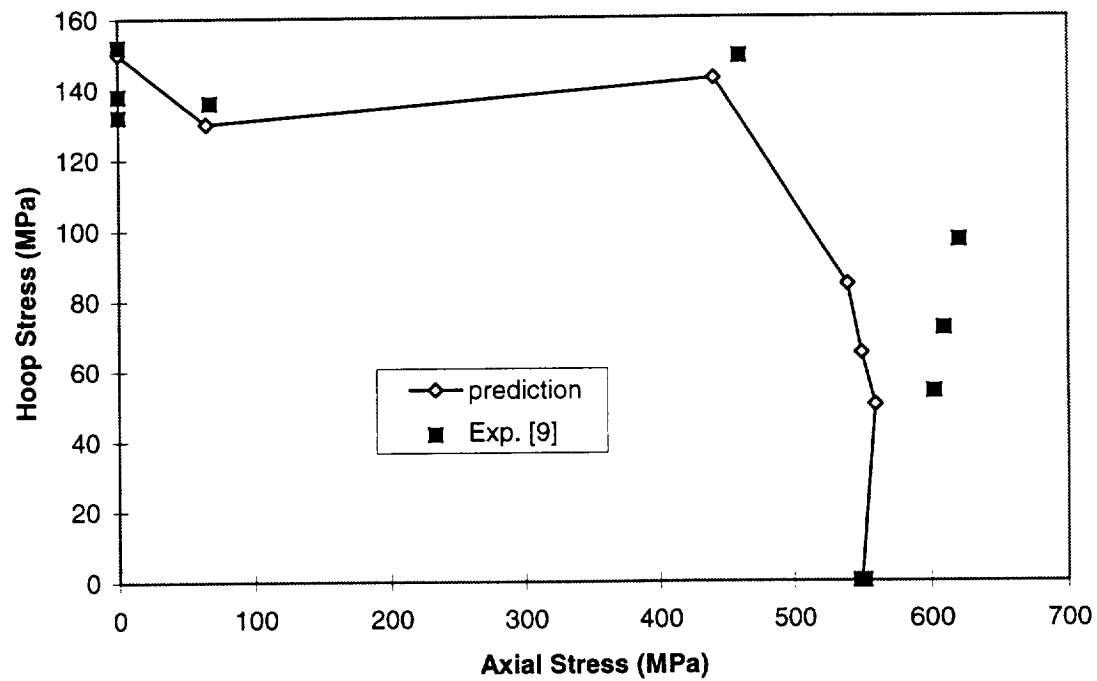


Figure B1-19. Comparison of Strength for Architecture LLS

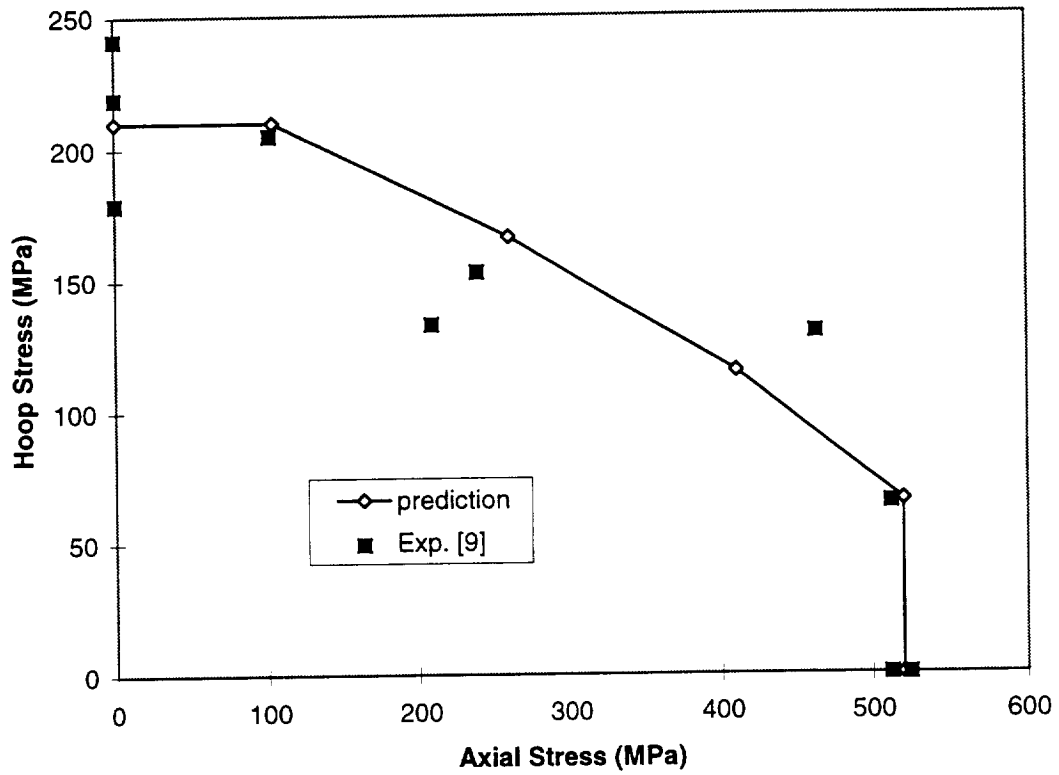


Figure B1-20. Comparison of Strength of Architecture SLL

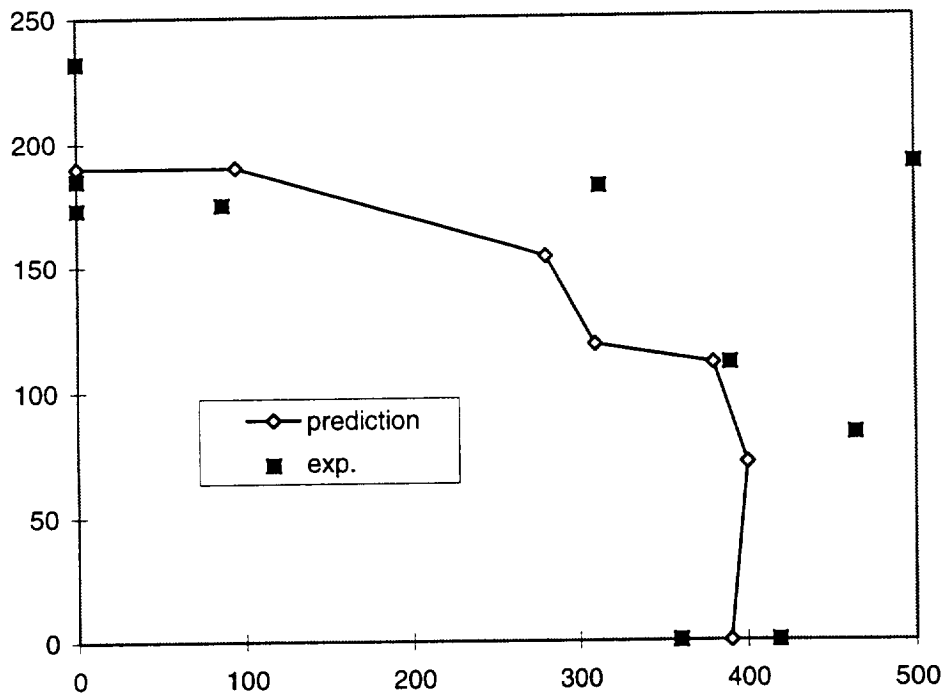


Figure B1-21. Comparison of Strength of Architecture LLL

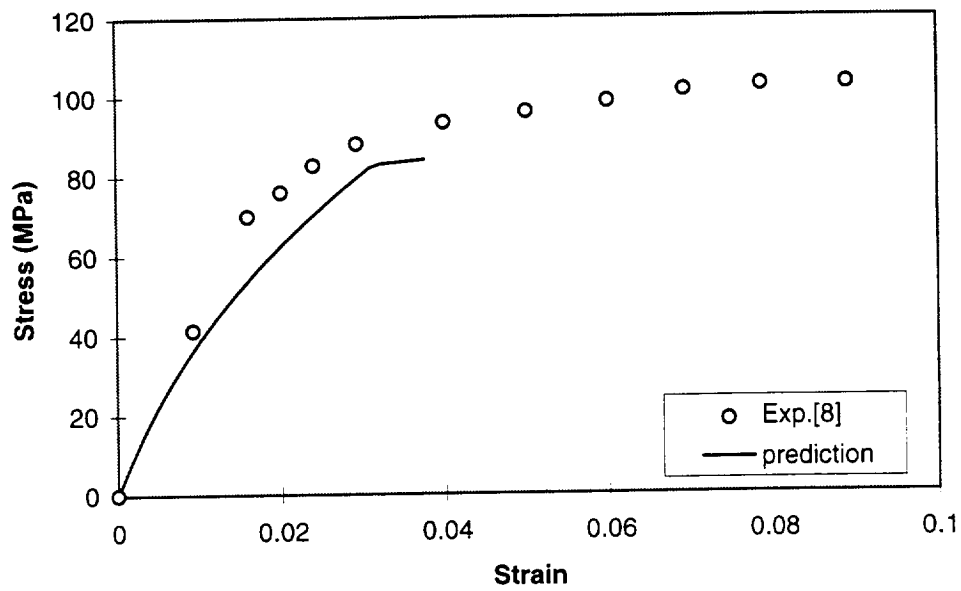


Figure B1-22. Shear stress-strain response for the plain weave composite (3k yarns)

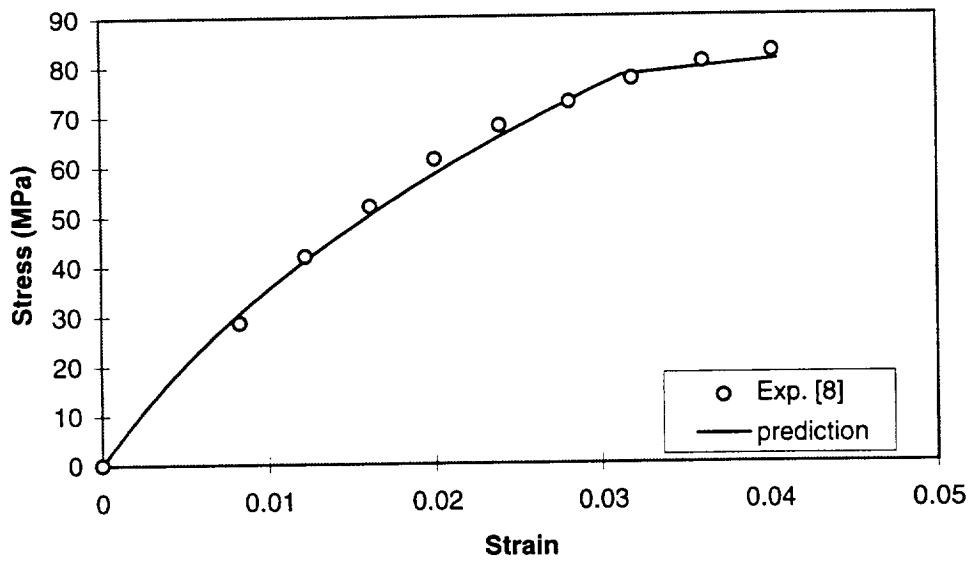


Figure B1-23. Shear stress-strain response for the plain weave composite (12k yarns)

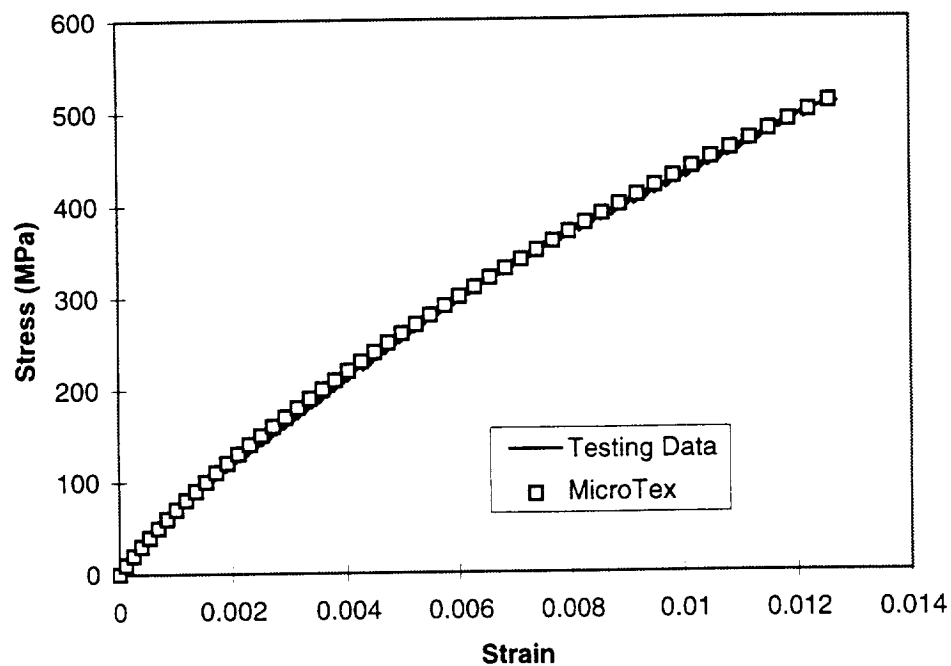


Figure B-24. Stress-strain results for a (0/90) C/SiC plain weave composite

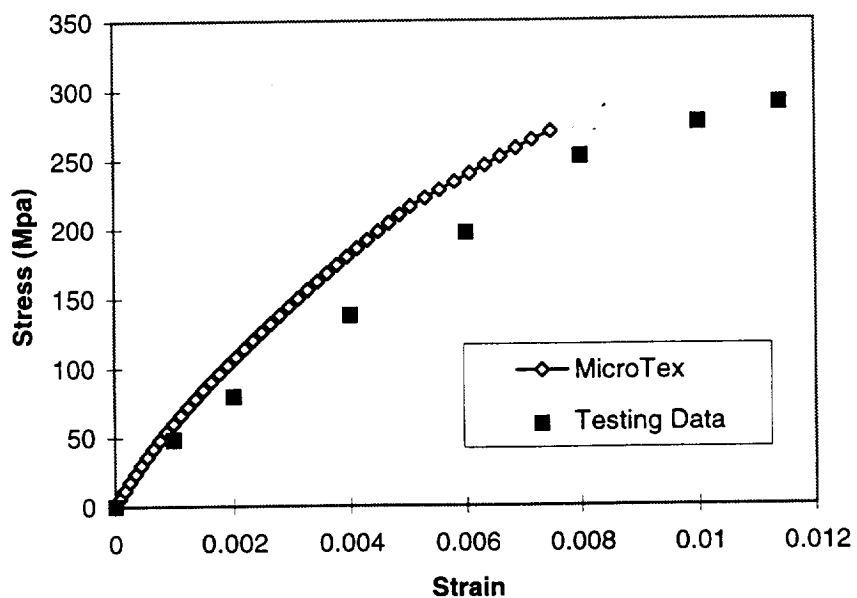


Figure. B1-25 Stress-strain results for a (0/+60-60) C/SiC plain weave composite

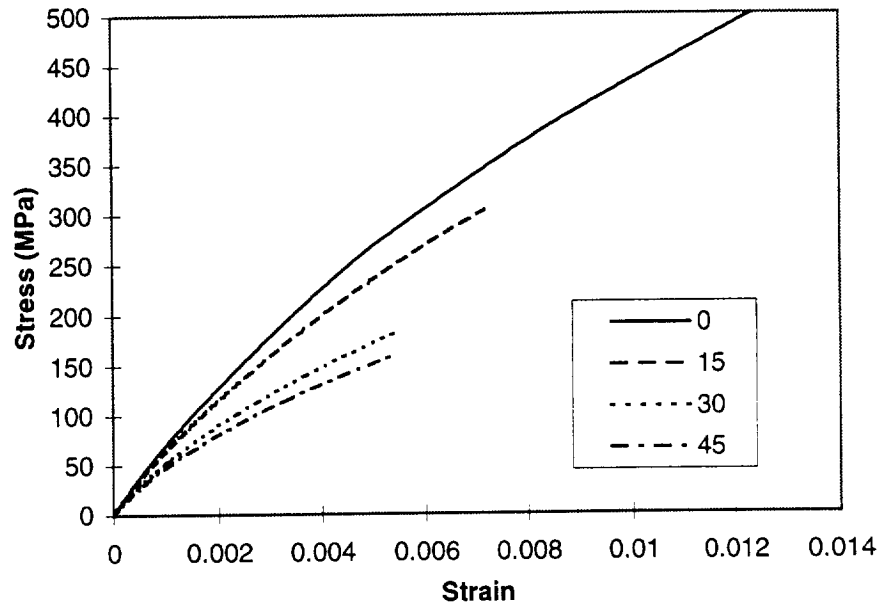


Figure B1-26. Stress-strain results for plain weave C/SiC composite under tension at different directions

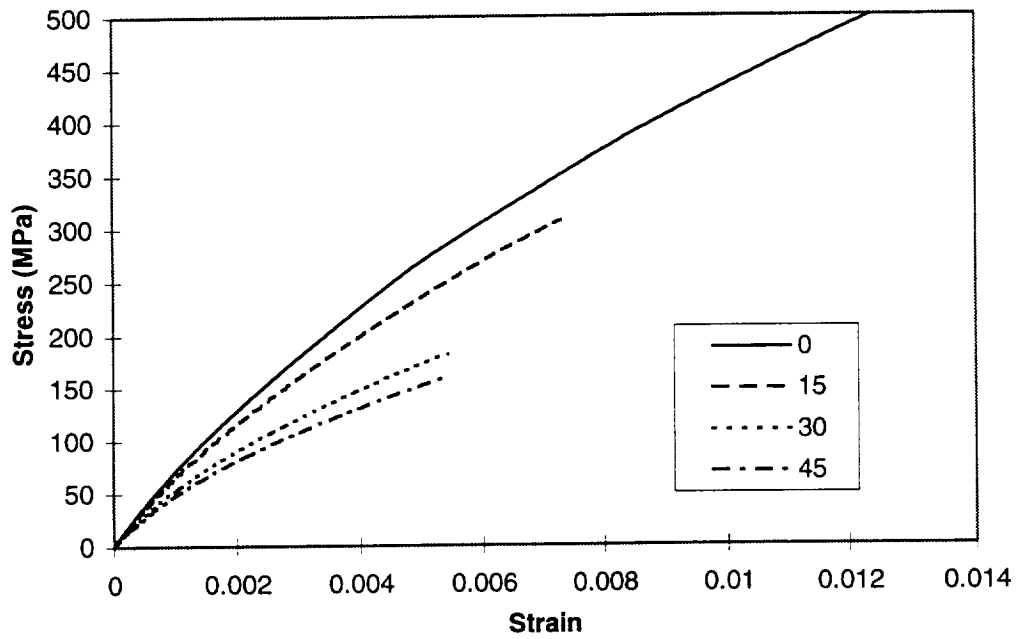


Figure B1-27. Strain-stress results for angle-ply plain weave composite under tension

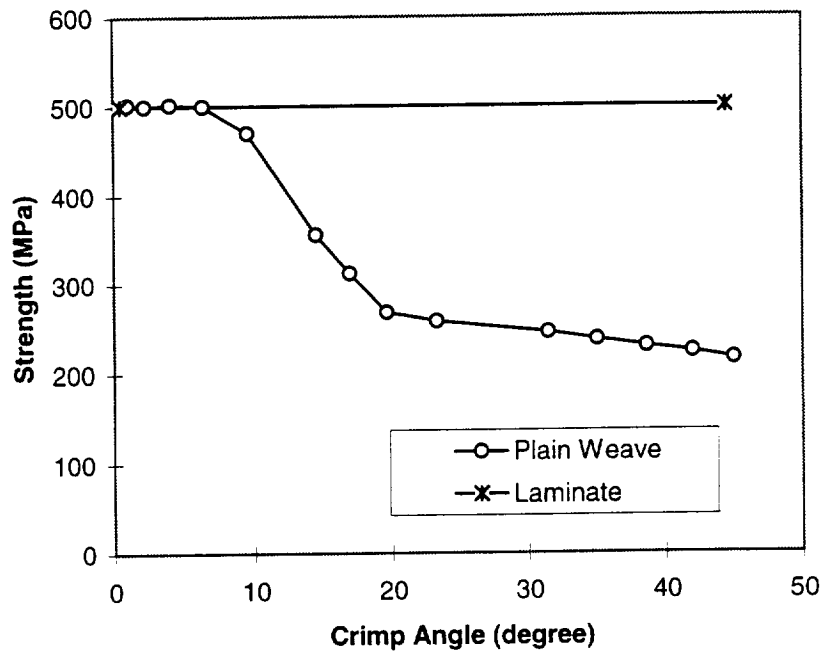


Figure B1-28. Tension strength of plain weave composite with different crimp angles

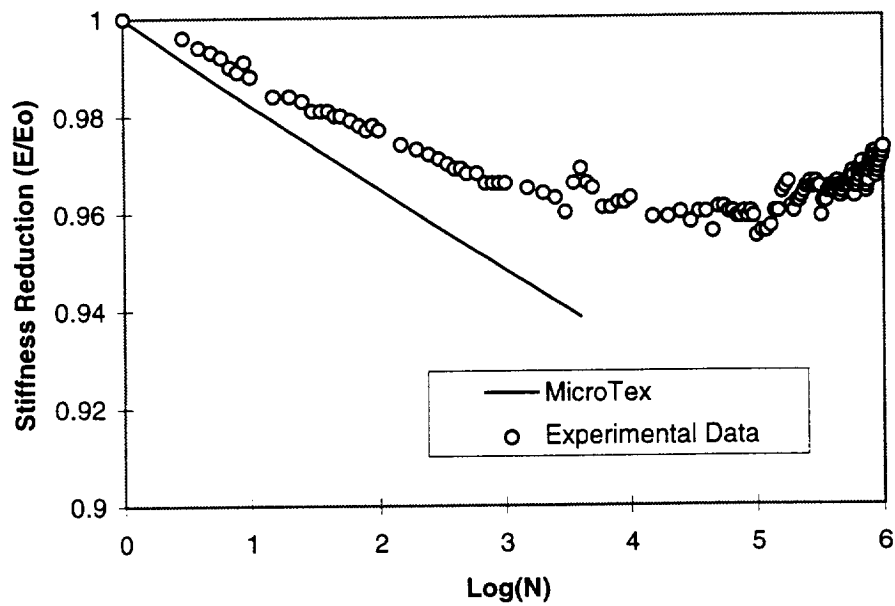


Figure B1-29. Stiffness Reduction for (0/90) C/SiC Plain Weave Composite for Maximum Stress at 458.85Mpa.

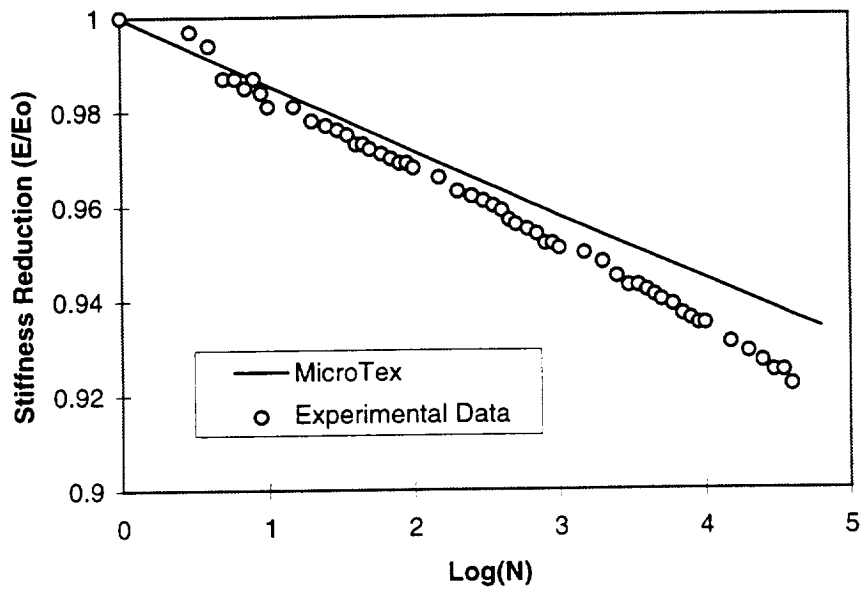


Figure B1-30. Stiffness Reduction for (0/90) C/SiC Plain Weave Composite for Maximum Stress at 410.60Mpa.

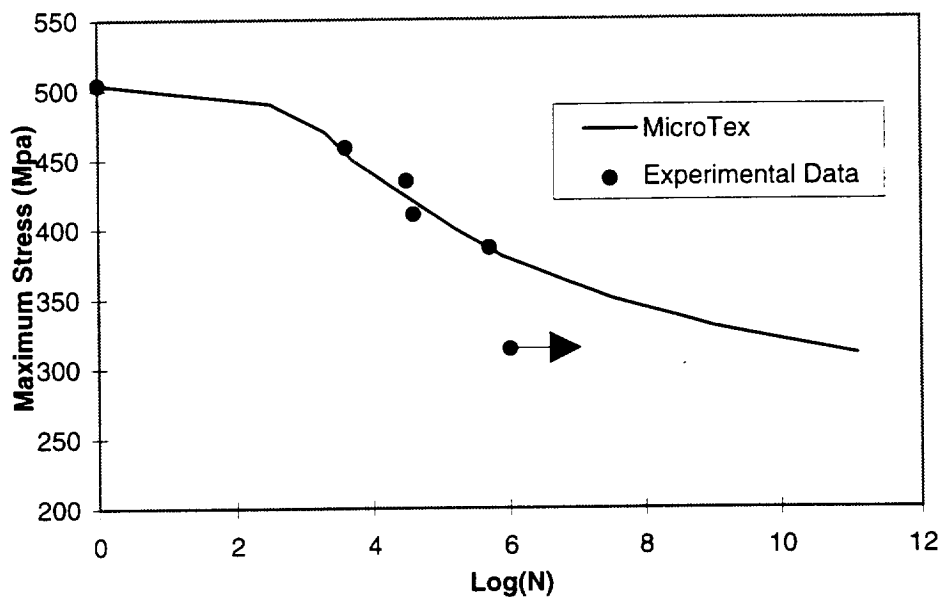


Figure B1-31. S-N Curve for (0/90) C/SiC Plain Weave Composite

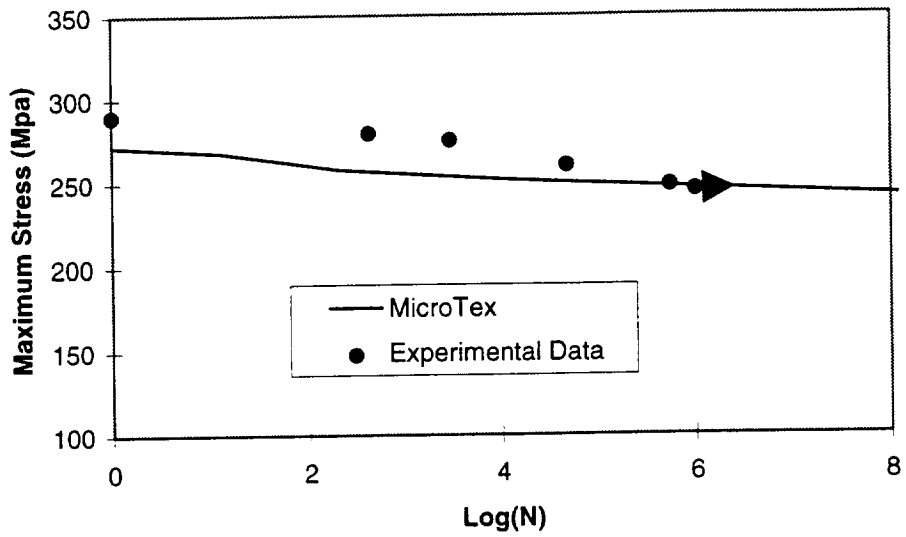


Figure B1-32. S-N Curve for (0/-60/+60) C/SiC Plain Weave Composite

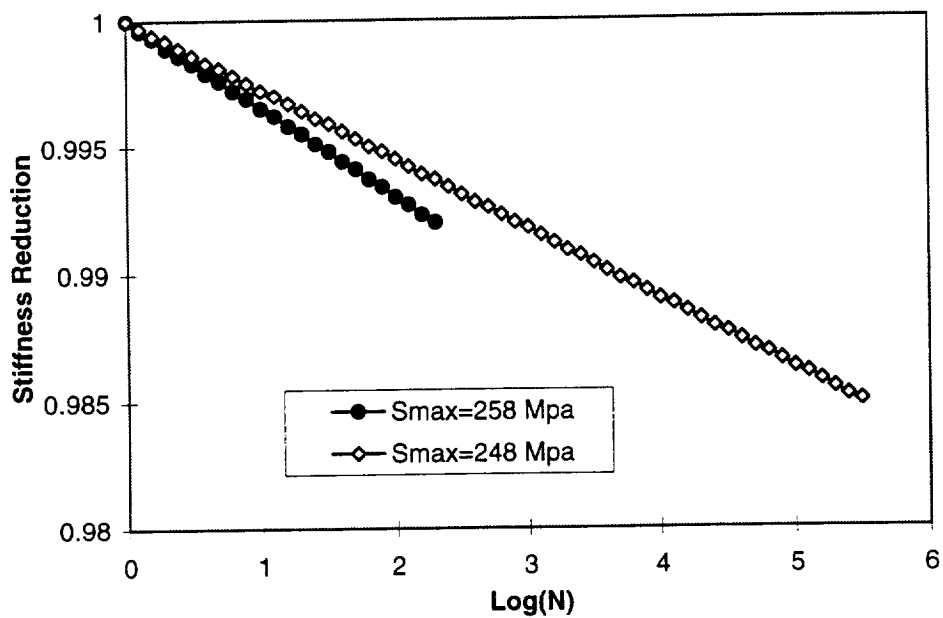
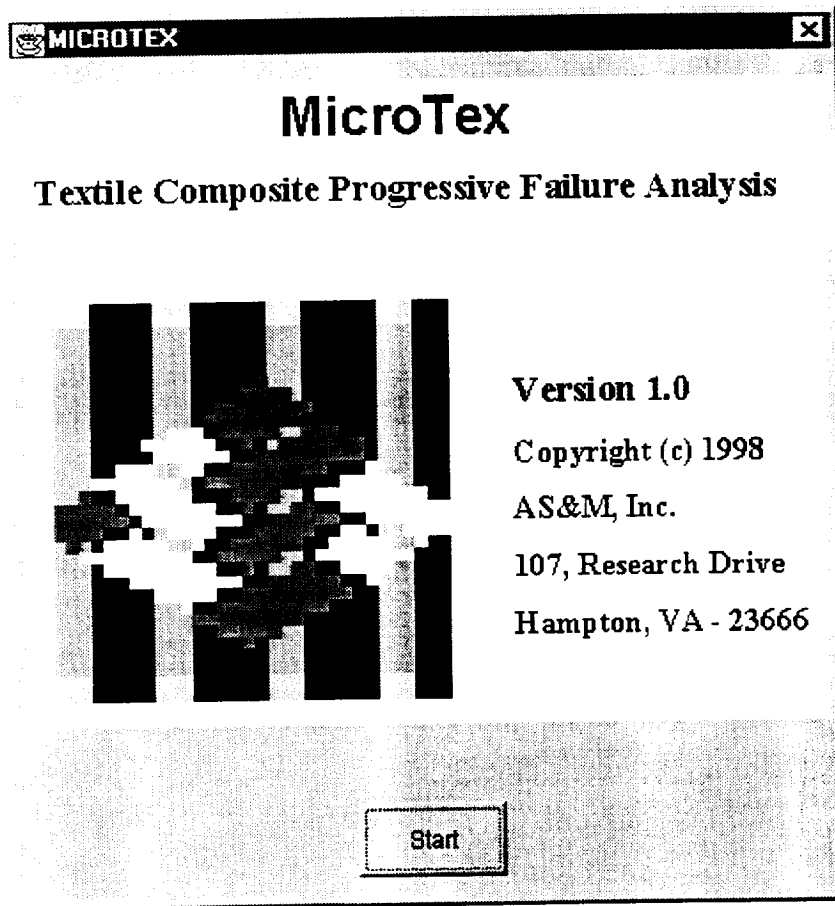


Figure B1-33. Stiffness Reduction for (0/-60/60) C/SiC Plain Weave Composite for Maximum Stresses at 258.0MPa and 248.0MPa.

B-2. MicroTex User's Manual



Introduction

The **Micro**-mechanics analysis for **Textile** composites (**MicroTex**) code provides the materials/design engineer with a user-friendly tool for the analysis of a wide variety of multi-layered, oriented, fabric reinforced woven and braided composites and laminated composites. Improved from a prior code (**TEXCAD**), MicroTex can be used to calculate overall thermal and mechanical properties along with engineering estimates of damage progression and strength. This code discretely models the yarn centerline paths within the textile repeating unit cell (RUC) by assuming sinusoidal undulations at yarn cross-over points and uses a yarn discretization scheme (which subdivides each yarn into smaller, piecewise straight yarn slice) together with either a 3D strain averaging procedure or a thin composite plate theory to calculate overall thermal and mechanical properties, stress distributions, and layer average strains[1-3].

For the failure analysis, the textile composite failure is defined as the loss of loading capability of the RUC, which depends on the stiffness reduction due to material slice failure and nonlinear material properties. Two models, a fracture model and a continuum model, are employed for material slices (matrix and yarn slices) failure analysis. In addition to the maximum

strain and maximum stress criteria of TEXCAD, a statistical criterion based on shear-lag model, fracture mechanics, and statistical principles are used to predict the tensile failure of yarn slices.

A fatigue analysis capability is also included in MicroTex. The damage due to fatigue loading is considered by overall stiffness reduction and material (matrix and yarn) strengths decreasing with cycle load.

Input to MicroTex consists of : (1) material parameters like yarn (or fiber) and matrix properties such as moduli, Poisson's ratios, coefficients of thermal expansion, nonlinear parameters, shear stress parameters, matrix stress intensity factor, initial matrix crack length, failure strains and stresses; (2) fabric parameters like yarn sizes, braid angle, yarn packing density, fiber diameter, yarn spacing, composite layer thickness; (3) applied loading like temperature and applied stresses. MicroTex output includes overall thermoelastic constants, yarn and matrix slices strains and stresses, slice failure history, in-plane stress-strain relation, ultimate strength, and overall stiffness reductions.

This manual consists of two parts. The first part includes the installation. The second part is a demonstration of the MicroTex application. The input to MicroTex is explained in detail according to the windows of the GUI and demonstrated using input files, output files are also explained with a sample problem.

System Requirement

MicroTex can be run on PC or UNIX system.

Since the GUI is written by JAVA, it requires JDK(Java Development Kit 1.1.3 or higher version) on the PC or UNIX system.

Installation and Execution

The software is distributed in tar format file `asm.tar`. The file contains all the required data files, source files and java class files required to execute the programs. To install the software components copy change directory to the destination directory and extract the files using the command: `tar -xvf asm.tar`. This command creates the ASM main directory and sub directories to copy the CPFail, MicroTex and ABAQUS interface programs. After extracting the files the default executable file names and paths have to set before running the any sample problems. This can be set either manually editing the configuration files or by executing the programs and modifying through the GUI using the menu command Configuration under Options menu. The executable commands for MicroTex are listed below:

change directory to	<code>\ASM\TEX\MICROTEX</code>	and
execute	<code>java asm.microtex.TXApp</code>	command

The MicroTex is developed using Sun's JDK 1.1.4. To execute these components Java runtime environment of version 1.1.3 or higher is required. Refer the JDK or JRE documentation for installation of Java.

Original code Files:

The following files are the original code files, user should carry over when change software installation directory, user can also carry over old saved files for previous cases:

pctexcad.exe	(for PC version, modify microtex.cfg)
utexcad.exe	(for UNIX version, modify microtex.cfg)
/asm/abaqus/*.*	(all files)
microtex.gif	
microtex.cfg	
TXMatrix.db	
TXYarn.db	

MicroTex Input

MicroTex is a user-friendly textile composites analysis code. Based on micro-geometry and micro-mechanics analysis, MicroTex can perform geometry analysis for various textile composite architectures which includes laminated composites, 2D, 2x2 and 1x1 triaxial braids, weaves (plain weave, 5-harness satin weave, and 8-harness satin weave), 2D braids (2D plain braid, 5-harness satin braid, and 8-harness satin braid), and 3D spatial oriented composites, and calculation of mechanical and thermal properties, such as overall Young's moduli, Poisson's ratios, and coefficients of thermal expansion for RUCs. MicroTex can calculate average and local strains and local stresses using plate theory or 3D iso-strain model, and performs local material slice failure judgment. MicroTex can also perform the overall stiffness reduction calculation due to material slice failure and non-linear material properties, and overall composite failure judgment.

MicroTex can be executed for static analysis by entering all the required material and architecture parameters through MicroTex Graphical User Interface (GUI). The GUI will then generate four data files: ***control.dat*** for control parameters, ***geom.dat*** for architecture parameters, ***mater.dat*** for material parameters, and ***load.dat*** for loading information. For fatigue analysis, MicroTex can be executed by providing fatigue information through the MicroTex GUI, and the GUI will generate an additional data file, ***fatigue.dat***.

Control data

Control data are input on "***Control***" window. The "***Failure criteria***" is for the judgment of composite failure. If the user assumes that the composite is failed when the overall stiffness of RUC is reduced *a*% of the initial stiffness, the number "*a*" is the input value.

This window also provides the options between static or fatigue analysis, plate model or 3D solid model, linear or nonlinear materials, and also if the fracture model should be employed.

If the fracture model is the choice, the statistical failure criterion will be used instead of the maximum tension strain criterion of yarns. Also matrix crack development will replace the strengths criteria to judge if a matrix slice is failed.

When the plate model is used, MicroTex will employ thin composite plate theory to analyze the stress and strain distribution among different layers, while for solid model, the strains are assumed to be uniform through thickness.

When the nonlinear material is used, MicroTex assumes both matrix and yarn material are nonlinear, and obey following equation

$$E = E_0 \left[1 + \left(\frac{s}{\beta s_c} \right)^\alpha \right]^{-(1+1/\alpha)} \quad (B2-1)$$

where E_0 represents the initial Young's modulus, S is the corresponding stress level, s_c is the critical values of failure criteria used, α and β were empirical constants; for matrix slices, β is taken as unity. Noticing that the transverse and shear moduli of the yarn slice are dominated by matrix material, the empirical constant α for transverse and shear moduli for the yarn slice is taken as the same value as matrix material, and β is unity. In the case of linear model, the only stiffness reduction comes from material slice failure.

When fatigue analysis is wanted, the user will be required to supply fatigue damage information like stiffness reduction due to fatigue loading for basic fatigue testing. This version assumes that the stiffness reduction due to fatigue loading obeys:

$$\frac{E}{E_0} = \frac{1}{1 + (c_1 + c_2 \sigma_{\max}) \text{Log}(N)} \quad (B2-2)$$

where modulus E/E_0 is the overall stiffness reduction, N is the number of cycles, σ_{\max} is the maximum stress, c_1 and c_2 are material constants to be determined by experimental data. The mean strength in the Weibull distribution and all the critical values in material failure criteria are assumed to be related to the stiffness reduction of composite to reflect the affect of fatigue loading on the composite strength. They can be expressed as

$$\sigma_N = \sigma_o \left(\frac{E}{E_0} \right)^{M(b_1 + b_2 \sigma_{\max}) \sigma_s} \quad (B2-3)$$

$$\sigma_{cN} = \sigma_c \left(\frac{E}{E_0} \right)^{M(b_1 + b_2 \sigma_{\max}) \sigma_s} \quad (B2-4)$$

where b_1 and b_2 are parameters, M is the Weibull modulus, σ_o is the mean strength of the yarn material, and σ_N is the yarn mean strength after N cycles, σ_c is the original critical value in any failure criteria, and σ_{cN} the critical value after N cycles, and σ_s is the static strength of composite which can be obtained by performing static analysis.

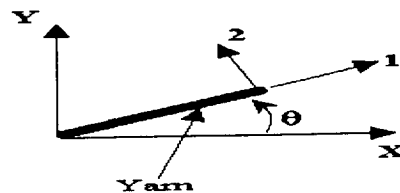
Architecture data

Architecture data can be provided on window "Geometry". The user is required to input the number of layers, layer orientation, layer thickness, and type of architectures. Then for each different architecture, the information user should provided are given as follows:

Architecture Option No. 1 -- Laminated composite

This option provides a classical lamination theory analysis for modeling two dimensional, stacked, orientated yarns (or plies). MicroTex requires material name for each ply. The layer orientations for laminated composite are measured with respect to x-axis (see Figure B2-1). The ply longitudinal and transverse direction are indicated by 1 and 2, respectively.

COORDINATE SYSTEMS FOR 2-D LAMINATE

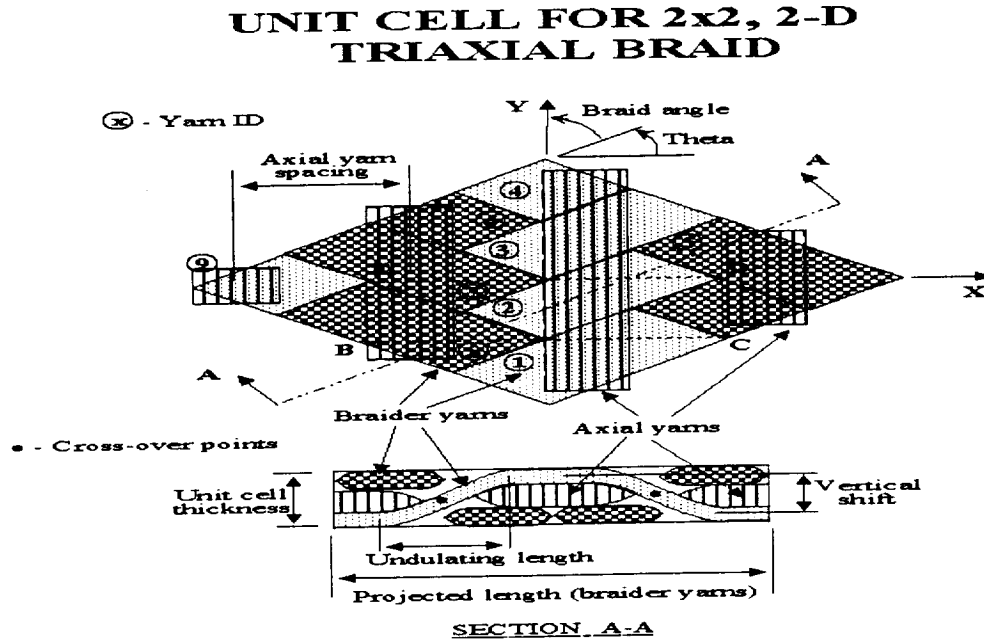


- 1-2-3 Coordinates refer to yarn material coordinates. The 2-axis is assumed to be always perpendicular to the Z-axis.

Figure B2-1. Reference coordinate system for the 2D laminated composite

Architecture Option No. 2 -- 2D, 2x2 triaxial braids

This option allows the user to model two dimensional, 2x2 triaxial braids. For each layer, MicroTex requires braid angle, axial yarn spacing, axial yarn contest, number of fiber in axial and braid yarns, and also material name ID for both matrix and yarns. The RUC is shown in Figure B2-2.



- Smallest unit cell = BCDE, where, $BC = 2 \times \text{Axial yarn spacing}$.
and $CD = 0.5 \times BC \times \tan(\theta)$.

Figure B2-2. RUC for the 2D, 2x2 triaxial braided composites

Architecture Option No. 3 -- 2D, 1x1 triaxial braids

This option allows the user to model two dimensional, 1x1 triaxial braids. The RUC of this architecture is shown in Figure B2-3. For each layer, MicroTex requires braid angle, axial yarn spacing, axial yarn contest, number of fiber in axial and braid yarns, and also material name ID for both matrix and yarns.

UNIT CELL MODEL FOR 1x1 2-D TRIAxIAL BRAID

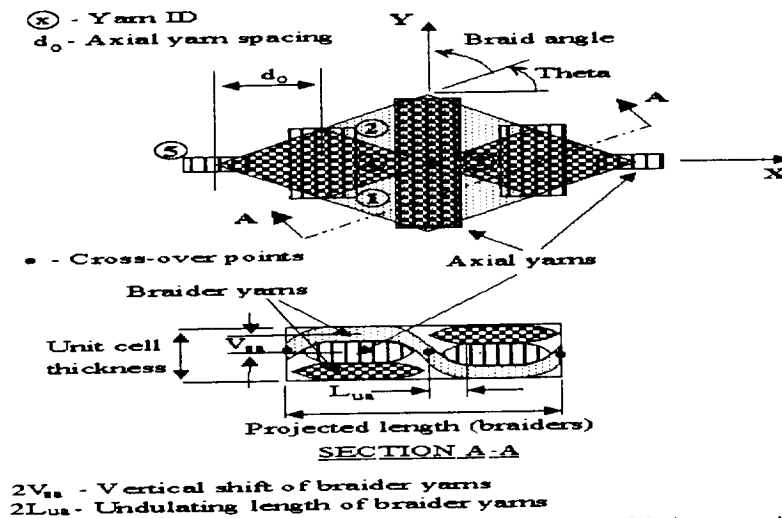


Figure B2-3. RUC for the 2D, 1x1 triaxial braided composites

Architecture Option No. 4 -- Weave and 2D braids

This option allows the user to model two dimensional weaves and two dimensional braids. The RUCs for plain weave, 5-harness satin weave, 8-harness satin weave, and plain 2D braid are shown in Figures B2-4 to B2-7.

For each layers, MicroTex requires weave type (for plain weave and plain 2D braid, 2; 5-harness satin weave and 5-harness satin 2D braid, 5; and for 8-harness satin weave and 8-harness satin 2D braid, 8), braid angle (for plain weave, 5-harness satin weave and 8-harness satin weave, 45 degree), axial yarn spacing, number of fiber in yarns, and also material name ID for both matrix and yarns.

UNIT CELL MODEL FOR PLAIN WEAVE COMPOSITE

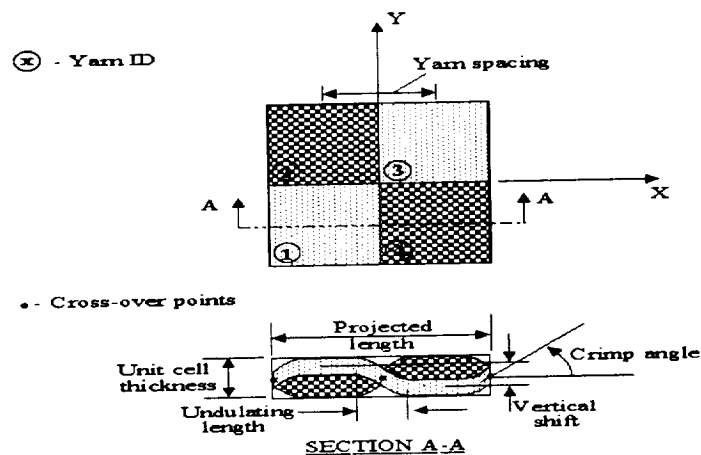


Figure B2-4. RUC for the plain weave composites

UNIT CEL FOR 5-HARNESS SATIN WEAVE

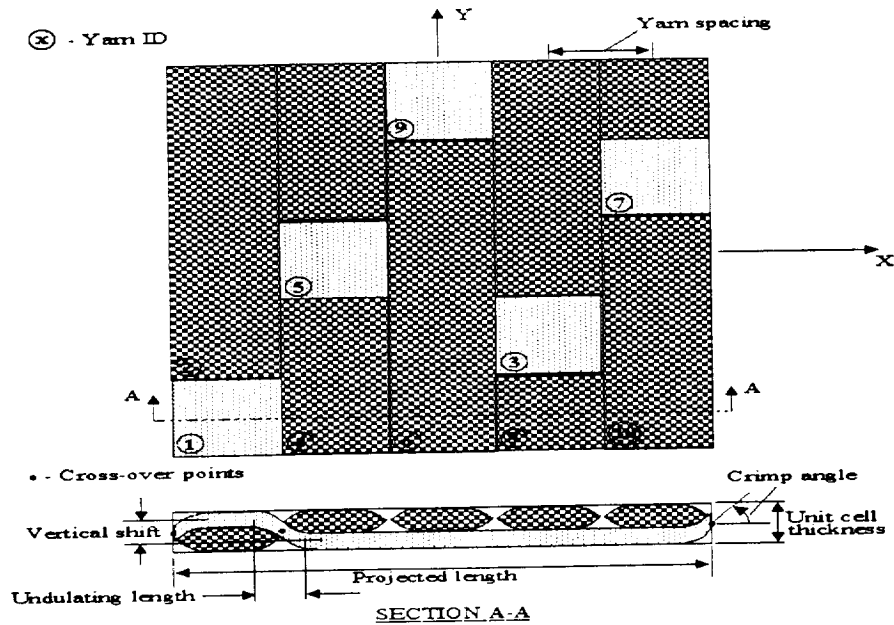
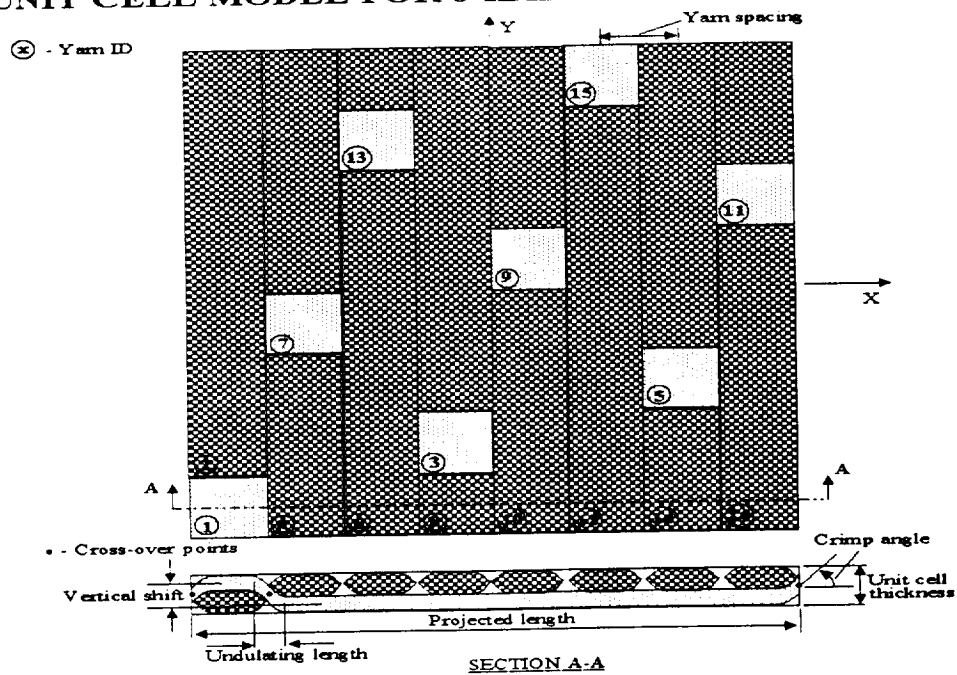


Figure B2-5. RUC for the 5-harness satin weave composites

UNIT CELL MODEL FOR 8-HARNESS SATIN WEAVE



UNIT CELL FOR 2-D BRAIDED COMPOSITE

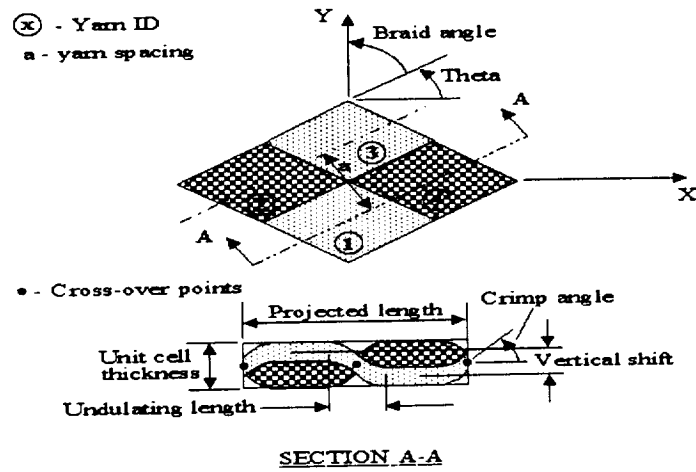
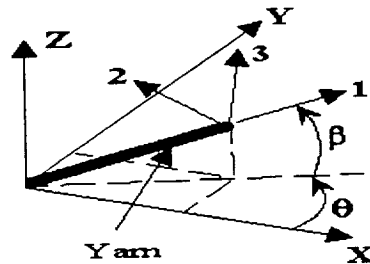


Figure B2-7. RUC for the plain 2D braided composites

Architecture Option No. 5 -- 3D spatially Oriented Composites

This option allows the user to model a three dimensional, spatially oriented composite which is made up of straight yarns oriented along different directions. The RUC is shown in Figure B2-8. For each layer, MicroTex requires the lengths of two sides of the unit cell, included angle, number of yarns, orientation, length, and cross-section area of each yarn, and also material name ID for both matrix and yarns.

ORIENTATION ANGLES FOR 3-D COMPOSITE



- 1-2-3 Coordinates refer to yarn material coordinates. The 2-axis is assumed to be always perpendicular to the Z-axis.

Figure B2-8. Reference coordinate system for the 3D spatially oriented composite

Loading information

Loading information should be input on the window "Loading". The user is required to provided processing temperature, temperature load, applied forces (stresses) in each direction, and number of steps. MicroTex will apply the temperature at the first step and equally divide the applied forces into each step.

Materials

Material parameters, for both yarn and matrix, are inputted use "database" windows.

The screenshot shows the MICROTEX Yarn Database window. It contains several input fields for material properties. The 'Identification' dropdown is set to 'DEFAULT' and the 'Name' field is 'Default Yarn Properties'. The 'Kind' dropdown is set to 'Fiber' and the 'Matrix ID' dropdown is set to 'DEFAULT'. The input fields are organized into three columns:

Property	Value	Property	Value	Property	Value
E11 (MPa)	123255.0	Max tension strain 11 (MPa)	0.014	Thermal exp. coef. in 1 dir (°C)	0.00000127
E22 (MPa)	56761.524	Max compression strain 11 (MPa)	0.01	Thermal exp. coef. in 2 dir (°C)	0.00000693
E33 (MPa)	56761.524	Max tension stress 22 (MPa)	84.9	Nonlinear parameter 1	0.85
G12 (MPa)	96250.0	Max compression stress 22 (MPa)	206.0	Nonlinear parameter 2	12.0
G23 (MPa)	96250.0	Max tension stress 33 (MPa)	84.9	Shear stress parameter	1.6
G13 (MPa)	96250.0	Max compression stress 33 (MPa)	206.0	Fiber diameter (m)	0.007
NU12	0.211	Max shear stress in 12 plane (MPa)	87.5	Fiber volume fraction	0.3
NU23	0.211	Max shear stress in 23 plane (MPa)	102.4		
NU13	0.211	Max shear stress in 13 plane (MPa)	87.5		

At the bottom of the window, there are four buttons: NEW, DELETE, UNDO, and EXIT.

Yarn Database:

This window allows user to input yarn material properties. The yarn is assumed to be anisotropic. The fiber direction here is denoted as 1, 2 and 3 are transverse directions.

The "kind" has two options: fiber or yarn. When fiber is chosen, the Young's moduli (E_{11} for fiber direction, E_{22} and E_{33} for transverse direction), shear moduli (G_{12} , G_{13} , and G_{23}), Poisson's ratios (μ_{12} , μ_{13} , and μ_{23}), and coefficient of thermal expansion (α_1 , α_2 , and α_3) should be entered, MicroTex will calculate the correspondent yarn parameters. If yarn is the choice, yarn properties should be inputted, and MicroTex will calculate the corresponding fiber parameters.

The "Assoc. Matrix" specifies the matrix material used in this yarn.

For the yarn material strengths, the maximum tension ($E11T$) and compression ($E11C$) strains in fiber direction, maximum tension, compression, and shear stresses in transverse direction ($S22T$, $S22C$, $S33T$, $S33C$, $S12S$, $S23S$, and $S13S$), should be also input on this window.

The two nonlinear parameters for yarn material are defined to include possible material nonlinearity, they are the constant β and α in equation (B2-1).

The last three parameters are the shear stress parameter, fiber diameter, and yarn fiber volume fraction. The shear stress parameter is the maximum shear stress that the fiber-matrix interface can resist, and an empirical constant which be determined by testing.

Matrix Database:

This window is used for create or modify matrix materials. The matrix is assumed to be isotropic. The "*Nonlinear Coefficient*" is the parameter α in equation (B2-1). The "*Crack Length c*" is the initial matrix crack length, which can be calculated using:

$$c = a \left[2 \sqrt{\frac{\pi}{2\sqrt{3}V_f}} - 1 \right] \quad (B2-5)$$

where a is the fiber diameter, V_f is the fiber volume fraction.

Sample problem:

A sample of a 2D 2x2 triaxial braid composite is provided here to demonstrate all the input files. Those data files are given here in case that user misunderstands any parameters. Users are usually not required to view those data files.

Material:

The material of this composite is graphite AS4 yarns and 3501-6 epoxy resin. The Young's modulus and shear modulus for matrix are 3448.0MPa and 1276.0MPa, respectively, Poisson's ratio is 0.35, coefficient of thermal expansion is $4.0e-05/^{\circ}C$, the nonlinear coefficient is taken as 2.34, and the normal and shear strength for matrix is 84.85MPa and 98.30MPa, respectively.

The initial crack length is $1.1e-05m$, and the stress intensity factor is $0.2MPa\sqrt{m}$.

For yarn material, the moduli, Poisson's ration, and coefficient of thermal expansion are given as:

$$E_{11} = 144.8e03MPa, E_{22} = E_{33} = 1.173e03MPa, G_{12} = G_{23} = G_{13} = 5.52e03MPa$$

$$\mu_{12} = \mu_{13} = 0.23, \mu_{23} = 0.3, \alpha_1 = -3.24e-07/^{\circ}C, \alpha_2 = \alpha_3 = 1.4e-05/^{\circ}C$$

The yarn material strengths are:

$$ST1T=0.014, ST1C=0.01, S22T=S33T=26.0MPa, S22C=S33C=206.0MPa,$$

$$S12S=S12S=102.4MPa, S23S=87.5MPa$$

The yarn fiber volume fraction is 0.75, fiber diameter is $7.0e-06m$, and the shear stress parameter is 0.4. The two nonlinear parameters are equation to 1.0 and 10.0, respectively.

We have the **mater.dat** file as:

```
***
1,
1

1
3448.0,1276.0,0.35,4.0E-5,
2.34
84.85,98.3
0.2,1.1E-5

2,0.75,2,
1
144800.0,11730.0,11730.0,5516.0,5516.0,5516.0,
0.23,0.3,0.23,-3.24E-7,1.4E-5
1.0,10.0
0.014,0.01,26.0,206.0,
26.0,206.0,87.5,102.4,87.5
0.4
7.0E-6
***
```

Geometry:

The composite is a single layer 2D, 2X2 triaxial braid. The layer thickness is 7.9e-04m, orientation is 0 degree, braid angle is 62.3 degree. Axial yarn spacing is 6.1e-03m, Number of fibers in axial yarn is 24K, number of fibers in braid yarn is 12K, percent of axial yarns is 0.37, and fiber diameter is 7.0e-06m.

We have the **geom.dat** file as:

```
***
1
2
0.0
1,7.9E-4,
62.3,
7.0E-6,0.0061,
24,
12,
0.37,
2,
2
***
```

Loading:

Assuming there is no temperature change, and applied stress in transverse direction as 600.0Mpa, and number of steps is 50. We have the **load.dat** file as:

```
***
0.0 0.0
0.0 600.0 0.0 0.0 0.0 0.0
50
***
```

Control:

Assuming the failure criterion is 10%, and using static analysis, fracture, and nonlinear model. There is no difference between plate model and solid mode for this case. We have the **control.dat** file as:

```
***
1,1,1,0,0.1,
***
```

Fatigue:

For fatigue analysis, The four parameters c_1 , c_2 , b_1 , and b_2 , and the static strength σ_s in equations (B2-2) to (B2-4) should be entered. For a C/SiC plain weave composite [3], the parameters in equation (B2-2) comes out as $-1.537e-02$ and $7.317e-05/MPa$, b_1 and b_2 in equations (B2-3) and (B2-4) come out as $4.147e-02$ and $-8.216e-05/MPa$, and static strength for (0/90) composite is 504.0MPa. we have the **fatigue.dat** file as:

```
***
-1.537E-02,7.317E-05,
-8.216e-05, 0.04147,
504.0,
***
```


MicroTex Output

The results created by the above MicroTex execution are stored in three different files. The input and calculated geometry parameters are saved in *geomout.dat*, the overall stress-strain relation and stiffness reduction are saved in file *stress.dat*, and the initial mechanical and thermal parameters, the local stresses and strains of each material slice at each step, and the failure information are saved in file *output.sta*. For fatigue analysis, an additional file, *damage.dat*, is created for predicted S-N curve.

The geometry model, stress-strain relation curve, stiffness reduction curve, S-N curve, and *output.sta* file can also be displayed in the "view" window.

Sample problem:

The result files for the sample problem are listed here.

geomout.dat:

Geometry Parameter
for 2D 2X2 Triaxial Braided Composite

Input data:

Braid angle:	62.300
Number of fibers in axial yarn:	24000.000
Number of fibers in braid yarn:	12000.000
Percent of axial yarns:	0.370
Thickness of each layer (m):	0.7900E-03
Axial yarn spacing (m):	0.6100E-02
Fiber diameter (m):	0.7000E-05

Calculated data:

Axial yarn thickness (m):	0.5659E-03
Braid yarn thickness (m):	0.1121E-03
Length of axial yarn (m):	0.2562E-01
Length of braid yarn (m):	0.1091E-01
Volume of RUC (m ³):	0.1235E-06
Fiber volume fraction:	0.52
Crimp angle (deg):	6.58

stress.dat

σ_x	ϵ_x	E_x	σ_y	ϵ_y	E_y	σ_{xy}	ϵ_{xy}	G_{xy}
.....								
.....								
0.0000E+00, -0.5960E-04, 0.8138E+05, 0.3600E+02, 0.4588E-03, 0.7288E+05, 0.0000E+00, 0.4588E-03, 0.2273E+05,								
0.0000E+00, -0.7960E-04, 0.7970E+05, 0.4800E+02, 0.6323E-03, 0.6918E+05, 0.0000E+00, 0.6323E-03, 0.2247E+05,								
0.0000E+00, -0.9967E-04, 0.7818E+05, 0.6000E+02, 0.8137E-03, 0.6615E+05, 0.0000E+00, 0.8137E-03, 0.2225E+05,								
0.0000E+00, -0.1198E-03, 0.7678E+05, 0.7200E+02, 0.1002E-02, 0.6359E+05, 0.0000E+00, 0.1002E-02, 0.2207E+05,								
0.0000E+00, -0.1401E-03, 0.7547E+05, 0.8400E+02, 0.1198E-02, 0.6137E+05, 0.0000E+00, 0.1198E-02, 0.2192E+05,								

```

0.0000E+00, -0.1604E-03, 0.7424E+05, 0.9600E+02, 0.1400E-02, 0.5940E+05, 0.0000E+00, 0.1400E-02, 0.2179E+05,
0.0000E+00, -0.1807E-03, 0.7307E+05, 0.1080E+03, 0.1608E-02, 0.5763E+05, 0.0000E+00, 0.1608E-02, 0.2167E+05,
0.0000E+00, -0.2012E-03, 0.7197E+05, 0.1200E+03, 0.1822E-02, 0.5603E+05, 0.0000E+00, 0.1822E-02, 0.2157E+05,
0.0000E+00, -0.2216E-03, 0.7093E+05, 0.1320E+03, 0.2042E-02, 0.5457E+05, 0.0000E+00, 0.2042E-02, 0.2148E+05,
.....
.....

```

output.sta:

UNIT CELL OVERALL PROPERTIES

```

EXX = 0.43473E+05   EYY = 0.40531E+05   EZZ = 0.10209E+05           !moduli

NuXY =  0.25985   NuYX =  0.24227           !Poisson's ratio

NuXZ =  0.25196   NuYZ =  0.28887

GXY = 0.12217E+05   GYZ = 0.41796E+04   GXZ = 0.41292E+04           !shear moduli

Alfa1= 0.23804E-05   Alfa2= 0.24915E-05   Alfa3= 0.26612E-04   Alfa12=-0.32894E-05

```

steps, load, stress, strain and failure flag:

```

- step = 1   load = 0.000E+00, 12.00, 0.00, 0.00, 0.00, 0.00,
    layer number: 1
      yarn slice number: 1
         $\sigma_{11}$        $\sigma_{22}$        $\sigma_{33}$        $\tau_{12}$        $\tau_{13}$        $\tau_{23}$       !local stress
        -0.96934E+01, 0.32277E+01, -0.21554E+00, 0.89005E-16, -0.12821E-15, -0.89963E+00,
         $\epsilon_{11}$        $\epsilon_{22}$        $\epsilon_{33}$        $\epsilon_{12}$        $\epsilon_{13}$        $\epsilon_{23}$       !local strain
        -0.71728E-04, 0.29607E-03, -0.85526E-04, 0.16136E-19, -0.23244E-19, -0.16309E-03,
      yarn slice number: 2
        0.30429E+02, 0.60667E+00, -0.17046E+00, 0.17237E+01, 0.67227E+00, -0.65681E+00,
        0.20945E-03, 0.77454E-05, -0.78381E-04, 0.31250E-03, 0.12188E-03, -0.11907E-03,
      .....
      .....
        0.32374E+01, 0.15839E+02, 0.27607E+01, -0.23205E-15, 0.24918E-15, -0.25639E+01,
        -0.10086E-02, 0.42373E-02, -0.12069E-02, -0.18954E-18, 0.20628E-18, -0.21304E-02,
      layer slice model
failure slice and model: 1, 1, 2,           !failure location and model

step = 14   load = 0.000E+00, 168.00, 0.00, 0.00, 0.00, 0.00,
    layer number: 1
      yarn slice number: 1
        -0.13670E+03, 0.34486E+02, -0.32706E+01, -0.26481E-14, 0.18309E-14, -0.12681E+02,
        -0.10942E-02, 0.46035E-02, -0.13087E-02, -0.48008E-18, 0.33423E-18, -0.22990E-02,
      .....
      .....

```

damage.dat

.....

.....

Log(N)	E/Eo
0.5000E+00,	0.9910E+00,
0.6000E+00,	0.9892E+00,
0.7000E+00,	0.9874E+00,
0.8000E+00,	0.9856E+00,
0.9000E+00,	0.9839E+00,
0.1000E+01,	0.9821E+00,
0.1100E+01,	0.9804E+00,
0.1200E+01,	0.9786E+00,
0.1300E+01,	0.9769E+00,
0.1400E+01,	0.9752E+00,
0.1500E+01,	0.9734E+00,
0.1600E+01,	0.9717E+00,
0.1700E+01,	0.9700E+00,
0.1800E+01,	0.9683E+00,
0.1900E+01,	0.9666E+00,

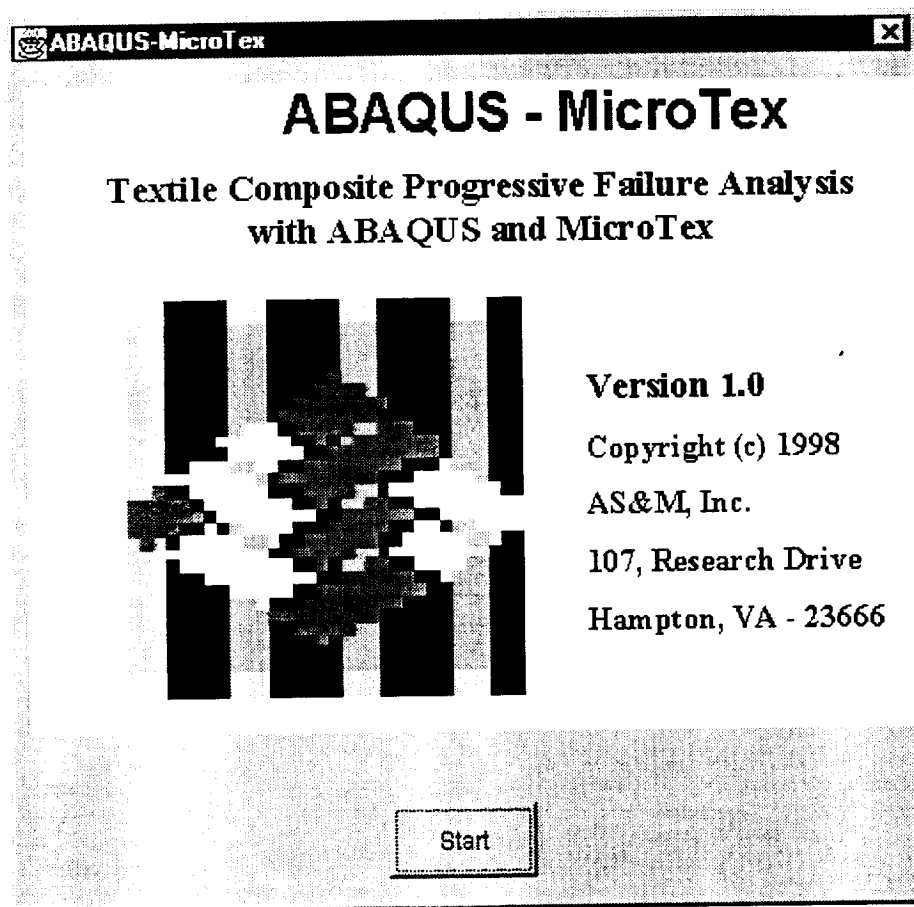
.....

.....

References

1. R. A. Naik: "TEXCAD - Textile Composite Analysis for Design, Version 1.0 User's Manual," NASA CR-4639, Dec, 1994.
2. R. A. Naik: "Analysis of Woven and Braided Fabric Reinforced Composites," NASA CR-194930, June, 1994.
3. Y. Shi, M.F. Card, V.V. Raman, and R.M.V. Murthi: "Prediction of Tension Failure of Textile Composites Using Micro-mechanics and Statistical Analysis," Presented at the 2nd Annual Cocoa Beach Conference of America Ceramic Society , January 20-2, 1998, Cocoa Beach, Florida.

B3. ABAQUS-MicroTex User's Manual



System Requirement

ABAQUS-MicroTex can be run on PC or UNIX system. The system requirement for running ABAQUS-MicroTex is the same as the requirement for running ABAQUS software.

Since the GUI is written by JAVA, it also requires JDK(Java Development Kit 1.1.3 or higher version) on the PC or UNIX system.

Installation, Path and Execution

Installation:

The software is distributed in tar format file `asm.tar`. The file contains all the required data files, source files and java class files required to execute the programs. To install the software components copy change directory to the destination directory and extract the files using the command: `tar -xvf asm.tar`. This command creates the ASM main directory and sub directories to copy the CPFail, MicroTex and ABAQUS interface programs.

The ABAQUS-MicroTex is developed using Sun's JDK 1.1.4. To execute these components Java runtime environment of version 1.1.3 or higher is required. Refer the JDK or JRE documentation for installation of Java.

Path:

After extracting the files, the following two path settings have to be completed.

1) The ABAQUS executable file with its path, xxx/xxx/xxx/**abaqus**, has to be set for GUI before running any sample problems. The path, xxx/xxx/xxx/, is the path where the ABAQUS software installed and **abaqus** is the ABAQUS executable file for UNIX version. This setting can be made by either manually editing the configuration file (abaqus.cfg) or by executing the program and modifying through the GUI using the menu command Configuration under Options menu.

2) In ABAQUS subroutine, UMAT, user need to set the full path in two 'open' statements. Modify the path '/xxx/xxx/ASM/TEX/ABAQUS-TEX/' for 'open(101,file= ---)' and 'open(102,file= ---)'. The UMAT subroutine is in the file jacobia.rut under the directory of xxx/xxx/ASM/TEX/ABAQUS-TEX/.

Execution:

The executable commands for ABAQUS-CPFail are listed below:

go to directory	/ASM/TEX/ABAQUS-TEX	and
execute	java asm.abaqus.ABApp	command
	TEXCAD	

Original code Files:

The following files are the original code files, user should carry over when change software installation directory, user can also carry over xxx.txc, xxx.ini and xxx.inp files for previous cases:

initial.rut	
jacobia.rut	
/asm/abaqus/*.*	(all files)
abmicrotex.gif	
abaqus.env	
abaqus.cfg	
TXMatrix.db	
TXYarn.db	

Finite Element Analysis of Textile Composite Structures

Introduction

As we mentioned in Part B1, the repeating unit cell (RUC) of a textile composite is usually used to represent the textile composite, and the thermal and mechanical properties of the RUC are considered as the same as the composite. The assumption behind this consideration is the same as the continuous assumption in Elasticity or other rational mechanics. In Elasticity, what we deal with is the material particle, the material continuity means that the particle is small enough that we can treat it as a mathematical point when we consider structures, and large enough that increasing the size will not affect the average material properties. For a textile composite, the concept of RUC is similar to the particle, it is so small that a textile composite structure can be considered as materially continuous, and so large it can fully represent the effect of textile composite microstructures.

It is clear that usually this argument is not true when we notice the dimensions of a RUC. The sizes of a RUC can easily reach to the magnitude of thousandth even hundredth of a meter. But the adopting of RUC concept may be the only way to perform stress analysis and failure prediction of textile composites without micro-level finite element analysis. Analyzing a real textile structures and considering all the woven and braided structures will be the last thing any engineer want to do, without even mention the matrix cracking or matrix-fiber interface slipping. On the other hand, the microstructures of textile composites do not have any repeating pattern in mathematical sense, the yarn paths, the distribution of matrix, even the cross-sections of yarns are far from regular.

The concept of RUC provides a reasonable approach for analyzing textile composite structures. The analysis in Part B1 is in fact a constitutive model of textile composite material. With this model the stress analysis of textile composite structures has no difference from traditional laminated composite structures but a different material. That means any finite element package with the capability of adoption to new materials can be employed to analyze textile composite structures. In this Part of this report, the combination of previous approach with ABAQUS is presented.

Two different material models, three dimensional solid model and two dimensional thin plate model, are developed in this Part for textile composite structures. Element tests are performed for both brick element and shell element and compared to the constitutive model. The failure analysis of a C/SiC plain weave composite plate with a circular hole located at the center is provided as a example.

The combining of MicroTex with ABAQUS: UMAT

As a commercial finite element analysis package, ABAQUS provides an extremely powerful and flexible tool for analysis by user subroutines. Since MicroTex only provides a material model to the finite element analysis, UMAT, the user subroutine to define material behavior, is the main subroutine we need to provide to ABAQUS. Another user subroutine, SDVINI, is also used to define the initial values of solution depended variables (SDV).

The UMAT subroutine retains part of the MicroTex's capabilities, such as the calculation of initial thermal and mechanical properties, material slices failure judgment, and the

calculation of stiffness reduction. The UMAT, in fact, calculates the Jacobean's matrix of the RUC at each stress states, the iteration scheme of ABAQUS is used to solve the system of nonlinear equations. The local stresses, strains, failure information, along with overall RUC material properties (Young's moduli and shear moduli), for each material slice are defined as solution dependent variables. Since the UMAT is called at each integral point on each iteration, all this information will be stored at each integral point, and can be output by the same way as ABAQUS standard variables. The capability of MicroTex to calculate geometry parameters for each material slice and material parameters for each matrix, yarn, and fiber, are provided using a separate code. The results of this code are sent to ABAQUS through input data files of UMAT.

Element test: Comparison with constitutive model

Generally, textile composites are three-dimensional architectures, and the constitutive relation developed in MicroTex is also three dimensional. The combining of MicroTex with ABAQUS through a 3D solid element is then straight forward. A single brick element model as shown in Figure B3-1 was analyzed to verify the UMAT code. As defined in Part B1, the material is C/SiC and the composite is plain weave, and the element type here is C3D8R which is a 3D 8-node brick element with reduced integral. An iterative scheme was used and the increment of applied force at each of the four nodes at the right end of the element is $P = 30.0 * H$, where H is the plate thickness. The comparison with MicroTex results for the two-layer (0/90) composite is given in Figure B3-2. The MicroTex analysis has a criterion for composite failure, so the stress-strain curve stops at the failure load, while for ABAQUS-MicroTex, there is no failure criteria, the predicted stress-strain curve using a single brick element model indicates a dramatic stiffness reduction. The maximum difference between MicroTex and ABAQUS model is less than 2%.

Usually, textile composites are used as plate or shell components which are difficult to model using 3D solid elements. Thus, the constitutive model has to be simplified to two dimensional. The 3D incremental stress-strain relation can be expressed as

$$d \begin{Bmatrix} \epsilon_x \\ \epsilon_y \\ \epsilon_{z1} \\ \epsilon_{xy} \\ \epsilon_{xz1} \\ \epsilon_{yz1} \end{Bmatrix} = \begin{bmatrix} c_{xx} & c_{xy} & c_{xz} & 0 & 0 & 0 \\ c_{yx} & c_{yy} & c_{yz} & 0 & 0 & 0 \\ c_{zx} & c_{zy} & c_{zz} & 0 & 0 & 0 \\ 0 & 0 & 0 & c_x & 0 & 0 \\ 0 & 0 & 0 & 0 & c_z & 0 \\ 0 & 0 & 0 & 0 & 0 & c_y \end{bmatrix} d \begin{Bmatrix} \sigma_x \\ \sigma_y \\ \sigma_z \\ \tau_{xy} \\ \tau_{xz} \\ \tau_{yz} \end{Bmatrix}$$

For thin plate or shell, assuming that $[\sigma_z, \tau_{xy}, \tau_{xz}] = 0$, we have

$$\begin{Bmatrix} d\sigma_x \\ d\sigma_y \\ d\tau_{xy} \end{Bmatrix} = \begin{bmatrix} c_{xx} & c_{xy} & 0 \\ c_{yx} & c_{yy} & 0 \\ 0 & 0 & c_{zz} \end{bmatrix}^{-1} \begin{Bmatrix} d\epsilon_x \\ d\epsilon_y \\ d\epsilon_{xy} \end{Bmatrix}$$

A single shell element model was analyzed for the same problem, the element type is S8R5. The results shown in figure B3-3 indicated that the UMAT for those two elements is correct.

MicroTex-ABAQUS User Interface: GUI

The screenshot shows the MICROTEX Yarn Database GUI. It features a title bar with the text 'MICROTEX: Yarn Database'. The main window contains several input fields and buttons. At the top, there are dropdown menus for 'Identification' (set to 'DEFAULT') and 'Name' (set to 'Default Yarn Properties'). Below these are 'Kind' (set to 'Yarn') and 'Matrix ID' (set to 'DEFAULT'). The central area is divided into three columns of input fields. The first column contains moduli (E11, E22, E33, G12, G23, G13) and Poisson's ratios (NU12, NU23, NU13). The second column contains maximum strains and stresses in different directions (1 dir, 2 dir, 3 dir) for tension and compression, as well as maximum shear stresses in different planes (12, 23, 13). The third column contains thermal expansion coefficients, nonlinear parameters, shear stress parameters, fiber diameter, and fiber volume fraction. At the bottom, there are four buttons: 'NEW', 'DELETE', 'UNDO', and 'EXIT'.

Property	Value
E11 (MPa)	142845.0
E22 (MPa)	65783.1
E33 (MPa)	65783.1
G12 (MPa)	27029.7
G23 (MPa)	27029.7
G13 (MPa)	27029.7
NU12	0.21
NU23	0.21
NU13	0.21
Max tension strain in 1 dir (MPa)	0.014
Max compression strain in 1 dir (MPa)	0.01
Max tension stress in 2 dir (MPa)	84.9
Max compression stress in 2 dir (MPa)	206.0
Max tension stress in 3 dir (MPa)	84.9
Max compression stress in 3 dir (MPa)	206.0
Max shear stress in 12 plane (MPa)	87.5
Max shear stress in 23 plane (MPa)	102.4
Max shear stress in 13 plane (MPa)	87.5
Thermal exp. coef. in 1 dir (1/C)	0.00000127
Thermal exp. coef. in 2 dir (1/C)	0.00000693
Nonlinear parameter 1	0.85
Nonlinear parameter 2	12.0
Shear stress parameter	1.6
Fiber diameter (m)	0.000007
Fiber volume fraction	0.55

A graphical user interface was developed for finite element analysis using ABAQUS package. The user is required to provide finite element model, boundary conditions, and loading history through a standard ABAQUS input file as an initial file.

No blank space after comma in the material and section definition lines.

ABAQUS allows different material in single model. The user should define textile composite materials (assuming MicroTex as their constitutive model) through the GUI and all other materials as standard ABAQUS input.

The ABAQUS-MicroTex GUI provides windows for user to input yarn and matrix material properties, such as moduli, Poisson's ratio, coefficients of thermal expansion, maximum strains and stresses, nonlinear coefficients, stress intensity factor, initial crack length, shear stress parameters, and yarn packing density; geometry parameters, such as yarn orientation, layer thickness, axial yarn spacing, axial yarn content, and yarn sizes, of textile composites; and analytical control parameters, such as linear or nonlinear materials, plate theory or 3D iso-strain analysis, fracture model or continuum model. The GUI also provides user opportunity to modify orientations of each composite layers. Those input windows are very much similar to the MicroTex GUI. The main difference is that the user is required to specify element groups to which all material and geometry properties are defined.

The GUI will first generate a set of data files containing material, geometry and control data, and will allow the user to choice between creating a new ABAQUS input file or

overwriting the original one. Before executing ABAQUS, the GUI will execute a FORTRAN code based on the input material and geometry parameters to generate two data files for UMAT for each textile composite material.

Following is the ABAQUS input file for the shell element testing problem. It is noticed that element group “*allel*” is made up of material “*shell*” which is not defined (no modulus or Poisson’s ratio is given). ABAQUS- MicroTex reserves material names with the first five letter being “*shell*” to materials defined by UMAT with the 2D stress-strain relation, and all the other user-defined material names as defined by UMAT with the 3D stress-strain relation. There is neither indication in the input file that “*shell*” is a user defined material, nor the location of UMAT. The user is required to define this material with GUI by specifying material and geometry parameters for this material under element group “*allel*”.

```
*heading
Textile composite plate, single shell elements model
S8R5 element
SI units
**
**      Model definition      **
*node, nset=alln
101, 0.00, 0.00, 0.00
102, 0.25e+03, 0.00, 0.00
103, 0.50e+03, 0.00, 0.00
201, 0.00, 0.25e+03, 0.00
202, 0.50e+03, 0.25e+03, 0.00
301, 0.00, 0.50e+03, 0.00
302, 0.25e+03, 0.50e+03, 0.00
303, 0.50e+03, 0.50e+03, 0.00
*nset, nset=middle
201, 202
*nset, nset=left
101, 201, 301
*element, type=s8r5, elset=allel
1, 101, 103, 303, 301, 102, 202, 302, 201
*shell selection, elset=allel, composite
6.0e-04, 1, shell, np0      !!shell material is used for element group allel
6.0e-04, 1, shell, p90    !!layer orientation is defined (p90), and can be modified in GUI
*transverse shear stiffness
5.0e04, 5.0e04, 5.0e04
*material, name=shell      !! shell is the material to be defined using UMAT
*elastic
1.0,2.0,3.0,4.0,5.0,6.0
*orientation, name=np0, system=rectangular
1.0, 0.0, 0.0, 0.0, 1.0, 0.0
3, 00.0
*orientation, name=p90, system=rectangular
1.0, 0.0, 0.0, 0.0, 1.0, 0.0
3, 90.0
**
```

Finite Element Analysis of Textile Composite Structures

Introduction

As we mentioned in Part B1, the repeating unit cell (RUC) of a textile composite is usually used to represent the textile composite, and the thermal and mechanical properties of the RUC are considered as the same as the composite. The assumption behind this consideration is the same as the continuous assumption in Elasticity or other rational mechanics. In Elasticity, what we deal with is the material particle, the material continuity means that the particle is small enough that we can treat it as a mathematical point when we consider structures, and large enough that increasing the size will not affect the average material properties. For a textile composite, the concept of RUC is similar to the particle, it is so small that a textile composite structure can be considered as materially continuous, and so large it can fully represent the effect of textile composite microstructures.

It is clear that usually this argument is not true when we notice the dimensions of a RUC. The sizes of a RUC can easily reach to the magnitude of thousandth even hundredth of a meter. But the adopting of RUC concept may be the only way to perform stress analysis and failure prediction of textile composites without micro-level finite element analysis. Analyzing a real textile structures and considering all the woven and braided structures will be the last thing any engineer want to do, without even mention the matrix cracking or matrix-fiber interface slipping. On the other hand, the microstructures of textile composites do not have any repeating pattern in mathematical sense, the yarn paths, the distribution of matrix, even the cross-sections of yarns are far from regular.

The concept of RUC provides a reasonable approach for analyzing textile composite structures. The analysis in Part B1 is in fact a constitutive model of textile composite material. With this model the stress analysis of textile composite structures has no difference from traditional laminated composite structures but a different material. That means any finite element package with the capability of adoption to new materials can be employed to analyze textile composite structures. In this Part of this report, the combination of previous approach with ABAQUS is presented.

Two different material models, three dimensional solid model and two dimensional thin plate model, are developed in this Part for textile composite structures. Element tests are performed for both brick element and shell element and compared to the constitutive model. The failure analysis of a C/SiC plain weave composite plate with a circular hole located at the center is provided as a example.

The combining of MicroTex with ABAQUS: UMAT

As a commercial finite element analysis package, ABAQUS provides an extremely powerful and flexible tool for analysis by user subroutines. Since MicroTex only provides a material model to the finite element analysis, UMAT, the user subroutine to define material behavior, is the main subroutine we need to provide to ABAQUS. Another user subroutine, SDVINI, is also used to define the initial values of solution depended variables (SDV).

The UMAT subroutine retains part of the MicroTex's capabilities, such as the calculation of initial thermal and mechanical properties, material slices failure judgment, and the

```

**      analysis history      **
*step
*static
0.05, 1.0
*boundary
left, 1
left, 3, 6
middle, 2
*cloud
103, 1, 2.5
202, 1, 10.0
303, 1, 2.5
**
**      output      **
*restart, write
*node print, nset=alln, frequency=1
u
*node file, nset=alln, frequency=1
u
*el print, elset=allel, frequency=1
s,e
*el file, elset=allel, frequency=1
s,e
*end step

```

The GUI can save all the GUI input information in a file, xxx.txc, for re-opening. A new ABAQUS input file will be created by GUI. This new file will be the same as the original one for the model, boundary condition and loading history, output requirement, the only difference is the material property part. The new one will appear as follows. The solution dependent variables are defined at each integral point and updated in each iteration. The first six solution dependent variables here are used to store the local moduli, and can be exported as standard ABAQUS variables.

```

.....
.....
*shell selection, elset=allel, composite
6.0e-04, 1, shell, np0
6.0e-04, 1, shell, p90
.....
.....
*material, name=shell
*depvar
822
*user material, constant=0
*initial conditions, type=solution, user
*user subroutine, input=...\...\initial.rut
*user subroutine, input=...\...\jacobia.rut
.....
.....

```

!!number of solution variables

!!initial data for UMAT

!!UMAT, define material

Finite element analysis of a C/SiC plain weave composite plate with a center hole

A two-layer (0/90) C/SiC plain weave composite plate with a hole at the center has been analyzed using ABAQUS. The plate is 8 inches long and 1 inch wide, the radius of the hole is 0.125 inches. A total of 768 shell elements (S4R) and 844 nodes were used to model the plate, and 3 integral points were used for each layer; the mesh which was generated by PATRAN is shown in Figure B3-4. The load is applied through uniform displacement boundary condition at two ends. In each increment, the displacement increases $5.0\text{e-}04$ m.

Figures B3-5 to B3-9 give the distribution of normal stress and tangent stiffness moduli in loading direction at increments 5, 7, 8, and 10, respectively. The moduli are all normalized by the initial material properties of the RUC. When any material slice fails, the corresponding modulus is reduced to 1%.

The distributions of moduli clearly indicate the failure process of the plate on the element base. It can be seen that, at increment 5, the maximum stress is less than 490.0MPa, the modulus indicates that there is no element failed although the nonlinear material properties cause some stiffness reductions. At increment 7, the distribution of modulus indicates that element failure happens near the hole. The failure range increases at increment 8, and at increment 10, the plate failed in the sense that the modulus in loading direction across the width of the plate had been reduced near to 1%.

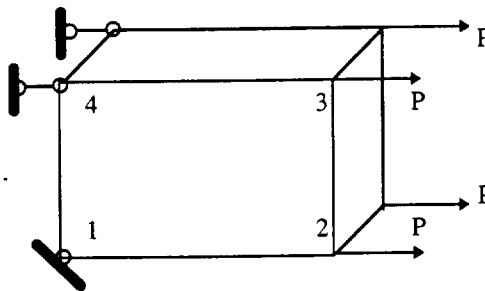


Figure B3-1. Brick element model for (0/90) C/SiC plain weave composite

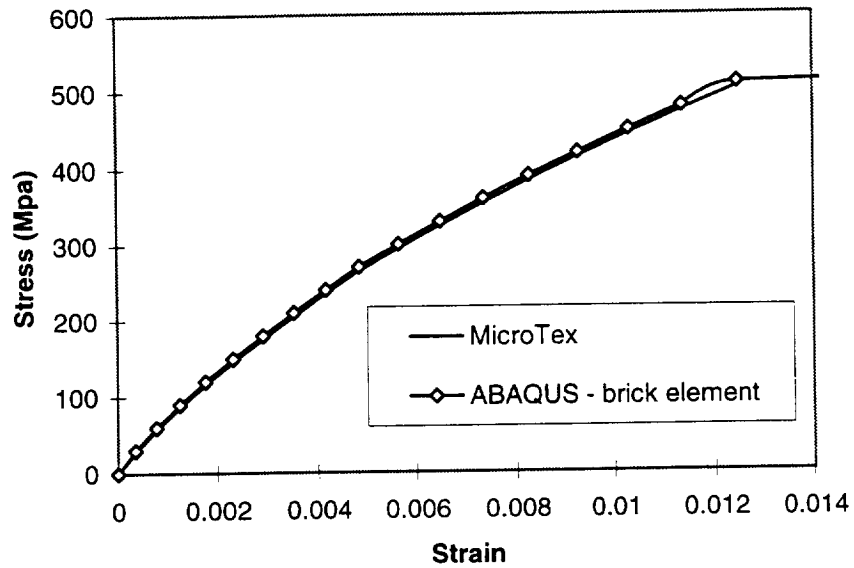


Figure B3-2. Comparison for a 2-layer (0/90) C/SiC plain weave composite: Brick element

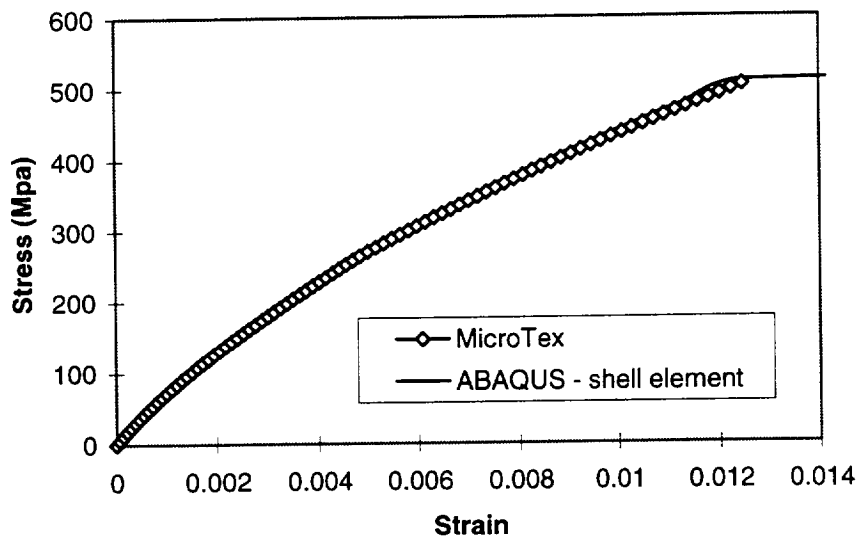


Figure B3-3. Comparison for a (0/90) C/SiC plain weave composite: Shell elements

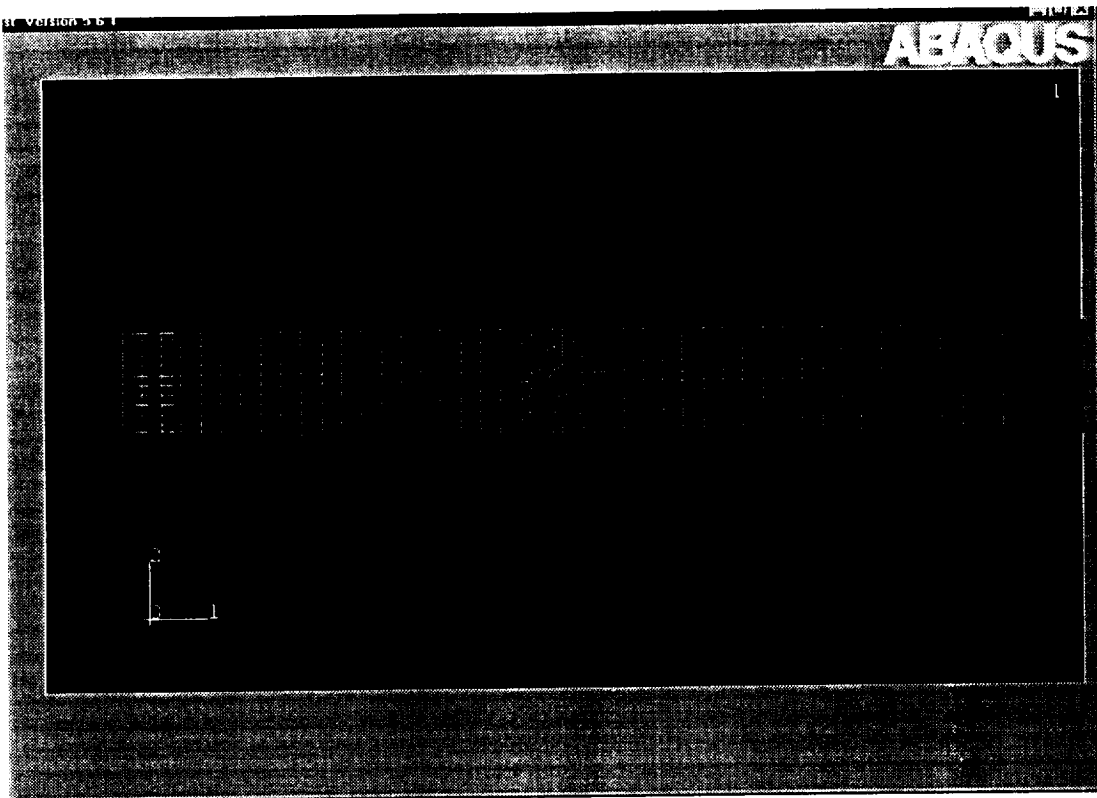


Figure B3-4. Finite element model for a two layer plane weave composite plate with a hole

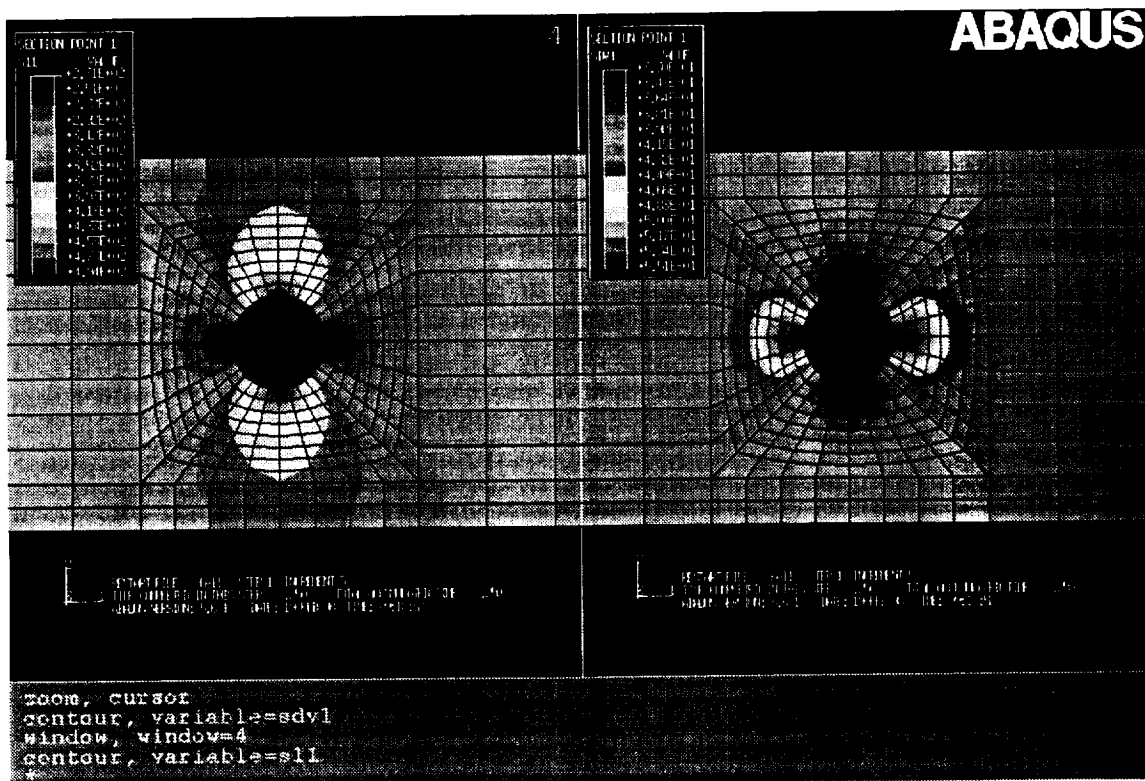


Figure B3-5. Distribution of normal stress and tangent modulus at increment 5.

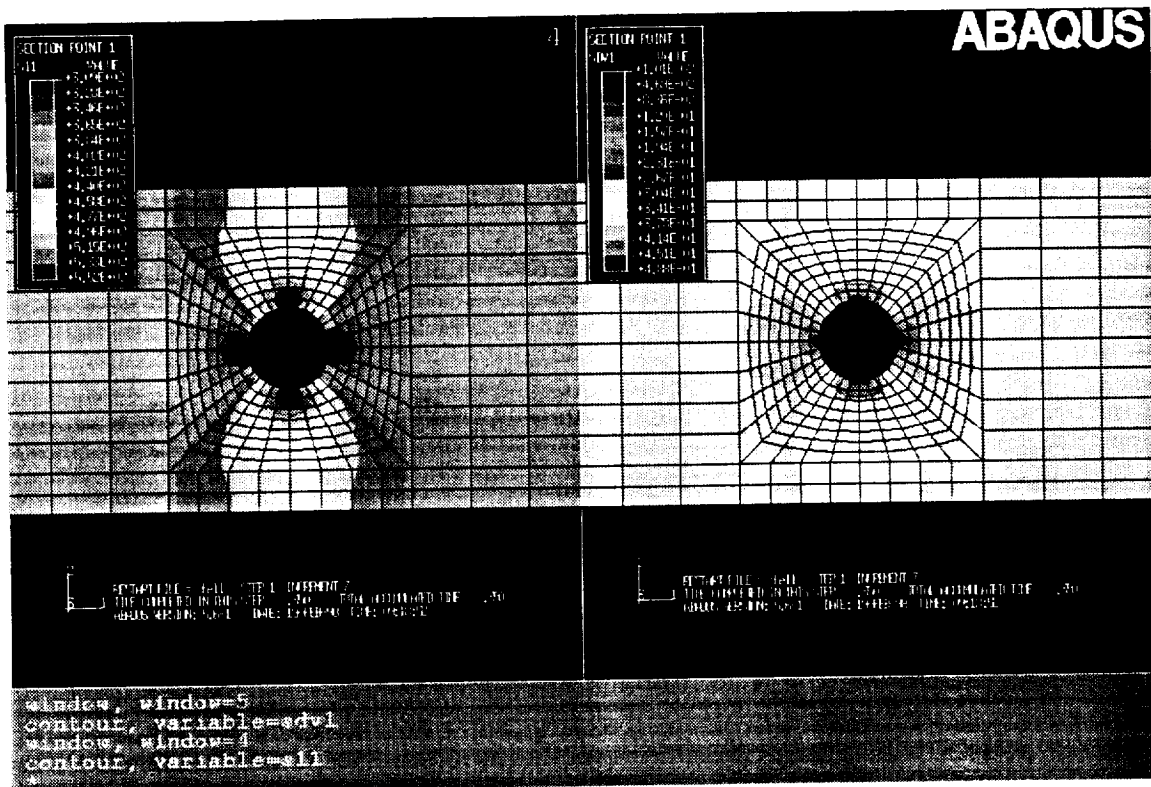


Figure B3-6. Distribution of normal stress and tangent modulus at increment 7.

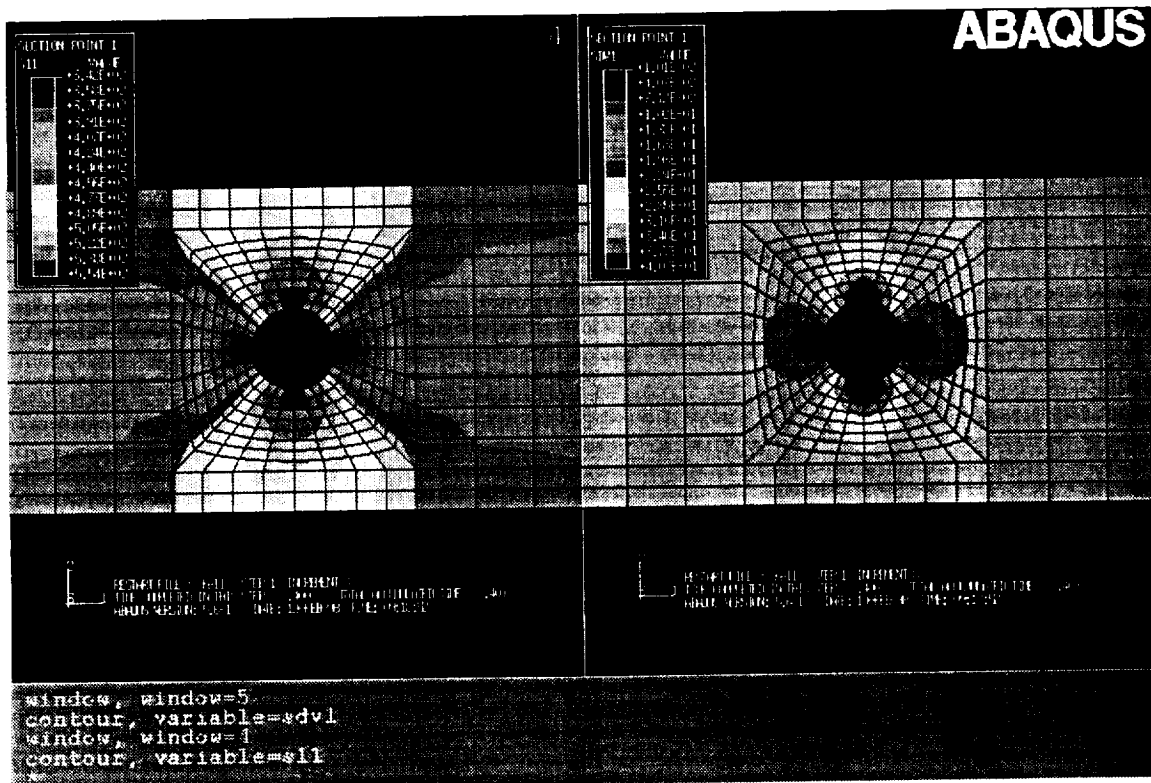


Figure B3-7. Distribution of normal stress and tangent modulus at increment 8.

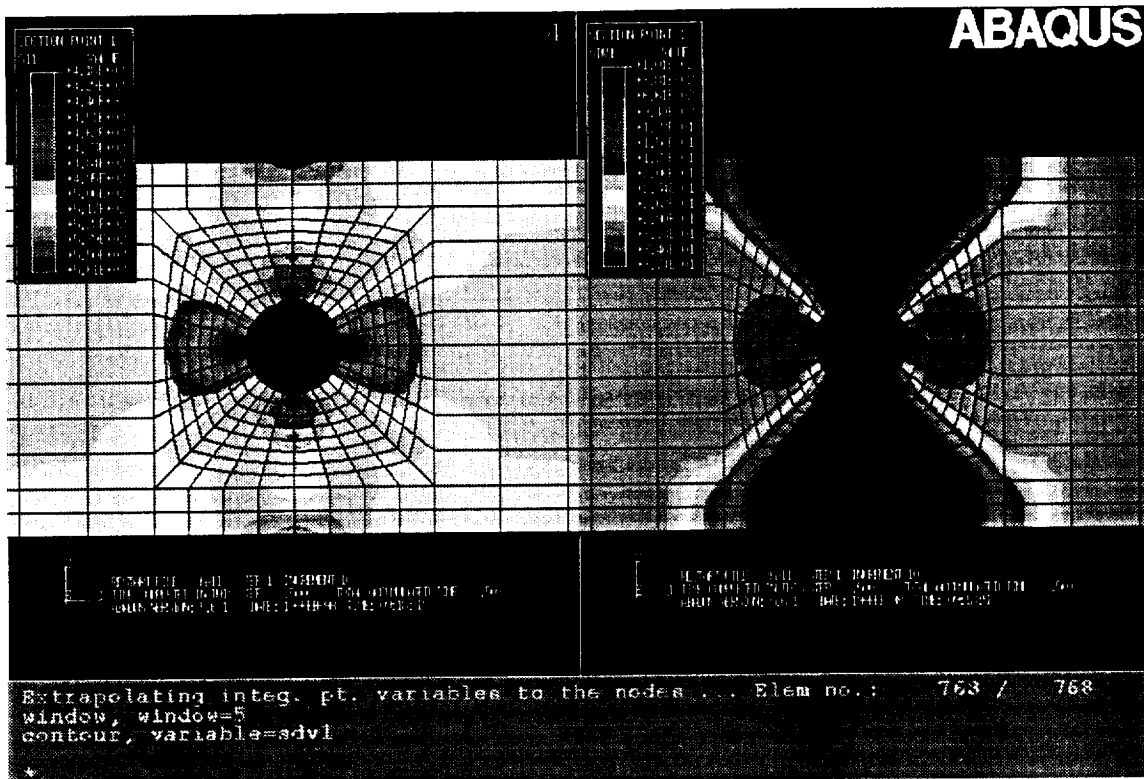


Figure B3-8. Distribution of normal stress and tangent modulus at increment 10.

Part C. Experiments

Introduction

An experimental investigation was performed to determine the fatigue and static behavior of two lay-ups of Carbon/Silicon Carbide (C/SiC) composite specimens. The specimens were loaded in static tension and in tension-tension fatigue under isothermal fixed-frequency conditions. Two temperature levels and a range of stress levels for fatigue were used to assess performance. The tests were conducted at 23°C and 1000°C. Measurements were made of modulus and cycles to failure several times during the test.

Experimental Program

The experimental program was divided into two parts to develop an understanding of the fatigue performance of the material. The first part consisted of an investigation to determine the static properties of the material and determine how the modulus of the material changes as a function of maximum applied static strain. The second portion of the testing consisted of an investigation of the high cycle fatigue behavior of the material. The specimens were tested to failure or 1,000,000 cycles.

Tests were performed on two lay-ups of a C/SiC composite material system with a CVIP coating by DuPont. The coating provided protection from oxidation at high temperature. This composite system consisted of plain woven carbon fibers in a silicon carbide matrix produced in two 24 ply symmetric lay-ups. The test panels, produced with a [0/90] and a [0/±60] lay-up, both had a nominal thickness of 0.12 in. after manufacture. The panels were machined into 6 inch "dog-bone" specimens with a 2-inch long by approximately 0.50 inch wide gage section.

Test Procedure and Equipment

Static Properties

The static test used on the C/SiC was performed in load control at a loading rate of 5000 lb./min. on a 50 KIP servo-hydraulic test stand equipped with an automated data acquisition system. The load was increased by 150lb, then decreased by 100 lb, in order to take the stiffness measurements. This loading series was repeated until the specimen failed. This loading and unloading provided the advantage of allowing the calculation of the modulus as a function of the maximum strain experienced by the specimen for each unloading segment during the test. A 25.4 mm (1 in.) gauge length extensometer was mounted on the edges and centered with respect to the gage section to provide strain data. Load and strain were recorded at half-second intervals during all of the tests.

Property calculations consisted of ultimate strength and modulus. Ultimate stress was calculated using the area of the un-notched cross-section and the highest load carried by the laminate. Modulus was calculated using a least squares fit to the unloading segments of data during static tests.

Fatigue Properties

The tension fatigue tests were performed on a 50 KIP capacity servo-hydraulic test stand. Load, strain, actuator displacement and time were recorded using an automated digital data acquisition system. All fatigue tests were performed under load control at a frequency of 5 Hz (except during data cycles) with a min./max. stress ratio of $R=0.1$ and a sinusoidal wave form. Tests were concluded after 1,000,000 cycles if failure did not occur.

The strain and load were measured during specified cycles of the fatigue test as summarized in Table C-1 and allowed for determination of changes in modulus. For high temperature testing, a clamshell furnace maintained the test temperature over the entire gage length of the specimen. A high temperature ceramic extension rod extensometer with a 25.4 mm (1.0 in.) gage length was edge mounted on the gage section center to measure strain.

Applied load and measured strain were used to calculate an effective modulus for the gage section during fatigue tests. Stiffness calculations were performed by making a least squares linear fit to the stress versus strain data. Stress was calculated using the specimen gage section area and the load from the data acquisition system. Strain was taken from the extensometer attached to the gage section. The fit was performed on the loading and unloading data over the entire fatigue cycle.

Experimental Results

Static Tests

The static tests at 23°C and 1000°C were conducted for both lay-ups. The ultimate stress for each testing condition is shown in Table C-2. There was a 57% reduction in strength of the [0/90] lay-up between room temperature and 1000°C while the [0/±60] lay-up experienced a 35% reduction in strength. Results from the room temperature static tests are shown in Figure C-1 for both lay-ups. Elastic modulus as a function of maximum strain for these two static tests is shown in Figure C-2.

Fatigue Tests

The 23°C fatigue tests are summarized in Tables C-3 and C-4, and Figures C-3 and C-4. Tables C-3 and C-4 display the maximum stress and cycles to failure of individual [0/90] and [0/±60] specimens respectively during fatigue. The fatigue life diagrams for each material lay-up are shown in Figures C-3 and C-4. These figures allow visualization of both the fatigue data and the static results.

Similarly the 1000°C fatigue tests are summarized in Tables C-5 and C-6, and Figures C-5 and C-6. The fatigue data is tabulated in Tables C-5 and C-6 for [0, 90] and [0/±60] specimens respectively. The fatigue life diagrams for each material lay-up are shown in Figures 5 and 6. Notice that none of the fatigue tests lasted to run out.

The modulus is shown in Figures C-7 and C-8 as a function of cycle count during fatigue. Data for the [0/90] lay-up is shown in Figure C-7. Data for the [0/±60] is displayed in Figure C-8. These figures demonstrate how the modulus of both lay-ups decreases with fatigue loading.

Table C-1. Ultimate Stress for the C/SiC Static Tests

Cycle Count Range	Reading Interval
1-10	1 cycle
10-50	5 cycles
50-100	10 cycles
100-500	i-99050 cycles
500-1,000	100 cycles
1,000-5,000	500 cycles
5,000-10,000	1,000 cycles
10,000-100,000	5,000 cycles
100,000-1,000,000	10,000 cycles

Table C-2. Ultimate Stress for the C/SiC Static Tests

Lay-up	Temperature (°C)	Ultimate Stress (ksi)
[0/90]	23	73.0
[0/90]	1000	31.3
[0/±60]	23	42.0
rdrl[0/±60]	1000	27.1

Table C-3. Cycles to failure for the [0/90] C/SiC Fatigue Tests at 23°C
(R = 0.1, f = 5Hz.)

Maximum Stress σ_{\max} (ksi)	Cycles to Failure n
66.5	4369
62.7	37332
59.5	42334
56.0	515176
45.5	> 1000000

Table C-4. Cycles to failure for the [0/±60] C/SiC Fatigue Tests at 23°C
(R = 0.1, f = 5Hz.)

Maximum Stress σ_{\max} (ksi)	Cycles to Failure n
40.53	423
39.9	2924
37.7	48754
36.0	546514
35.6	> 1000000

Table C-5. Cycles to failure for the [0/90] C/SiC Fatigue Tests at 1000°C
(R = 0.1, f = 5Hz.)

Maximum Stress σ_{\max} (ksi)	Cycles to Failure n
28.0	1853
25.1	5417
21.7	8028
15.4	37751
rdrs9.1	95525

Table C-6. Cycles to failure for the [0/±60] C/SiC Fatigue Tests at 1000°C
(R = 0.1, f = 5Hz.)

Maximum Stress σ_{\max} (ksi)	Cycles to Failure n
21.8	6060
19.2	7861
16.2	33829
13.5	55309
10.8	114676

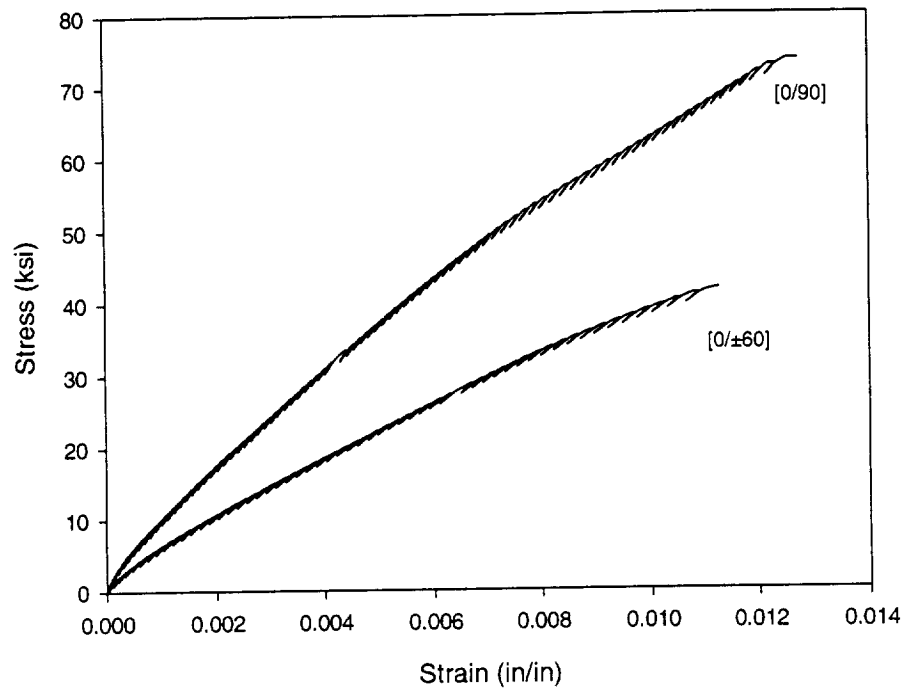


Fig. C-1 Static Results for C/SiC at 23°C

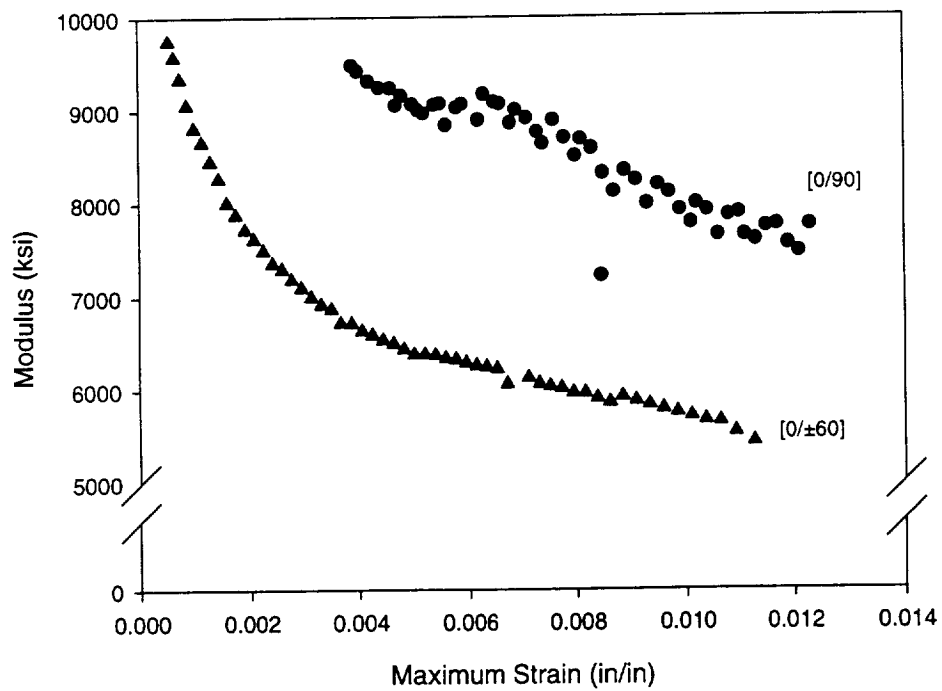


Fig. C-2 Modulus Shown as a Function of Maximum Strain for C/SiC Tests at 23°C

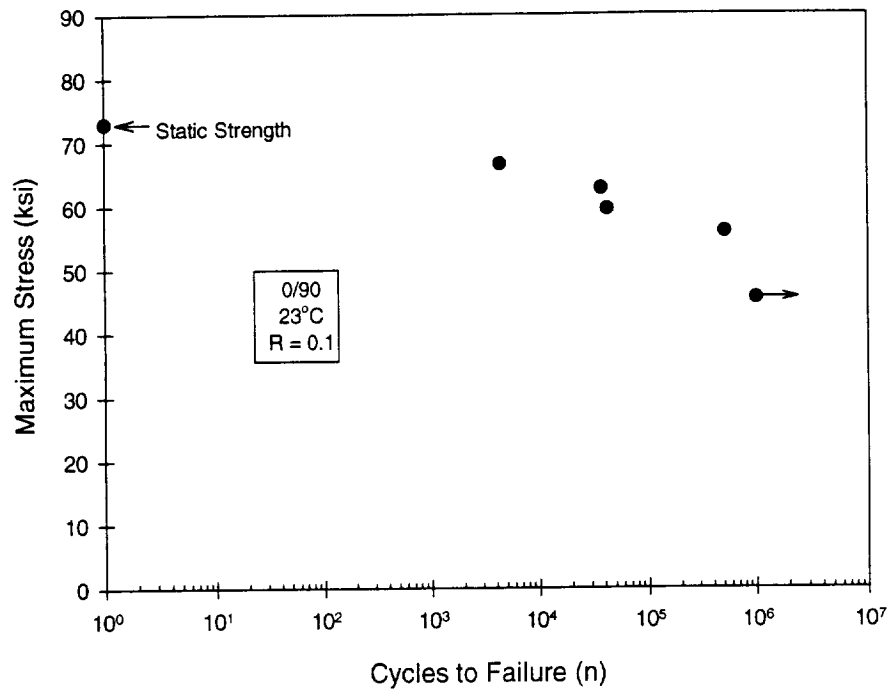


Fig. C-3 Fatigue Life Diagram for C/SiC at 23°C

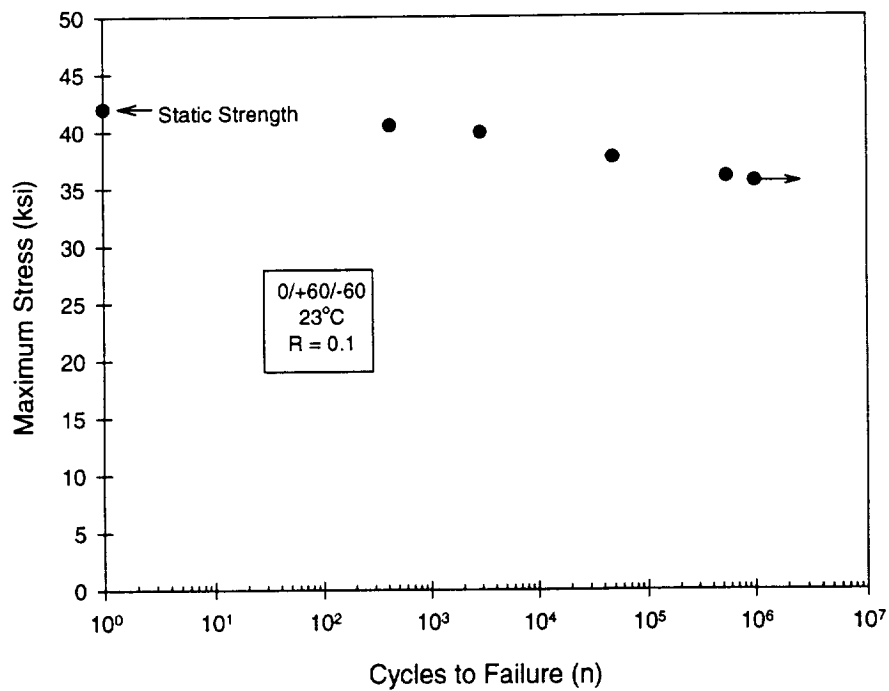


Fig. C-4 Fatigue Life Diagram for C/SiC at 23°C

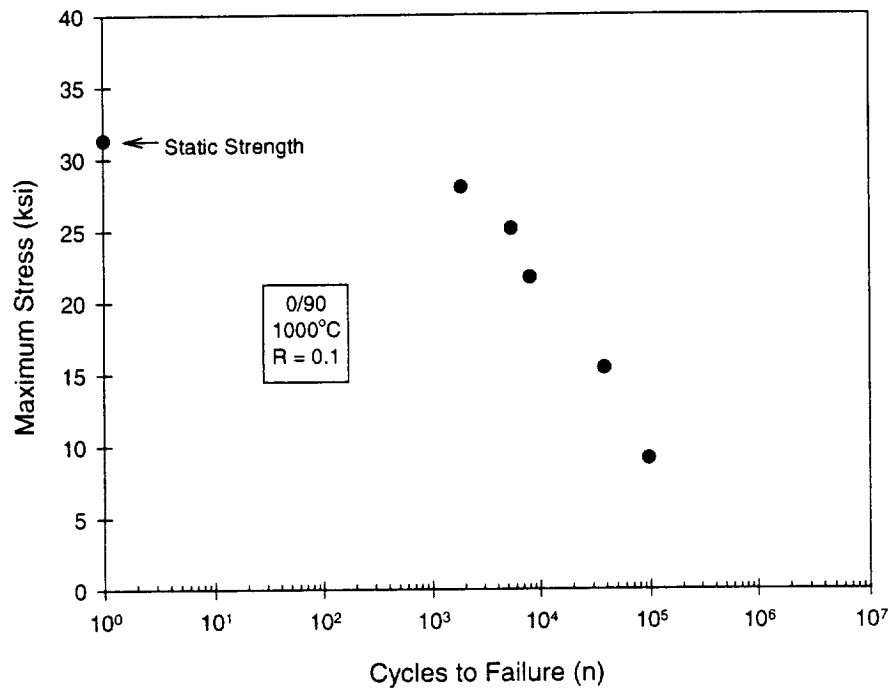


Fig. C-5 Fatigue Life Diagram for C/SiC at 1000°C

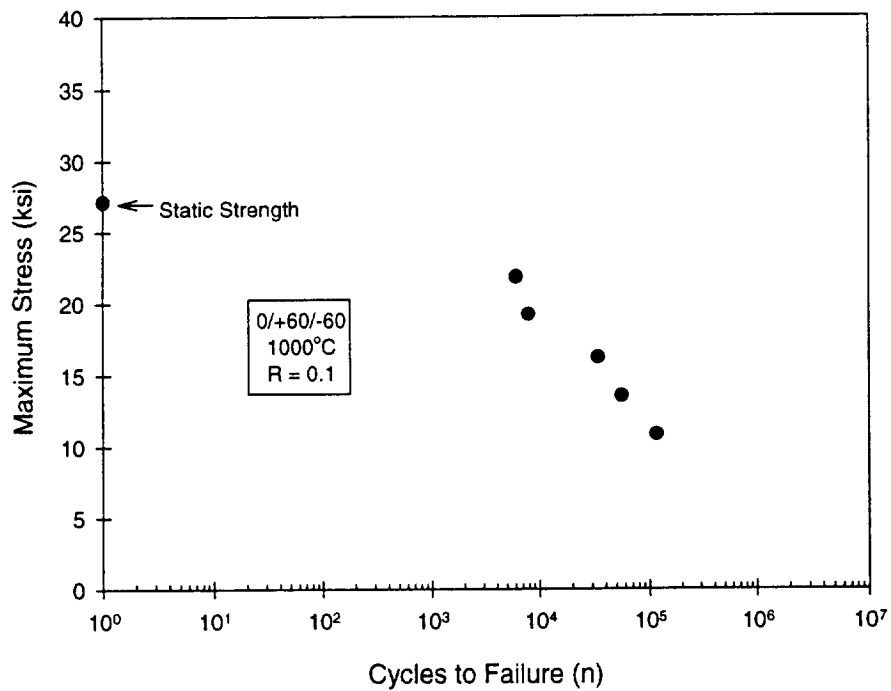


Fig. C-6 Fatigue Life Diagram for C/SiC at 1000°C

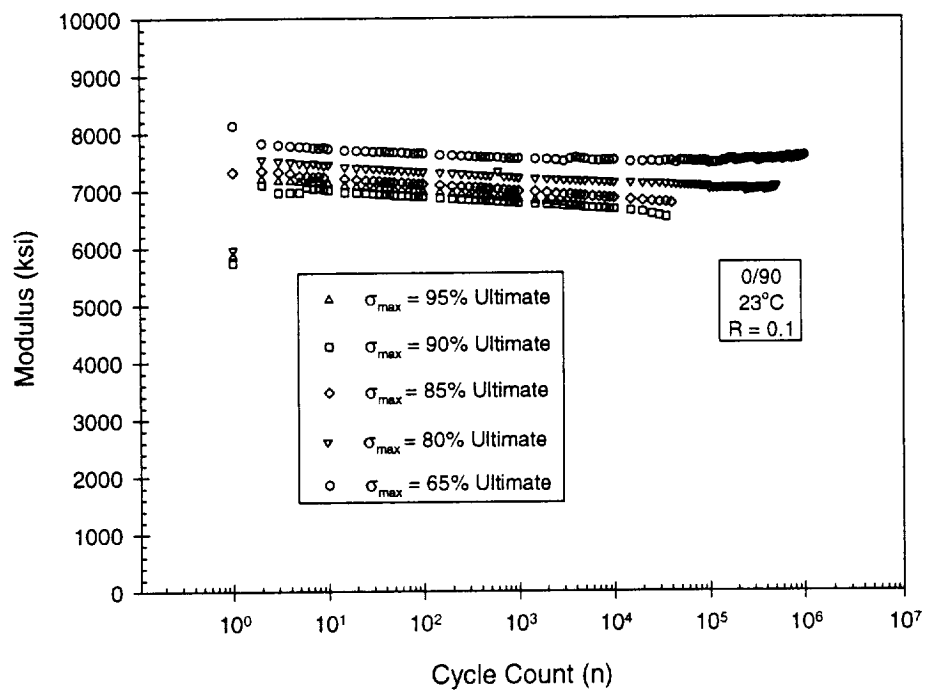


Fig. C-7 Modulus as a Function of Cycle Count Diagram for C/SiC at 23°C

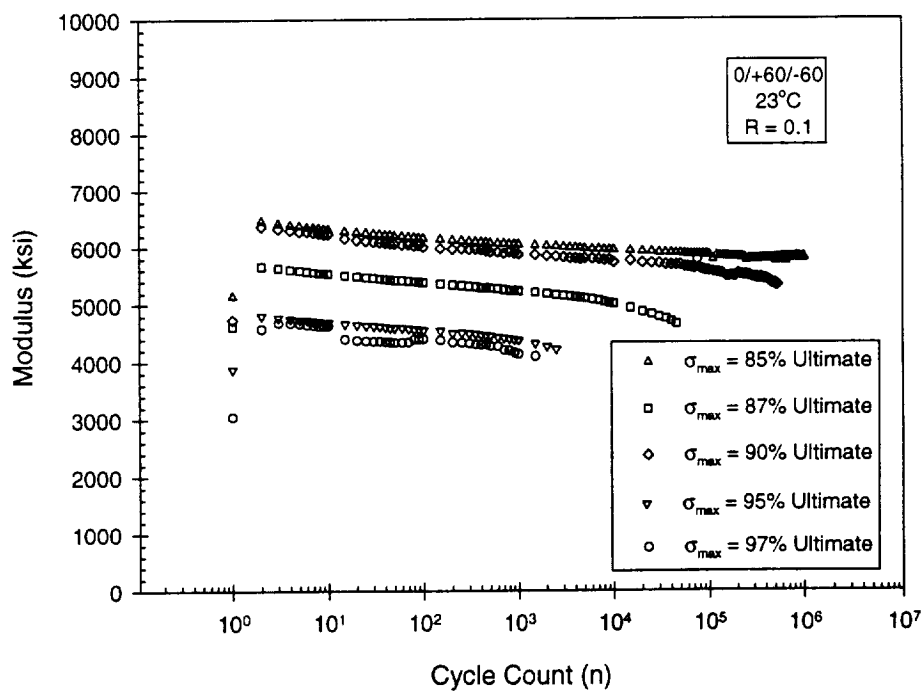


Fig. C-8 Modulus as a Function of Cycle Count Diagram for C/SiC at 23°C

Part D. Publications

Two paper related to this project were published in technical conferences.

- 1) D. Y. Xue and M. F. Card, "Prediction of Laminate Damage Processes Using Combined Micro-Mechanics, Fracture Mechanics and Statistics," AIAA-97-1188, 38th Structures, Structural Dynamics and Materials Conference, Kissimmee, FL, April 7-10, 1997
- 2) Y. Shi, M. F. Card, V. V. Raman and R.M.V. Murthi, "Prediction of Tension Failure of Textile Composites Using Micro-Mechanics and Statistical Analysis," 22nd Annual Cocoa Beach Conference and Exposition on Composites, Advanced Ceramics materials and structures, , Cocoa Beach, FL, Jan. 20-24, 1998

Part E. Commercialization Plan

MICROTEX and CPFail developed by Analytical Services and Material, Inc. are the user-friendly softwares which combined the degradation analysis of composite materials (textile and laminate) into ABAQUS structural analysis. The softwares have the capability to perform structural progressive failure analysis for laminate and textile composite structures.

Progressive failure analysis is very important to the structure safety, especially for aging aircraft structures. Comparing to the conventional structural analysis, the progressive failure analysis can more accurately predict the structural damage development and the structure life.

Many composite failure analysis theories have been developed, but not much of them actually been used in real structural analysis. This is due to either the theory is not applicable (theoretical research) or not available for commercial or practical users. MICROTEX and CPFail were developed under the consideration of practical application. They are combined with ABAQUS commercial structural analysis code, therefore they are available for the general structural analysis.

The following suggestions are for Phase III or commercialization MICROTEX and CPFail:

- 1) Provide free maintenance service to NASA Marshall and any buyer
- 2) Continuously update MICROTEX and CPFail, distribute updated version to current users
- 3) Provide consulting and training service for using MICROTEX and CPFail
- 4) Advertise MICROTEX and CPFail in technical conferences, seminars, internet, universities and research institutes.
- 5) Apply MICROTEX or CPFail technology to other projects, get the support from new projects to update MICROTEX and CPFail.
- 6) Find potential new users, keep in touch with the current users
- 7) Give free simple sample version to new user to test
- 8) Combine MICROTEX and CPFail to other commercial codes, for example, NASTRAN, COMET, ----.

The key point of Phase III is to find potential users. Composite structure manufacture company and airplane, automobile companies are the possible potential users.

Part F. Computer Codes

The software codes for CPFail, MicroTex, ABAQUS-CPF and ABAQUS-TEX are distributed in tar format file `asm.tar`. The file contains all the required data files, source files and java class files required to execute the programs. To install the software components copy change directory to the destination directory and extract the files using the command: `tar -xvf asm.tar`. This command creates the ASM main directory and sub directories to copy the CPFail, MicroTex and ABAQUS interface programs. After extracting the files the default executable file names and paths have to set before running the any sample problems. This can be set either manually editing the configuration files or by executing the programs and modifying through the GUI using the menu command Configuration under Options menu. The executable commands for software components are listed in the sections 'Installation and Execution' of each manual.

The CPFail is developed in C/C++ using X-Windows and Motif toolkits. Where as other components are developed using Sun's JDK 1.1.4. To execute these components Java runtime environment of version 1.1.3 or higher is required. Refer the JDK or JRE documentation for installation of Java.

All the software codes currently have been installed in merlin.msfc.nasa.gov under the directory `/xfs/merlin/lv00/home/xuedx`:

- (1) `/xfs/merlin/lv00/home/xuedx/ASM/CPF/ABAQUS-CPF`
Execution: `java asm.abaqus.ABApp CMLIFE`
- (2) `/xfs/merlin/lv00/home/xuedx/ASM/CPF/CPFAIL`
Execution: `./cpfail`
- (3) `/xfs/merlin/lv00/home/xuedx/ASM/TEX/ABAQUS-TEX`
Execution: `java asm.abaqus.ABApp TEXCAD`
- (4) `/xfs/merlin/lv00/home/xuedx/ASM/TEX/MICROTEX`
Execution: `java asm.microtex.TXApp`

REPORT DOCUMENTATION PAGE

Form Approved
OMB No. 0704-0188

Public reporting burden for this collection of information is estimated to average 1 hour per response, including the time for reviewing instructions, searching existing data sources, gathering and maintaining the data needed, and completing and reviewing the collection of information. Send comments regarding this burden estimate or any other aspect of this collection of information, including suggestions for reducing this burden, to Washington Headquarters Services, Directorate for Information Operations and Reports, 1215 Jefferson Davis Highway, Suite 1204, Arlington, VA 22202-4302, and to the Office of Management and Budget, Paperwork Reduction Project (0704-0188), Washington, DC 20503.

1. AGENCY USE ONLY (Leave blank)		2. REPORT DATE March 1998		3. REPORT TYPE AND DATES COVERED Final Report February 1996 to March 1998	
4. TITLE AND SUBTITLE Progressive Failure and Life Prediction of Ceramic and Textile Composites				5. FUNDING NUMBERS	
6. AUTHOR(S) David Y. Xue, Yucheng Shi, William M. Johnston, Madhu Katikala and Micheal F. Card					
7. PERFORMING ORGANIZATION NAME(S) AND ADDRESS(ES) AS&M, Inc. 107 Research Drive Hampton, VA 23666				8. PERFORMING ORGANIZATION REPORT NUMBER	
9. SPONSORING / MONITORING AGENCY NAME(S) AND ADDRESS(ES) NASA Marshall Space Flight Center Huntsville, AL				10. SPONSORING / MONITORING AGENCY REPORT NUMBER	
11. SUPPLEMENTARY NOTES Final Report under NAS8-40638					
12a. DISTRIBUTION / AVAILABILITY STATEMENT Generally Available				12b. DISTRIBUTION CODE	
13. ABSTRACT (Maximum 200 words) An engineering approach to predict the fatigue life and progressive failure of multilayered composite and textile laminates is presented. Analytical models which account for matrix cracking, statistical fiber failures and nonlinear stress-strain behavior have been developed for both composites and textiles. The analysis methods use experimentally derived empirical coefficients to account for the interface of fiber and matrix, fiber strength, and fiber-matrix stiffness reductions. Similar considerations were applied to textiles using Repeating Unit Cells. Fatigue analyses included use of Walker's equation for cyclic matrix cracking and Heywood's formulation for stress degradation. The analysis has been compared with experiment with good agreement. Comparisons were made with Graphite-Epoxy, C/SiC and Nicalon/CAS composite materials. For textile materials, comparisons were made with triaxial braided and plain weave materials under biaxial or uniaxial tension. Fatigue predictions were compared with test data obtained from plain weave C/SiC materials tested at AS&M. Several computer codes were developed to perform the analysis. Composite Progressive Failure Analysis for Laminates is contained in the code CPPFail. Micromechanics Analysis for Textile Composites is contained in the code MicroTex. Both codes were adapted to run as subroutines for the nonlinear Finite Element code ABAQUS and MicroTex-ABAQUS.					
14. SUBJECT TERMS Ceramics, Textiles, Progressive, failure				15. NUMBER OF PAGES	
				16. PRICE CODE	
17. SECURITY CLASSIFICATION OF REPORT Unclassified	18. SECURITY CLASSIFICATION OF THIS PAGE Unclassified	19. SECURITY CLASSIFICATION OF ABSTRACT Unclassified	20. LIMITATION OF ABSTRACT None		